ABSTRACT

Title of dissertation: CAPACITY OF FROZEN SOIL FOR SHALLOW TUNNEL PRE-SUPPORT UNDERNEATH A BUILDING FOUNDED ON WOODEN PILES

Vojtech Gall, Doctor of Philosophy, 2004

Dissertation directed by: Associate Professor Charles W. Schwartz, Department of Civil and Environmental Engineering

The ever-increasing density of urban environments poses new challenges to tunneling for transit projects. Tunneling methods are called for that meet these challenges while minimizing the impact on every day routines. With only a few exceptions, urban tunneling is confronted with soft ground conditions resulting from two basic facts. Historically, dwellings were established near rivers for reasons of logistics situating cities on alluvial deposits. In addition, tunnel alignments must be kept at shallow depths to optimize access and passenger circulation.

This dissertation analyzes implementation of a binocular tunnel underneath a historic building at low cover using ground freezing for tunnel pre-support and building underpinning. The shallow depth required tunneling through a large number of timber piles arranged in groups that serve as foundations for the steel frame, brick and masonry building. Tunneling was carried out using a sequenced excavation with shotcrete for tunnel support, commonly referred to as the New Austrian Tunneling Method (NATM). During the tunneling the building remained operational for its mainly commercial purpose. The analysis focuses on the performance of the building foundations, frozen

soil and tunnel opening. Observations from the construction-monitoring program are utilized in the development of a numerical model to study the performance of the support system consisting of timber piles, frozen soil and tunnel lining. Adfreeze strength that develops between the frozen soil and wooden piles provides a significant increase in shear capacity of the pile-frozen soil interface as compared with unfrozen conditions. The analyses suggest that the interconnect between frozen soil and pile is of such structural capacity as to allow for a substantial reduction of frozen soil thickness when compared to the one implemented on this project. This reduction provides for economies in freezing and in mitigation measures such as compensation systems for initial building heave and subsequent settlement due to freeze consolidation.

It is further suggested that ground freezing in combination with NATM tunneling offers a methodical concept for tunnel construction through vertical foundation elements. A thorough testing program for adfreeze strength must support its implementation, since adfreeze strength is the primary contribution to the capacity of the hybrid tunnel-frozen ground-pile support system.

CAPACITY OF FROZEN SOIL FOR SHALLOW TUNNEL PRE-SUPPORT UNDERNEATH A BUILDING FOUNDED ON WOODEN PILES

By

Vojtech Gall

Dissertation submitted to the Faculty of the Graduate School of the
University of Maryland, College Park, in partial fulfillment
of the requirements for the degree of
Doctor of Philosophy
2004

Advisory Committee:
Associate Professor Charles W. Schwartz, Chair
Professor Mohamed S. Aggour
Assistant Professor Ahmet H. Aydilek
Professor Deborah J. Goodings
Professor Sung W. Lee

Dedication

To my family

Acknowledgements

I would like to thank my advisor Dr. Charles Schwartz for all his support that he has given me during my studies under his guidance. In particular his dedication to my work throughout the past year is greatly appreciated. I also thank all dissertation committee members for their contribution and support.

This dissertation practically started in 1996 when the Massachusetts Bay Transportation Authority initially accepted the mined tunneling with ground freezing for the Russia Wharf complex in Boston. Soon it became apparent that the application was unique and the limits of proven tunnel engineering practice have been reached. To further the understanding more detailed analyses and further research into the principles involved were called for. Because the work presented builds on actual tunnel design and construction over a period of over eight years, many professionals representing owners, designers and contractors were involved whom I would like to acknowledge.

Foremost I would like to thank Messrs. David Ryan and Howard Haywood of the MBTA for their permission to utilize project information in my work and their strong support for innovation in tunneling. Dr.-Ing. Peter Jordan and Mr. Helmut Hass of CDM Jessberger shared their ground freezing expertise in many discussions. I would like to thank Dr. Gerhard Sauer and Mr. Franz Langer of the Dr. G. Sauer Corporation, Messrs. Hugh Lacy and Frank Arland of Mueser Rutledge Consulting Engineers, Dr. Marco Boscardin of Boscardin Consulting Engineers, and Ms. Katy Wood of GEI Consultants for their cooperation during the design and for providing monitoring data during tunnel construction. I would like to thank Messrs. Stephen DelGrosso and Thomas Hennings of

Modern Continental and Mr. Norbert Fuegenschuh of Beton und Monierbau for sharing construction-monitoring data and for the open discussions about the tunneling performance. In particular I would like to express my gratitude to my colleague of many years Dr. Kurt Zeidler for his time spent and the insight he provided to the many discussions evolving around the tunneling and research aspects associated with this dissertation.

Most importantly I would like to thank my family; my wife Gerda-Marie for her incredible support, my children Vojtech and Helen, with a promise not to miss their activities as I have in the past, my brother Dr. Martin Gall for his simple, but effective advise 'just do it,' my mother Milada Gall for encouraging me throughout the years, and my father Vojtech Gall for his guidance which made all this work possible.

Table of Contents

List of Tables

List of Figures

Chapter 1: Introduction

1.1 General

Tunneling beneath two buildings at Russia Wharf for the Massachusetts Bay Transit Authority's new South Piers Transitway in Boston called for different means of building underpinning. The tunneling was carried out using sequential excavation and shotcrete support methods in soft ground, commonly referred to as the New Austrian Tunneling Method (NATM). The buildings, which are founded on timber piles, remained in service during the tunneling operation. Thus, all underpinning systems have been designed to enable tunneling within permissible foundation deformations.

As shown in Figure 1.1, the tunnel structure traverses the Russia Wharf complex entering at the west corner (Congress Street/Atlantic Avenue intersection) and passes easterly toward Fort Point Channel. The Russia Wharf complex consists of three buildings, the Russia, Graphic Arts and Tufts building (Figure 1.2), of which the first two are affected by the tunnel construction. The investigation in this dissertation focuses on the Graphic Arts building.

Underneath the Russia building, frozen ground was used for tunnel pre-support purposes only. The underpinning was accomplished by a mini pile based permanent underpinning system. Underneath the Graphic Arts building on the contrary, ground freezing was used as the sole means of temporary building support as the tunnel excavation cut through the existing timber pile supports. The frozen soil encapsulated the timber piles and acted as a supporting structure for the building loads above until the cut-off piles were integrated into the tunnel lining. Following thawing of the frozen soil, the

tunnel double lining system, which includes a shotcrete initial lining and a reinforced shotcrete final lining, supports the wooden piles and serves as a large strip foundation. At the time of writing all tunneling and final lining installation has been completed and the thawing of the frozen soil is in progress. The combination of ground freezing for underpinning and pre-support together with NATM tunneling and the approach to cut off and re-integrate the timber pile supports into the tunnel liner constitute an innovative engineering solution which has not been implemented elsewhere to date.

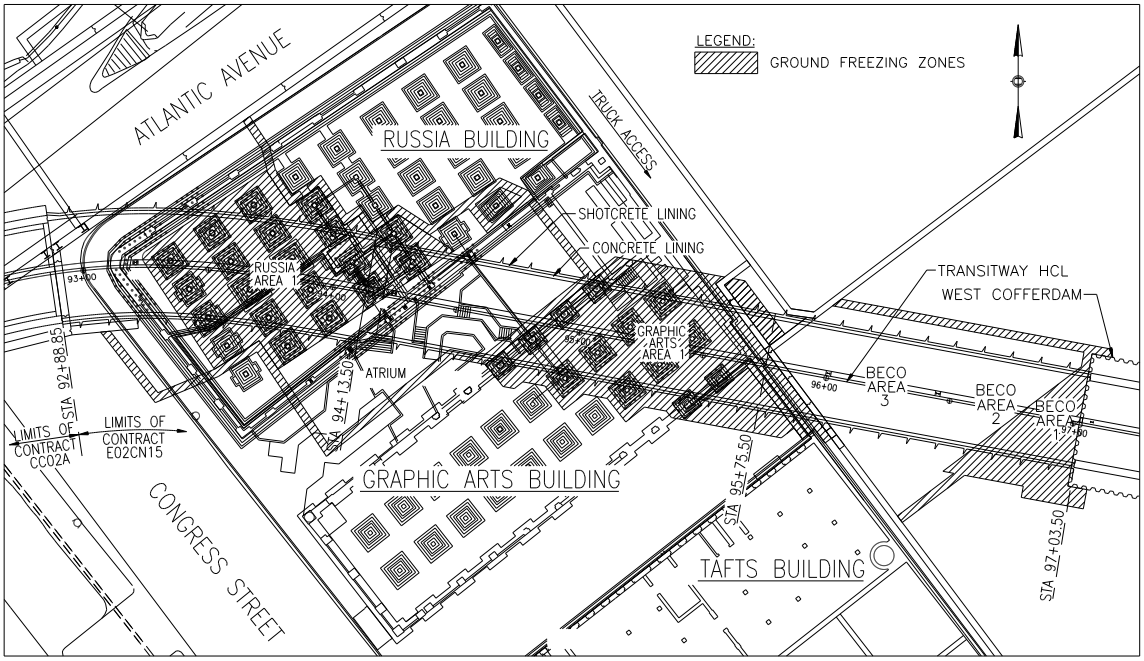

Figure 1.1: Tunnel Alignment Beneath Russia and Graphics Arts Building

The selected design imposes the least disruption to building tenants while maintaining significant economic, schedule and construction staging advantages. It replaced other, more traditional design solutions, for example one that relied on a large

scale steel girder underpinning system with construction of the tunnels by cut-and-cover methods, that would have resulted in the taking of several lower building floors during construction.

The acceptance of the ground freezing solution was based on a multi-phased review process of relevant case histories and the adaptation of engineering principles under the review of nationally and internationally renowned experts in the fields of geotechnical engineering, tunneling, underpinning, and ground freezing.

Figure 1.2: Russia Wharf Complex with Graphic Arts Building in the Middle and Russia Building to the Right

1.2 Ground Freezing for Tunneling and Underpinning

Ground freezing is an established geotechnical engineering method for tunneling and shaft sinking in difficult ground conditions (Jessberger, 1981). However, it is often considered the last resort, primarily because of the high cost involved. To establish a frozen soil body, a cooling agent, supplied by a refrigerating plant must be circulated through freezing pipes to extract heat energy from the ground. The ground freezing method, in combination with NATM tunneling has been successfully applied on several urban transit projects in soft soils, particularly in Europe (Germany, Switzerland, and Austria) and has been used for temporary building support during tunneling underneath. Two European projects supported the ground freezing concept proposed for Russia Wharf in particular: At the Oberbilker Markt, Metro Düsseldorf, Germany (Jessberger and Partner, 1996) and Vivenotgasse, Metro Vienna, Austria (Deix and Braun, 1988) settlement sensitive buildings were underpinned with frozen ground to facilitate tunnel construction. In both cases, tunneling was carried out with minimum clearance between the tunnel roof and the building foundations, and the buildings remained in operation during the ground freezing and tunnel construction process. Though using different freezing configurations, these and other case histories yielded valuable information for the development of the concepts at Russia Wharf. For example, the experience at the Milchbuck Tunnel project, Zurich, Switzerland (Schmid, 1981) suggested use of the so-called 'intermittent freezing' method to reduce excessive heave during the ground freezing period.

The proposed underpinning system for the Graphic Arts building, the focus of the present study, consists in principle of a multi-staged load transfer process of:

- Integration of the timber pile foundation into a frozen soil body, which temporarily supports the pile caps on which the building steel columns rest,
- Cutting off the timber piles during tunneling and founding their ends on the tunnel lining for permanent support, once the soil body is thawed,
- Permanent foundation support provided by the tunnel tube, which acts as a large-scale strip foundation.

This system constitutes a unique concept in the multi-functionality that is assigned to the frozen soil. Figure 1.3 shows a hybrid configuration of frozen ground extent, cut-off and integrated piles into the shotcrete lining.

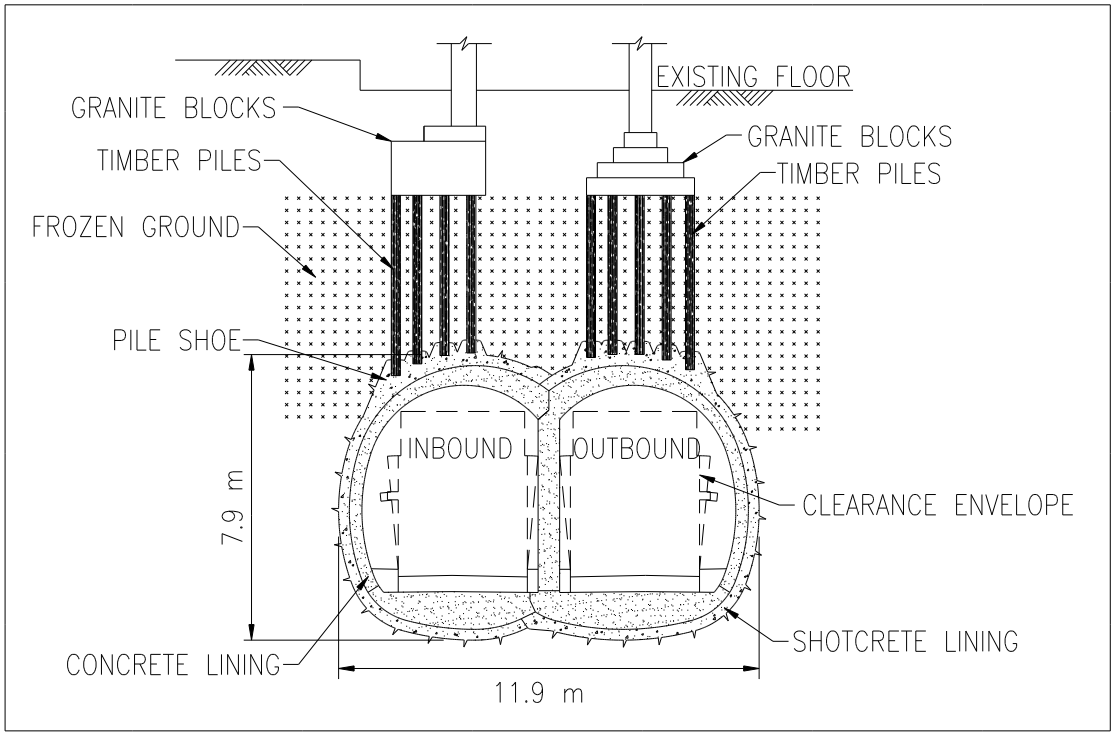

Figure 1.3: Underpinning of Graphic Arts Building (Frozen Ground Shown)

1.3 Purpose of This Investigation

The ground freezing concept at the Graphic Arts building is based on generally accepted tunneling, ground freezing, and geotechnical engineering principles and is backed by a review of relevant case histories. The prediction of the behavior of the soil mass during tunneling was based on numerical modeling. The accuracy of this numerical modeling depends on many factors, and in particular on assumptions such as material properties for input, constitutive material models, geometric modeling, etc. Often, the numerical modeling is used to predict behavior tendencies only rather than provide estimates of ground movements and stresses. Because of these facts, the final design must include a large degree of conservatism to ensure safety.

The concept implemented at the Graphic Arts building for the underpinning by frozen ground was based on the assumption that the frozen soil extends completely to the granite pile caps and that these are thus supported by the frozen soil mass during tunneling. An alternative approach is to create a limited frozen soil zone around the tunnel perimeter and to rely on a pile-frozen body interaction for support. A schematic of this alternate approach is shown in Figure 1.4. Although initially considered for the project, this alternate concept did not offer a sufficient degree of conservatism, as it would rely on a thinner frozen soil body and introduce another unknown, or at least difficult to describe, structural interaction between the piles and the frozen soil. It is, however, more economic due to the smaller volume of frozen soil. It also alleviates to a greater extent any surface heave phenomena associated with soil freezing.

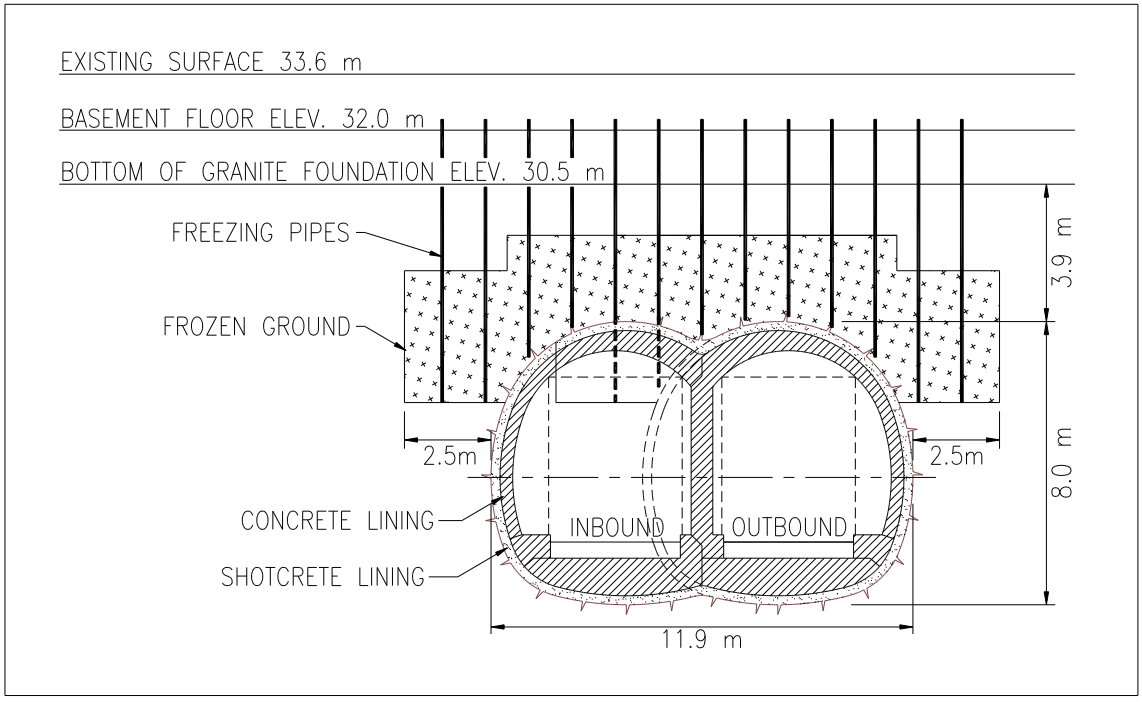

Figure 1.4: Alternate Arrangement of Frozen Arch for Underpinning

The actual design used for the Graphic Arts building (Figure 1.3) is based on a relatively massive frozen soil body in vertical extent. While from an engineering and risk analysis point of view the additional cost for an additional frozen soil volume is justified, the question arises as to the limits to the required thickness. At the Russia building, in contrast to the initially proposed concept, the final design abandoned the frozen soil for the purpose of underpinning because it was viewed too thin. Instead, a permanent underpinning by mini piles was implemented.

More precise determination of the required frozen soil thickness and extent as well as its function as an underpinning element (in combination with embedded pile supports) can only be achieved through a more fundamental understanding of the frozen

ground behavior during tunneling and the subsequent load transfer process. In particular understanding of the frozen soil-pile interaction is important.

The work presented herein analyses the interaction between the frozen soil and the wooden piles using finite element (FE) modeling. The calculations take into consideration the staged excavation of the NATM tunneling and lining installation process thus simulating the complex frozen soil-pile-tunnel lining support system. The calculations consider construction monitoring data collected during the tunneling and field observations related to the tunneling process and piles encountered. This information is used to verify assumptions and calibrate the numerical model for in-situ conditions. The model verification utilizes the frozen ground extent according to the engineering design. Subsequently, the frozen soil extent is reduced and a methodological approach is developed for the investigation and acceptance of a thinner frozen soil layer. The calculation techniques developed, in particular for the representation of the wooden pile-frozen soil interface along with the methodological investigation of frozen soil requirements offer a novel tool for tunnel designs under similar conditions. The findings further suggest utilizing the wooden piles as active support members for the buildings during NATM tunneling. This new concept and the procedures developed to investigate frozen soil requirements will benefit urban tunneling in many aspects. The concept provides economy. It further offers a new flexibility in tunneling when encountering pile or other vertical supports within the tunnel alignment. Finally, the methodology developed may be readily adopted by tunnel engineers for the planning and design of tunnels in urban, difficult ground conditions.

The description of the work in this dissertation is organized as follows:

Chapter 1 introduces the problem statement and derives the benefits of the proposed concept.

Chapter 2 reviews a selected number of case histories where soil freezing in combination with underground construction has been applied. While these case histories greatly supported the development of ground freezing with NATM tunneling at Russia Wharf, they also demonstrate the uniqueness of the tunneling carried out at the Graphic Arts building. The information collected from these case histories is used in later chapters when analyzing surface heave.

Chapter 3 examines frozen soil in terms of its constitutive behavior and summarizes frozen soil and pile testing performed for the ground freezing at Russia Wharf. It further proposes adfreeze strength values derived from a broad literature review. Adfreeze strength is a major contributing factor in the proposed concept as it supplies the strength of the frozen soil-pile interface.

Chapter 4 summarizes project soil characteristics and design elements. The ground freezing and NATM tunnel design is described. The chapter also reports on the geotechnical, tunnel, ground freezing and building related instrumentation and monitoring utilized.

Chapter 5 describes the finite element modeling and assumptions made for the simulation of the tunneling process and materials and their behavior involved. A simplified, three-dimensional FE model was used for the derivation of a softening factor

(S) to be used in two-dimensional FE modeling as a representation of the three-dimensional state of stress at the tunnel heading.

Chapter 6 develops a refined two-dimensional FE model and implements the wooden piles as part of the modeling. The interface between piles and frozen soil is represented using interface elements with a Mohr-Coulomb failure criterion. Observed surface heave associated with freezing and subsequent surface settlements as a result of the tunneling is analyzed in detail. Observed frozen soil temperatures throughout the freezing and tunneling period are evaluated. The FE model is verified for field conditions and calibrated to represent deformations observed in-situ. The calibration involves reduction of the modulus of elasticity of frozen soil to account for creep.

Chapter 7 utilizes the verified two-dimensional FE model to systematically vary frozen soil thickness and adfreeze strength values. Variations are implemented for the tunnel excavation stages as carried out in the field. Acceptance criteria are developed to determine minimum frozen soil requirements. These are based on engineering principles and appraise the load carrying capacity of the pile-frozen soil interface, pile strength, strength of the frozen soil, and the tunnel lining capacity. A hybrid, frozen soil-pile-NATM tunnel support system is suggested. The frozen soil extent may be as thin as 1.2 m above the tunnel roof provided minimum adfreeze strength is developed in the pile-frozen soil interface.

Chapter 8 lays out the benefits of the proposed concept for the tunneling industry, in particular in urban settings:

- A thinner frozen soil offers greater economy directly, by reducing installation and freezing costs, and indirectly by reducing heave mitigation measures.
- Frozen soil can be used systematically for the temporary arrest of vertical support members while tunneling underneath and through them. This may occur at shallow, or deep tunneling horizons and for single supports or pile groups. This offers a significant flexibility for tunneling in urban areas where vertical foundations are present.
- The calculation methods presented offer a systematic approach for tunnel designers for the planning and investigation of tunneling applications where frozen soil is to be used for underpinning in association with existing, vertical support members.

Chapter 2: Tunneling Case Histories Using Frozen Soils As Pre-Support

2.1General

The use of ground freezing as a means to improve the soil strength properties in geotechnical applications is generally thought of as the last resort for ground improvement. This is primarily because of the high cost involved with the ground freezing operation. However, the cost disadvantage of ground freezing operations diminishes very quickly when other project constraints are considered. For example, the use of ground freezing for soil stabilization to tunnel underneath railroad tracks or buildings under shallow cover may make a project economically feasible because of the savings that are achieved by non-disruption of services. As described earlier, ground freezing with shotcrete supported tunneling permitted continuous usage of the buildings at Russia Wharf throughout the tunnel construction period. Furthermore the building repair needs were minimal when compared to other alternatives considered.

The prospect of these benefits led to the consideration of ground freezing and shotcrete supported tunneling for the Russia Wharf project. Although the individual elements of the concept, namely ground freezing, NATM tunneling in soft ground, and use of freezing for both tunneling pre-support and building underpinning had been utilized elsewhere before, the particular combination of those methods was novel. In particular, the use of ground freezing as the sole means of building underpinning while the supporting timber piles were cut and subsequently integrated into the tunnel lining shell for permanent support was a unique solution.

To demonstrate the engineering feasibility of the proposed concept a review of case histories of relevant projects including ground freezing and tunneling beneath sensitive structures was carried out (Gall, *et al*., 2000). The study collected and evaluated data on well over twenty-five international projects (Dr. G. Sauer Corporation, 1996). The criteria under which the screened projects would qualify as relevant case histories included the following:

- The tunnel passes underneath sensitive structures, preferably buildings,
- The sensitive structures remain in operation during construction beneath,
- Ground conditions are characterized by soft soils with high ground water level,
- Ground freezing has been utilized for soil stabilization to:
    - Increase stand-up time, and
    - Underpin the above lying structures.

The collected data and experience gained were also evaluated to support the development of engineering details for the tunneling and ground freezing design at Russia Wharf including:

- Magnitude of subsurface and surface deformations as related to:
    - Frost heave,
    - Settlements associated with consolidation as a result of the thawing process, and
    - Deformation as related to the excavation and support process,
- Geotechnical parameters needed for the structural computations for frozen soils.

2.2 Case Histories

The following table summarizes 17 selected tunnel case histories with direct relevance to the project based on the criteria detailed above. The summary indicates project name, location and general date of construction, tunnel size and length and the type of ground freezing used. The first column of the table assigns a project number and project details given in individual project tables, one for each project are contained in the Appendix.

Table 2.1: Summary of Tunnel Case Histories Using Frozen Soils as Pre-support and/or Underpinning

Project No.	Project Name	Location / Date	Tunnel Cross Section A [m^2], Diameter [m]	Tunnel Length	Type of Freezing
USA					
1	Syracuse Tunnel	Syracuse, New York 1980	3.0 m	36.6 m	cooled brine
2	Heights-Hilltop Interceptor Sewer Tunnel	Cleveland, Ohio 1987	4.6 m	42.7 m	cooled brine
3	Naval Research Lab - Large Acoustic Tank	Washington, DC 1989	19.5 m	depth 16.8 m	cooled brine
Germany					
4	Urban Rapid Transit Rail Stuttgart Contract Section 12	Stuttgart 1974-78	50 to 162 m^2	505 m	cooled brine

Project No.	Project Name	Location / Date	Tunnel Cross Section A [m^2], Diameter [m]	Tunnel Length	Type of Freezing
5	Sewage Collector - Center, Düsseldorf	Düsseldorf 1978	5.2 to 6.3 m	115 m	cooled brine
6	Metro Frankfurt am Main Crossing under the River Main Contract Section 81	Frankfurt a. Main 1976-81	2 x 38.5 m^2	2x193 m	cooled brine
7	Metro Nuremberg Contract Section 258/1.3	Nuremberg 1984	5.6 m	11 m	liquid Nitro-gen
8	Urban Rail System Hannover Contract Section C23	Hannover 1988-91	37.4 to 55.4 m^2	251 m	cooled brine
9	Fahrlach Highway Tunnel Mannheim	Mannheim 1989-92	2 x 100 m^2	184 m	cooled brine
10	Urban Railroad Mühlheim a. d. Ruhr Contract Section 8	Mühlheim a. d. Ruhr 1991-92	38 to 65 m^2	30 m	liquid Nitro-gen
11	Metro Düsseldorf Contract Section 3.4 H	Düsseldorf 1991-93	96 m^2	3 x 40 m	cooled brine
12	Metro Düsseldorf Contract Section - Oberbilker Markt	Düsseldorf 1995-98	60 m^2	38 m	cooled brine
Switzerland					
13	Milchbuck Road Tunnel	Zürich 1978-84	145 to 195 m^2	350 m	cooled brine

Project No.	Project Name	Location / Date	Tunnel Cross Section A [m^2], Diameter [m]	Tunnel Length	Type of Freezing
14	Station Quay / Limmat Contract Section 2.04 Neumühle Quay / Publicitas Contract Section 4.03	Zürich 1987	13.50 to 10.50 m 2 x 7.65 to 9.30 m	80 m & 40 m	cooled brine
Austria					
15	Metro Vienna Contract Section U6/3 Vivenotgasse	Vienna 1985-87	2 x 34 m^2	60/64 m	liquid Nitro-gen
16	Metro Vienna Contract Section U3/10	Vienna 1987	6.60 - 8.60 m	70 m	liquid Nitro-gen
Italy					
17	Santa Lucia Tunnel	Salerno 1973	85 m^2	71 m	cooled brine

2.3 Proposed Concept

The review of the case histories indicated that the use of the ground freezing and NATM for tunneling at Russia Wharf appeared to be a feasible concept. Development of a tunnel cross section and the concept for the ground freezing, in particular the installation of the freeze pipes for the establishment of the frozen soil zone, was carried out considering site specific limitations:

- Cross section

The relatively shallow alignment and the need to incorporate a twin vehicle clearance envelope, which requires a wide footprint, prohibited the use of a single cross section to accommodate a single tunnel tube. Such a cross section, carried out as a rounded profile would result in a roof too high for project constraints. Therefore, a twin bore binocular tunnel arrangement was chosen for the tunnel cross section. There is a significant additional benefit of this arrangement in that the excavation sizes are kept relatively small in the sequential top heading and bench/invert excavation approach.

- Freeze pipe installation

In principle, freeze pipes can be installed vertically or sub vertically from the surface or horizontally from access points such as shafts and pipes located close to the theoretical excavation perimeter. The spatial difficulties at the project site did not favor the installation of temporary shafts for freeze pipe installation. The installation of horizontal freeze pipes would have furthermore required drilling through a dense arrangement of vertical wooden piles. Using standard, one drill per freeze pipe arrangement, this was viewed as a very difficult and inaccurate freeze pipe installation procedure. An alternative was to use micro tunneling techniques having bore diameters in the range of 1 meter with subsequent installation of freeze pipe bundles within the micro tunneled bores arranged around the tunnel perimeter and above the springline. However this alternative was viewed as cost prohibitive.

Although the basement space beneath the buildings provides for only limited vertical space for vertical drilling equipment, it was viewed sufficient for the installation of vertical freeze pipes. The major advantage of vertical pipe installation is increased placement accuracy and the capability to install pipes parallel to existing wooden timber piles with, in general, no interference. Therefore, the vertical pipe installation was chosen for soil freezing.

Preliminary frozen soil computations indicated the need for a frozen soil arch above the tunnel crown as shown in Figure 2.1 below. This Figure also depicts the typical binocular tunnel cross section. A longitudinal section is displayed in Figure 2.2. The configuration shown established the basis for the tunnel and ground freezing design at Russia Wharf. The proposal aimed at the use of ground freezing as the sole means of building underpinning for the Graphic Arts building.

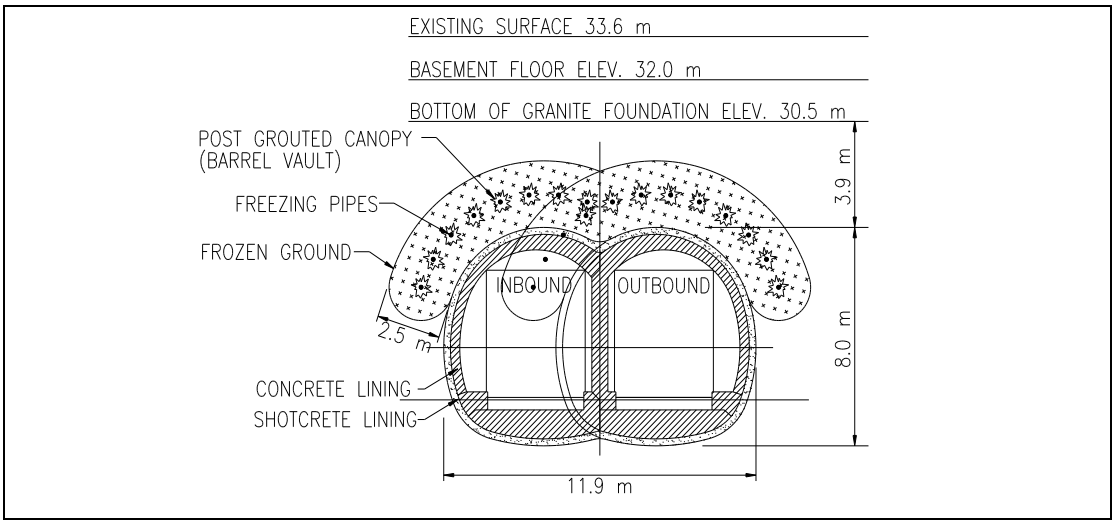

Figure 2.1: Typical Tunnel Cross Section and Frozen Arch

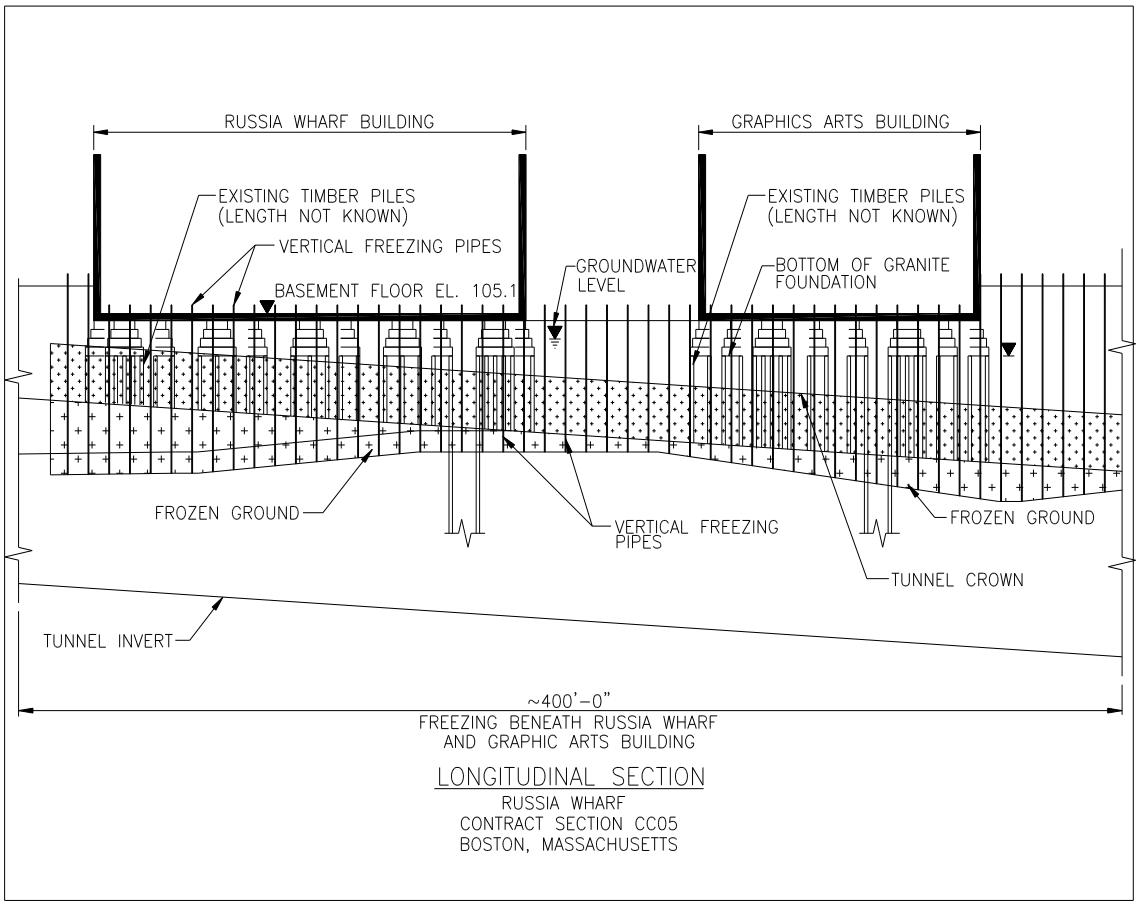

Figure 2.2: Longitudinal Section for Ground Freezing as Sole Means for Underpinning at Russia Wharf

Chapter 3: Strength of Frozen Soils and Behavior of Piles in Frozen Ground

3.1 General

Frozen soil is used for tunnel pre-support and building underpinning at the Graphic Arts building. Thus, its behavior as a structural member is of importance. This chapter examines the behavior of frozen soils and factors that influence its strength and provides a basis for detailed assessments discussed in later chapters. Further, the load carrying behavior of wooden piles embedded in frozen soil is reviewed.

Frozen soil is a composite that consists of four different components: solids (soil particles which may be of mineral or organic nature), unfrozen water, ice, and gases (Andersland and Ladanyi, 1994). There are two types of unfrozen water present in soils: the strongly and weakly bound water. The strongly bound water may resist freezing down to very low temperatures. Frozen water, which fills the pores is only of one type (normal hexagonal ice of type 1h). Despite the amount of unfrozen water when frozen water fills the majority of the void space the mechanical behavior of frozen soil strongly resembles that one of ice.

Ting, Martin, and Ladd (1983) concluded that the shear behavior of frozen sands is controlled essentially by the four following mechanisms: (1) pore ice strength, (2) strength of the soil skeleton, (3) increase in the effective stress due to the adhesive ice bonds resisting dilatation during shear of a dense soil, and (4) synergestic strengthening effects between the soil and ice matrix preventing the collapse of the soil skeleton. From this postulation, failure mechanisms can be derived and models developed. Other characteristics and conditions such as ice content, temperature, soil density, etc. will

govern the behavior in detail. For example, in high particle concentration soils the soil strength will be governed by soil particle interaction rather than ice strength.

Many researchers have studied the behavior of frozen soils and the many factors that influence its strength, deformation and creep behavior. Andersland and Ladanyi (1994) provide an overview of these factors and describe the behavior of the various types of frozen soils and compositions as a function of applied stress and strain, both constant and variable, the impact of the temperature, expansion (segregation potential) over time, and even the effect of salinity content on the behavior of the frozen soil.

The composition of the soils at the project site was well studied and described. Tests were performed on the frozen soils to study their elastic properties and their uniaxial compressive strength and creep behavior, characteristics that are of importance when evaluating the behavior of the frozen soil. A summary of these tests is provided below preceded by a general discussion of the creep behavior of frozen soils. Based on the test data obtained, creep functions for the soils at the Russia Wharf project have been derived. The general discussion of creep along with the empirical creep equations for the site soils shall aid in the incorporation of creep in back-calculations of observed deformations. A discussion of the expansion-inducing segregation potential is also provided. Although tests have not been performed to determine the segregation potential values for the project soils, literature references (Deix, 1992) are used to estimate its value and compute the observed heave. Thus a comparison can be made between estimated and observed surface heave at selected locations.

3.2 Creep Behavior

A schematic description of creep behavior of frozen soils is presented in Figure 3.1, which also demonstrates the influence of the applied uniaxial stress σ on the creep rate (Jessberger, 1981). Figure 3.2 shows several measured creep curves of frozen cohesive soils after Vyalov (1962) and Sayles (1968) as examples at temperature values of –10 °C (close to project conditions as will be described later). Figures 3.1 and 3.2 demonstrate that the creep rate is dependent on stress level and the soil type. Similarly, temperature dependence can be demonstrated (Jessberger, 1981). This indicates that it is important to investigate each individual soil under expected temperatures and stress regimes to find the appropriate creep behavior.

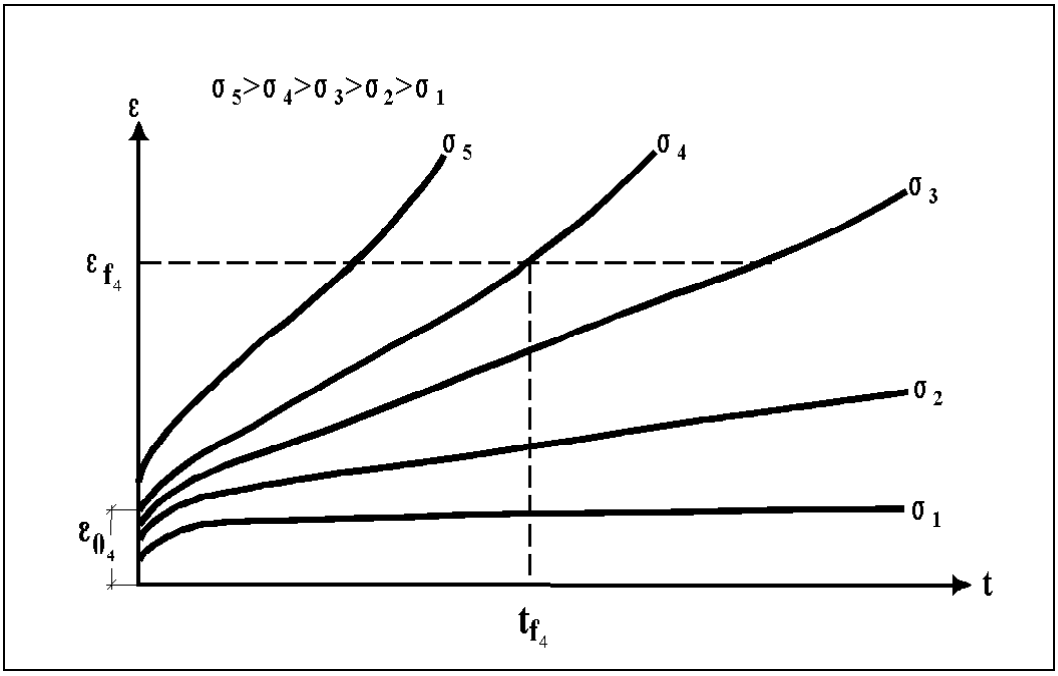

Figure 3.1: Schematic Creep Curves of Frozen Soils (after Jessberger, 1981)

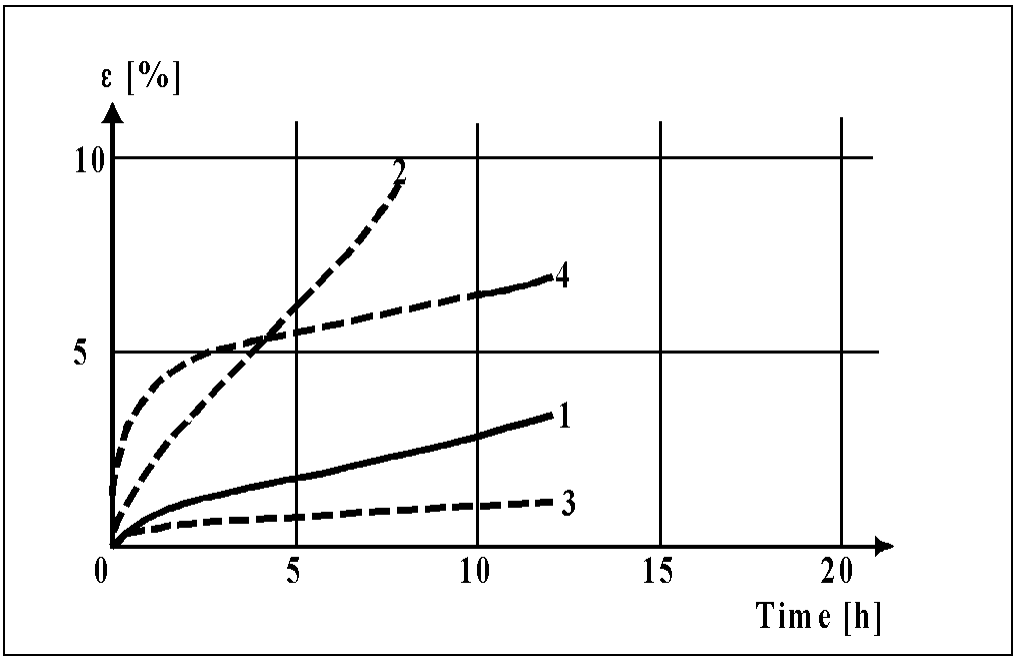

Curve	Soil	σ_1 (N/mm^2)	T (°C)
1	Bat-Baioss Clay	2.0	-10.0
2		3.0	-10.0
3	Callovian Sandy Loam	2.0	-10.0
4		3.0	-10.0

Figure 3.2: Creep Curves for Cohesive Soils (After Vyalov, 1962 and Sayles, 1968)

Creep behavior is typically described using empirical relations (Vyalov, 1962 and Ladanyi, 1972). There is similarity of creep characteristics between soils and metals, which have been studied extensively in the past. However, the creep behavior of metals is typically measured from constant uniaxial tensile stress tests at high temperatures while for geotechnical materials the creep of frozen soils under compression at low temperatures is of interest.

The uniaxial creep curve is often the reference state that is characterized by suitable empirical creep functions. In particular for design purposes, it is useful to have a

simple creep relationship with only a few material parameters present derived from laboratory testing. The total strain (Figure 3.3) consists of an elastic instantaneous part and a plastic creep part expressed as follows:

$$\varepsilon = \varepsilon_0^e + \varepsilon^p \tag{3.1}$$

$$\varepsilon = \varepsilon_0^e + \varepsilon_1^c + \varepsilon_2^c + \varepsilon_3^c \tag{3.2}$$

where:

ε_0^e = instantaneous strain;
ε_1^c = creep strain in the primary stage (Phase I in Figure 3.3);
ε_2^c = creep strain in the secondary stage (Phase II in Figure 3.3);
ε_3^c = creep strain in the tertiary stage (Phase III in Figure 3.3);

The tertiary stage ultimately leads to instability and failure; it is neglected in the following, theoretical study. Neglecting the third stage is admissible for the purpose of this study as the shotcrete initial lining will be installed immediately following excavation of each short (2'-6") advance of the top heading. It is anticipated that due to the short unsupported span failure of the frozen soil mass due to creep does not occur. For conditions of non-increasing creep strain rate the primary and secondary stages maybe combined and one can refer to the creep function after Vyalov as follows:

$$\varepsilon = \varepsilon_0^c + (\varepsilon_1^c + \varepsilon_2^c) = \frac{\sigma}{E_0} + A\sigma^B t^C, \quad (\sigma = \text{constant}) \tag{3.3}$$

where:

E_0 = initial Young's modulus, and
A, B, C = material parameters.

Vyalov describes creep by a power law function with C<1, which is of a damped nature.

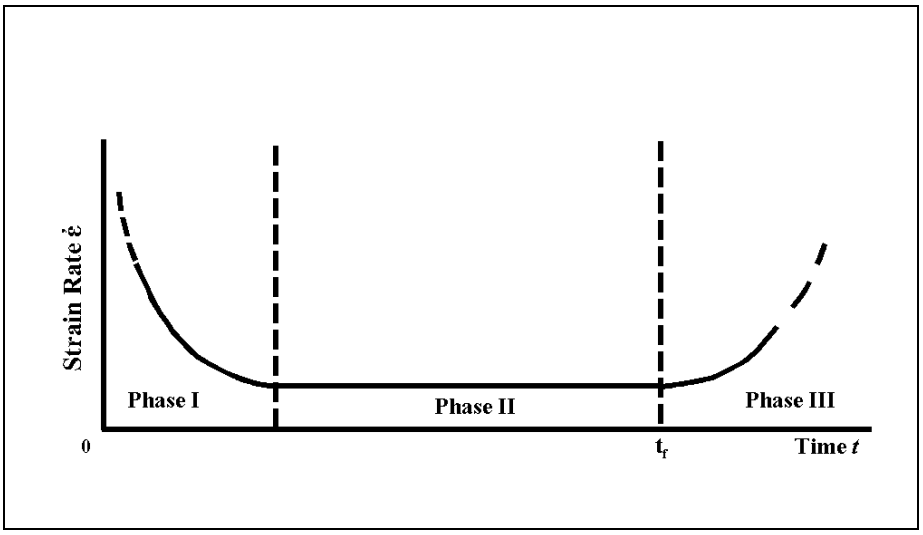

(a)

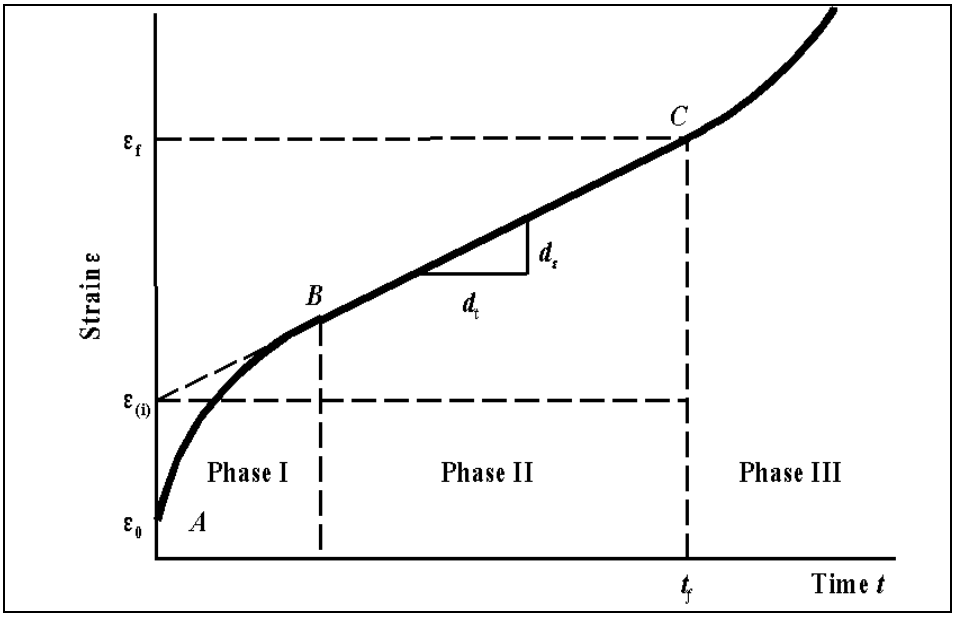

(b)

Figure 3.3: Idealized Creep Curves, (a) Basic Creep Curve, (b) Strain Rate vs. Time (After Klein and Jessberger, 1979)

Odquist and Hult (1962) proposed an idealization of creep in the form of a pseudo-instantaneous strain, where the strain at t=0 contains instantaneous elastic strain ε_0^e as well as damped plastic strain increments ε_0^c:

$$\varepsilon = (\varepsilon_0^e + \varepsilon_0^c) + \varepsilon_2^c = (\frac{\sigma}{E_0} + A_0\sigma^{B_0}) + \bar{A}\sigma^B t^C, \qquad (C=1,\ \sigma = \text{constant}). \qquad (3.4)$$

Equation (3.4) may generally be selected for the description of creep behavior of frozen soils at the project site with determination of the material parameters from creep tests as described later in this Chapter. This creep equation is used for an approximation of creep behavior in connection with the excavation and support of the tunnels at Russia Wharf.

3.3 Segregation Potential

Due to the temperature gradient established as part of the freezing process water will be transported to the colder sections of the soils. Once the temperature falls below the freezing point a portion of the pore water will be frozen. Because of their composition the site soils are considered to be susceptible to frost heave. In such soils a suction occurs at the freezing front that causes a transport of water to the ice front and a creation of an ice lens which in turn causes an expansion of the ice in direction of the temperature gradient. Konrad and Morgenstern (Andersland, 1994) analyzed a thin section of partially frozen soil between the ice lens and the unfrozen soil in which a water intake flux v_0 occurs. A proportionality between the water intake flux and the

temperature gradient within this frozen fringe exists and has been termed the segregation potential SP as follows:

$$v_0 = SP \cdot gradT \tag{3.5}$$

The segregation potential may be considered as an index property of a soil that uniquely characterizes its frost-heave susceptibility. Consequently it may be used to determine the frost heave of a given soil in a freezing application. The magnitude of heave and thereby the segregation potential will be qualitatively a function of the following factors:

- Soil characteristics:

  Gradation, specific surface volume, clay mineral content, water content, density, thermal conductivity, and

- Other factors:

  Water supply (hydraulic conductivity), rate of heat extraction, and external loading (overburden pressure).

For the description of the heave associated with the freezing operation the segregation potential can be rewritten as (Deix, 1992):

$$SP = \frac{\dot{h}}{grad\ T} \tag{3.6}$$

where:

$\dot{h}$ = heave rate (mm/s), and

grad T = temperature gradient in the soil (°C /mm).

The total amount of frost heave can then be determined for the frozen soil as follows:

$$h(t) = d(t) \cdot n \cdot F + SP \int_0^{t_1} gradT(t_1) d\,t_1 + SP \cdot gradT(t - t_1) \qquad (3.7)$$

where:

h(t)	=	frost heave,
d(t)	=	frozen soil thickness,
n	=	void ratio,
F	=	(0 … 0.09),
grad T (t_1)	=	temperature gradient at the frozen soil boundary during the initial freezing period (establishing the frost body),
grad T	=	temperature gradient at the frozen soil boundary during maintenance freezing period,
t_1	=	time duration of initial freezing period, and
t	=	time duration for total freezing period.

The first expression in Eq. (3.7) represents the frost heave associated with the volume increase due to freezing, with F depending on the type of soil and the overburden thickness. The second expression refers to the development of the ice lens during establishment of the frozen soil body during which the temperature gradient is generally time dependent. The third expression describes the frost heave due to ice lens development during the maintenance period. Equation 3.7 assumes that the frozen soil body is located beneath the ground water table and that water is continually supplied. The segregation potential is evaluated in later chapters based on literature (Deix, 1992) to validate the order of magnitude of surface heave associated with the freezing.

The direction of frost expansion is also important. The expansion of the frozen soil in the horizontal direction will lead to an ‘interlocking’ effect between the soil and

the piles within the soil. This is in particular true in the Russia Wharf project, because the temperature gradient from the vertical freeze pipes will be in horizontal direction which will enhance the 'lock-in' effect. For the purpose of this work pressure exerted onto the piles in the horizontal direction is not considered in detail. The interlocking effect is described solely by the cohesive phenomenon termed 'adfreeze.' The neglect of frictional interface resistance is justified because it is only mobilized in the granular fill stratum and not in the cohesive Organic and Marine Clays. Therefore a conservative assumption for pile resistance is provided by relying on the adfreeze strength only.

3.4 Laboratory Testing of Frozen Soils

3.4.1 General

A series of frozen soil tests was performed by the University of Alberta in Edmonton, Canada to provide frozen soil properties for the design and evaluation of the frozen ground for underpinning at the Russia Wharf building complex. These frozen soil tests were performed on undisturbed tube samples of Fill, Organic Clay, Peat and Marine Clay from the site (See Figure 4.1 for a subsurface geological profile of the Russia Wharf site). Seven borings were taken from the site within the tunnel alignment and beneath the Russia and Graphic Arts buildings (Mueser Rutledge Consulting Engineers, 1998). From these seven borings a total of twenty-one samples were prepared for testing. Nine of the samples were Marine Clay, six were Organic Clay, two were Peat and four were Fill.

The frozen soil test program consisted of twelve unconfined compression tests, four creep strength tests, three unfrozen water contents tests, six thermal conductivity

tests, and two freeze thaw tests. Only the results from the unconfined compression tests and creep tests are given here as they relate directly to the strength behavior of the frozen soil mass. The results of the water content test are reported here because the amount of frozen water content affects the soil behavior under load. The other tests are relevant primarily to the layout of the freezing system and to assess the potential soil settlement upon the thawing.

3.4.2 Unconfined Compression Tests

The results of the unconfined compression tests are summarized in Table 3.1. The twelve samples were tested at nominal temperatures of -5, -10, and -15 °C to evaluate the influence of temperature on strength. All the samples were loaded at a constant strain rate of 1% per minute, and the load and displacements were recorded digitally using load cells and displacement transducers connected to a data logging system. The samples were loaded to failure in less than 20 minutes. Details of the stress testing are available in the relevant Mueser Rutledge Consulting Engineers, 1998 report. The Marine Clay samples exhibited a large stress reduction after failure. The ratio between the peak stress and the residual stress generally increased with decreasing temperature, and the strain at failure decreased. The Organic Clay, Peat and Fill samples generally exhibited small changes in stress above 2% strain (Figure 3.4). For many of the samples the stress continued to rise with increasing strain. Others displayed a small reduction after failure, particularly at the coldest temperatures.

Figure 3.5 plots unconfined compressive strength vs. sample temperature. The Organic Clay and Peat samples show a comparable strength and therefore a combined regression curve is displayed in the Figure. The short-term compressive strengths q of the Marine Clay, Fill, and the Organic Clay/Peat at -10 °C are 3.5 MPa, 2.4 MPa, and 2.0 MPa respectively. In Figure 3.5 and also 3.4 the reporting concentrates on a temperature of around –10 °C because the frozen soil freezing design concentrated on this general temperature level.

Table 3.1: Unconfined Compressive Tests - Summary of Results

Soil Type	Boring No.	Sample No.	Sample Elev. (ft)	Water Content (%)		Temp (°C)	Compr. Strength (MPa)	Strain at Failure (%)
				Initial Avg.	Final			
Marine Clay	RW-2	UF-5	85.7	29.2	28.3	-4.5	1.72	11.5
	RW-5	UF-7	81.1	19.8	23.5	-9.5	4.39	6.7
	RW-2	UF-7	80.4	36.4	35.4	-10.4	2.94	3.8
	RW-4	UO-10	76.3	34.6	34.8	-14.8	4.87	9.7
Organic Clay	RW-4	UO-4	92.9	70.2	46.3	-9.3	1.37	14.0
	RW-2	UO-3	91.9	55.5	70.1	-10.0	1.97	11.0
	RW-6	UO-1	93.2	33.2	30.4	-10.0	2.39	20.0
Peat	RW-3A	UO-5	89.6	346.7	330.2	-5.0	0.72	17.7
	RW-3A	UO-5	89.6	214.3	312.5	-14.8	3.51	12.3
	RW-4	UF-5	88.9	399.1	306.2	-9.8	1.60	19.7
Fill	RW-3A	UF-2	99.5	18.9	19.1	-10.2	2.45	19.2
	RW-5	UF-4	95.6	32.4	32.5	-15.6	4.51	3.8

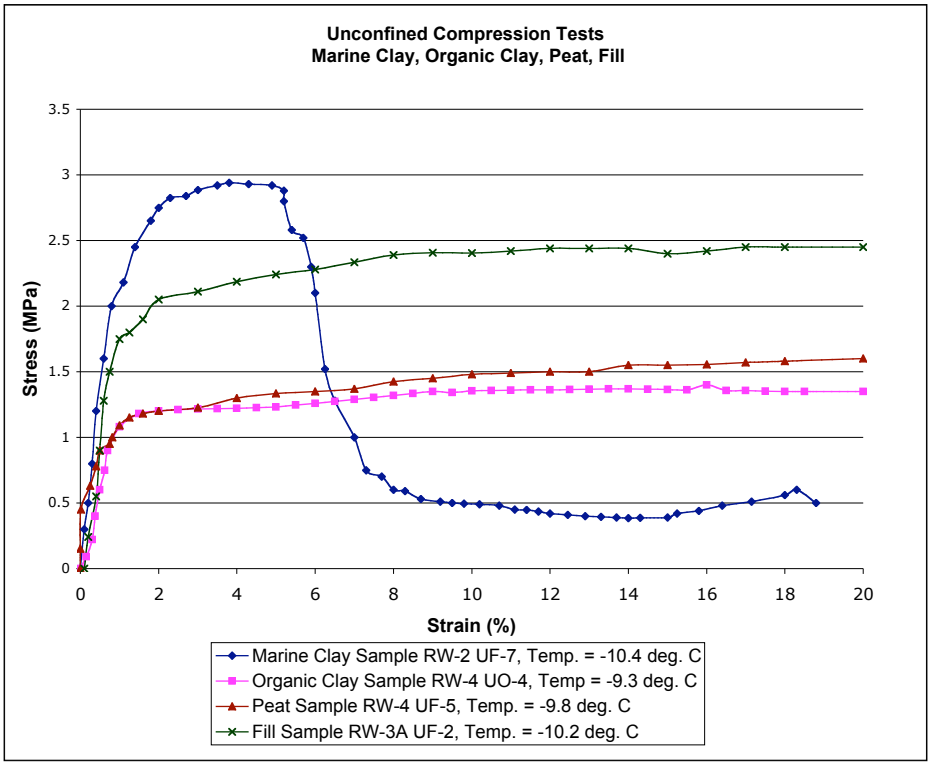

Figure 3.4: Unconfined Compression Tests - Marine Clay, Organic Clay, Peat and Fill

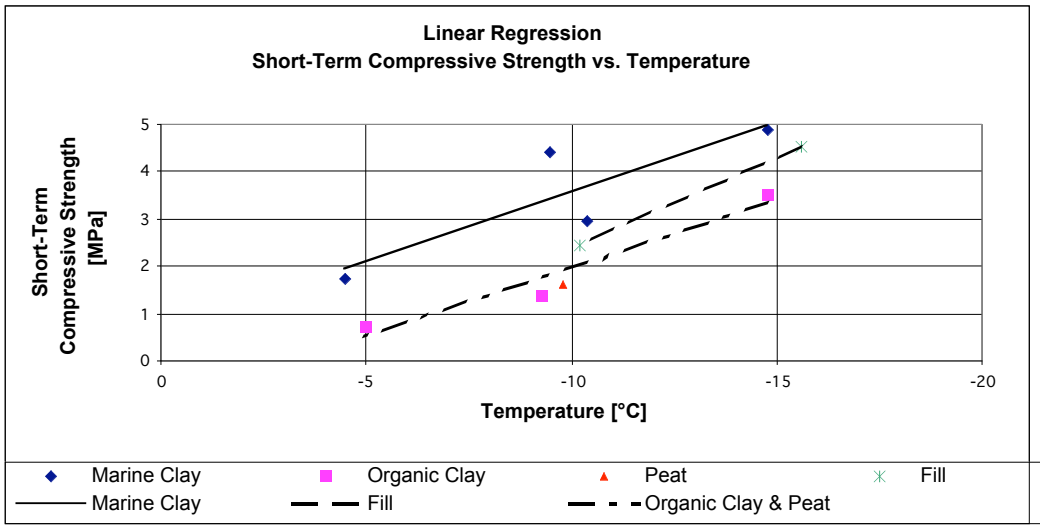

Figure 3.5: Unconfined Compressive Strength vs. Selected Temperature

3.4.3 Creep Tests

A total of four creep tests were performed, two on Marine Clay and two on Organic Clay. These tests follow the testing procedure as called for by ASTM D5520-94 'Standard Test Method for Laboratory Determination of Creep Properties of Frozen Soil Samples by Uniaxial Compression.' All creep tests were performed at a temperature of about -10 °C. Two types of tests were performed for the two soil types. Single-stage tests were carried out over a seven day period at a constant stress level of 70% of the short-term unconfined compressive strength q. Multiple-stage tests were also conducted in which the creep was measured over a 48 hour period at constant stress levels of 30%, 40% , 50% and 70% of the short-term unconfined compressive strength q. The short-term compressive strengths for the Organic Clay and Marine Clay were estimated from the unconfined compression test results.

The creep test results are summarized in Table 3.2. Because the single stage test on sample UF-7 was canceled due to problems with the testing apparatus only the multiple stage test for the Marine Clay is reported here.

The data from these tests were used to calibrate the material parameters in equation 3.4 (Section 3.2) to define the relationships for creep of frozen Organic and Marine Clay as follows:

$$\varepsilon_{C,OrganicClay} = 1\times10^{-3}(\sigma) + 6\times10^{-5}(\frac{\sigma}{7.9})^{3.05}\times t \tag{3.8}$$

$$\varepsilon_{C,MarineClay} = 4.5\times10^{-4}(\sigma) + 6\times10^{-5}(\frac{\sigma}{14.7})^{6.73}\times t \tag{3.9}$$

where:

ε_C = total creep strain,

σ = constant stress in tsf, and

t = time interval for creep in hours.

These equations are utilized in Chapter 6 to estimate creep deformations during tunneling under the Graphic Arts building.

Table 3.2: Creep Tests - Summary of Results

Soil Type	Boring No.	Sample No.	Sample Elev. (ft)	Water Content (%)		Temp (°C)	Applied Stress (MPa)	Pseudo Inst. Strain ε_0^e	Min. Creep Rate $\dot{\varepsilon}_2^c$
				Initial Avg.	Final				
Marine Clay	RW-5	UF-9	77.1	33.0	31.1	-10.0	1.0	.0029	1.8E-07
							1.5	.0053	5.3E-07
							1.8	.0076	6.4E-07
							2.5	-	[1]
Organic Clay	RW-6	UO-1	93.2	33.2	30.4	-10.0	0.945 [2]	0.0611	2.7E-06
	RW-2	UO-3	91.1	55.5	70.1	-10.0	0.405	0.0042	2.8E-07
							0.540	0.0052	2.7E-07
							0.675	0.0059	4.8E-07
							0.945 [3]	0.0099	1.3E-06

1) Sample failed at 4th load increment
2) Unconfined Compression test performed on sample after creep test; compressive strength = 2.46 MPa
3) Unconfined Compression test performed on sample after creep test; compressive strength = 1.98 MPa

3.5 In-Situ and Laboratory Tests on Wooden Piles

3.5.1 Load Tests

In-situ load tests were performed on the piles to determine their loading conditions and elastic parameters. These tests were conducted in test pits, which exposed the pile groups and the granite pile caps inside the Russia and Graphic Arts buildings (Mueser Rutledge Consulting Engineers, 1998). The summary of the test pit investigation and load testing is as follows:

- A total of 39 piles were exposed and by visual inspection appeared to be in good to excellent condition.
- Two selected piles were loaded incrementally to a maximum load of 15 tons. The elastic moduli determined were 1.34×10^6 psi (9,240 MPa) and 1.40×10^6 psi (9,650 MPa).
- The estimated capacity of the piles at the Russia building was about 40 tons each.
- Calculated foundation loads for the two piles were 4.5 and 2.2 tons.

3.5.2 Laboratory Tests on Frozen and Unfrozen Wooden Piles

Laboratory test were performed on unfrozen and frozen wooden pile samples (Mueser Rutledge Consulting Engineers, 1998) to determine their in-situ strength, frozen strength, and any impact the freezing process may have on strength once thawed. For this purpose samples were taken from two piles under the Russia building. The results of this testing program are summarized as follows:

- The piles were identified as spruce (Picea Spp). The piles were either red, black or white spruce and can be grouped as eastern spruce.
- A microbiological examination revealed that some deterioration had occurred at the perimeter of the piles, generally limited to the outer 1/2 to 3/4 inch of the piles. The cell structure more than 1 1/2 inch to 2 inch into the piles was sound and showed no influence of bacterial organisms.
- The average compressive strength with or without freezing in the parallel-to-grain direction ranges between a minimum of 2,191 psi (15.11 MPa) and 3,304 psi (22.79 MPa). This range equates well with the published data in ASTM D2555 for the three eastern spruce species.
- No statistically significant difference was found between the average compressive strength of samples with and without a freezing history. Therefore, it was concluded that no adverse impact on pile strength and condition would result from the freezing.

3.6 Adfreeze Strength

The strength between frozen soil and pile is important for the proposed load carrying mechanism being investigated here. The load carrying capacity of the pile will depend on the strength that develops at the interface between the frozen soil and the pile surface. This is referred to as adfreeze strength. According to the definition by the National Snow and Ice Data (NSIDC, www.nsidc.colorado.edu) and Johnston (1981) it is defined as "the tensile or shear strength, which has to be overcome to separate two objects that are bonded together by ice."

Chapter 4 of the Technical Manual TM-852-2/AFM 88-19 (Joint Departments of the Army and Air Force USA, 1985) provides information on the pile supporting capacity in permafrost that is derived primarily from the strength of the adfreeze bond. According to the current state of practice clean metal, untreated smooth wood or smooth concrete surfaces may all be assumed to have similar adfreeze bond potentials. Rough concrete and rough wood have greater potential; however, the potential for increasing tangential shear strength by increasing roughness is limited by the shear strength of the adjacent frozen soil.

Values for the adfreeze strength were derived from three different sources. Chapter 4 of the Technical Manual TM-852-2/AFM 88-19 (Joint Departments of the Army and Air Force USA, 1985) reports data from tests carried out in permafrost at Fairbanks, Alaska for uncoated steel piles embedded in a silt under natural freezing conditions. Adfreeze strengths as high as 60 psi (0.414 MPa) were measured in these tests. The adfreeze strength is dependent on the frozen soil temperature. Andersland and Ladanyi (1994) propose maximum short-term design adfreeze strengths for steel piles for different soil types and soil temperatures based on data from the literature. The adfreeze strengths generally reach their highest values at a temperature of –5 °C and remain constant at lower temperatures. The values proposed by Andersland and Ladanyi (1994) are as follows:

- 0.250 MPa for ice-rich silt or fine sand,
- 0.350 MPa for sand, and
- 0.300 MPa for clay.

Bowles (1982) approximates the ultimate adfreeze strength of several materials as follows:

$$\tau_a = F + G \times (T)^{0.7} \tag{3.10}$$

where:

τ_a = adfreeze strength in kPa

T = degrees below 0 °C,

F = 0 for pure ice; about 40 for silty soils and 70 for sand, and

G = 75 for pure ice; about 80 for silty soils and about 150 for sand.

Orders of magnitude estimates for adfreeze strength for ambient soil temperatures of – 1 °C to –3 °C are reported in Table 3.3 (Bowles, 1982). The lower values of the ranges provided are applicable to soil temperatures close to 0 °C, limiting values are reached at temperatures of about –10 to –12 °C.

Table 3.3: Adfreeze Strength (–1 °C to –3 °C Ambient Temperature)

Soil	Wood (MPa)	Steel (MPa)	Concrete (MPa)
Sand	0.400-1.600	0.625-1.000	0.500-3.000
Silt	0.120-1.000		
Clay	0.300-1.200	0.100-1.300	0.500-1.300
Gravel	< 0.160		

Evaluation of the values provided in Table 3.3 and equation 3.10 by Bowles, 1982, the adfreeze data recommended for design by Andersland and Ladanyi (1994) and the values reported by Chapter 4 of the Technical Manual TM-852-2/AFM 88-19 (Joint

Departments of the Army and Air Force USA, 1985) the adfreeze strength for the soil types at the project site can be estimated as summarized in Table 3.4. For reference the table also lists the cohesion obtained from laboratory testing of the frozen soils at the project site.

Table 3.4: Proposed Adfreeze Strength Ranges for Analyses

Frozen soil	Cohesion (at T = -10 °C) (MPa)	Adfreeze Range (MPa)	Percent of Frozen Soil Cohesion [%] (MPa)
Fill	1.440	0.935 – 0.350	65 – 24
Organic Deposits	0.860	0.496 – 0.250	58 – 29
Marine Clay	1.130	0.600 – 0.300	53 – 26

Chapter 4: Project Design Elements

4.1 General

The tunneling at Russia Wharf emphasizes the restrictions under which tunneling in urban areas must be conducted today. The brief project history outlined in this Chapter portrays the planner's, architect's, and engineer's search for the most appropriate solutions to meet socioeconomic transportation demands under difficult urban constraints. The accommodation of these tunneling demands and constraints ultimately leads to new solutions in geotechnical engineering.

Following a brief portrait of the project's development, Chapter 4 describes the local geotechnical conditions at the Russia Wharf site, lays out the ground freezing and tunneling concepts adapted, and details the instrumentation system implemented to monitor the construction.

4.1.1 Project History

Located below the historic Russia Wharf complex, the Russia Wharf Segment is one section of the Massachusetts Bay Transportation Authority (MBTA) Transitway project. Connecting the South Boston Piers/Fort Point Channel area with the Central Business District, the Transitway project has an important role in connecting a fast growing development area to the public transit system of the Greater Boston, MA area.

The MBTA initiated a feasibility study in 1987 that provided a preliminary evaluation of new public transit service alternatives to meet the future travel demands in the South Boston Piers/Fort Point Channel Area. Alternatives included conventional

surface bus service, elevated and underground people mover alignments, elevated guided busses, and a relocation of the existing Red Line. As a result and as recommended by the feasibility study, a Draft Environmental Impact Report (DEIR) was initiated in the fall of 1987. The DEIR concluded that the Fort Point Channel Underground Transitway, using either trackless trolleys or dual mode busses with possible conversion to light rail technology, was the preferred alternative. Staged implementation opportunity, attraction of more riders, ability to serve other areas, including Logan International Airport, and the joint construction opportunity with the northbound Central Artery were the deciding factors for the underground option. Finalized in 1993, the Final Environmental Impact Statement/Final Environmental Impact Report further analyzed impacts of the underground option. After a positive review, the design process started with alignment studies, construction feasibility studies and operations analyses for Phase 1, starting at South Station and proceeding to the World Trade Center in South Boston.

Initial alignments showed the Russia Wharf Segment of the Transitway passing through the ventilation building of the Central Artery project. Significant risk of vehicular accidents due to sharp corners in the horizontal layout and conflicts with the ventilation building layout required a relocation of the twin travel way tunnel structure beneath the Russia Wharf Buildings. As shown in Figure 1.3 (Chapter 1), the tunnel structure traverses the Russia Wharf property, entering at the southwest corner (Congress Street/Atlantic Avenue intersection) and passing northeasterly to the Boston Edison parcel. The Russia Wharf complex consists of three buildings, the Russia, Graphic Arts

and Tufts Building, of which the first two are affected by the tunnel construction. All buildings are founded on timber piles.

During the preliminary design phase, a cut and cover tunnel, with underpinning of the Russia and Graphic Arts buildings, was developed which required partial demolition of the buildings in order to install the excavation support and underpinning. A Value Engineering Review, carried out after the 30% design completion as required by the Federal Transit Administration (FTA), found that the proposed cut and cover scheme was the most expensive option and recommended the demolition of the buildings to build the tunnel. This proposal received great resistance from the Massachusetts Historical Commission (MHC), which encouraged the MBTA in March 1996 to develop additional alternatives that minimized any demolition of the existing structures. Four alternative scenarios were evaluated:

Option A: Open Cut and Cover

This modified cut and cover alternative eliminated long underpinning girders by introducing post-tensioned concrete. Excavation support was provided by low headroom mini-piles at close spacing. These measures reduced but did not eliminate demolition of the lower floors of the buildings. Furthermore, cost and schedule considerations did not satisfy project needs.

Option B: Shield Tunnel with Liner Plates

To accommodate both in- and outbound lanes, a circular shield tunnel with steel liner plates had the largest cross section of the proposed methods. Excavation would require hand mining after the underpinning of the building foundations. However,

difficulties with the numerous timber foundation piles and the high cost of a shield machine for the short length of tunnel as well as unresolved alignment details in adjacent tunnel sections made the mechanized shield option unfeasible.

Option C: Elliptical Pipe Arch with Micro Tunneling

In this option an elliptical pipe arch is installed at the crown of the tunnel cross section before advancing with the tunnel excavation. Individual pipes are excavated using micro tunneling techniques. The tunnel is then excavated beneath the completed arch and supported typically by steel ribs and lagging. Difficulties with the feasibility and accuracy of micro tunneling through the vast number of foundation piles plus high costs and low advance rates made this method unfeasible in comparison with other methods proposed.

Option D: Rectangular Jacked Box

Jacking a pre-cast reinforced concrete tunnel box of the proposed size through the ground requires high jacking forces. Underpinning of the foundations and additional face support with either grouting or ground freezing would be required prior to excavation. Cost, schedule, excavation through the timber pile foundations, but most of all, the very limited and restricted working zone at the site made this option virtually impossible.

None of these alternatives provided the level of feasibility and economy required to realize the project. A more viable option was sought after and, based on precedent examples, ground freezing (see Chapter 2), in combination with shotcrete support tunneling techniques, was suggested. This new proposal became Option E and along with Option B was evaluated in a more detailed feasibility study. This feasibility study

was completed in early fall 1996 and following numerous reviews by industry peers representing the geotechnical and underground construction professions, the shotcrete support method with ground freezing was found to be the most technically and economically feasible method while providing schedule advantages and allowing the buildings to remain occupied by the tenants during construction.

4.2 Sub-surface Profile Along the Tunnel Section

The general subsurface profile along the alignment below the Russia Wharf building complex is shown in Figure 4.1. The profile consists of the following strata (from ground surface proceeding downwards): fill, organic deposits (organic clays), marine clay, glacial till, and bedrock. At Russia Wharf, the total thickness of soil overburden ranges from 70 to 90 feet, with the top of bedrock ranging between El. 20 and El. 40.

The fill thickness varies from 1.5 to 9 meters, generally becoming thicker towards the channel at the eastern edge of the project. The organic deposits are typically 1.5 to 5 meters thick where encountered in the borings. The top of the organic deposits slopes gently toward the channel from El. 100 to 85. The clay thickness increases from approximately 3 meters near the west of the Russia Building to some 15 meters east of the Graphic Arts Building. The glacial till thickness decreases from approximately 12 meters at the west corner of the Russia Building to just about 1.5 meters at its thinnest location east of the Graphic Arts building. As shown in Figure 4.1, the crown of the binocular tunnel is located near the top of the clay stratum but extends into the overlying

organic deposits and fill. The majority of the tunnel invert is located in the clay stratum except for a portion beneath the Russia Building where it is located in the glacial till.

Groundwater measurements from the borings indicate groundwater elevations to be generally well above the tunnel crown to an elevation near the base of the pile caps, so that the freezing scheme will be under submerged soil conditions. Measurements were also taken to determine the effect of tidal variation in Fort Point Channel. The tide cycle data indicate that tidal variation in the channel has almost no effect on the water levels at the locations measured.

4.2.1 Soil Descriptions

The soil descriptions given here are aimed at providing the general characteristic of each stratum in the project section. Detailed data on soil geotechnical properties are given in the relevant reports (Final Geotechnical Data Report by GEI Consultants, Inc., July 1998). Detailed test data for the unfrozen soils along with the test data on the frozen soil samples (Chapter 3) were utilized to derive the soil properties used for the numerical modeling in Chapters 5 through 7.

Fill

The fill is highly variable in composition. In general, it consists of fine to coarse sand with varying amounts of gravel and slightly plastic fines. Brick fragments, wood, ash, and cinders, as well as organic matter and clumps of clay were encountered in many of the fill samples taken. The fill generally is gray-brown in color. SPT-N values in the fill ranged from 2 to 47 blows per foot. The SPT data indicate that the density of the fill is highly variable, ranging from very loose to dense. The permeability of the fill is highly

variable due to its composition. The permeability was expected to range from 1 x 10^{-7} to 1 x 10^{-4} m/sec. Localized high permeability flow paths may occur along existing and abandoned building foundations, old seawall and wharf structures and other remnant structures at the site.

Salinity in the fill samples ranged from 0.1 to 6.6 ppt. Where salinity is measured from samples taken from the ground water or Fort Point Channel directly, it ranged between 9.6 and 20.8 ppt.

Organic Deposits (Organic Clay)

The organic deposits typically consist of gray to black, low to high plasticity organic silt with fine sand, frequent peat fibers and occasional shell fragments. The organic deposits also contain occasional zones or layers of fine sand and peat. Peat layers of up to 1.2 meters were encountered. The SPT-N values range from 1 to 17 with an average of 7 blows per foot, indicating a very soft to stiff consistency.

Field borehole permeability tests were performed in the organic deposits at three locations in the project area. These tests were performed near the bottom of the deposits at the interface with the underlying clay stratum, because experience at other sites has indicated that relatively continuous layers of sand are occasionally encountered at this interface. At one test location for example, the tests indicated a relatively high permeability of 4 x 10^{-5} m/sec and 1 x 10^{-4} m/sec. In general, the organic deposits were expected to have a low permeability (1 x 10^{-8} to 1 x 10^{-7} m/sec) in the organic silt, with localized zones of higher permeability (up to 1 x 10^{-4} m/sec) where layers of sand and peat are present.

Salinity in the organic deposit samples ranged from 4.8 to 12.0 ppt.

Marine Clay

The marine clay, commonly known as the Boston Blue Clay, is gray in color and consists of low to medium plasticity clay with frequent thin partings and laminae of silty fine sand. The upper part of the clay deposit (above approximately El. 75, which on the average is above the tunnel springline) is highly over consolidated due to desiccation during a period when it was exposed above sea level. The clay in this upper desiccated crust is often distinguished by a yellow-brown color resulting from oxidation. The N-values in the desiccated crust were typically in the range of 10 to 30 blows per foot, indicating a stiff to very stiff consistency. N-values below the desiccated layer were typically in the range of 5 to 15 blows per foot, indicating a medium to stiff consistency.

Consolidation tests were performed on the clay within the tunnel section below the desiccated crust. The test data indicate that the over consolidation ratio (OCR) decreases generally from west to east along the alignment. Measured values of OCR varied from 4 at station 94+65, 3 at stations 95+67, 97+66 and 96+50 just below the crust to 1.5 at the bottom of the clay at this location.

Salinity in the clay samples ranged from 1.0 to 6.4 ppt.

Glacial Till

The glacial till typically consists of a heterogeneous mixture of sand, silt, clay, and gravel, with occasional cobbles and boulders. For descriptive purposes, the till deposit has been subdivided into two subunits based on fines content (material passing the No. 200 sieve). Glacial till with typical fines content greater than 30% is described as

cohesive till and till with typical fines content less than 30% is described as granular till. The fines in the cohesive till typically consist of clayey silt with low plasticity, and the fines in the granular till vary from non-plastic silt to clayey silt with low plasticity. Most of the till encountered within the alignment is cohesive till. SPT-N values in the till ranged from 33 to > 100 blows per foot, with an average SPT-N value of 90, indicating a dense to very dense condition.

Permeability tests indicate permeability values ranging from 6×10^{-8} to 1×10^{-6} m/sec in the cohesive till and 4×10^{-7} to 2×10^{-6} m/sec in the granular till.

Bedrock

The bedrock formation in this area is predominantly a gray, fine-grained, very thinly bedded argillite (also known as Cambridge Argillite). Because of its depth, the influence on the tunneling and ground freezing is thought to be very limited and no further descriptions are provided here.

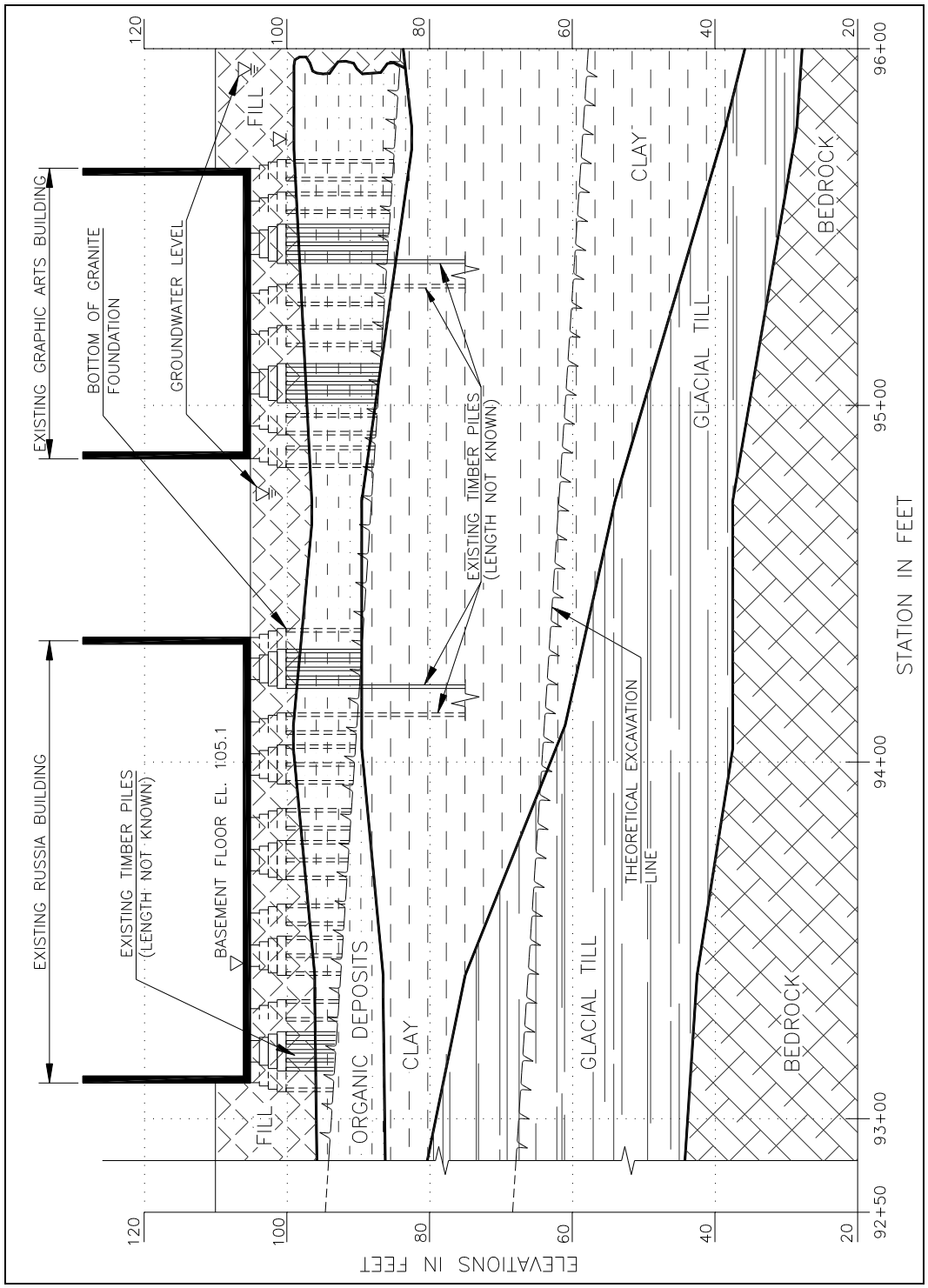

Figure 4.1: Geologic Profile at Russia Wharf

4.3 Building Foundations

The buildings at Russia Wharf were constructed in the late 1800's / early last century. All of the buildings are founded on timber piles. From a review of historic documents, it may be concluded that the piles were driven into the ground until the capacity of the driving equipment was reached. Therefore their depth is not known. The piles may act as friction piles, and bearing piles if the desiccated upper layer of the Boston Blue Clay has provided sufficient bearing capacity, or a combination of both. The piles were typically arranged in groups of about 30 wooden piles per pile group. The wooden piles are generally about 30 cm in diameter and each pile group occupies a plan area of some 3 x 3 m. This results in a pile arrangement such that the piles have typically about a 30 to 50 cm clear pile-to-pile distance.

Granite blocks of varying sizes were used to create pyramid shaped pile caps in typically four layers. These pile caps constituted the direct foundations for the steel columns of the steel frame, brick/masonry building construction. See Figure 4.3 (Stage 1 & 2) in Chapter 4.4.3 below for a schematic pile and granite block arrangement. Based on the building construction and use, loads resulting in pile cap pressures of 0.300 MPa were assigned to pile groups within the center of the Graphic Arts building, which translates in a load per pile of approximately 10 tons.

4.4 Ground Freezing

4.4.1 General

As mentioned in Chapter 2, the vertical freeze pipe installation had many advantages over other methods, mainly in accuracy of the drilling operation, access and cost and was therefore implemented in the contract. The vertically installed freeze pipes also bear the advantage of producing qualitatively less surface heave as a result of the freezing operation. This is due to the fact that the freeze-associated expansion is in the direction of the propagating frost front. Because the freeze pipes are installed vertically, the frost front therefore propagates horizontally and radially around the freeze pipes and not towards the surface.

Despite the above phenomenon, the potential for heave exists. Freezing associated heave has been reported extensively in the case histories studied, although mainly associated with horizontal freeze pipe installation. At the Milchbuck tunnel in Zurich, Switzerland (see Appendix, Project 13) for example, the surface heave in the first freezing section reached a maximum of 105 mm. The introduction of the so-called "intermittent" freezing reduced the heave to 10 mm in the third freezing section and to only about 4 to 6 mm in subsequent freezing sections (Aerni, 1980). The intermittent freezing is based on the principle that following the initial build up of the frozen soil mass, further freezing for the maintenance of frozen soil temperatures is carried out in "on-off sequences" in which the cooling medium is circulated through the system in "on" sequences and is shut off during "off" sequences. Successful application of this method

is also reported by Deix (1992) for freezing sections at the Vienna, Austria subway construction.

The design at the Russia Wharf implemented some heave mitigating measures. Arrays of vertically drilled drainage pipes to provide drainage of excessive ground water during the initial freezing operation were installed. For example, at the Graphic Arts building, vertically installed drain pipes were placed where the frozen soil is in close proximity to wooden pile foundations. The drain pipes were located just outside of the frozen soil boundaries and between the frozen soil and wooden piles. Drain pipes were also foreseen beneath the granite pile caps at the Graphic Arts building to drain excess pore water. At critical locations, as for example in close proximity to neighboring CA/T slurry walls, warming pipes were installed to mitigate horizontal propagation of the ice front and associated deformations. The freezing was also established in phases to match a phased tunneling. This phased freezing further minimized the total duration of freezing and provided economy.

4.4.2 Extent of Ground Freezing

The ground freezing, as related to tunneling, was accomplished underneath the Russia and Graphic Arts Buildings. It should be noted that ground freezing was also utilized for the sole purpose of ground water cut-off. These ground water cut-off walls were required for the installation of the permanent underpinning system for the Russia building and at the Fort Point Channel side of the Graphic Arts building.

Figure 4.2 depicts the extent of ground freezing at the Graphic Arts building in a typical cross section. In general, the frozen soil extended horizontally to both sides of the binocular tunnel sidewalls by about three meters. Ground was frozen vertically to the granite pile caps at the top and about one meter into the marine clay layer at the bottom. This distance was viewed to be a good compromise between the need to freeze the Organic Clay/Marine Clay interface to prevent any ground water flow and assure increased stand-up time in this interface while not subjecting too large a volume of the Marine Clay to freezing and subsequent unwanted thaw settlements. While zones A and D, which lie completely outside of the tunnel profile, were frozen in their entirety, Zone C was only frozen to approximately 30 cm outside the tunnel clearance in the roof section. Zone B initially specified freezing to elevation B to assure that ground beyond the top heading sidewall of the outbound tunnel during its excavation was frozen. During the excavation and support of the inbound tunnel, however, the freezing pipes that extended to about elevation B were switched off and cut off during tunnel excavation and support, and only the freeze pipes that reach to some 30 cm outside of the tunnel envelope were used for maintaining the frozen ground.

The freeze pipe layout called for an arrangement of freeze pipes such that a freeze pipe density of 2.5 m^2 of surface area per freeze pipe was not exceeded at the Graphic Arts Building and 5.8 m^2 per freeze pipe at the Russia Building. With these minimum requirements, the detailed freeze pipe layout was left to the freezing contractor who installed and operated the freezing system based on performance criteria. It was also the

contractor's responsibility to implement secondary ice growth mitigation measures described above to maintain deformations within permissible limits.

The frozen ground temperature criteria called for a minimum of 80% of all the frozen ground viewed in plan underneath the Graphic Arts building to be colder than -12 ºC with the warmest temperature at any measured location not to exceed -7 ºC. Similarly, 70% of the frozen volume viewed in plan underneath the Russia Building had to be cooler than -7 ºC and the warmest point allowed at any location could not exceed -5 ºC. Because of the large volume of freezing and the long freezing durations, natrium chloride solution (brine) was used as the coolant medium.

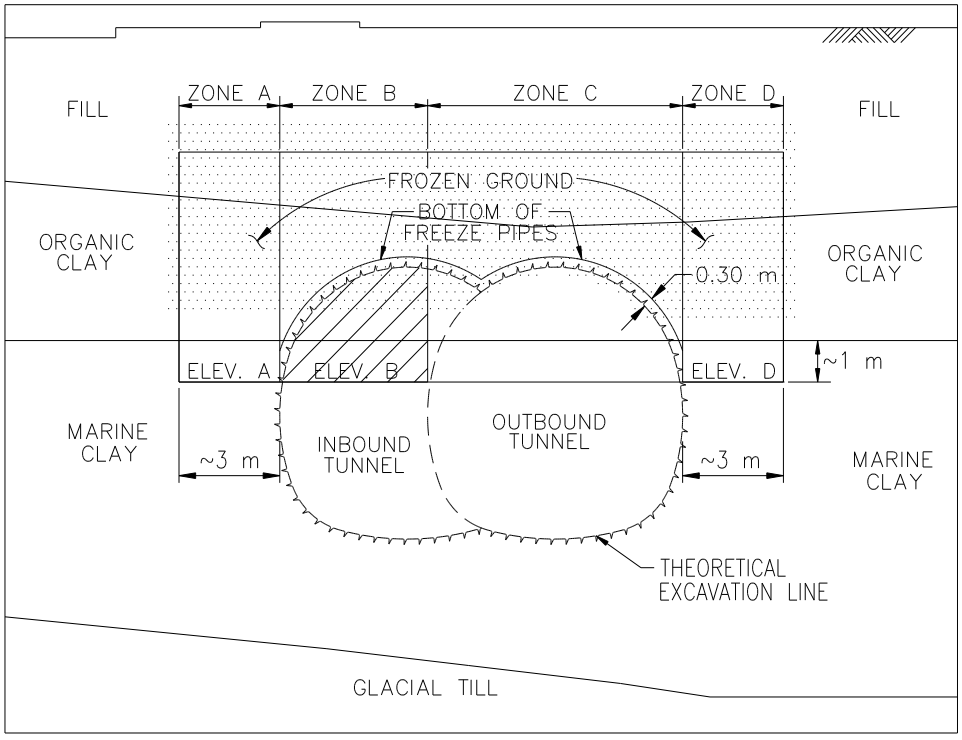

Figure 4.2: Extent of Ground Freezing

4.4.3 Temporary Jacking for Building Columns at Graphic Arts Building

A temporary jacking system was implemented at all 14 building columns of the Graphic Arts building, where the wooden piles were cut-off during the tunneling operation and load transfer onto the tunnel lining would occur after thawing. This temporary underpinning system was laid out as a "two-way" system that accommodated pile cap heave and any subsequent thaw related settlements. The temporary jacking system is displayed in Figure 4.3.

- In a first stage (stage 1), before the tunneling operation commenced, the existing floor slab, fill and brick arches were removed, exposing the two upper granite blocks. Following build-up of the frozen soil zone, timber cribbing was constructed and the temporary jacking system with transfer beams, jacking beams, column brackets and jacks was installed.
- The jacking system was engaged (stage 2) for compensation during tunneling whenever the permissible column deformation limits were exceeded. During jacking, the column was separated from the pile caps and the load transferred onto the cribbing and therefore onto the frozen soil mass.
- Once the tunnel construction will be completed, including placing of the inner shotcrete lining stage 3 of the temporary jacking procedure will be implemented. At the time of writing, this work is on-going. Within stage 3, the upper two granite block layers will be removed and replaced by a reinforced concrete pad. Spreader beams and lock-nut jacks between the spreader beams and the jacking beams of stage 1 will be installed. By activating these jacks, the loads will be

transferred from the cribbing system back onto the concrete pad. Once this load transfer has taken place, wedge and shim plates will be inserted between the column base and the concrete pad. This arrangement will be kept in place throughout the entire ground thawing period and some time thereafter until absence of continuing deformation has been verified. Any thaw consolidation related settlements will be compensated by this stage 3 jacking system.

- Following completion of stage 3, the jacking system will be removed and the pile caps restored as displayed under stage 4 in Figure 4.3.

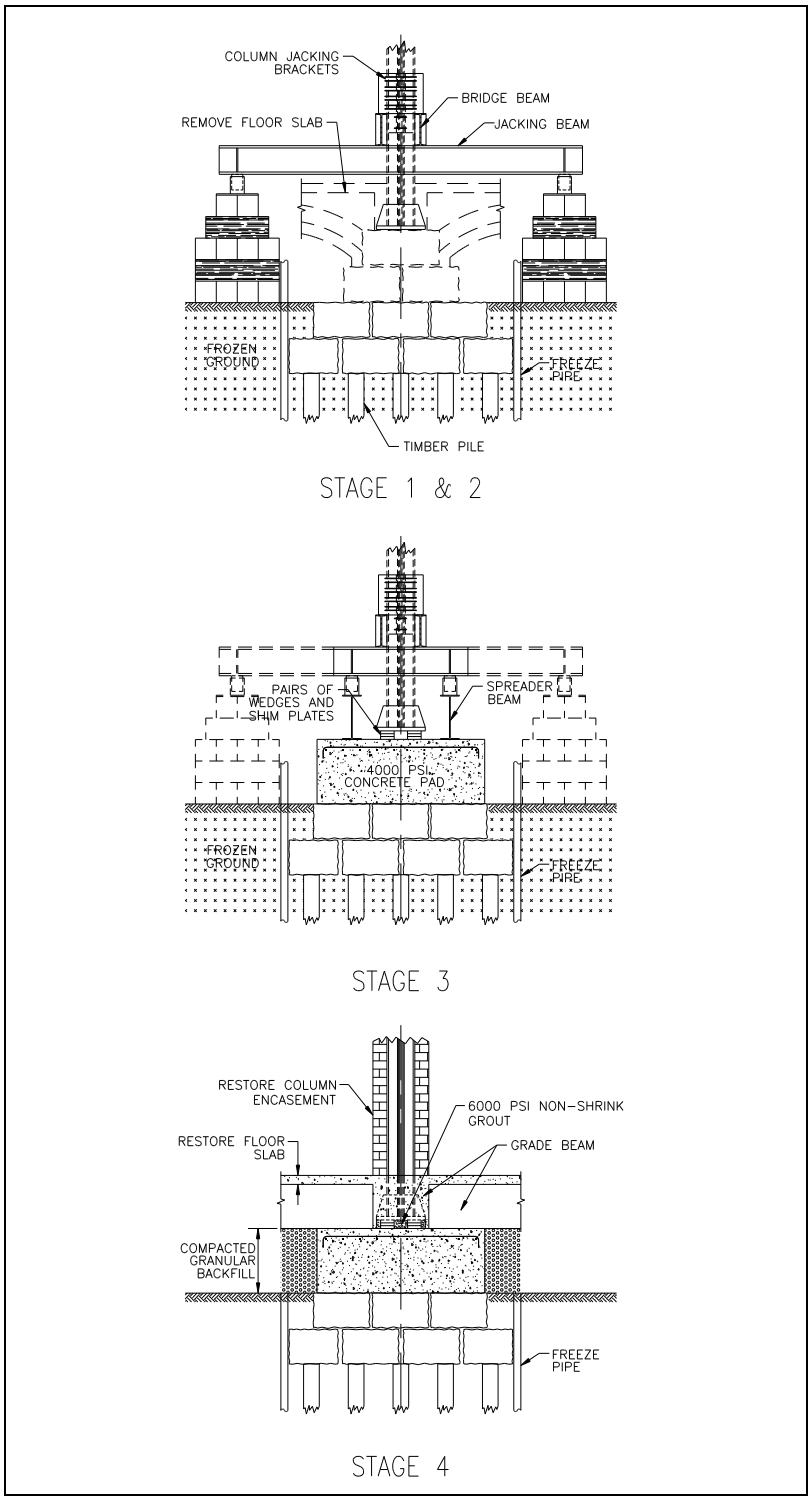

Figure 4.3: Temporary Jacking System for Building Columns at Graphic Arts Building

4.5 Tunneling

The tunneling method selected for excavation and support of the binocular tunnel follows principles of the New Austrian Tunneling Method (NATM). The tunnel cross section has been laid out in a binocular arrangement (Figure 4.4). The binocular arrangement offers the advantage that the overall height of the cross section is smaller than an otherwise full, oval cross section. This allows for more cover between tunnel roof and the granite pile caps. In the binocular tunnel, the overall cross section is subdivided into two distinct tunnel excavations, i.e. an outbound and inbound tunnel. This further minimizes the excavation area and therefore reduces settlements.

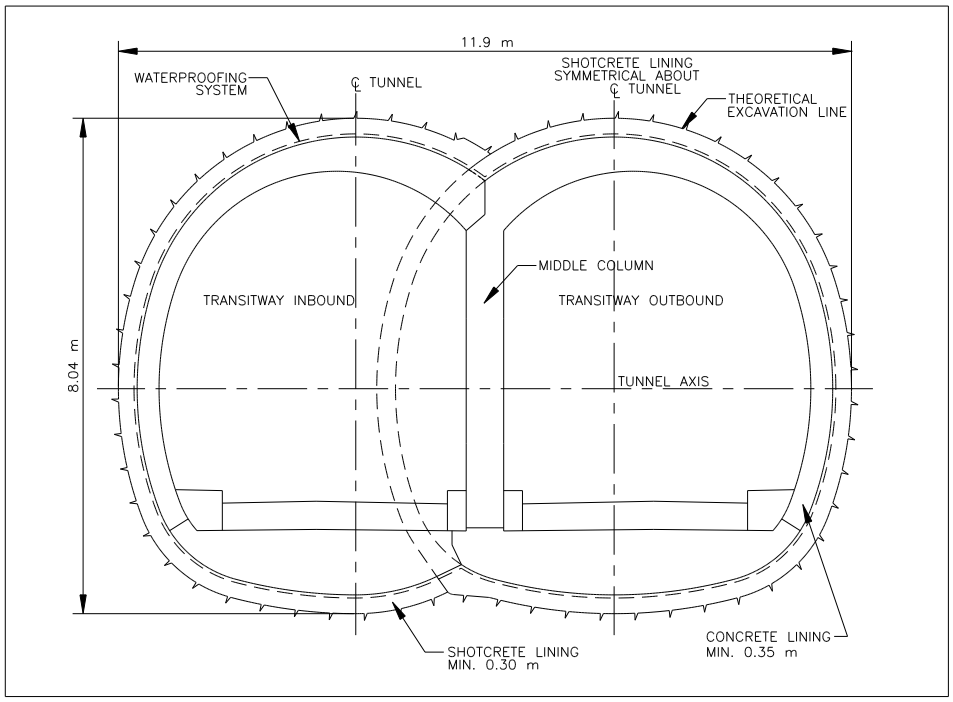

Figure 4.4: Typical Dual Lining Tunnel Cross Section

The overall cross section is designed as a double lining structure. The initial shotcrete lining provides immediate support to the excavated ground. Once installed, a waterproofing membrane is installed for water tightness. The contractor changed the planned concrete inner lining (Figure 4.4) to a more economic, shotcrete final lining. The geometry remained unchanged. The timber piles supporting the building were cut off during the tunneling process and integrated into the shotcrete lining. Prior to installation of the final lining, the building was supported by the frozen ground, which in turn rested on the tunnel initial shotcrete lining. Only after installation of the final lining shotcrete lining and thawing of the frozen soil will the tunnel structure support the piles and therefore the Graphic Arts building (Figure 4.5).

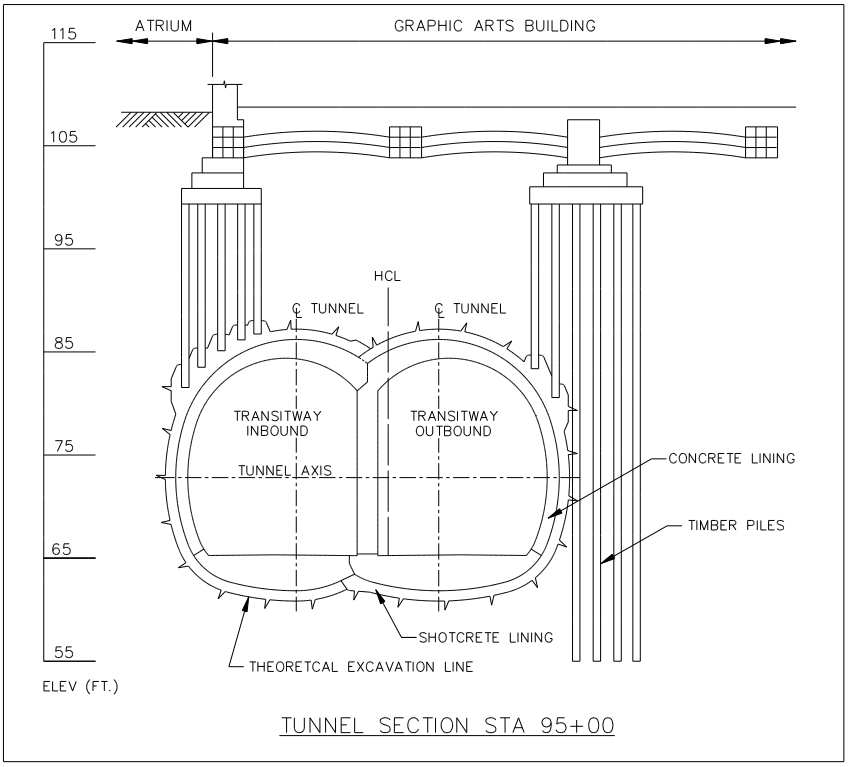

Figure 4.5: Tunnel, Piles, and Building Support

The tunnel longitudinal alignment is sloped downward towards the Fort Point Channel at 3.25 %. Figure 4.6 displays the longitudinal alignment as it relates to tunneling beneath the Russia and Graphic Arts buildings. The section is taken along the outbound tunnel centerline. As shown, the minimum thickness of the frozen soil at the Graphic Arts Building is 3.8 m and the maximum frozen soil thickness overlying the tunnel is 4.5 m. In contrast, the minimum thickness of frozen soil cover at the Russia Building is 2.0 m and the maximum is 3.1 m.

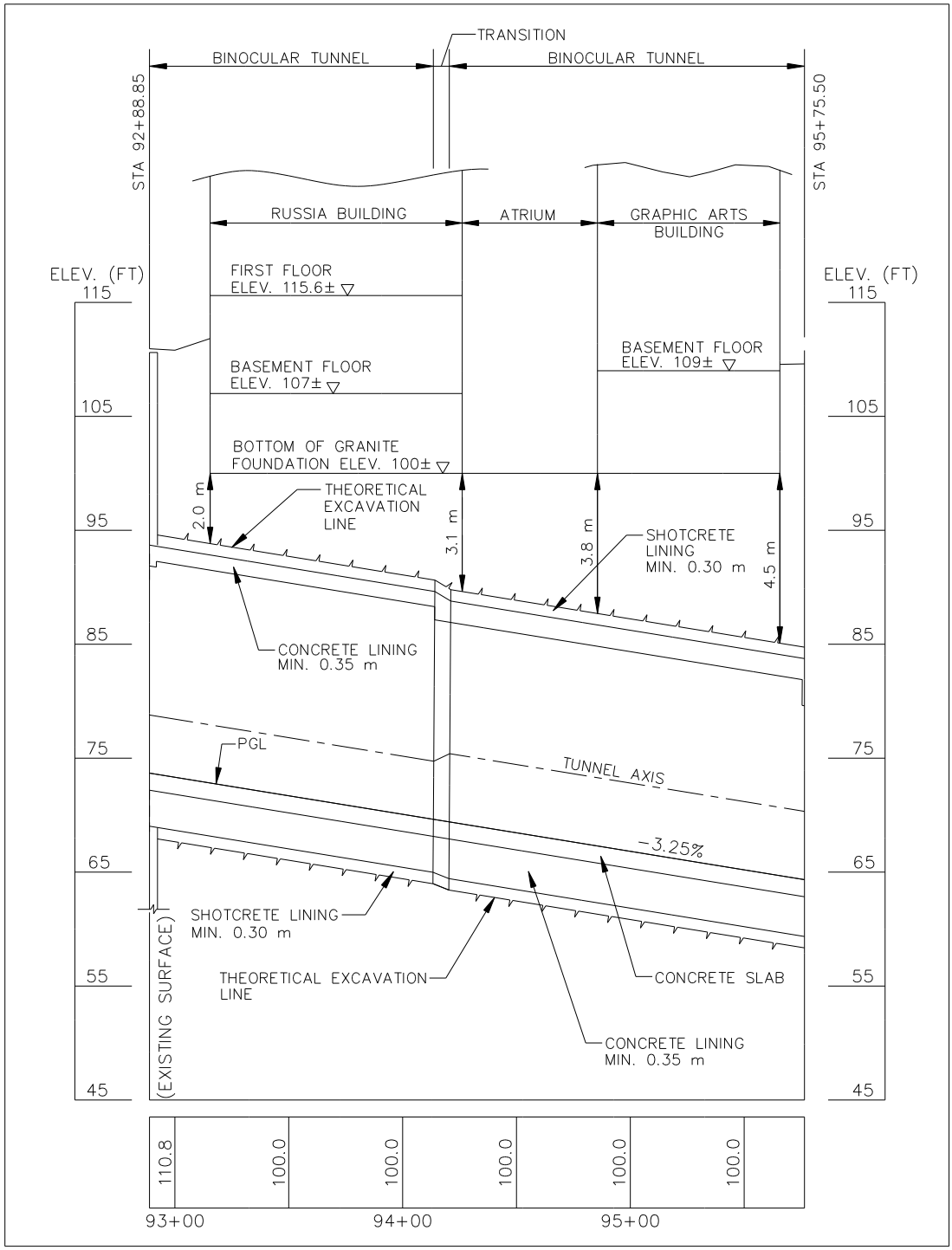

Figure 4.6: Tunnel Longitudinal Section at Russia and Graphic Arts Buildings (Outbound Tunnel)

4.5.1 Excavation Sequences and Shotcrete Lining

The excavation and support of the tunnels commenced after the temperature of the frozen ground met minimum temperature criteria established. Tunneling commenced from the Fort Point Channel side of the Graphic Arts building and proceeded first underneath the Graphic Arts building, then underneath the Russia Building towards Atlantic Avenue. Tunneling generally first involved the top heading of the outbound tunnel at the Graphic Arts building. After the top heading was completed, the bench and invert excavation commenced. The excavation and support sequence is shown in Figure 4.7.

The tunnel excavation and support has been laid out adhering to NATM principles (Sauer, 1988). The cross section has an oval shape. Because of the soft ground conditions, shallow cover, and overlying buildings, the ring closure distance has been shortened to only about 0.8 m behind the excavation face. A temporary invert shotcrete of 0.2 m thickness provides ring closure. In each advance length (round), a lattice girder was set to provide shotcrete reinforcement along with two layers of welded wire fabric. Also, 4-bar lattice girders were installed as longitudinal beam abutments supporting the lower section of the top heading shotcrete lining. The very limited size of the top heading offers for quick response to unforeseen conditions without compromising structural integrity and safety.

The specifications called for high early strength shotcrete, which was designed to achieve a compressive strength of 15 MPa within 24 hours. Once the top heading was completed, the bench and invert excavation removed the temporary top heading invert

shotcrete and completed the tunnel shotcrete lining with excavation rounds generally not exceeding 1.6 m (twice the top heading excavation round).

Following completion of the shotcrete lining in the outbound tunnel and installation of the waterproofing membrane, the outbound tunnel final shotcrete lining was placed. This shotcrete lining included a middle cast-in-place concrete pillar wall, which serves as an abutment for the subsequent inbound tunnel construction.

The inbound tunnel was also generally excavated in very short rounds of 0.8 m in the top heading and 1.6 m in the bench but followed a staggered full-face excavation sequence. During excavation, the remainder of the outbound shotcrete tunnel was removed and the initial shotcrete lining was supported by the previously constructed outbound tunnel and its concrete middle wall (Figure 4.8).

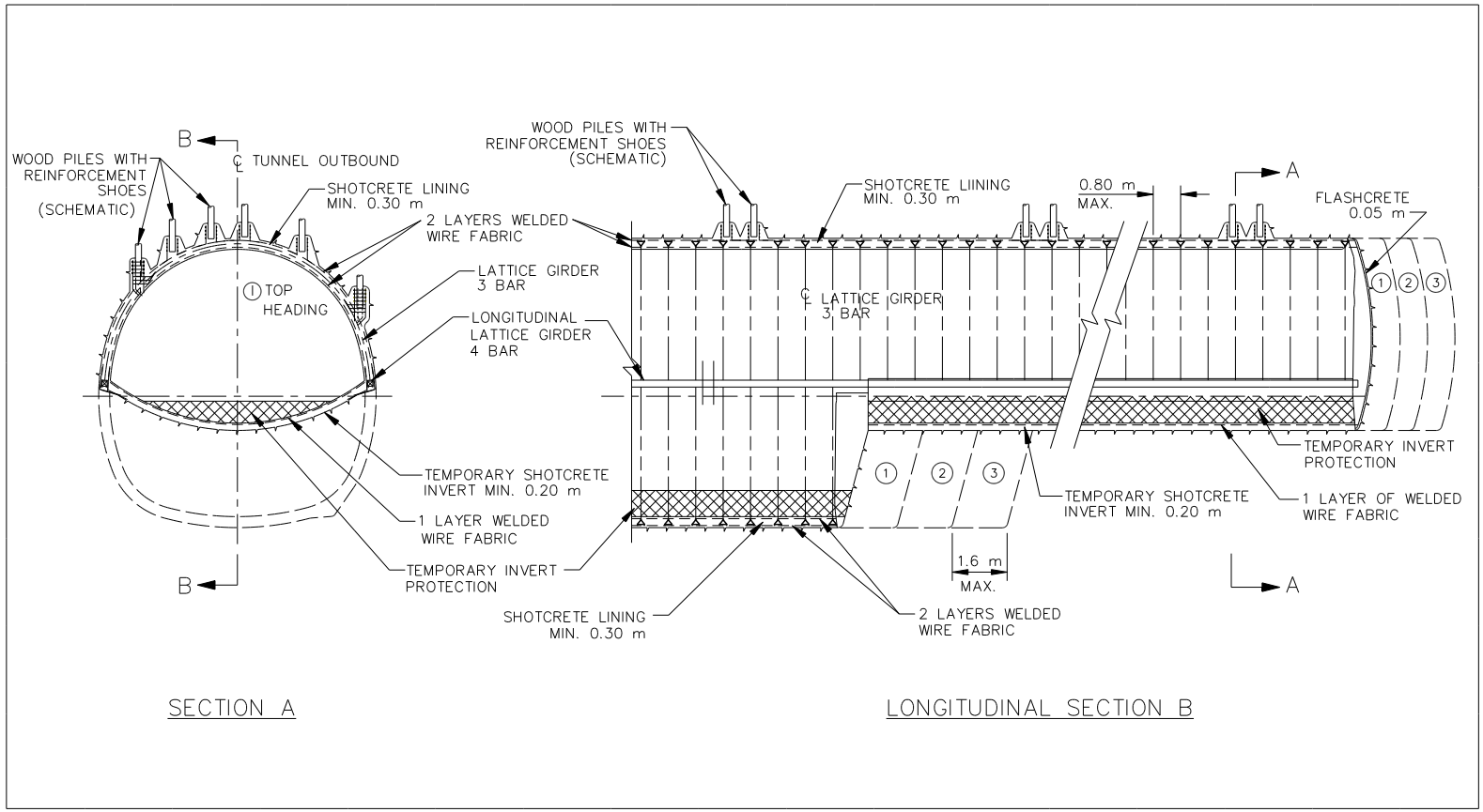

Figure 4.7: Excavation and Support of Outbound Tunnel

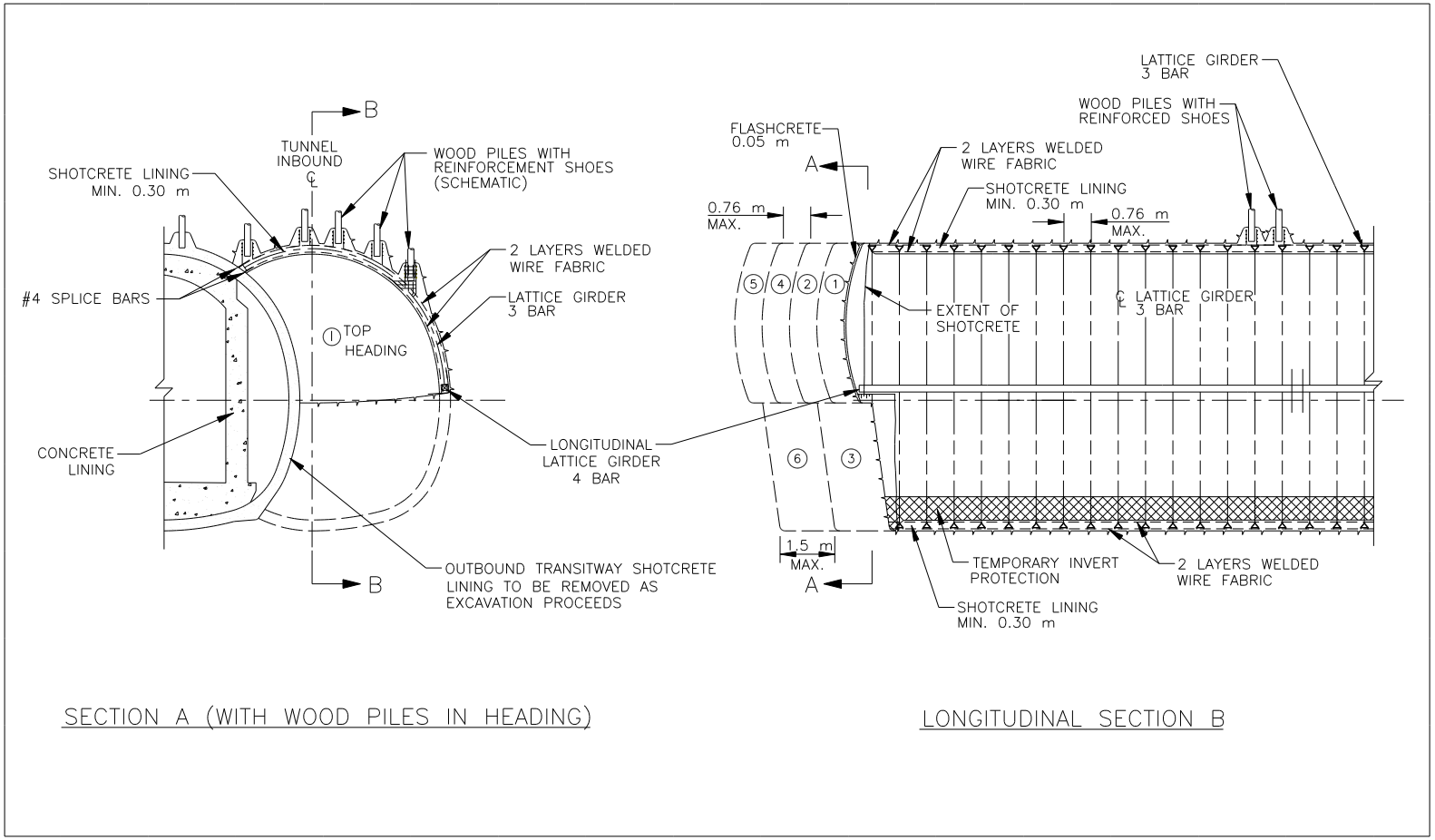

Figure 4.8: Excavation and Support of Inbound Tunnel

4.5.2 Pile Shoes

The pile supports of both the Russia and the Graphic Arts Buildings were encountered during tunneling. Underneath the Russia building, the existing pile supports were removed during tunneling because the building columns were underpinned by a permanent mini-pile underpinning system. Therefore, the wooden piles could be cut off and no special treatment was required.

In contrast, the wooden piles underneath the Graphic Arts building were to serve as permanent pile supports after the completion of tunnel construction. A careful cut-off procedure was therefore implemented for the piles at the Graphic Arts building. This cut-off procedure, along with an over-excavation around the lower portion of the piles, enabled the integration of the piles into the initial shotcrete lining as depicted in Figure 4.9. This Figure shows the construction of a "pile reinforcement shoe" in construction step II at a height of about 40 cm. As can be seen, this lower portion of the pile was separated from the shotcrete lining using a debonding layer which consisted of a polyvinyl chloride (PVC) membrane backed geotextile. This debonding permits free vertical movement of the pile tip. The pile tip itself is separated from the shotcrete lining by means of a neoprene pad. Once fully implemented (step VI, Figure 4.9), the debonding and neoprene padding will separate the pile from the shotcrete lining and minimize the transfer of construction-induced vibrations and, more importantly, traffic-induced vibrations when the tunnel is in operation for busway traffic.

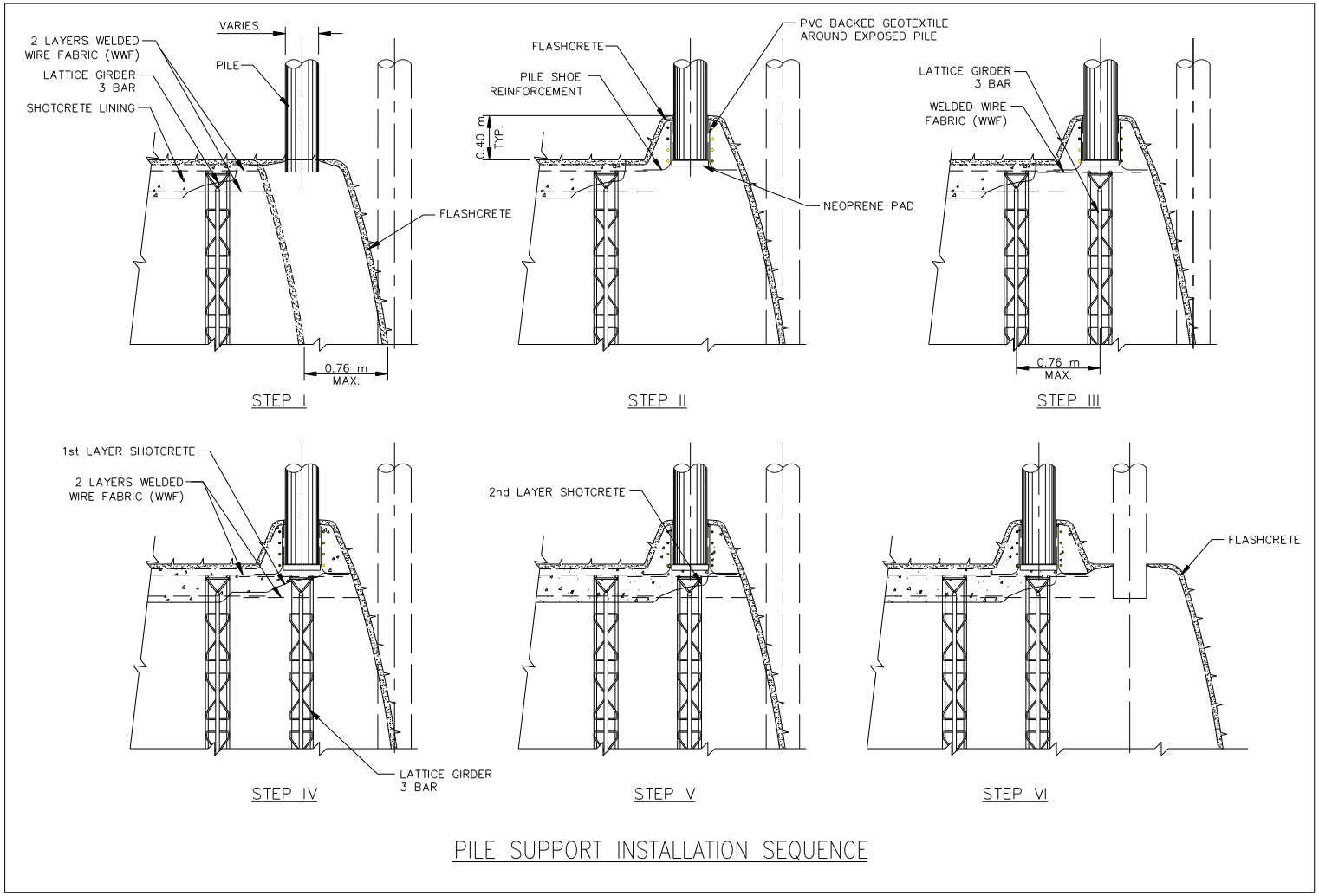

Figure 4.9: Pile Support Installation Sequence

4.6 Instrumentation and Monitoring Program

4.6.1 General

A comprehensive instrumentation program was established to monitor the performance of the freezing and tunneling and the associated impact on ground behavior and building structures. Selected elements of this instrumentation program are used in later chapters to calibrate the finite element model that is used to derive a new support mechanism. The FE model has been placed at Station 95.20. This station has an average overburden depth above the tunnel within the Graphic Arts building, provides for a representative pile cap arrangement and has therefore been equipped with a dense instrumentation array. Instrumentation at this Station is described along with the project wide range of instruments used to monitor the tunneling and ground freezing operation and the building response to it.

The geotechnical instrumentation program provides information on the deformational behavior of the ground, its surface and the buildings. For building monitoring instruments were installed at pile caps and building columns. This geotechnical instrumentation was supplemented by instrumentation installed from within the tunnel. The tunnel instrumentation provided information on the performance of the tunnel and its construction. Stress cells were installed between the shotcrete lining and the bottom of the cut-off piles at the "pile shoe" locations.

As part of the geotechnical instrumentation, an array of temperature sensors was installed to measure the temperature regime of the frozen soil. The information gained on frozen soil temperatures was used to verify the performance of the freezing system

and in interpretations of the surface heave. For the purpose of the evaluation in later chapters, in particular the building instruments installed at pile caps and columns are utilized. These are indicative of the deformation of the frozen ground and the wooden pile foundations embedded therein.

An initial baseline of readings was established prior to any tunnel construction and ground freezing activities. This baseline included all deformations that may have occurred as part of the on-going construction activities at Russia Wharf and at the adjacent Central Artery Tunnel project. For example, the construction of the ventilation building No. 3 was found to have had an impact on the Russia Building complex.

4.6.2 Geotechnical Instrumentation

4.6.2.1 Instruments

The instrumentation installed to observe the ground behavior included an array of geotechnical instruments:

Deformation Monitoring Points (DMPs): There are a total of five different types of DMPs. These DMPs differ in type and layout, depending on where they were installed. They include masonry nails (DMP-1) for masonry structures, stainless steel socket-head cap bolts (DMP-2) for steel column members, stainless steel round head bolts screwed into tamp-in screw anchors (DMP-3) for horizontal concrete and rock surfaces such as granite curbstones, steel rods installed in surface roadway boxes (DMP-4) where installed directly in soil, and observable points punched in steel sheets or soldier piles (DMP-5) and sprayed with fluorescent spray paint.

Borros Points: Borros points are typically 1/4" steel pipes installed in casings and surface roadway boxes for the measurement of shallow subsurface deformations. The steel rod is inserted in a casing in a pre-drilled hole. The steel rod is attached to a borros anchor with anchor prongs for proper anchoring of the steel rod tip into the soil.

Convergence Gages: Convergence gages are tape extensometers with read-out gages to measure changes in distance between selected anchorage points.

Inclinometers: the inclinometer probe is biaxial, consisting of two force balance accelerometers mounted at 90 degrees with a 2-foot wheelbase. The probe is inserted into a casing with broached internal keyways for a twist tolerance that is better than one degree per 10 feet. The inclinometer extends 15 feet into the glacial till.

Probe Extensometer: The probe extensometers have magnetic settlement targets, which are pneumatically or mechanically attenuated spider magnets with 6 leaf springs in 4.5 to 5.5 inch diameter boreholes. The spider magnets are at 5 feet distances and the extensometer extends 12 feet below the top of glacial till.

4.6.2.2 Instrument Locations

A consolidated location plan for this geotechnical instrumentation is depicted on Figure 4.10 below.

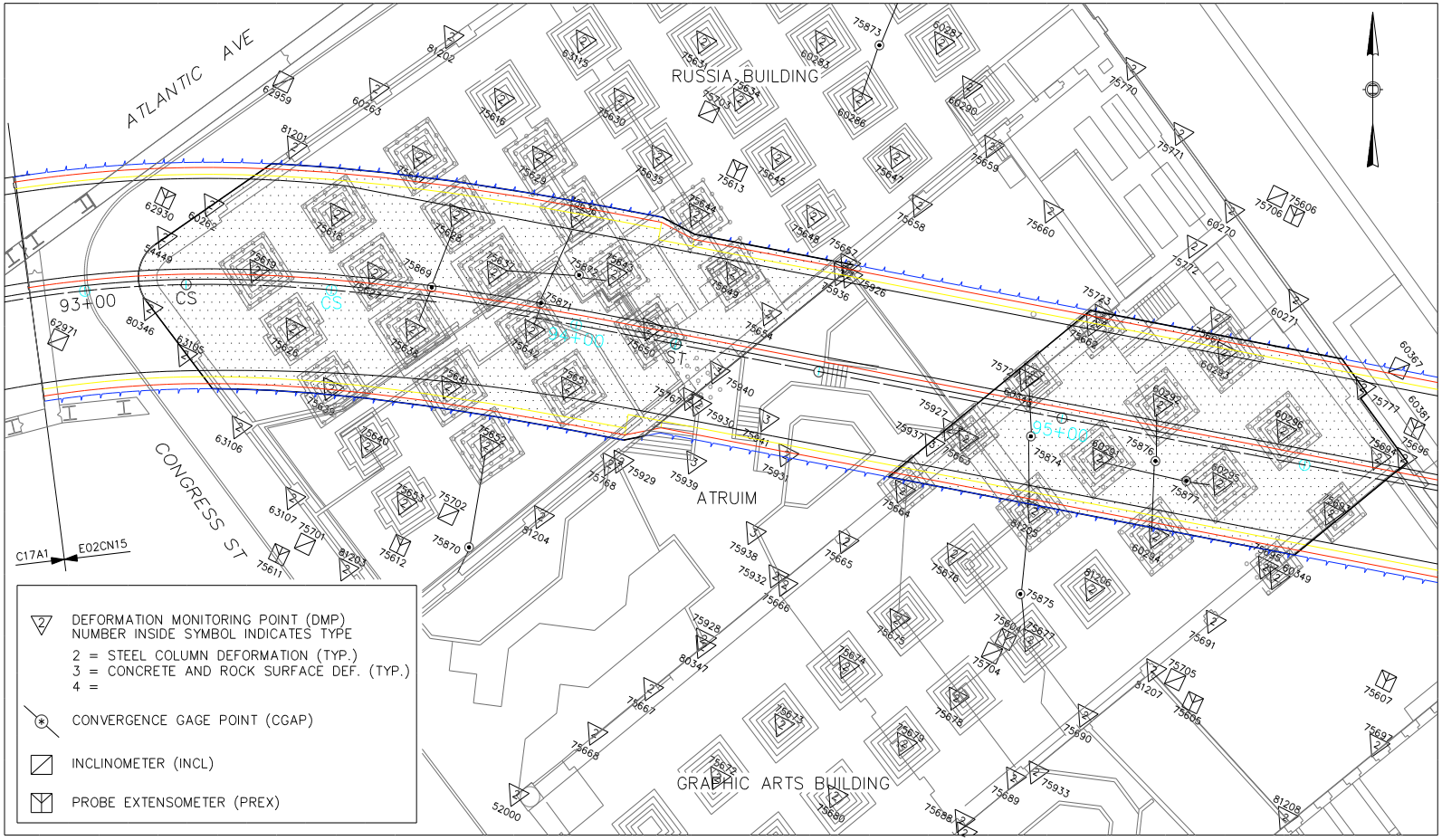

Figure 4.10: Geotechnical Instrumentation Location Plan

4.6.2.3 Instrumentation Monitoring Schedule

The geotechnical instruments were generally read according to the schedule as shown in Table 4.1.

Table 4.1: Instrumentation Schedule for Geotechnical Instrumentation

INSTRUMENT	SCHEDULE
All geotechnical instruments	Instrument verification and formal initial reading; Weekly until the construction of the tunnel; One reading directly before the construction of the tunnel;
DMPs Borros Points Inclinometers Probe Extensometers	*Twice a day* for instrument located within one tunnel diameter front and back of tunnel face *Daily* for instrument located between one and two diameters front and back of tunnel face *Weekly* for instrument located outside of two tunnel diameters until completion of tunnel construction *Monthly* until frozen ground has thawed
Convergence Gages	*Twice a day* when tunnel face is located within one tunnel diameter front and back of building limits *Daily* when tunnel face is located between one and two diameters front and back of building limits *Weekly* when tunnel face is located greater than two tunnel diameters front and back of building limits until completion of tunnel construction *Monthly* until ground has thawed

4.6.3 Instruments to Observe Behavior of the Tunnel Lining, and Between Piles and Lining

4.6.3.1 Instruments

Convergence Bolts: Bolts inserted into the shotcrete lining to measure deformations of the shotcrete lining.

Roof Leveling Points: Devices used to monitor the vertical movement of the tunnel roof centerline. Measurements for both convergence bolts and roof leveling points are made by optical survey methods. Figure 4.11 depicts the arrangement of tunnel convergence and roof leveling arrangements monitoring cross sections (MCS-1) in the inbound and outbound tunnels.

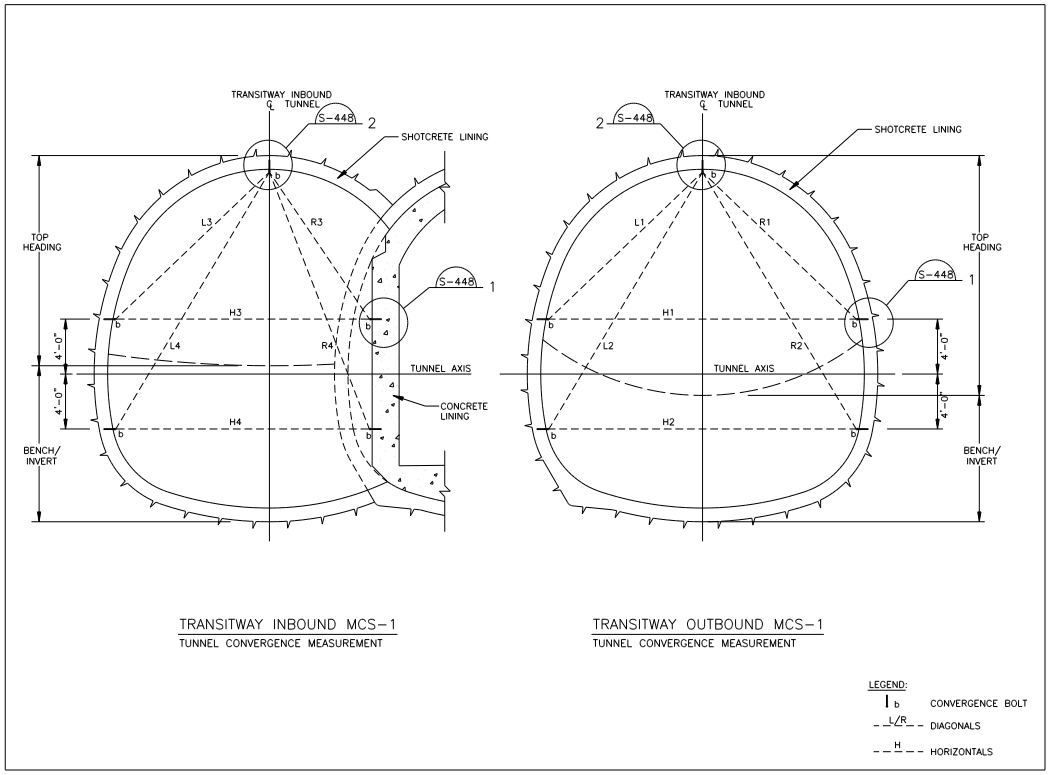

Figure 4.11: Monitoring Cross Section 1 - Convergence Measurement

Concrete (Shotcrete) Pressure Cells: Mercury filled measuring systems ("Gloetzl type") used for monitoring the actual stress in the circumferential direction within the shotcrete lining during and after the excavation process. They are based upon a membrane balanced hydraulic pressure system and are equipped with a re-pressurizing tube to compensate for gaps between cell and shotcrete arisen from the shrinkage in the

shotcrete after application. Shotcrete pressure cells are either equipped with an electric transducer and connected with cables to a remote automatic data logger or are connected with tubing to a change-over box inside the tunnel for readings with a hand or motor operated oil pressure pump.

Ground Pressure Cells: Oil filled measuring systems ("Gloetzl type") used for monitoring the actual stress on the shotcrete lining during and after the excavation process. The ground pressure cells are either equipped with an electric transducer and connected with cables to a remote automatic data logger or are connected with tubing to a change-over box inside the tunnel for readings with a hand or motor operated oil pressure pump. Figure 4.12 depicts the arrangement of ground load cells and concrete pressure cells in monitoring cross sections (MCS-2) in the inbound and outbound tunnels. Figure 4.13 depicts the installation details for the concrete and ground pressure cells.

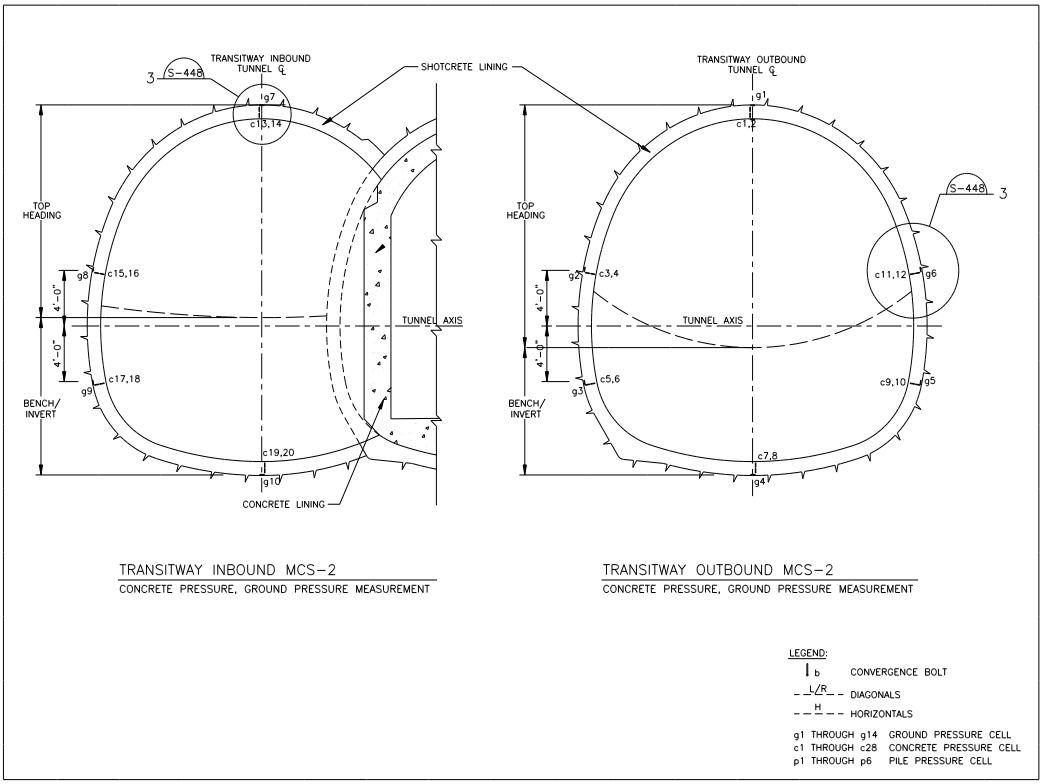

Figure 4.12: Monitoring Cross Section 2 - Concrete Pressure and Ground Pressure

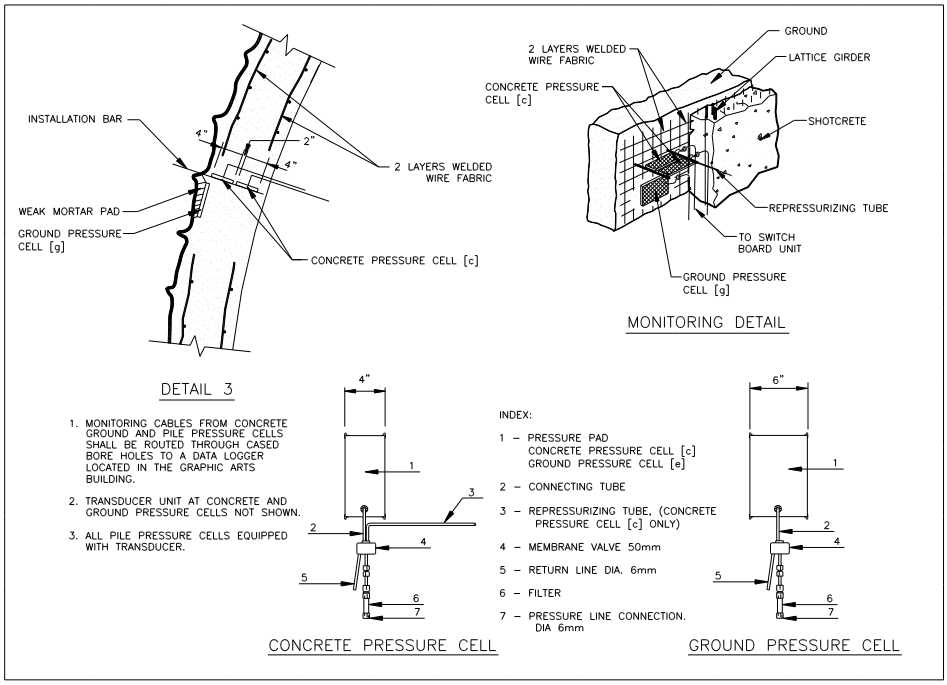

Figure 4.13: Pressure Cell Installation Details

Pile Pressure Cells: Hydraulic fluid filled piston pads installed between the neoprene pad at the bottom of the wood piles and the shotcrete lining to measure the pile load acting on the shotcrete lining after thawing. The pads are equipped with an electric transducer and connected with cables to a remote automatic data logger.

A monitoring cross section for pile pressure monitoring is shown in Figure 4.14. A pile pressure cell detail is shown in Figure 4.15. The PVC backed geotextile and the neoprene pad shown provide separation layers between shotcrete and pile. The purpose of this separation is to minimize transmission of vibrations from tunnel traffic to the buildings. Because of the separation layers, it is expected that the entire pile load will act on the lining and the pile pressure cells will allow for monitoring of those loads.

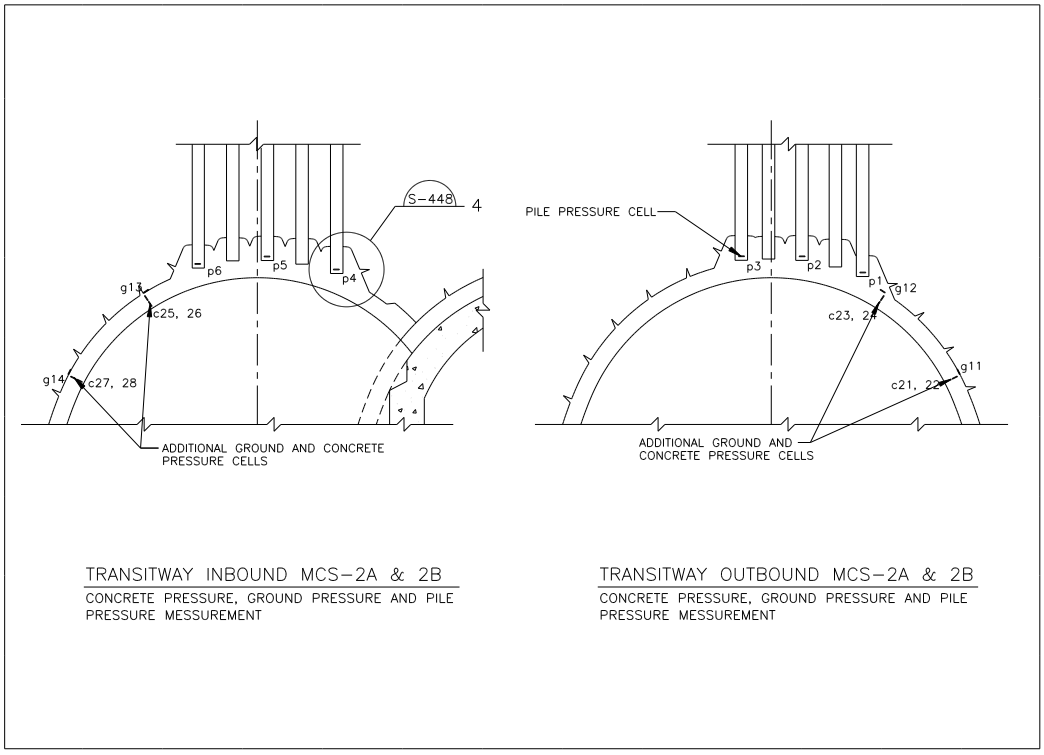

Figure 4.14: Pile Monitoring Cross Section 2A and 2B

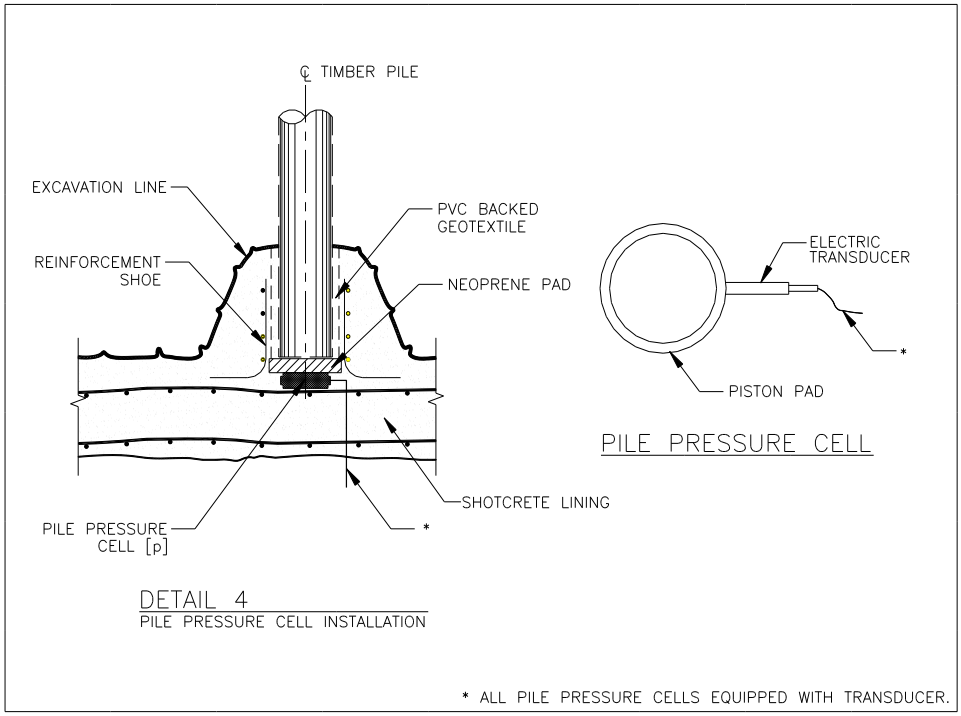

Figure 4.15: Pile Pressure Cell Installation Detail

4.6.3.2 Instrument Locations

Figure 4.16 shows the location of instruments along the tunnel alignment. MCS-1 sections were generally placed in intervals of every 20 feet. Two stress monitoring sections (MCS-2A) and two pile monitoring sections (MCS-2B) were placed within the Graphic Arts Building and in the immediate vicinity of Station 95.20 as shown in the detail in Figure 4.16.

4.6.3.3 Instrumentation Monitoring Schedule

Initial readings for Convergence Bolts and Roof Leveling Points were generally taken within 6 hours after their installation. Initial readings for pressure cells were

generally taken within 24 hours of their installation. Convergence and Roof Leveling Bolts were read as indicated in Figure 4.17.

Pressure cells within the Graphic Arts Building were read with an automatic data logger in hourly intervals. All other pressure cells were generally read according to the frequency indicated in Figure 4.17.

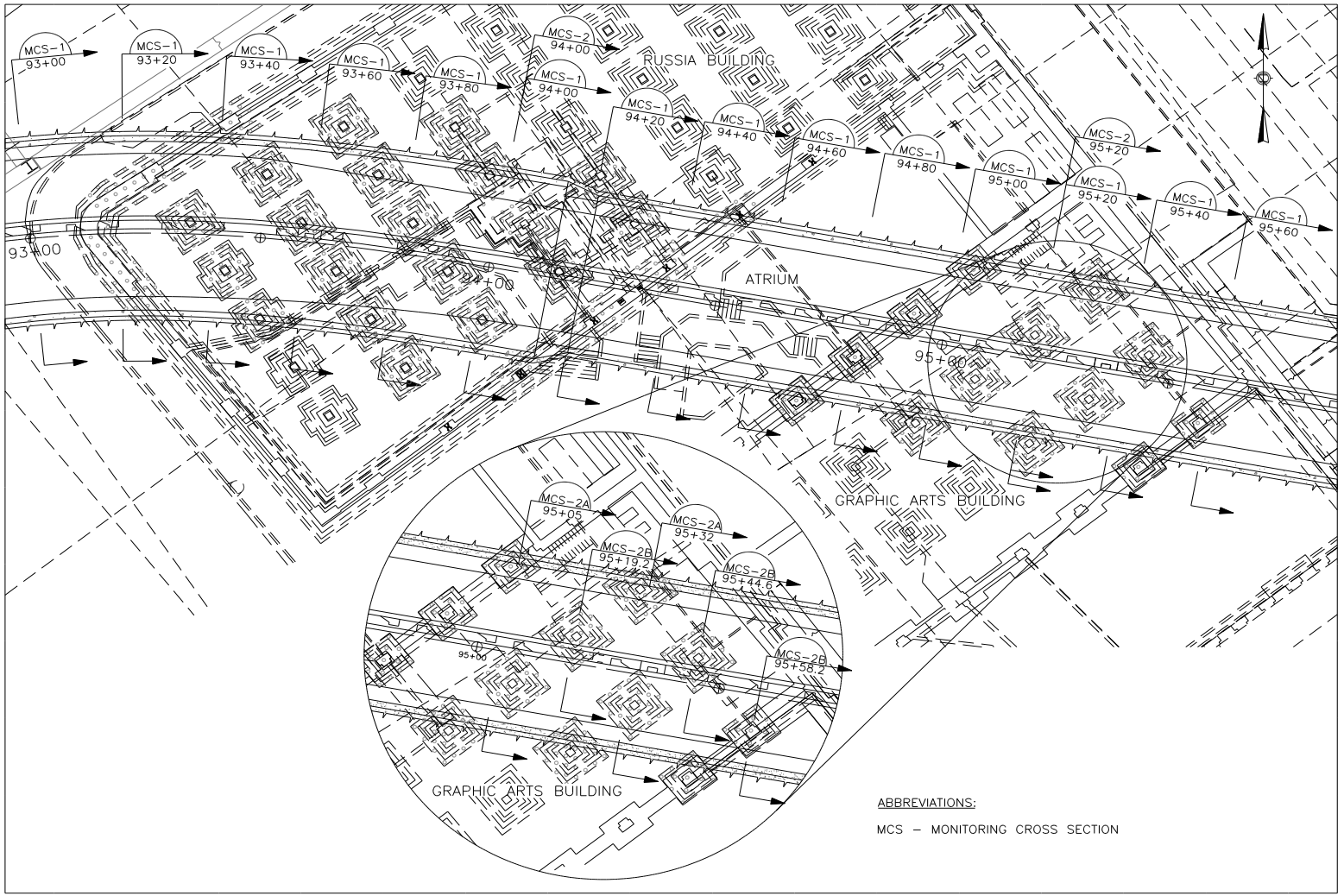

Figure 4.16: Monitoring Cross Sections – Location Plan

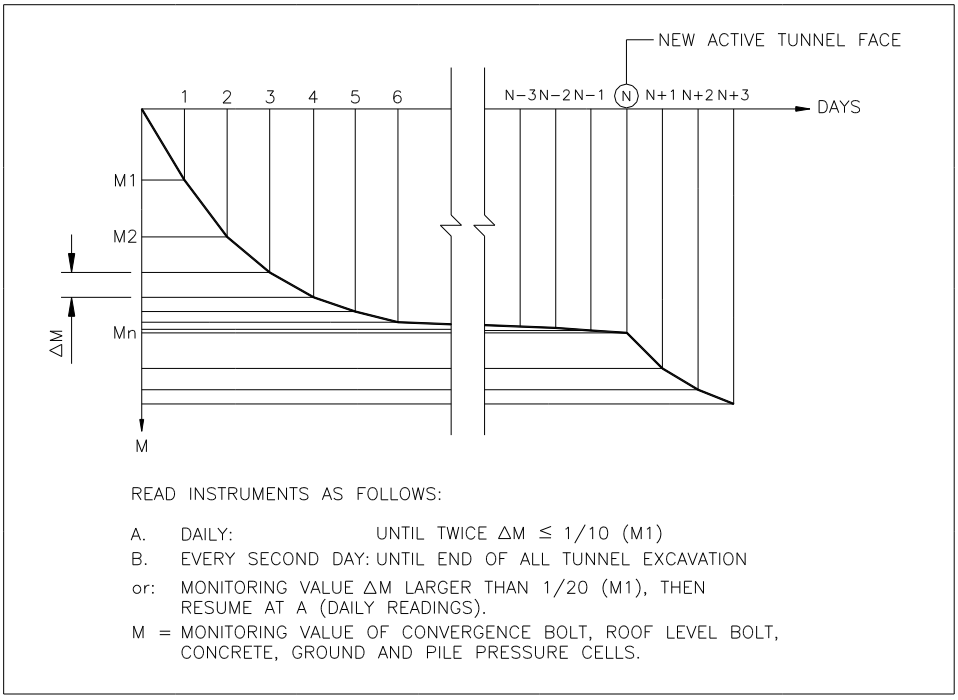

Figure 4.17. Monitoring Schedule

4.6.4 Instrumentation for Temperature Distribution in Frozen Soil

4.6.4.1 Instruments

There were two basic types of temperature monitoring devices foreseen to monitor the temperature distribution in the frozen soil:

Driven Temperature Monitoring Point (DVTP): This is a heavy-duty threaded steel rod with a conical tip and temperature sensor embedded at the tip.

Drilled Temperature Pipe (DTP): This is a 4.5" OD Schedule 40 seamless pipe with a welded base plate.

A schematic section of temperature monitoring is shown in Figure 4.18.

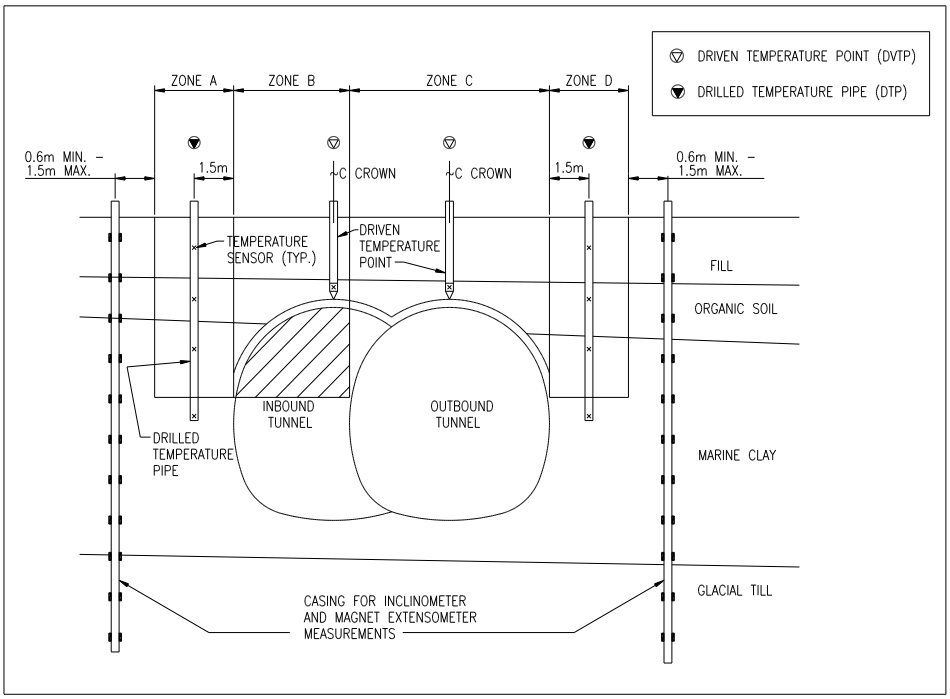

Figure 4.18. Schematic Section of Ground Freezing Monitoring

4.6.4.2 Instrument Locations

Figure 4.19 shows a general location plan of the DVTPs and DTPs to installed in the field according to design. The actual location of temperature points relevant to validation of the modeling at Station 95.20 is provided in later Chapters.

4.6.4.3 Instrumentation Schedule and Readings

The ground temperatures to determine the progress of ground freezing and freeze maintenance were monitored on a daily basis.

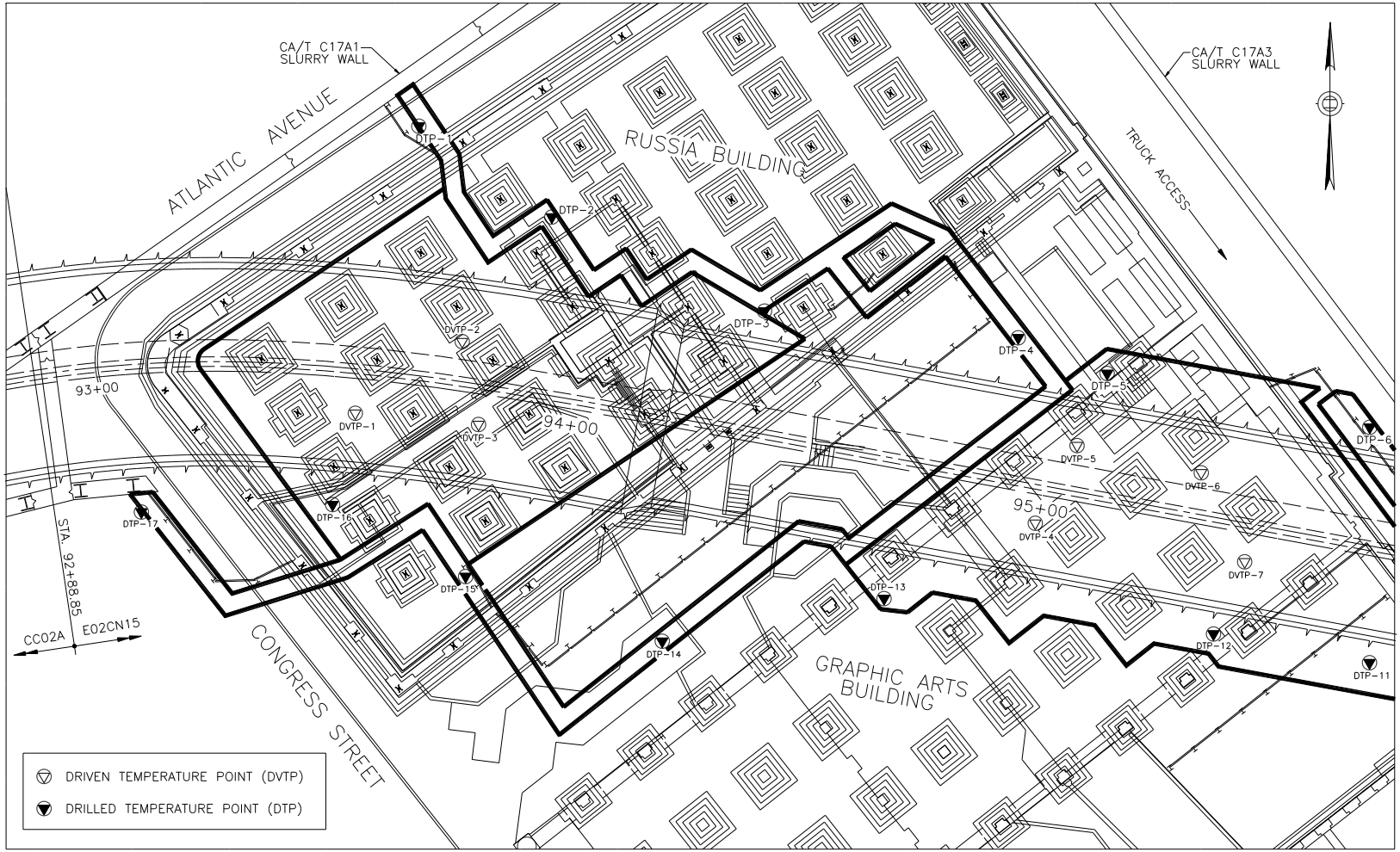

Figure 4.19: Temperature Monitoring Points – Location Plan

Chapter 5: Finite Element (FE) Modeling and 3-D to 2-D Conversion

5.1 General

The finite element modeling has been carried out in two distinct stages based on the purpose and the development of the computations. First, a three-dimensional (3-D) finite element modeling was used to assess ground and frozen soil behavior in general and the impact of tunneling on surface deformations under the Graphic Arts building. Due to the modeling complexity associated with an implementation of piles in 3-D, pile supports were not considered. The 3-D finite element model was further developed to assess the feasibility of an arched frozen soil configuration around the tunnel openings as initially envisioned (see Figure 2.1 in Chapter 2). For tunnel design purposes in terms of lining stresses and associated deformations this frozen soil configuration provided a conservative approach because it relied on a reduced pre-support and underpinning capability of the frozen soil. The stresses, thus the load carrying capability of this frozen soil was assessed in this model. The 3-D modeling bears one important advantage in that the stress redistribution ahead of the tunnel face and behind it can be appropriately assessed in comparison with two-dimensional (2-D) simulations. Without the use of arbitrary simulation measures, stresses and strains in the frozen soil, as they result from the excavation of a 'round' were evaluated. This is an important aspect of the simulation, as the time that it takes to excavate a round until the installation of the shotcrete lining will represent the time that the frozen ground will be unsupported. From these 3-D computations the feasibility of a frozen soil arch was established. The 3-D model was utilized for the design of tunnel construction sequencing and linings.

In a second stage and for the purpose of this dissertation a refined, two-dimensional model was established at Station 95.20 at the Graphic Arts building. This model is refined in that it incorporates a detailed modeling of the wooden piles using interface elements to represent the pile-frozen and unfrozen soil interface. To obtain detailed results a very fine mesh discretization was selected. This refined 2-D model is used in Chapter 6 for model verification and calibration to represent in-situ conditions. It is subsequently used in Chapter 7 to study frozen soil thickness requirements. These simulations rely on the frozen soil-pile interaction for building support.

A 2-D model has to rely on arbitrary simulation techniques to represent the three-dimensional stress redistribution and stress relief around the tunnel face that accompanies the tunnel excavation and support. This work uses the so-called "softening approach" to achieve this effect. According to this approach the modulus of elasticity of the material to be excavated in a round is reduced from its original value. With this reduction a pre-deformation of the surrounding ground is achieved. The factor with which the original material elastic modulus is reduced is referred to as the "softening factor" S. This softening factor was derived by a comparison of surface settlements of the 3-D model with surface settlements determined from a 2-D model. For this purpose an intermediate 2-D FE model was developed with the same geometrical configurations of the strata and frozen soil arch as used for the 3-D analyses. The same material parameters were used in both models.

This Chapter details the derivation of the softening factor S and describes the simulation techniques for excavation and support sequencing and constitutive material

laws used. The softening factor derived is then utilized in Chapter 6 for model verification and in Chapter 7 for the analysis of the various frozen soil configurations for the proposed frozen soil-pile-tunnel support system.

The FE program ABAQUS (ABAQUS, Inc., 2002) was utilized for the three-dimensional simulations, while the program Phase2 (RocScience, Inc., 2002) was utilized for the two-dimensional modeling. Both programs feature element types intended for the simulation of solids, i.e. the ground as well as the shotcrete structural tunnel supports.

Within ABAQUS rectangular (element type C3D20R) and triangular prisms (element type C3D15) are used for representation of the ground, and curved shell elements (element type S8R) are used for the linings.

Phase2 utilizes plane strain triangular elements for the representation of the ground and (Timoshenko) beam elements for the liners. The vertical boundaries are generally constrained in the horizontal direction and the horizontal boundaries in the vertical direction.

Within ABAQUS, the Drucker-Prager constitutive model is used to represent strength of both frozen and in-situ soils, whereas in Phase2 a Mohr-Coulomb failure criterion is implemented. In both cases the modeling does not account for the time dependent creep behavior of the frozen soil mass. However, this frozen soil characteristic is estimated for use in the detailed two-dimensional model in Chapters 6 and 7.

5.2 Soils and Soil Properties

Detailed descriptions of soil properties have been provided in Chapter 4. Material parameters used in the analyses were derived from laboratory testing on unfrozen and frozen soils (Mueser Rutledge Consulting Engineers, 1998). These are summarized in Table 5.1.

Table 5.1: Material Properties Utilized in the Numerical Modeling

Soil Type / Tunnel Lining	Friction Angle φ [°]	Shear Strength [MPa]	Unit Weight γ [MN/m^3]	Lateral Earth Pressure Coeff. K_0 [-]	Elastic Modulus E [MPa]	Poisoin's Ratio ν [-]
Fill	33	0	0.01922	0.50	47.9	0.35
Frozen Fill	0	1.440	0.01922	0.50	239.4	0.35
Organic Deposits (Clays. Silts)	0	0.036	0.01762	0.50	11.97	0.45
Frozen Organic	0	0.860	0.01762	0.50	239.4	0.25
Marine Clay	0	0.048	0.01874	0.75	23.94	0.45
Frozen Clay	0	1.130	0.01874	0.75	311.2	0.25
Glacial Till (granular)	37	0	0.02000	0.43	167.6	0.30
Shotcrete ("green")	-	-	0.02500	-	10,000.0	0.17
Shotcrete (hardened)	-	-	0.02500	-	27,000.0	0.17

5.3 Finite Element Modeling Analyses

5.3.1 Finite Element Models

Each of the models presented here and in Chapter 6 is established such that:

- The mesh appropriately models the ground strata in the tunnel area and reflects the geometry of tunnel cross section and incorporates the structural support elements.
- The appropriate geotechnical and structural material properties are assigned to the individual elements.
- The modeling of excavation and support installation is accomplished in stages by removal (3-D) or softening with subsequent removal (2-D) of ground elements and addition of elements representing the shotcrete initial and final linings. In particular, the mesh is set up to simulate the intended construction sequence closely and to assess the induced displacements and stresses of the ground/lining.

The 3-D model is located below the Graphic Arts building, at which location high vertical building loads are combined with greater overburden. The vertical alignment of the tunnel is assumed to be horizontal. The 2-D model is established at Station 95.20, approximately beneath the center of the Graphic Arts building. At this station an array of instruments is available for back-calculations.

Coarser mesh grading is generally used in the vicinity of the model boundaries to keep the number of elements and therefore the computation time economic. In the 3-D model a finer mesh is used towards the center to model the excavation rounds in their

length of 0.8 m as prescribed in the design. All results discussed herein are obtained from the center of the model (approximate Station 95.20). The total length of the 3-D FE model is 28.4 m and this is subdivided along the tunnel's longitudinal axis into the following sections: 6m, 4m, 2m, 1m, 0.8m, 0.8m, 0.8m, 1m, 2m, 4m and 6m. The FE models for the Graphic Arts building are shown for the 3-D model in Figure 5.1 and for the 2-D model at Sta. 95.20 in Figure 5.2.

Both programs permit input of a geostatic stress field as an initial condition. Using a consistent set of geotechnical properties, the initial conditions establish the initial equilibrium from which loading, freezing and tunneling is modeled. Deformations associated with the geostatic stress field, freezing and pile loading of the analysis are set as reference stages prior to the onset of tunneling.

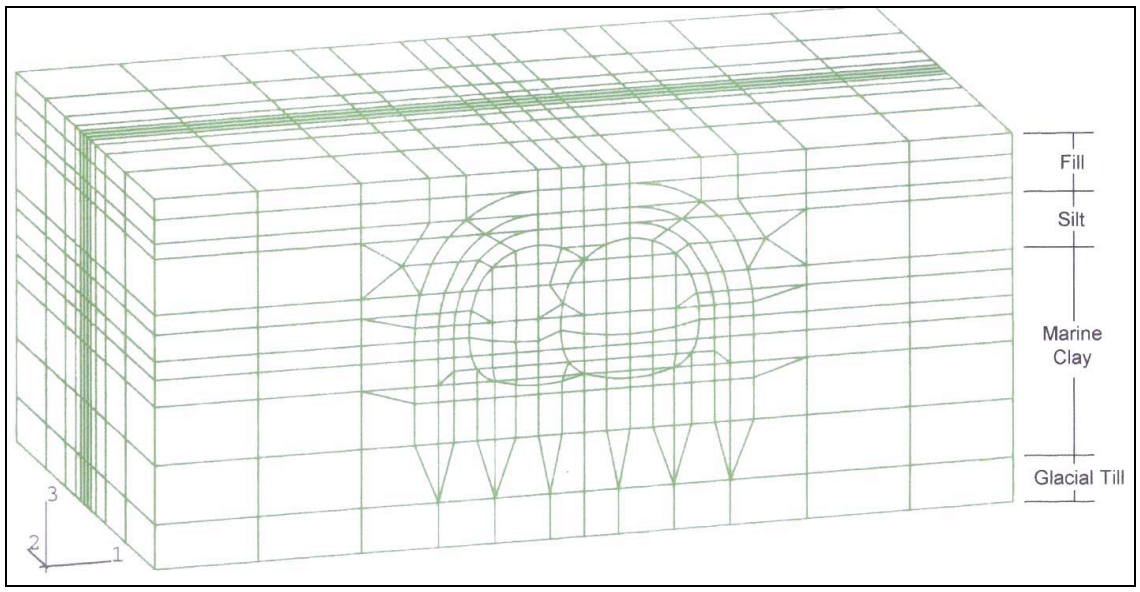

Figure 5.1: 3-D Finite Element Model at Graphics Arts Building

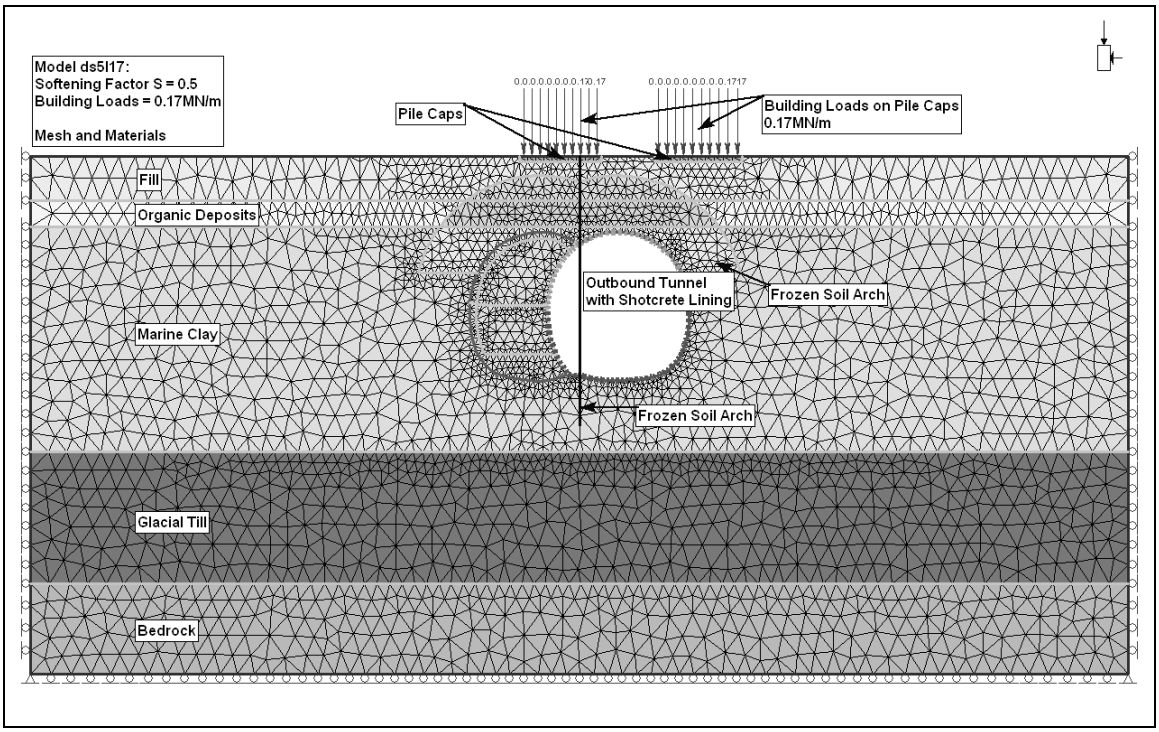

Figure 5.2: 2-D Finite Element Model With Outbound (OB Tunnel) Excavated - Graphics Arts Building at Sta. 95.20

5.3.2 Assumptions for FE Modeling

In the initial unfrozen condition, building loads are transferred by the timber piles into the ground. It is assumed that the piles are end-bearing and that the loads are transferred onto a layer of desiccated clay at the interface between the Organic Silt and Marine Clay strata. The model is balanced for this situation, i.e., there are no deformations associated with this loading condition. After ground freezing, the building loads are transferred onto the frozen ground. Based on building load calculations, a distributed pressure of 0.30 MPa is transferred to each pile cap location within the 3-D FE model. In the 2-D FE model however, and because of the skew of the alignment vs. pile cap arrangement, an adjustment has to be made for this load magnitude. The tunnel

alignment and arrangement of pile caps at the Graphic Arts building is shown in Figure 5.3. This figure shows the 2-D FE calculation section at Station 95.20 at a unit model width (depth) of 1 meter. In the center of the alignment the 2-D section cuts a 1 m unit model depth through the pile cap. Based on the geometrical configuration of the square pile cap at that location the 2-D model incorporates a pile cap width of 4.35 m at a unit model depth of 1 m. The associated pile load or cap pressure for this area is then calculated to 0.17 MPa (see Figure 5.2). Thus the 2-D FE modeling assumes an endless strip, rather than localized cap pressure and thus provides a conservative load assumption.

Freezing of the soil is modeled by increasing the stiffness and altering other soil properties for the elements forming the frozen body in the FE mesh according to material parameter values of Table 5.1.

In the 3-D model tunnel excavation is modeled using two different approaches throughout the analysis. In the center regions of the model, where a fine mesh is utilized, excavation is modeled by first removing the elements inside the tunnel. Once an equilibrated solution has been obtained, the shotcrete elements are installed. In regions with a coarser FE mesh, excavation is modeled by first reducing the element stiffness inside the tunnel. Then in the next step, the shotcrete elements are installed and the soil elements are removed. This approach is selected because at locations of coarser mesh grading the removal of elements within the excavation section would result in an unsupported length of up to 6 m. This in turn does not comply with the excavation sequencing (short rounds of 0.8 m in the top heading of the actual tunneling as described in Chapter 4.5.1, Figure 4.7). It would cause an overstressing and yielding of the above

lying ground and result in an overestimate of deformations, and potentially lead to instabilities in the simulations. A parameter study has been performed to determine an adequate reduction so that the model produces the same behavior during excavation in areas with fine and coarse elements.

Shotcrete application is modeled by activating shotcrete structural elements and "tying" them to the soil (shotcrete and soil elements at the tunnel circumference use common nodes). Therefore the shotcrete and surrounding soil form an interacting load carrying system.

The final shotcrete lining elements are "pinned" to the initial shotcrete lining elements, i.e., associated nodes are free to rotate; translations are restricted to a common value.

In the 2-D FE analyses of this Chapter the softening factor has been varied to produce deformations predicted within the center of the 3-D model and thus to incorporate the three-dimensional stress state and pre-deformation at the face. The use of the softening approach is a modeling technique commonly applied in tunnel designs to estimate ground deformations and design tunnel linings in 2-D modeling (Mohr and Pierau, 2004, and Wittke, 1999). Kielbassa and Duddeck (1991) provide an overview of stress-strain conditions at the tunneling face comparing three-dimensional and two-dimensional analyses based on a systematic study and literature review.

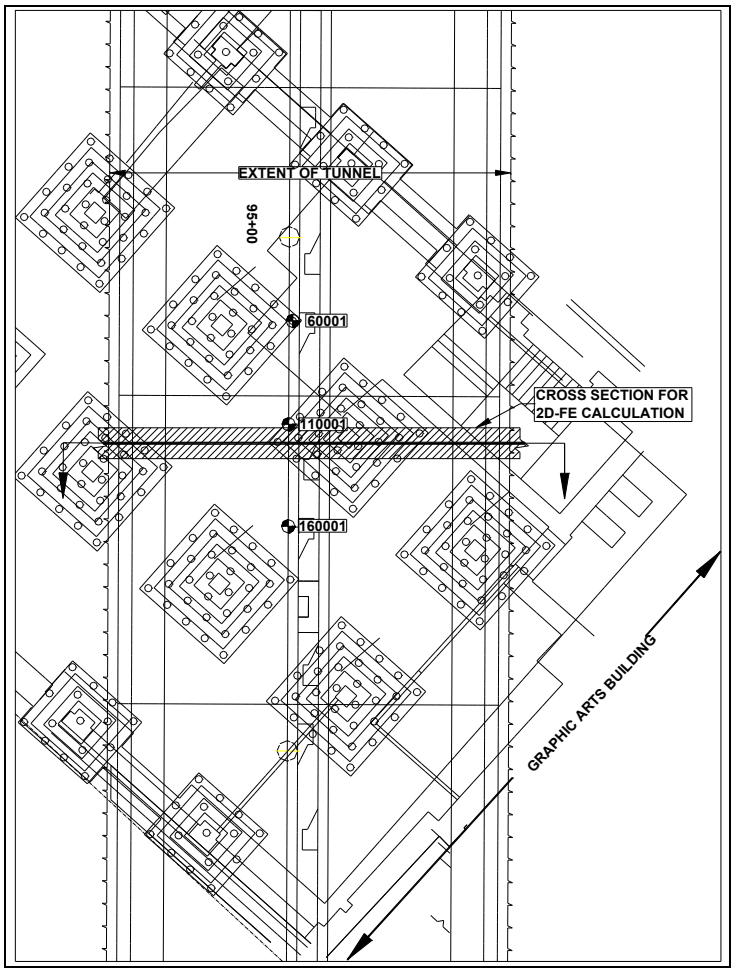

Figure 5.3: Element vs. Pile Cap Locations – Graphic Arts Building

5.3.3 Constitutive Models

Both the Drucker-Prager and Mohr-Coulomb failure criteria are commonly used in soil mechanics. A relationship between the two constitutive models is provided here.

The yield surface according to the Drucker-Prager criterion is given by:

$$F(\sigma_{ij}) = \alpha I_1 + \sqrt{I_2} - \beta \tag{5.1}$$

In which I_1 and I_2 are the first and second stress invariants, which can be written in terms of principal stresses as follows:

$$I_1 = \sigma_1 + \sigma_2 + \sigma_3 \tag{5.2}$$

$$I_2 = \frac{1}{6}\left[(\sigma_1 - \sigma_2)^2 + (\sigma_2 - \sigma_3)^2 + (\sigma_3 - \sigma_1)^2\right] \tag{5.3}$$

The coefficients α and β can be expressed in terms of Mohr-Coulomb parameters, cohesion (c) and internal angle of friction (φ). For values of c and φ obtained from a triaxial compression test, i.e., $\sigma_1 > \sigma_2 = \sigma_3$,

$$\alpha = \frac{2\sin\varphi}{\sqrt{3}(3 - \sin\varphi)} \tag{5.4}$$

and

$$\beta = \frac{6c\cos\varphi}{\sqrt{3}(3 - \sin\varphi)} \tag{5.5}$$

The yield surface for the Drucker-Prager failure criterion is cone shaped and yield occurs at:

$$F(\sigma_{ij}) = 0 \tag{5.6}$$

Figure 5.4 shows how the failure cone of the Drucker-Prager failure criterion compares with the Mohr-Coulomb envelope in three dimensional principal stress space. Figure 5.5 clarifies this comparison using a two-dimensional representation. It can be seen that the Drucker-Prager criterion generally allows greater stress before yield, although under special conditions it reduces to the Mohr-Coulomb criterion.

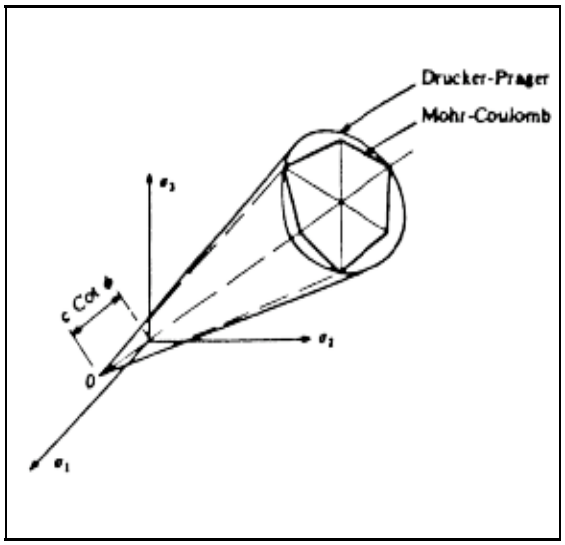

Figure 5.4: Geometrical Representation of the Mohr-Coulomb and Drucker-Prager Yield Surfaces in the Principal Stress Space

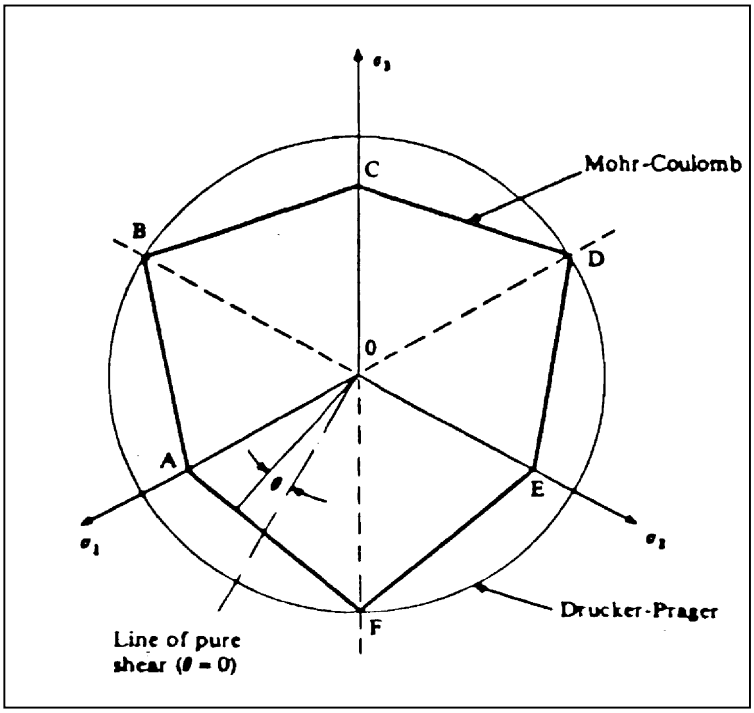

Figure 5.5: Two-Dimensional Representation of the Mohr-Coulomb and Drucker-Prager Yield Criteria

5.3.4 Excavation and Support Sequence

The excavation and support sequence is modeled in a series of steps in the analyses. Each individual manipulation in the model, such as change of material properties or removal and addition of elements to simulate excavation and support, is performed in different stages. The stages are described as follows and are depicted in Figures 5.6 through 5.9 for the outbound (OB) tunnel excavation and support. The same staged approach is utilized for the inbound (IB) tunneling.

Stage 1 through 4: Geostatic stress conditions, freezing of the ground, i.e. changing the stiffness and material parameters of soils forming the frozen arch, insertion of pile caps and loading of the model with pile loads.

Stage 5: Excavation of top heading (TH) of the first, OB tunnel. In 2-D the elastic modulus of the soil within the TH is reduced using a softening factor S (varies for the purpose of this modeling). In 3-D the crown elements are removed.

Stage 6: In 2-D application of shotcrete in the TH and the temporary invert of the OB tunnel and removal of the first set of softened elements. In 3-D insertion of shotcrete lining elements.

Stage 7: Excavation of bench and invert (B/I) of the OB tunnel. In 2-D reduction of the elastic modulus of the soil within the B/I using a softening Factor S. In 3-D the B/I elements are removed.

Stage 8: In 2-D application of shotcrete in the B/I of the OB tunnel and removal of softened elements. In 3-D insertion of shotcrete lining elements in B/I.

Stage 9: During this stage the final lining and the middle supporting column is inserted into the model.

Stages 10 through 15: Similar to Stages 5 through 8 the inbound tunnel is excavated and supported and the final lining is inserted in stage 15.

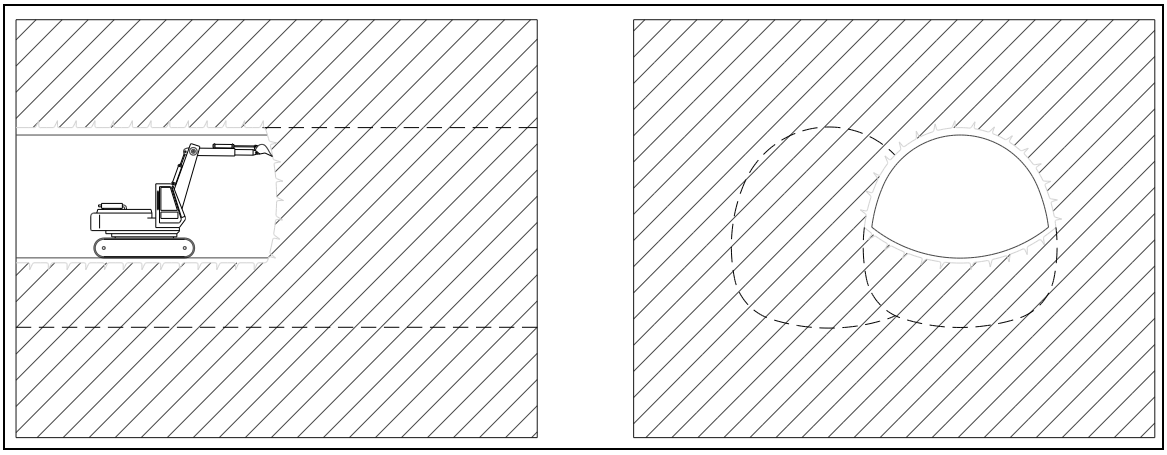

Figure 5.6: Stage 5 – Excavation OB Tunnel TH

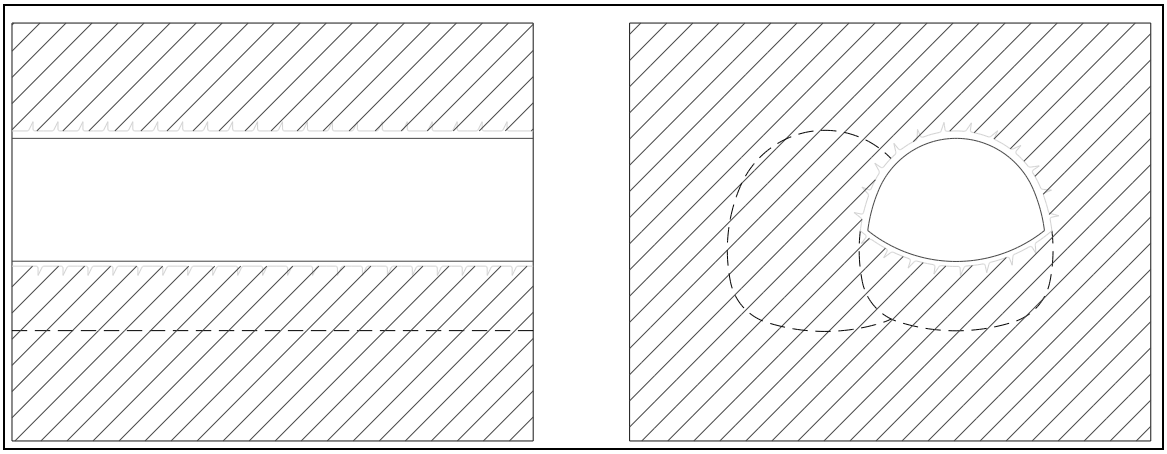

Figure 5.7: Stage 6 – OB TH Excavated and Shotcrete Lining Installed

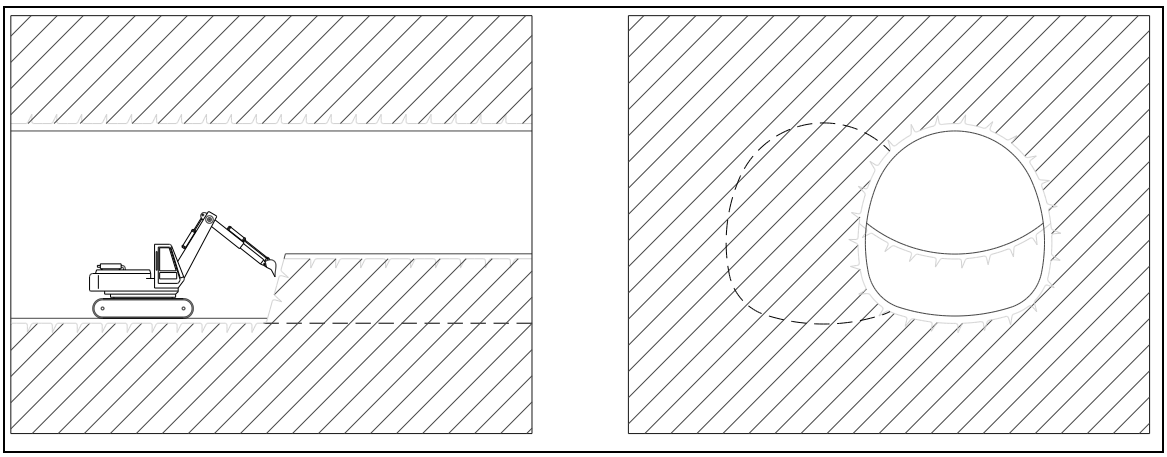

Figure 5.8: Stage 7 – Excavation OB Tunnel B/I

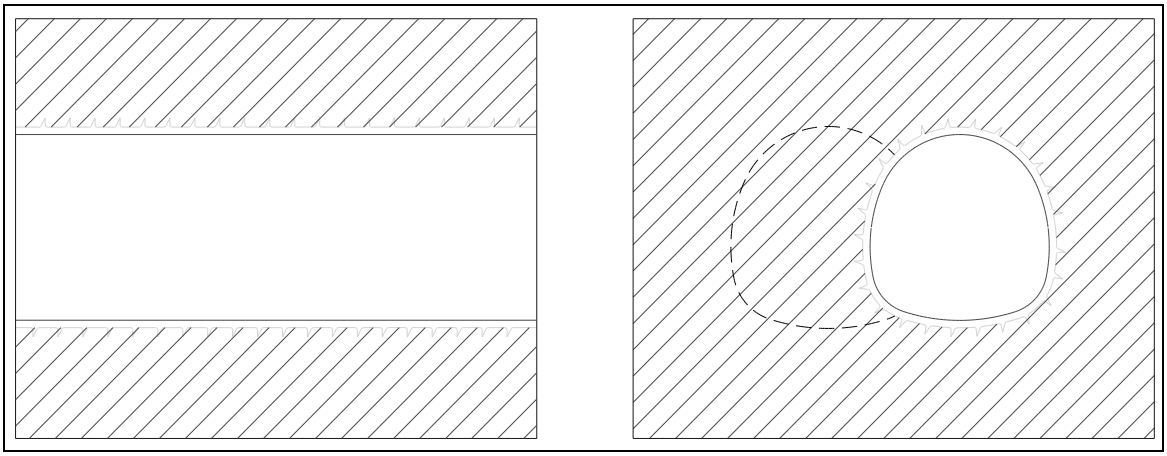

Figure 5.9: Stage 8 – OB Tunnel B/I Excavated and Shotcrete Lining Installed

5.3.5 3-D FE Results

5.3.5.1 General

The general behavior in terms of stresses in the frozen and unfrozen soil is described along with surface deformations that occur in the center of the model at and around Sta. 95.20.

As the given boundary conditions at the front edge of the model do not allow for full redistribution of load due to tunneling in the vicinity of the boundaries, displacements at the first few stages of the analyses may be overestimated. For the same reasons, elements at the rear edge of the model act overly stiff, and therefore, displacements at the last few stages of the analyses may be underestimated. The results of the analyses, given at the center part of the model, are free of boundary effects.

5.3.5.2 Stresses In The Frozen Soil

The material model utilized for modeling the frozen soil arch is a Drucker-Prager material model. Tension and compression stresses above the elastic limit will cause plastic strains to develop. For the construction sequence analyzed in the model however, no yielding or plastic strains developed. In other words, the actual stresses in the frozen arch are lower than permissible stresses for the frozen soil. For the Graphic Arts building vertical stresses S33 in the overall model are shown in Figure 5.10, for the frozen ground in Figures 5.11 and 5.12.

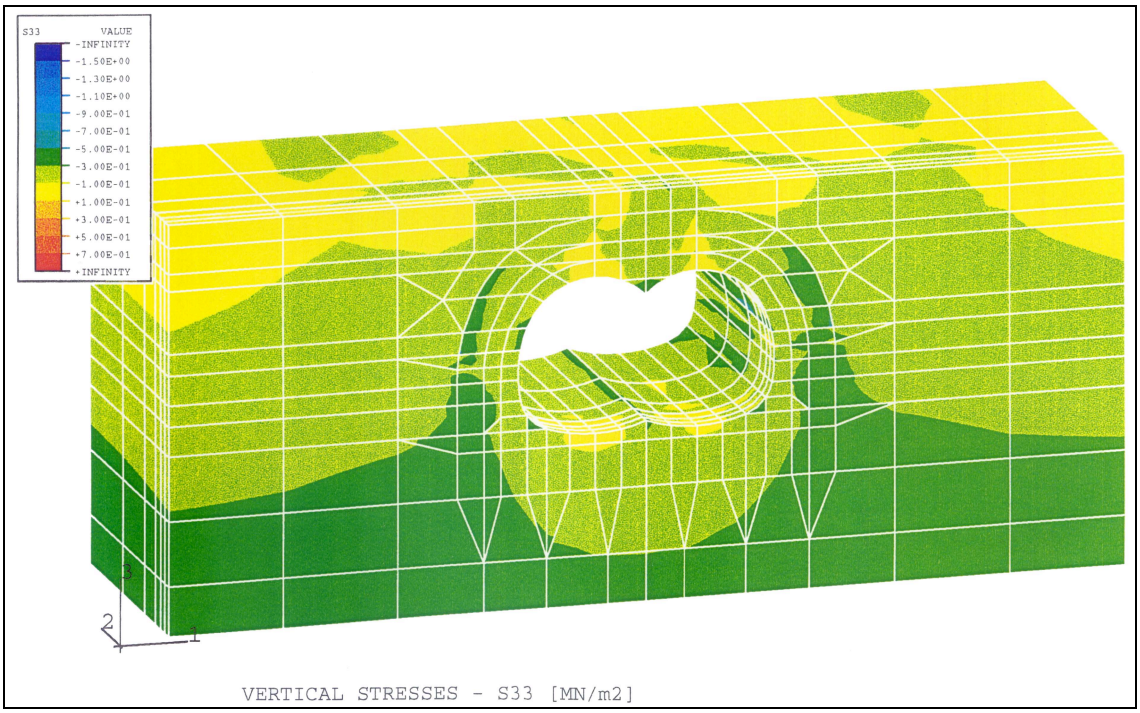

Figure 5.10: Vertical Stresses After Excavation and Support of OB and IB Tunnel – Graphic Arts Building

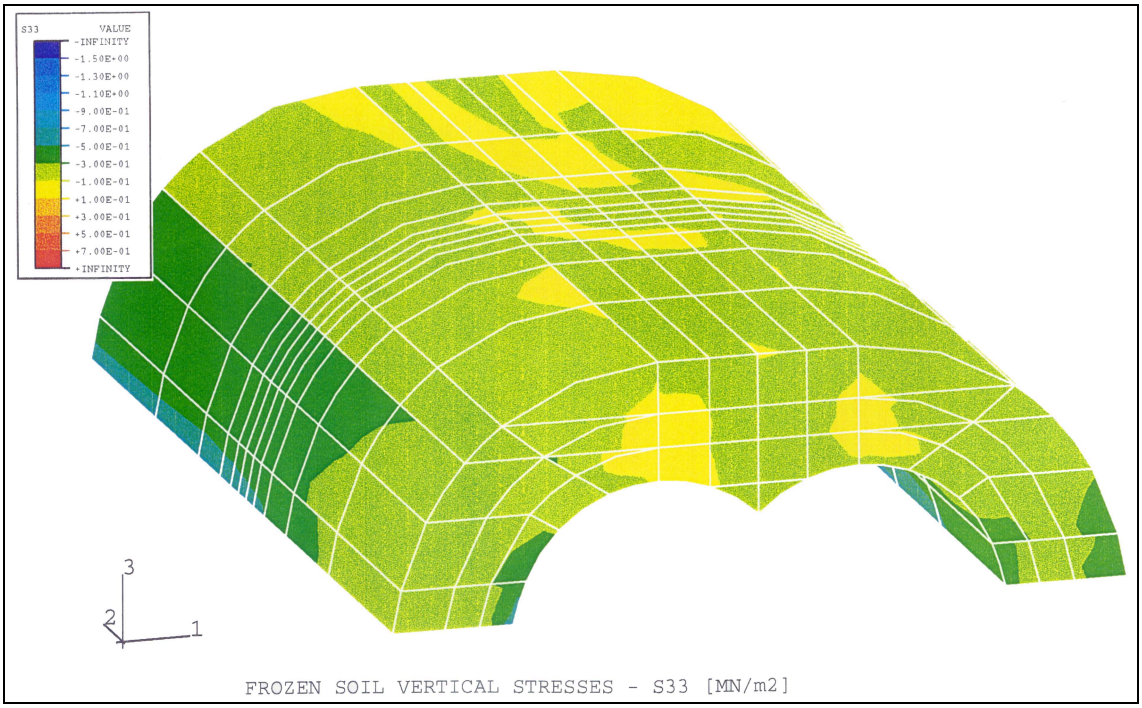

Figure 5.11: Vertical Stresses in Frozen Arch After Excavation and Support of OB and IB Tunnel – Graphic Arts Building (Top View)

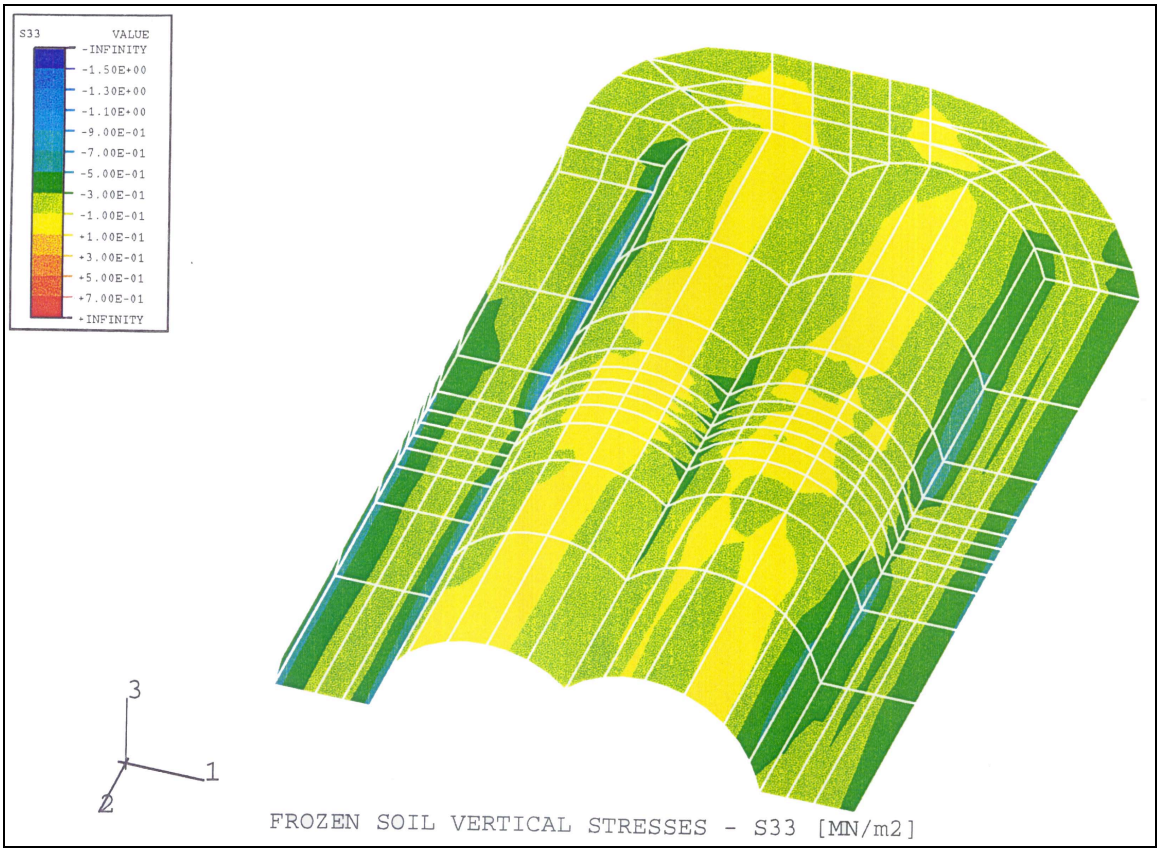

Figure 5.12: Vertical Stresses in Frozen Arch After Excavation and Support of OB and IB Tunnel – Graphic Arts Building (View from Below)

5.3.5.3 Surface Settlements

The increase in displacement for nodes at the surface (Graphic Arts Building) is shown in Figure 5.13 through 5.15. Displacements are shown for nodes 60001, 110001 and 160001 (see Figure 5.3 for node locations).

The three plots characteristically show the settlement ahead of the progressing tunnel face and an asymptotic trend towards a maximum settlement which occurs approximately 1.5 to 2 tunnel diameters behind the excavation face during excavation of the top heading. This is consistent with observations in the field as shown in Chapter 6.

The decrease in settlement during excavation of the invert of the first tunnel is interpreted as a "squeezing " effect of the tunnel lining after the temporary TH invert is removed, resulting in an upward movement in the finite element model.

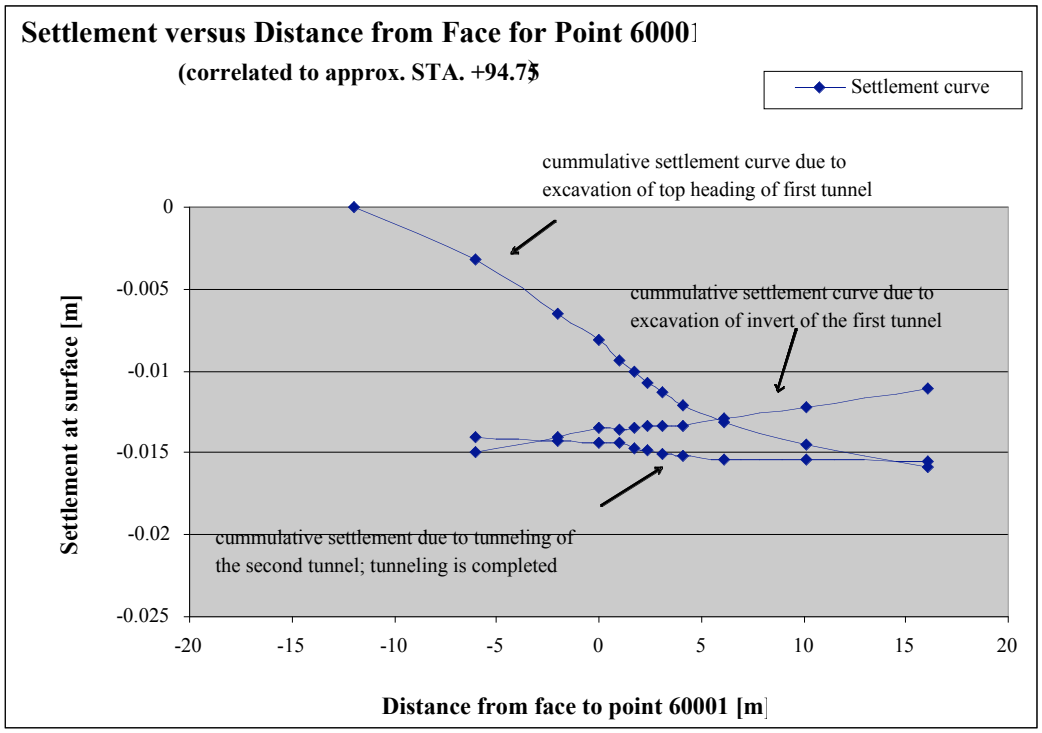

Figure 5.13: Settlement Under the Graphics Arts Building for Point 60001

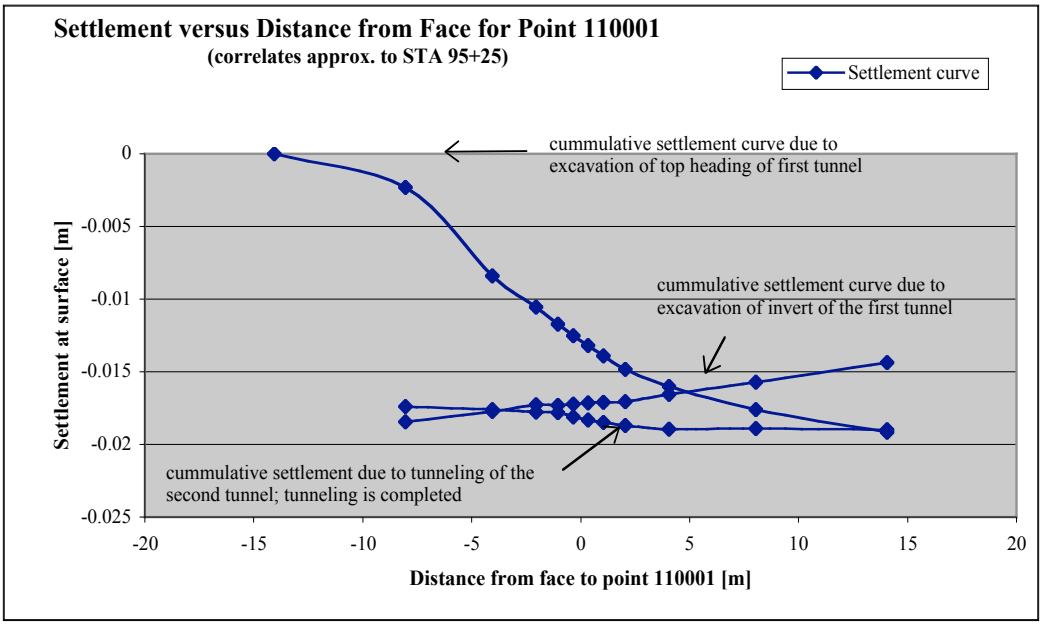

Figure 5.14: Settlement Under the Graphics Arts Building for Point 110001

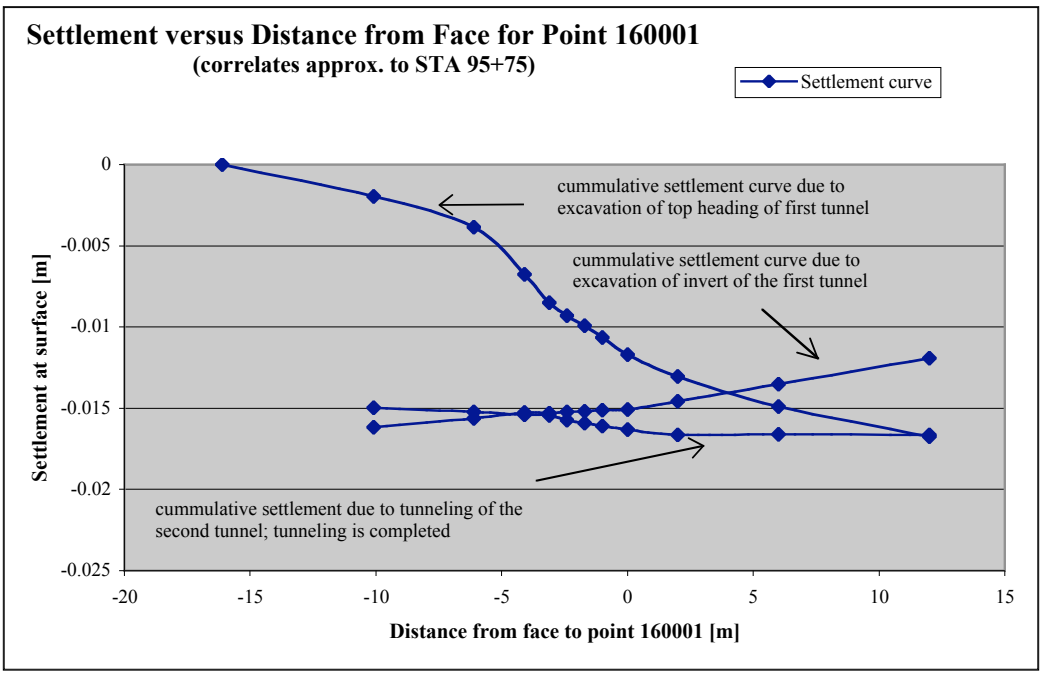

Figure 5.15: Settlement Under the Graphics Arts Building for Point 160001

5.3.6 Derivation of Softening Factor (S)

The three dimensional model was compared in terms of calculated surface displacements with the 2-D model presented in Figure 5.2. The same assumptions regarding frozen arch extent, frozen and unfrozen material parameters, and structural materials of the shotcrete linings were employed. Loading conditions on the pile caps were applied as described in Chapter 5.3.2, resulting in pile cap pressures of 0.17 MPa at Station 95.20. The settlement behavior of Figure 5.14 at Station 95.25 was selected for the 2-D vs. 3-D comparisons, because of its close proximity to Station 95.20. The comparisons were carried out for the excavation of the OB tunnel only. The modeling of the OB tunnel is "free" of any other modeling effects that are introduced by inclusion of the final structural lining.

To assess the sensitivity of pile cap loading and further validate the use of a pile cap load of 0.17 MPa, a pile cap pressure of 0.09 MPa or about 50% of the calculated pressure induced by the column loads was implemented in this parametric study. The results of this study are portrayed in Figure 5.16.

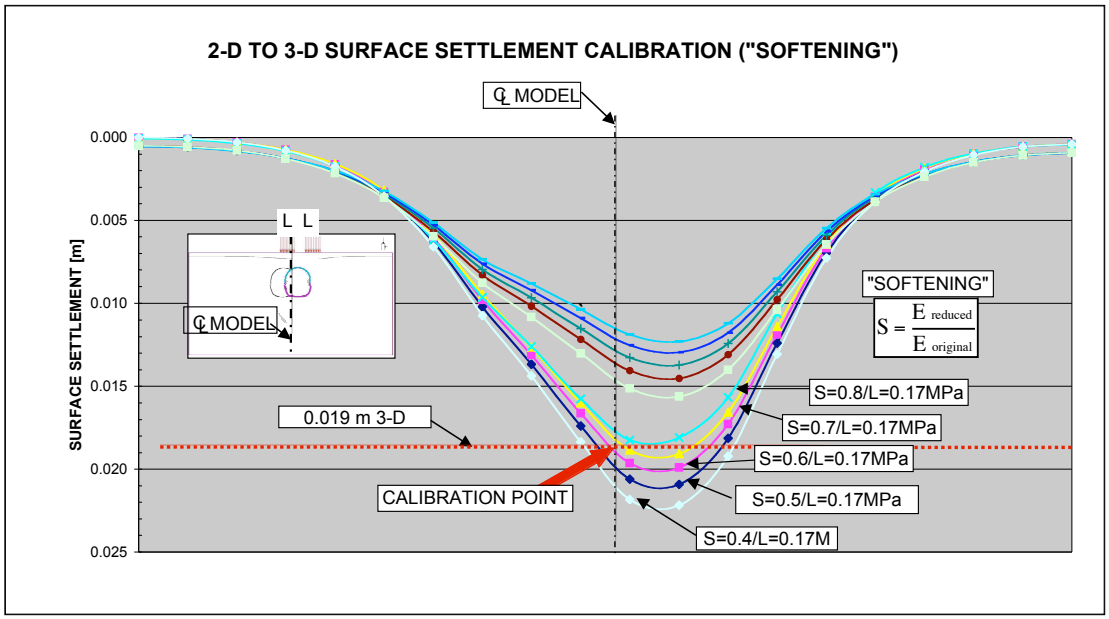

Figure 5.16: Evaluation of Softening Factor for 3-D to 2-D Model Conversion

The graphs in Figure 5.16 are surface settlement troughs for varied softening factors S. S is defined as the ratio between the reduced elastic modulus and the original elastic modulus of the material encountered in the tunnel heading: $S=E_{reduced} / E_{original}$. There are two clusters of settlement troughs, one for a pile cap load of L=0.17 MPa and one for a pile cap load of L=0.09 MPa. For the cluster of settlement troughs associated with L=0.17 MPa the softening factors for the individual settlement troughs are labeled and include, going from the deepest trough to the shallowest, 0.4, 0.5, 0.6, 0.7 and 0.8. All troughs are graphed vs. the centerline of the model. The graph contains surface settlement values on the ordinate. From the 3-D FE surface settlements at Station 95.25 the maximum settlement for the OB tunneling at the tunnel centerline was found to be 0.019 m. A dotted, horizontal line has been graphed at that elevation. This line intersects the centerline of the tunnel in midst between the surface settlement troughs produced by

S=0.6 and S=0.5. This intersection is defined as the calibration point. A surface settlement trough that would intersect this calibration point would be produced by a softening factor of approximately S=0.55. It can be further seen that column loads that would induce pile cap stresses of 0.09 MPa clearly underestimate the surface settlement magnitudes. This further justifies the use of 0.17 MPa as the pile cap load in further analyses. This load along with a softening factor of S=0.55 was utilized in further studies related to model calibration in Chapter 6 and the investigations of Chapter 7. The factor of 0.55 utilized in 2-D FE modeling to represent 3-D conditions compares well with the literature values reported and studies developed (Mohr and Pierau, 2004 and Coulter and Martin, 2004).

The deformed model following OB tunnel excavation with pile cap loads of 0.17 MPa utilizing a softening factor of S=0.50 is displayed in Figure 5.17.

The analyses of stresses in the ground and frozen soil, and assessment of surface displacement in these simplified models indicate the feasibility of a limited frozen soil arrangement for tunneling and building underpinning. More detailed analyses in Chapters 6 and 7 implement the piles as part of a hybrid frozen soil-pile-tunnel lining support system and attempt to determine minimum frozen soil requirements.

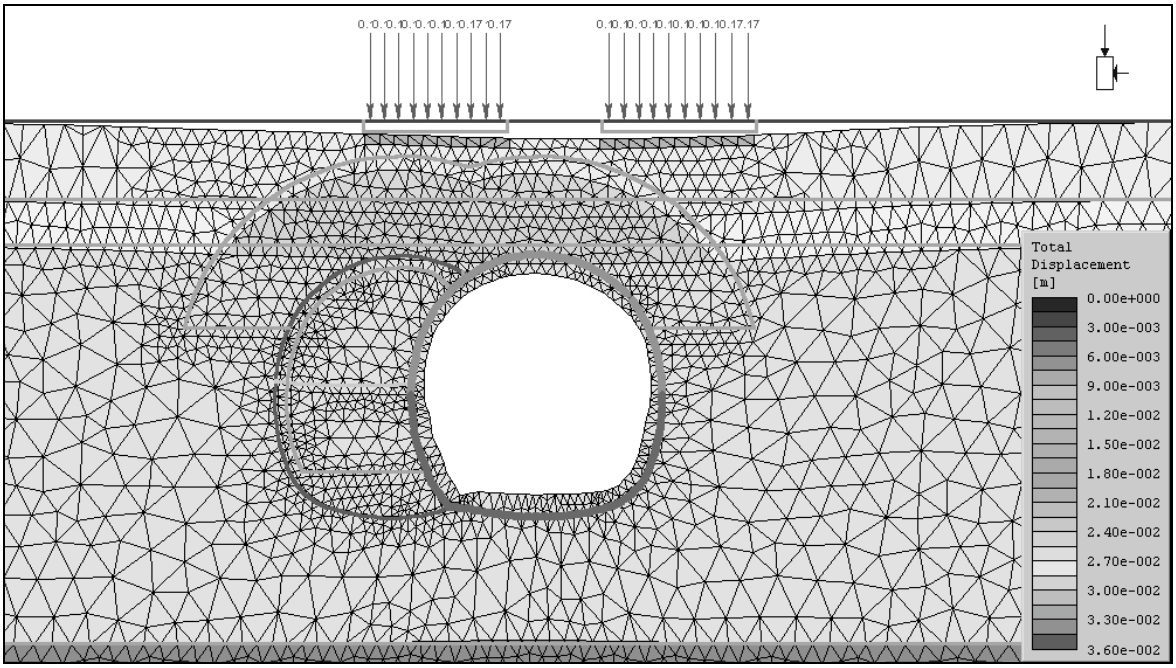

Figure 5.17: Deformed Model Following OB Tunneling at Station 95.20 Utilizing Pile Cap Loads of 0.17 MPa and Softening Factor S=0.50

Chapter 6: Finite Element (FE) Model With Wooden Pile Supports and Model Verification

6.1 General

Wooden piles were implemented into a new finite element model at Sta. 95.20 in order to investigate in more detail the composite structural system. This was accomplished using plane strain elements to represent the wooden piles with joint elements for the pile-frozen soil interface. The joint elements transmit shear stresses across the interface using an elastic-plastic stiffness relation governed by a Mohr-Coulomb failure criterion. This refined finite element model also included the actual extent of the frozen soil as implemented during construction. For the purpose of frozen soil parametric studies in Chapter 7 the mesh also allows variation of the extent of elements representing the frozen soil.

Once implemented, this refined FE model was calibrated and verified using deformations from the field. In-situ conditions with respect to loading, frozen soil temperatures and as-built lining thickness were considered. Creep behavior of the frozen soil mass and surface heave were also evaluated as part of the model verification.

Station 95.20 was selected for the purpose of modeling because this station has a dense array of building, geotechnical, and tunnel monitoring instruments. It also represents and average overburden height within the Graphic Arts building. The FE model at Sta. 95.20 is displayed in Figure 6.1. Figure 6.2 shows the actual tunnel construction of the outbound tunnel and Figure 6.3 displays construction of the inbound tunnel with the outbound tunnel completed including shotcrete final lining and middle concrete column.

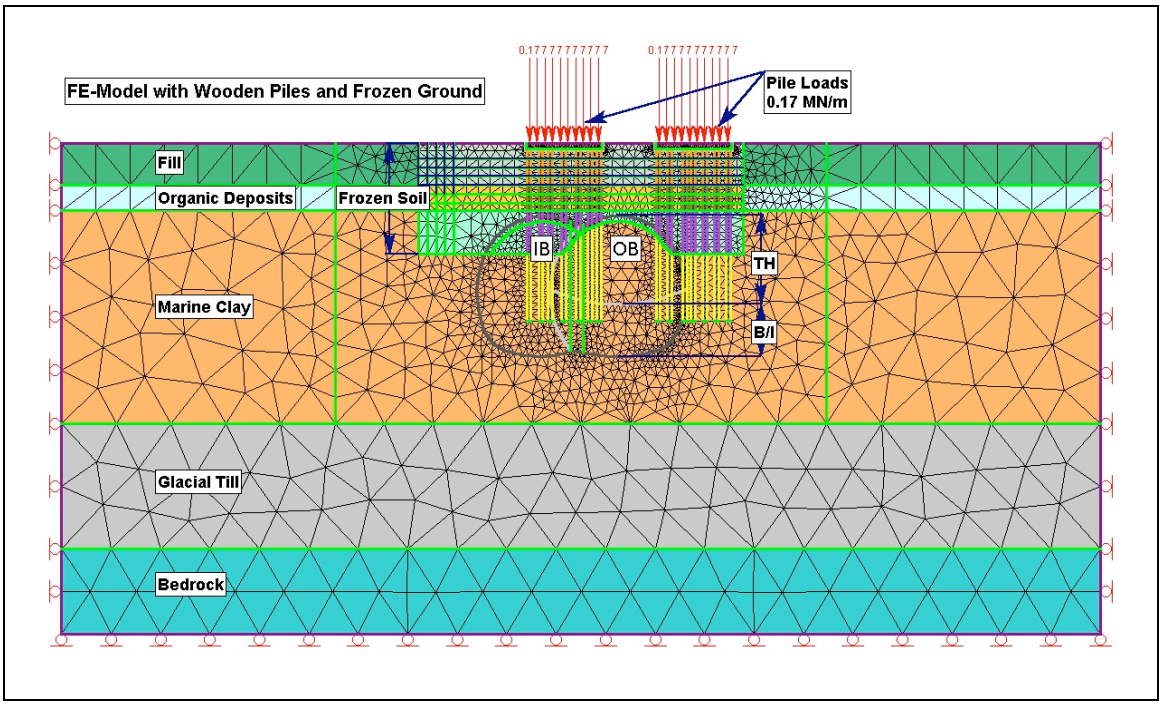

Figure 6.1: FE Model with Wooden Piles and Project Frozen Soil Mass Extent at Sta. 95.20

Figure 6.2: Excavation of the Outbound Tunnel

Figure 6.3: Excavation of the Inbound Tunnel

6.2 Pile-Soil Interaction and Pile Test Model

6.2.1 General

Research work on the effects of tunneling on pile foundations appears to be sparse (Chen *et al.*, 1999). It is generally limited to the investigation of effects due to tunneling that does not directly interfere with the piles but merely causes a deformation of the ground surrounding piles and individual piles or pile groups.

Further, piles arranged into pile groups as presented here are traditionally investigated and designed as pile group foundations, which generally neglects the soil-pile interaction of the individual piles and instead considers the reinforced soil body

acting as one quasi large pile (Bowles, 1982, Terzaghi, *et al*. 1996). The arrangement of the piles in the FE model, and in particular the fact that a number of individual piles will be cut off at certain depths, favored the development of a model that would assess the piles as individual structural members. This modeling allows for the assessment of pile structural behavior, in particular as it relates to their supporting function in terms of stresses in the pile-surrounding ground interface and pile tip stresses.

6.2.2 Modeling of Piles

The joint element feature in Phase2 (RocScience, 2001) incorporates a Mohr-Coulomb slip criterion. The slip strength is expressed as a function of cohesion, friction angle and the tensile strength in the joint. Where the piles are located within the frozen soils the cohesion is expressed by the adfreeze strength. Adfreeze values and elastic pile properties are assigned according to Chapter 3. The timber piles are modeled using elastic constitutive behavior only with elastic properties derived from the pile in-situ tests (Mueser Rutledge Consulting Engineers, 1998).

Terzaghi *et al.,* 1996 report that after driving of piles into soft clays and plastic silts the ultimate shear strength that is mobilized between the soil and piles is approximately equal to the undrained shear strength averaged over the length of the pile. Merritt, 1983 also allows for the use of the undrained shear strength as a representative value for the adhesion between pile and surrounding soil up to a value of 0.024 MPa, but reduces the resistance by a factor $\alpha < 1$ for higher undrained shear strengths, for example $\alpha = 0.9$ for a shear strength of 0.036 MPa. Where the piles are located outside of the

frozen soils the calculations were performed setting the adhesion between the pile and the soil to be equal to the undrained strength of the surrounding cohesive soils. The shear strength of the interface between piles and Fill (utilized in Chapter 7) is defined by the friction angle only, thus neglecting any additional strength that may be derived from the fines content of the Fill (see Chapter 4). Based on SPT-N values ranging from 2-47 an average friction angle of $\varphi = 30°$ was assigned to describe the pile skin friction in the Fill (Terzaghi, *et al.,* 1996).

Joint elements have a normal and shear spring stiffness. These relate the normal and shear stress across the element to the normal and shear displacements. The stiffness of the joint is derived from an assumed thickness and modulus of the infilling material. The infilling material was assumed to consist of the material of the surrounding ground and the corresponding elastic properties were assumed accordingly. The thickness of the joint was assumed small at 1 mm. The stiffnesses are then derived as follows:

$$K_n = E_0 / h \tag{6.1}$$

$$K_s = G_0 / h \tag{6.2}$$

where:

K_n = joint normal stiffness,
K_s = joint shear stiffness,
E_o = Elastic modulus of the infilling material (surrounding soil, frozen or unfrozen),
G_o = Shear modulus of the infilling material (surrounding soil, frozen or unfrozen), and
h = joint thickness.

Test simulations were conducted to verify the pile behavior within the FE model. An FE model for a simple pile test is shown in Figure 6.4. The model includes the simulation of excavated space below the pile tip to approximate conditions when the

tunnel excavation cuts through the piles. Comparative runs were carried out to investigate the transfer of loads onto the pile skin, i.e. the pile joints, when the void was implemented. These simplified runs correctly represented that the pile was supported by either a combination of pile skin friction and pile tip stress when calculated without the excavated space below, or the skin friction alone when the void beneath the pile tip was implemented. Typical analysis results for the stresses along within the piles are provided in Figure 6.5.

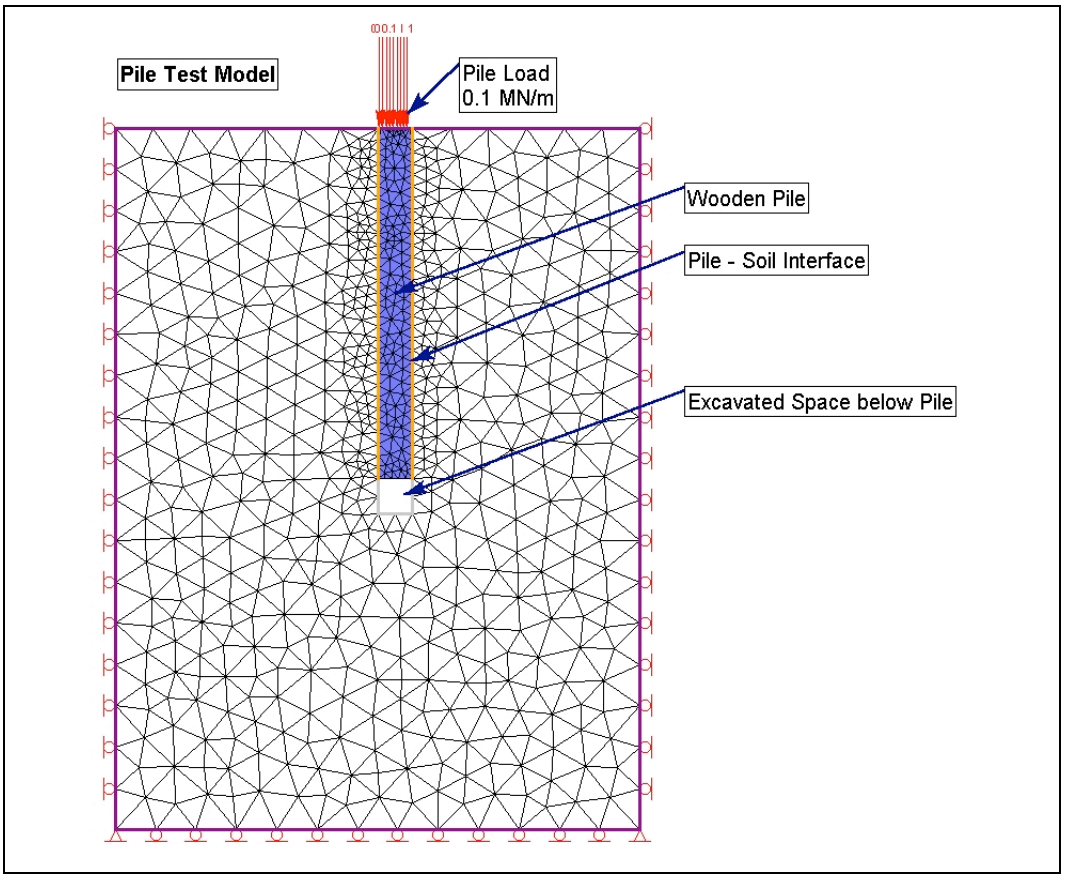

Figure 6.4: FE Pile Test Model

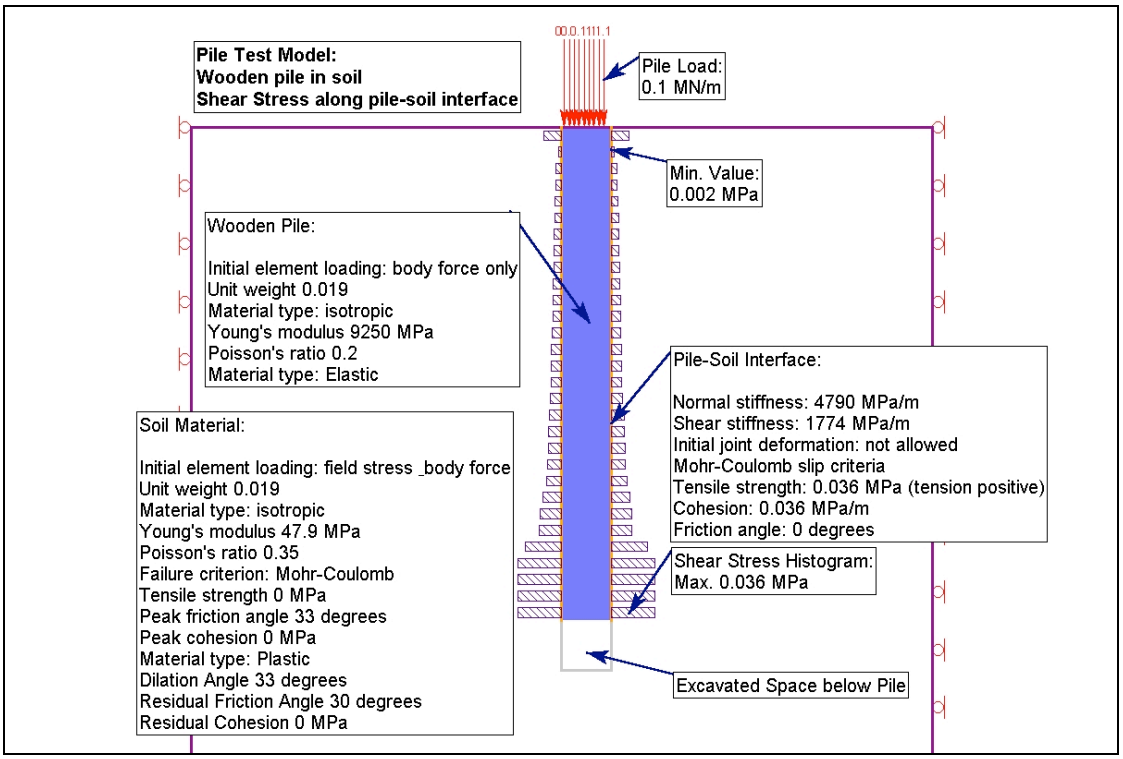

Figure 6.5: FE Pile Test Results

The number of piles implemented in the FE model as shown in Figure 6.1 was derived from historic Russia Wharf construction documents (Mueser Rutledge Consulting Engineers, 1998). These documents portray the intent to install about 32 piles per pile group to support granite pile caps of about 10 ft. x 10 ft. in plan. The piles are reported to range from 10.5 inch in diameter at the top and under the pile cap and to taper down to some 7 inch at their tips. When such a pile cap is crossed by the skewed alignment of the tunnel at Sta. 95.20 a representative pile cap width at its widest location is approximately 4.35 m as derived in Chapter 5 (Figure 5.3). The 2-D plane strain FE calculations were implemented in SI units with a unit width of 1 m. From a review of the construction documents, a plan area of 4.35 m x 1 m would contain about 14 piles.

With each pile on the average 0.20 m (10 inch) in diameter this results in a total pile surface area per 1 m depth of (0.20 m x π) x 14 ≈ 11 m^2. In comparison, 7 piles with two sides each in a 2-D model, with a 1 m unit thickness and per 1 m depth result in a total model pile surface area of 7 piles x 2 (sides) x 1 m (depth) = 14 m^2. The 2-D FE model thus overestimates the available pile surface area for the development of resistance by about 21%. However, and as described in paragraph 6.3.2 below, about 22% more piles were encountered during the outbound (OB) tunnel excavation than computed based on the construction documents. For the purpose of the calculations of this and Chapter 7, the number of piles implemented in the model is therefore viewed to be adequate.

6.2.3 Pile-Frozen Soil Interface Strength for Model Verification

For the purpose of model verification the piles do not act as supporting members because the frozen soil mass as actually constructed extends to the pile caps. The piles therefore merely increase the overall "stiffness" of the frozen soil mass to a certain degree. However, and as part of the modeling, adfreeze strength values are required for input. For model verification adfreeze values were taken from Table 3.4 (Chapter 3) to represent interface strength in the frozen soil. Arbitrarily higher values reported by Bowles (1982) were selected with 0.935 MPa, 0.496 MPa, and 0.600 MPa for the piles in frozen Fill, frozen Organic Clay and frozen Marine Clay respectively. Other material properties for the soils and the structural members were implemented in the FE model in accordance with Chapter 5.

6.3 Model Verification For As-built Conditions

6.3.1 Column Loads

At the beginning of the freezing operation the pile caps are loaded by column loads. To mitigate column displacements from initially soil heave and subsequent thaw consolidation a temporary jacking system redistributes the column loads onto the wooden cribbing located to the sides of the pile caps and thus onto the surrounding frozen ground surface. Figure 4.3 in Chapter 4 displays the design for the jacking system, Figure 6.6 below its actual construction. The loading conditions imposed onto the surface of the model must be modified accordingly. An accurate depiction of re-distributed loads in the 2-D model onto neighboring surfaces is difficult because the loads according to site conditions were re-distributed to the sides of the columns and to locations ahead and behind the actual pile cap location viewed in tunnel direction. Two different cases were investigated to bracket the transfer of column loads onto locations adjacent to the pile caps:

- Column loads redistributed from pile caps directly to neighboring locations in the 2-D model, and
- Column loads distributed to locations around the pile caps and assumed as an evenly distributed ("smeared") load over the entire width of the frozen soil surface, in the 2-D model.

The re-distributed column load cases along with load magnitudes assumed are portrayed in Figure 6.7. The first case is referred to as re-load case 1, or RC1, the latter as re-load case 2, or RC2.

Calculation results are presented for these two cases, but also for the case where column loads remain on the pile caps. Although theoretically not compatible with the actual load transfer intent in the project it represents the fact that loads existed at Station 95.20 above the tunnel. These resulted from cribbing loaded from the temporary load transfer of neighboring columns, possibly resulting in similar load magnitudes as imposed on the pile caps. This load case is referred to as load case RC0 in the reporting of results.

Figure 6.6: Jacking System and Installed Freeze Pipes within Graphic Arts Building

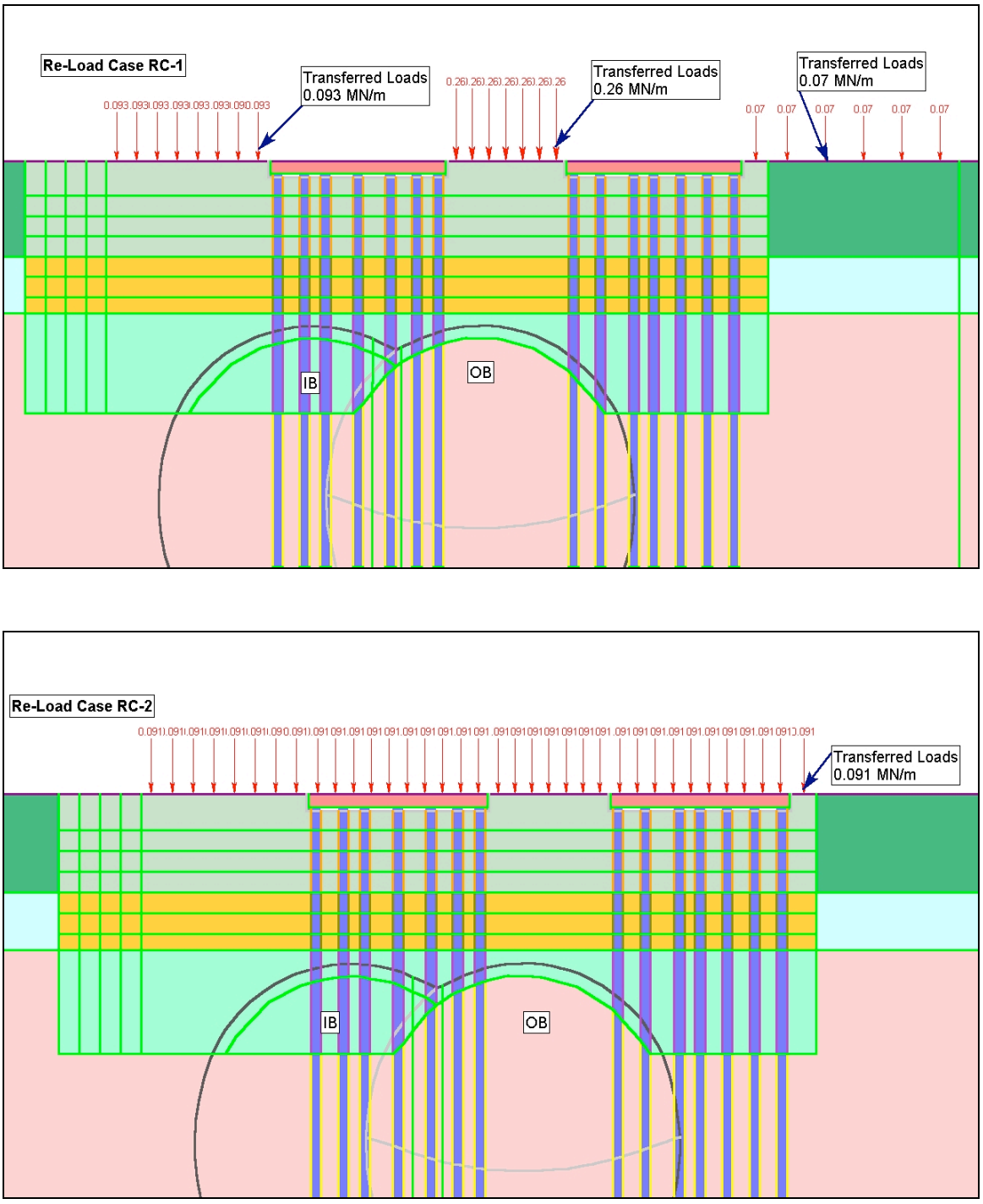

Figure 6.7: Re-Distribution of Pile Cap Load Alternatives Due to Temporary Column Jacking (Re-Load Case RC1, Re-Load Case RC2)

6.3.2 Number of Piles Encountered During Excavation

Two hundred forty one (241) wooden piles were encountered during outbound tunneling between Station 95.72 and 94.72. Figure 6.8 shows piles encountered at approximate station 95.05. Of these 241 piles, 212 piles were equipped with a pile shoe-reinforcing cage (Dr. G. Sauer Corporation, 2002) and therefore had a structural function for the future tunnel-pile support composite foundation. Assuming some 32 piles for the structural support per average pile group as stated in building construction drawings (Mueser Rutledge Consulting Engineers, 1998) the corresponding number of piles as measured by percentage of pile groups crossed during tunneling between the two stations would be about 190 piles. Therefore, 22% more wooden piles were encountered than assumed. However, as described previously, this greater number of piles in actuality is more compatible with the design assumptions made in the FE model.

Figure 6.8: Piles in Outbound Tunnel Top Heading at Approximate Station 95.05

6.3.3 Lining Thickness

Figures 4.7 and 4.8 of Chapter 4 indicate the pile embedment into the shotcrete lining after cut-off during tunneling. Execution of this arrangement in the field results in an over-excavation not only at pile locations but also generally around the tunnel crown circumference. Figure 6.9 illustrates the over-excavation at pile shoe locations in the field. To investigate the impact of lining thickness on surface deformations three different lining thicknesses were analyzed in the 2-D model: 0.30 m (the actual design thickness), 0.45 m and 0.60 m. The values of 0.45 m and 0.60 m account for the lining thickness actually built at Sta. 95.20 (Dr. G. Sauer Corporation, 2002). The influence of lining thickness on surface settlement is described in Section 6.3.6.

Figure 6.9: Excavation and Reinforcement Installation at Pile Locations

6.3.4 Frozen Soil Temperatures

In-situ temperature information was monitored using driven temperature monitoring points, drilled temperature points, and pile cap temperature points. The temperature monitoring point locations near Station 95.20 and up to a horizontal distance of 50 ft. within the frozen soil body are provided in Table 6.1. This table amends the locations of temperature monitoring points provided in Chapter 4, in that it lists the location of instruments according to their depth and also contains information on pile cap temperature monitoring points that were added during construction. These were installed within the relief drains that failed to perform for their intended purpose (Chapter 4). Water was not displaced by the freezing front and the drainpipes froze and were converted to temperature monitoring points instead.

Frozen temperature values for the selected monitoring points and as a function of absolute time and tunneling progress are graphed in Figure 6.10. Temperature is shown on the graph's left ordinate. The tunneling progress is shown using the advance (defined by the respective heading station) of the outbound tunnel (OB) and inbound tunnel (IB) top heading (TH) and bench/invert (B/I) as a function of time. Time, as for the temperature, is the abscissa and the station location is the graph's right ordinate. Using this display the temperature regime can be related to the tunnel excavation progress and also to surface deformations provided in Section 6.3.5 below.

The data in Figure 6.10 give a good representation of temperatures within the frozen soil mass at and near Sta. 95.20. A close inspection of the temperature point locations (H and D in Table 6.1) in connection with the temperature graphs of Figure

6.10 indicates that temperatures in the core of the frozen soil body, i.e. closer to the tunnel centerline and close to the tunnel crown (CPCs and DVTPs in Table 6.1) were coldest. Temperatures increase near the boundaries of the frozen soil body (DTPs in Table 6.1). Generally, a temperature gradient between the core and the outer regions of the frozen body of about 10 °C / 20 ft (6 m) can be observed.

Table 6.1: Types and Location of Selected Temperature Points in the Vicinity of Surface Monitoring Points at Station 95.20

Surface monitoring point DMP2: Steel column deformation DMP3: Concrete surface deformation	Relative vs. Station in Direction of Tunneling (“ in front = - “) (“ behind = + “)	Temperature measurements CPC=Pile Cap Temperature DTP=Drilled Temperature Pipe DVTP=Driven Temperature Pipe R=Location radius relative to monitoring point H=Distance to tunnel centerline D=Depth below surface vs. top elevation =105 ft. or as noted N/A=Outside of frozen soil
DMP2 75690	-5 ft.	N/A
DMP2 81207	+ 8ft.	N/A
DMP2 60294	+4 ft.	DTP11 (R=50 ft., H=20 ft., D=37 ft.) DTP12 (R=24 ft., H=18 ft., D=36 ft.) DTP13 (R=44 ft., H=26 ft., D=34 ft.)
DMP3 60291	-10 ft.	CPC12 (R= 8ft., H=10 ft., D= 2 ft. above crown) DVTP4 (R=20 ft., H=10 ft., D=16 ft.)
DMP3 60292	-1 ft.	CPC13 (R=8 ft., H=2 ft., D=2 ft. above crown) DVTP5 (R=16 ft., H=10 ft., D=19 ft.) DVTP6 (R=12 ft., H=10 ft., D=19 ft.)
DMP2 60293	+10 ft.	CPC15 (R=10 ft., H-14 ft., D=2ft. above crown)
DMP2 75772	+1 ft.	N/A
DMP2 60270/75981	+6 ft.	N/A

In summary, frozen soil temperatures as required by the contract requirements and described in Chapter 4 were generally achieved. At locations the temperatures measured were colder than those required. Therefore, it can be assumed for the purpose of the computations that the frozen soil properties, and in particular the elastic moduli and the adfreeze values, may be assumed as derived in Chapter 3.

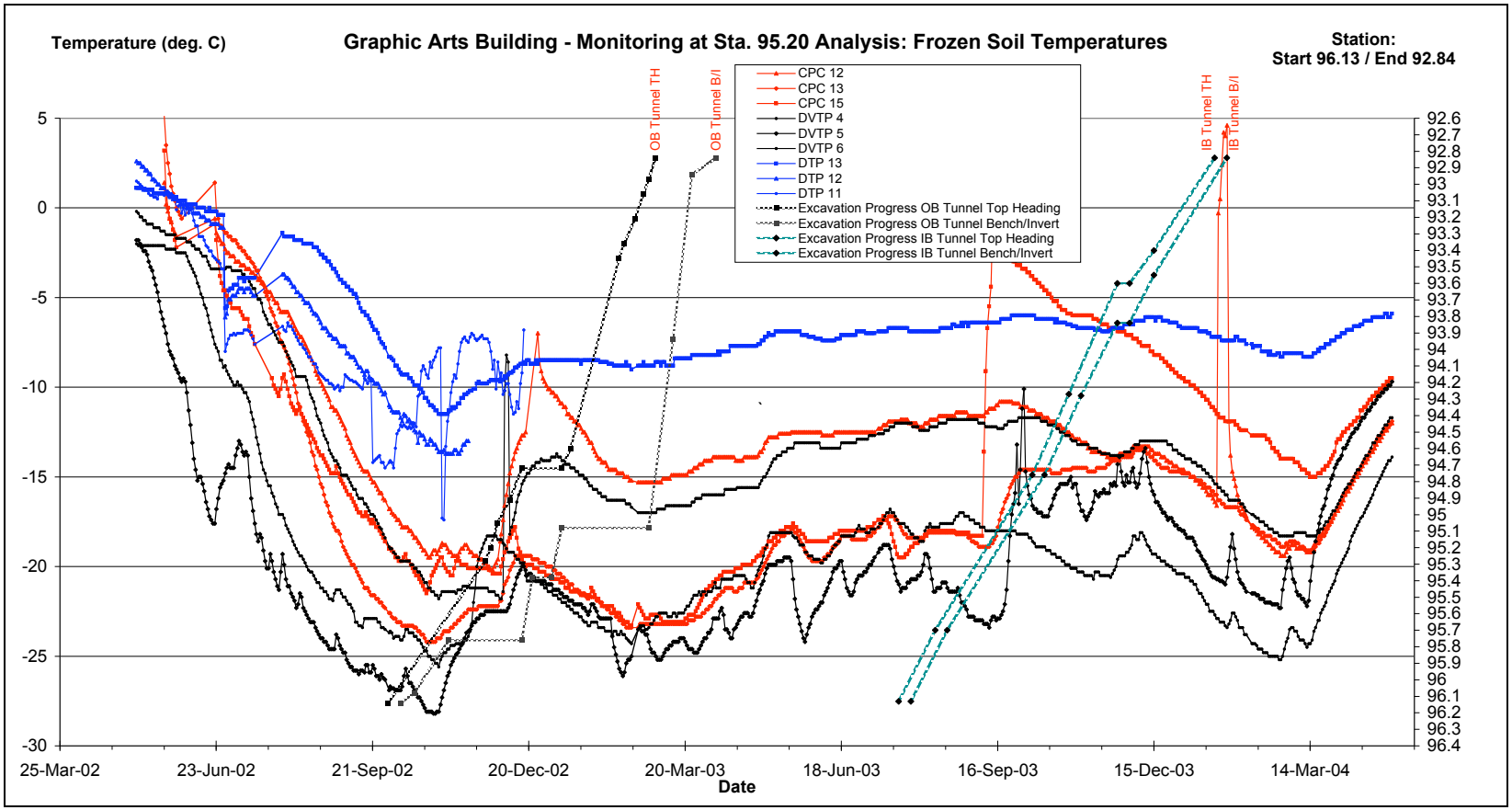

Figure 6.10: Frozen Soil Temperatures vs. Time and Tunnel Excavation Progress at Selected Monitoring Points (CPC, DTP, DVTP According to Table 6.1)

6.3.5 Evaluation of Monitored Surface Deformations

Monitored surface vertical deformations were evaluated for monitoring points at and around station 95.20. Point locations are represented in Figure 6.11. Location details for offset to Station 95.20 are provided in Table 6.1. The location of station 95.20 within the Graphic Arts building is shown in Figure 5.3 in Chapter 5. Figure 6.11 also shows the location of tunnel deformation monitoring points that are evaluated in Section 6.3.8.

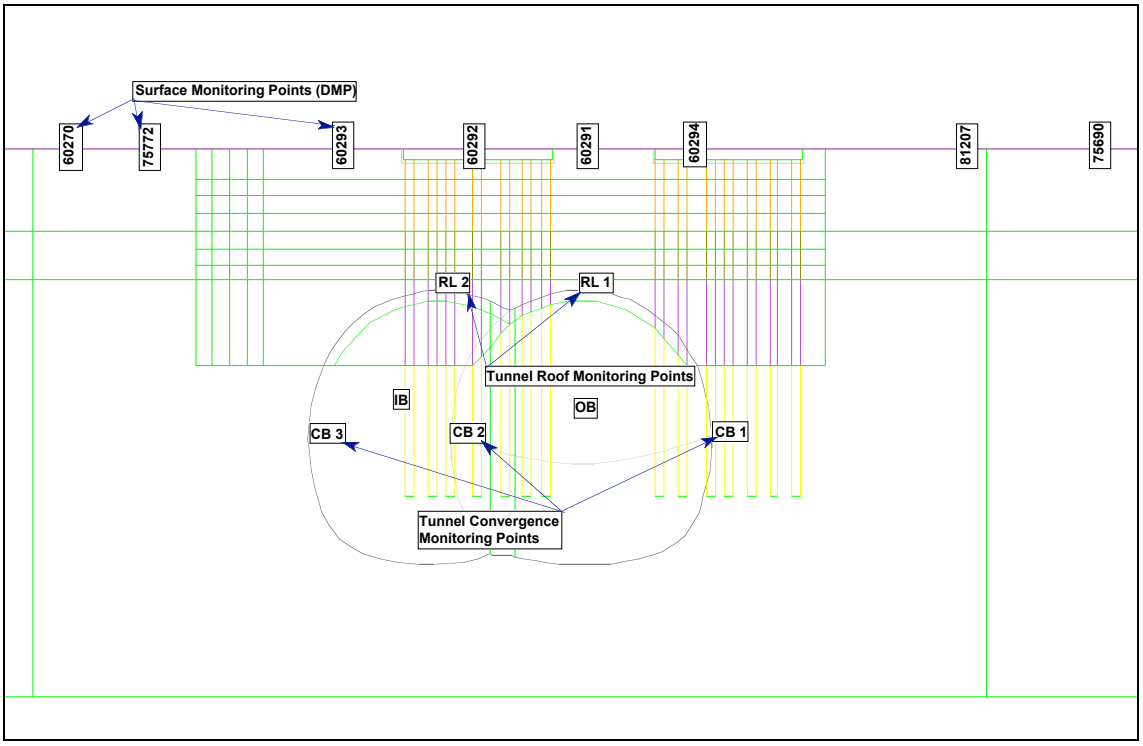

Figure 6.11: Location of Surface and Tunnel Deformation Points at Station 95.20

The surface monitoring results are summarized in Figures 6.12 through 6.14 that show the development of the surface deformation vs. time and vs. tunneling progress at selected locations. Surface deformation is shown on the graph's left ordinate. The tunneling progress is shown using the advance of the outbound tunnel (OB) and inbound

tunnel (IB) top heading (TH) and bench/invert (B/I) as a function of time. Time, as for the vertical deformation, is the abscissa and the station location is the graph's right ordinate. Using this display the deformation of the surface can be related to the tunnel excavation progress, thus relating cause and effect directly. By means of the time scale and the tunnel progress curves, the surface deformation can be further related to the temperature regime of Figure 6.10.

The graphs in Figure 6.12 (analysis 1 of 3) provide a general overview of the time related surface deformations caused by construction activities. The graphs in Figure 6.13 (analysis 2 of 3) are concerned with the freezing related surface heave prior to tunneling and show development of surface deformations for the entire tunneling period of about 14 months. The graphs in Figure 6.14 (analysis 3 of 3) are a further zoom into displacements associated with the OB tunnel excavation and support. These graphs are used for an evaluation of surface heave, settlement, and reoccurring heave at some locations. The phenomena observed are further set in relation to frozen ground temperatures vs. time provided in Figure 6.10.

The deformations are depicted using four vertical deformation points of type DMP3, one at each selected columns of the Graphic Arts Building; 60291, 60292, 60294, and 60270/75981. Three of these points (60291, 60292, 60294) provide a detailed assessment directly above the tunnels (60291, 60292, 60294) whereas the fourth point 60270/75981 is located outside of the tunnel footprint (see Figure 6.11).

Figure 6.12 shows an oscillating deformation behavior with a general tendency of settlement for all four points prior to the start of freezing. While the oscillating behavior appears to be associated with the reading accuracy at that time and construction activities

of a nearby ventilation building for the Central Artery project, the general tendency of settlement is explained by the installation of vertical freeze pipes and possibly the transfer of the columns onto the temporary jacking system prior to the start of mass freezing in mid April of 2002. Upon commencement of ground freezing all points show a pronounced heave due to the expansion of the frozen soil. This heave amounts to 0.119 ft. (36.27 mm) at point 60291 and 0.104 ft. (31.70 mm) at point 60294. These are total heave values prior to the onset of tunneling and include the amounts compensated for by lowering of columns at indicated points in the graph. As the tunnel heading approaches the monitoring points it induces settlements of the surface that cease once the tunnel bench and invert have passed the monitoring location and the heading has moved to a location of about 20-30 ft. distance. The outbound tunneling then has no further impact on surface settlements. The deformations show reoccurring heave between mid March and end of April 2003 of a maximum of about 0.010 ft. (3 mm). Subsequently, no further deformations generally occur until the onset of IB tunneling that causes further settlements of some 0.022 ft. (7 mm) maximum directly above the tunnels until the tunneling moves to a distance of about 60 ft. Thereafter the graphs generally show absence of any further deformations.

Figure 6.13 further details relationships between tunneling advance and surface deformation. A horizontal line is provided at Station 95.20, the location of the FE model station. Vertical lines indicate when tunneling of the individual faces passed underneath the surface at Station 95.20. Interpretation of settlements as caused by the tunneling is provided within the Figure. In particular the OB TH induced significant surface settlements. When tunneling ceased during the Christmas holiday period in 2002 as

indicated by the horizontal line in the OB TH tunnel progress curve, a reoccurring heave can be detected. When tunneling stopped at that time a shotcrete temporary top heading invert was installed in combination with a structural shotcrete lining at the face. Therefore, a stable tunnel structure was established providing an abutment for the frozen soil to heave against. All three DMPs located close to the center of the frozen soil indicate similar gradients for this heave. A similar observation can be made when the OB B/I excavation ceased for a longer period between the beginning of January and the end of February 2003. A comparison of this reoccurring heave with the temperature vs. time relationships of Figure 6.10 indicates that during the long OB B/I stoppage temperatures were generally lowered. This relationship between reoccurring heave can generally be made for the time during top heading stoppage as well. The temperatures were also lowered after an intermediate increase in the period between the beginning of October and mid December 2002.

A stable tunnel shell that provides a sufficient abutment in combination with lowering of temperatures generally leads to surface heave. Once the OB tunnel passed sufficiently far as to not cause any settlements, some minor heave occurs initially, but the displacement trend remains constant without any further heave, which is consistent with the increasing temperatures during the period between about mid April to mid August 2003 (Figure 6.10). The IB tunneling subsequently caused additional settlements as indicated in the graph. After the IB tunnel, which was driven in staggered full-face operation meaning that the B/I closely followed the TH excavation, advanced away from station 95.20 generally no further settlements were observed.

Figure 6.14 zooms into surface deformations for the OB tunnel. The heave in the period prior to tunneling is associated with the build up of the frozen soils mass. During this period the temperature gradients in the soil mass are greatest and cause the steady heaving of the surface. A linear regression curve based on the average of the heave of points 60291, 60292, and 60294 has been provided and is shown as a dashed line. The slope of this regression curve can be compared with the rate of heave during TH and B/I stoppages. As described above this heave appears to be caused by two events that must occur simultaneously to cause reoccurring heave: a stable tunnel lining shell that provides an abutment for the frozen soils for an upward expansion and a general cooling of the frozen soil that generates a temperature gradient. Under such circumstances, the linear regression curve could be used to estimate further heave, i.e. the 13.72 mm over a period of about 5 months (without tunneling) as labeled in the Figure. These observations are further validated by the fact that beginning of March 2003 and until influenced again by tunneling the surface displacements stagnate. An inspection of Figure 6.10 shows that during this time temperatures became warmer, consistent with the absence of any further heave.

Heave amounts measured at selected points and exemplary shown for point 60291 as d1=1.52 mm and d2=3.05 mm were considered in the derivation of absolute settlement values caused by tunneling. Deformations shown in Figures 6.12 through 6.14 along with similar graphs for the deformation points of Figure 6.11 not presented here have been used to derive average measured surface settlements for comparison with the calculated results from the FE analyses. These graphs are portrayed in Chapter 6.3.6 below.

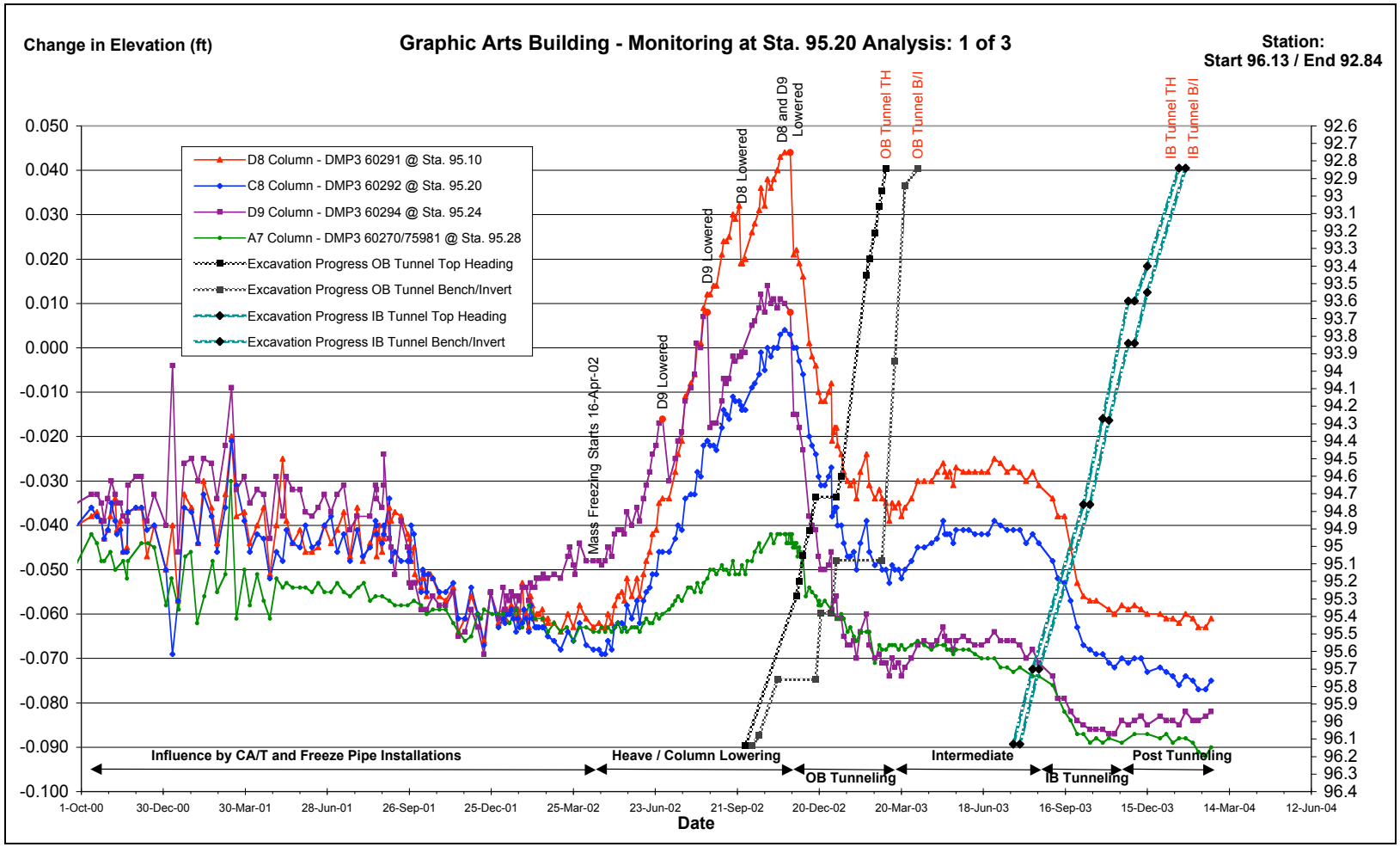

Figure 6.12: Graphic Arts Building - Monitoring at Sta. 95.20 - Analysis 1 of 3

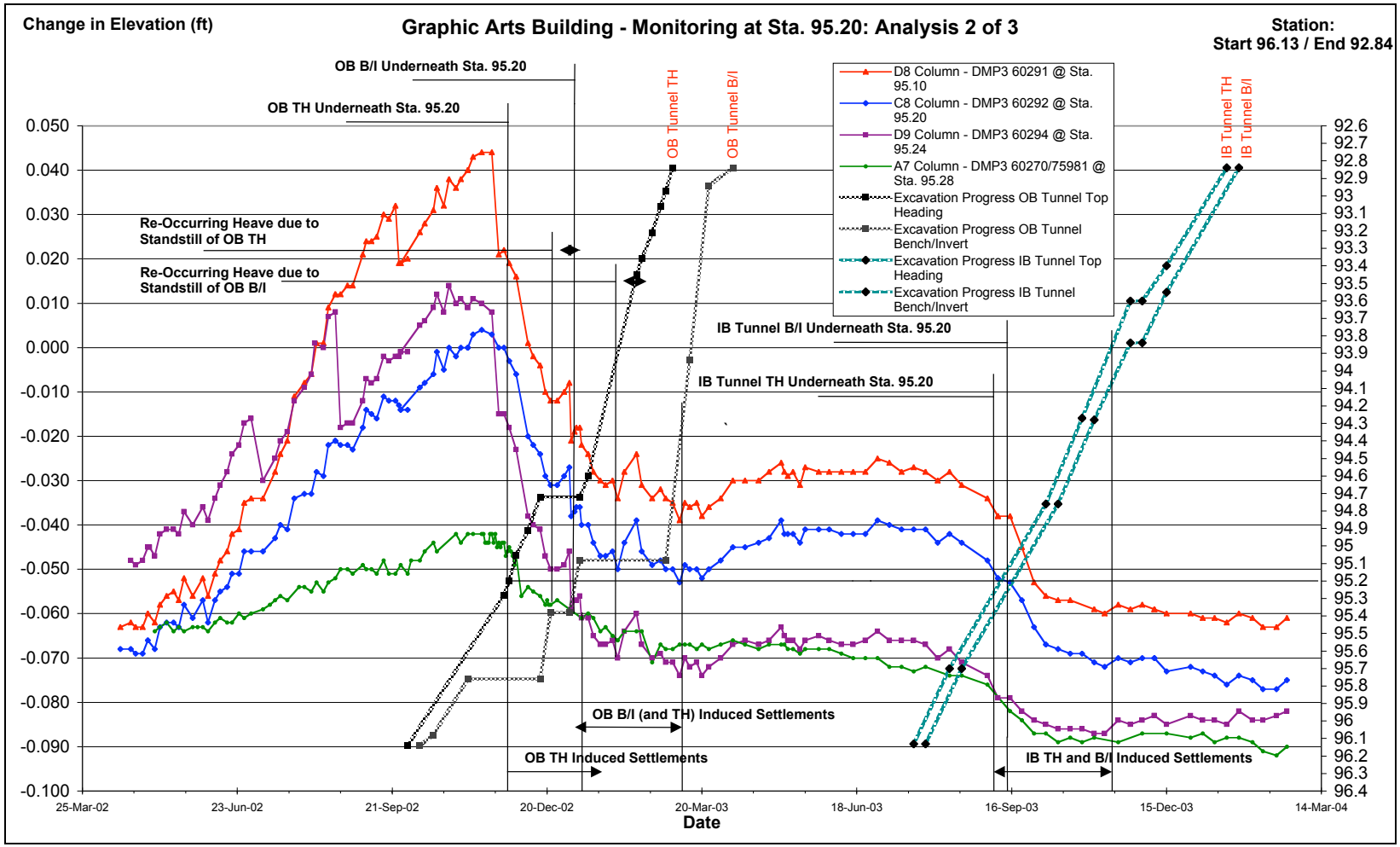

Figure 6.13: Graphic Arts Building - Monitoring at Sta. 95.20 - Analysis 2 of 3

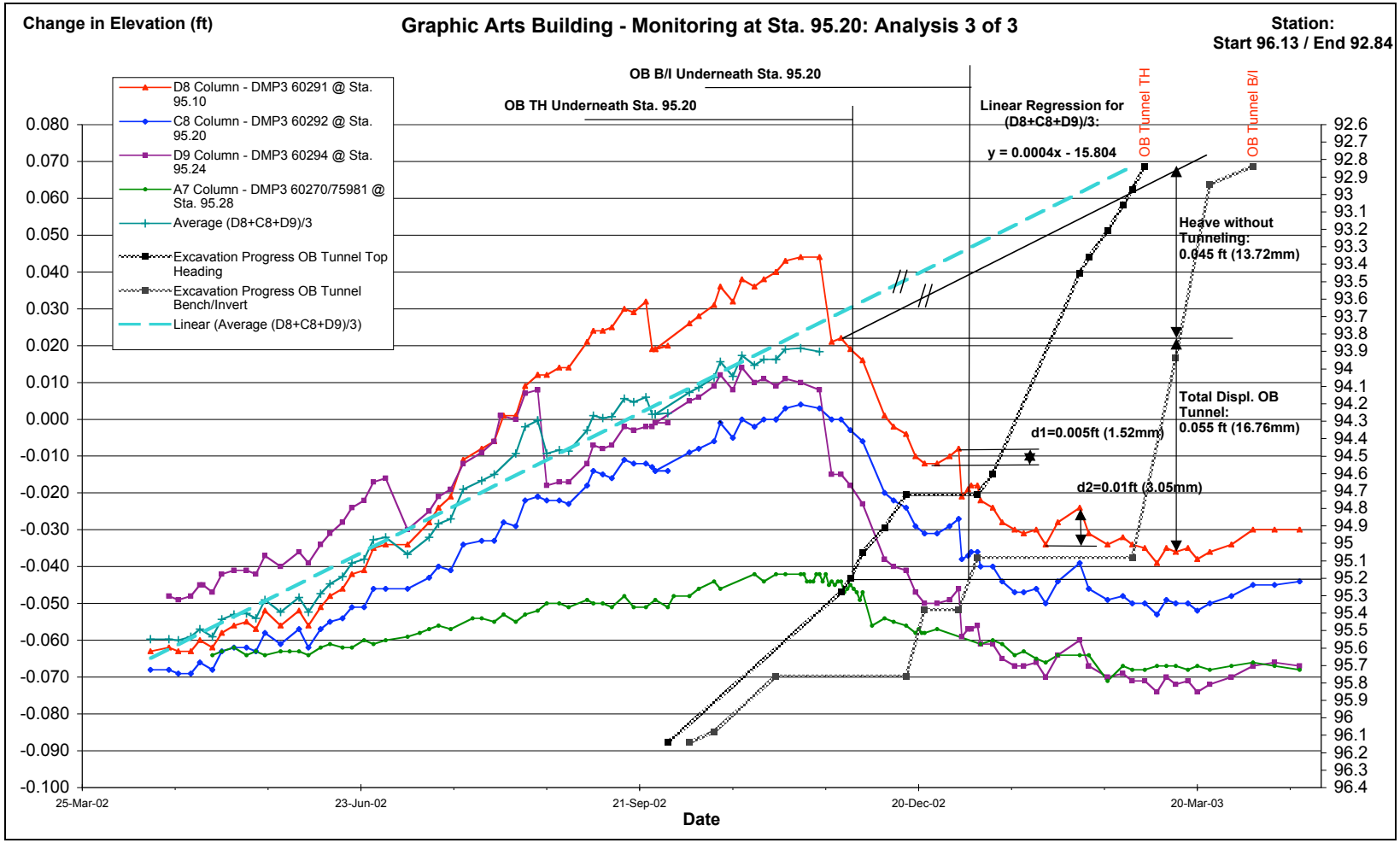

Figure 6.14: Graphic Arts Building - Monitoring at Sta. 95.20 - Analysis 3 of 3

6.3.6 Creep of Frozen Soil and Pile Frozen Soil Interface

Relationships derived in Chapter 3 are utilized to assess the amount of deformations associated with creep. The assessment is of importance to calibrate and validate the FE model. Deformation associated with the creep of the frozen soils is evaluated using equations 3.4, 3.8, and 3.9 of Chapter 3. An estimate of creep is based on the time required for the excavation of the OB tunnel. This creep amount is used as an indication for the need to implement creep related deformations in the FE modeling of the structural response around the advancing tunnel. The relevant creep deformation, if any, that has to be accounted for in the modeling associated with the OB tunneling will begin when the tunnel is about some 30 to 40 ft. distance (approximately 1.5 tunnel diameter) from Station 95.20. It will be of no further impact to the FE modeling once the entire tunnel (TH and B/I) has advanced to about 30 to 40 ft. beyond it. This represents the time for the excavation and support of the entire OB tunnel simulated in the FE modeling.

By inspection of Figure 6.14, the period to excavate the OB tunnel within the relevant Stations occurred between about 21 November 2002 and 13 March 2003, i.e. within 112 days or 2,688 hours. With regard to the loading conditions, the stresses for the Organic Deposits and Marine Clay are taken as the vertical stress at the top of the individual strata from the FE model from the load case RC1 (see Figure 6.7). The vertical stress for the Fill is taken from the applied surface load of 0.260 MPa. The average vertical stresses σ_V, acting on the top of the cohesive strata are as follows:

$\sigma_{V,OrganicDeposits}$ = 0.084 MPa, and

$\sigma_{V,MarineClay}$ = 0.055 MPa.

The creep strain within the Organic Deposits ($\varepsilon_{C,OrganicDeposits}$) and Marine Clay ($\varepsilon_{C,MarineClay}$) is evaluated using equations 3.9 and 3.8 (Chapter 3) respectively as follows for a total duration of 2,688 hours. Using the conversion of 1 tsf = 0.0958 MPa:

$\varepsilon_{C,OrganicDeposits} = 6\times10^{-5}(\frac{0.877}{7.9})^{3.05}\times 2{,}688 = 2\text{x}10^{-4}$, and

$\varepsilon_{C,MarineClay} = 6\times10^{-5}(\frac{0.574}{14.7})^{3.05}\times 2{,}688 = 8.165\text{x}10^{-6}$.

Multiplied by the individual thicknesses of the two layers (Chapter 4 of the Technical Manual TM-852-2/AFM 88-19, Joint Departments of the Army and Air Force USA, 1985) yields an estimate of the total deformation associated with the creep of these two frozen layers to be:

$2\text{x}10^{-4}$ x 1,400 mm + $8.165\text{x}10^{-6}$ x 1,700 mm = 0.280 mm + 0.014 mm = 0.298 mm.

Since the creep behavior of frozen Fill has not been investigated as part of the test freezing program the creep associated with the frozen Fill $\varepsilon_{C,Fill}$ is estimated using data provided by Jessberger (1981) in equation 3.4 neglecting the pseudo-instantaneous strain as follows:

$\varepsilon_{C,Fill} = \bar{A}\sigma^{B}t^{C}$

Creep constants $\bar{A}$, B, and C are taken for sand as an approximation of a frictional fill material with $\bar{A}$=1.67 [$(mm^2/N)^B h^C$], B=2.80 [-] and C=0.42 [-] for a temperature of -10 °C, thus:

$\varepsilon_{C,Fill} = 1.67\times10^{-3}\times(0.260)^{2.80}\times(2{,}688)^{0.42} = 0.0011$.

This yields an estimate of the total deformation associated with the creep of the frozen Fill of: 0.0011 x 3,000 mm = 3.30 mm. The total deformation caused by creep of the frozen soils is therefore 3.300 mm + 0.298 mm ≈ 3.6 mm.

These computations indicate that deformations associated with creep tend to exist, but play a minor role for the Organic and Marine Clays. When creep associated with the frozen fill is added then the deformations associated with creep are on the order of 20% of the total deformations. This indicates that the FE computations must incorporate a mechanism to account for creep. A reduction of the stiffness (elastic modulus) of the frozen soils within the model was analyzed for this purpose. Deix (1992) for example reports a reduction of the stiffness of frozen gravel at a temperature of –10 °C from an initial value of about 800 MPa to some 25% of this value or close to 200 MPa after a period of only 5 hours.

A parametric study was used to investigate the influence of the elastic modulus reduction of the frozen soils on the calculated surface vertical displacements. These were compared with monitoring results for the different tunneling excavation stages (OB TH, OB TH/B/I, and IB TH/B/I). Graphs in Figures 6.15.a through 6.15.c show these comparisons for the surface load arrangement of reload case 1 (RC1), Figures 6.16.a through 6.16.c for reload case 2 (RC2), and in Figures 6.17.a through 6.17.c for the case where the column loads remain on the granite pile caps (RC0).

Surface settlement troughs are provided for the reduced elastic moduli of frozen soil by reduction factors (Cr) of 0.25, and 0.15. For comparison troughs without a modulus reduction (Cr=1.0) are also displayed.

These graphs indicate that the form of the surface settlement trough greatly depends on the location of the loads on the surface. Generally reduction of modulus of elasticity to estimate the order of magnitude of settlements as a result of OB TH excavation is not required. A modulus reduction by a factor between 0.15 and 0.25 is required to depict the order of magnitude associated with the excavation of OB TH/B/I and IB TH/B/I. A modulus reduction of about 80% to simulate the final surface settlements may not be explained by the effect of creep alone as calculated above, although the calculations for the fill used material parameters from the literature only. Rather, this reduction is viewed to also contain a portion for the model calibration to account for miscellaneous unknowns that distinguish construction reality from the numerical modeling and its assumptions. For example, and based on review of the site reports (Dr. G. Sauer Corporation, 2002) the excavation of the OB B/I was carried out at increased lengths, up to three times the planned length, which deviates from the design and would cause larger deformations at the surface.

Use of a reduction factor of 0.15 for the frozen soils results in a close agreement between measured and calculated surface settlement data for OB TH/B/I and IB TH/B/I and was used in all further modeling.

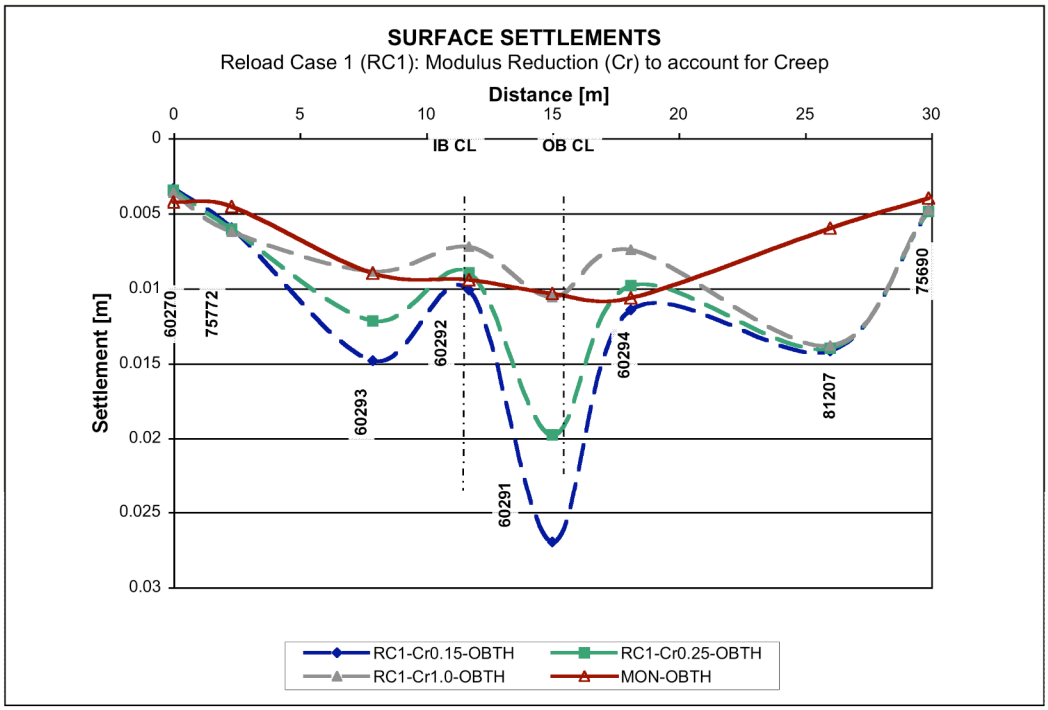

Figure 6.15.a: Comparison of Monitored (MON) vs. Calculated Surface Vertical Deformations for Reload Case 1 (RC1) – OB TH

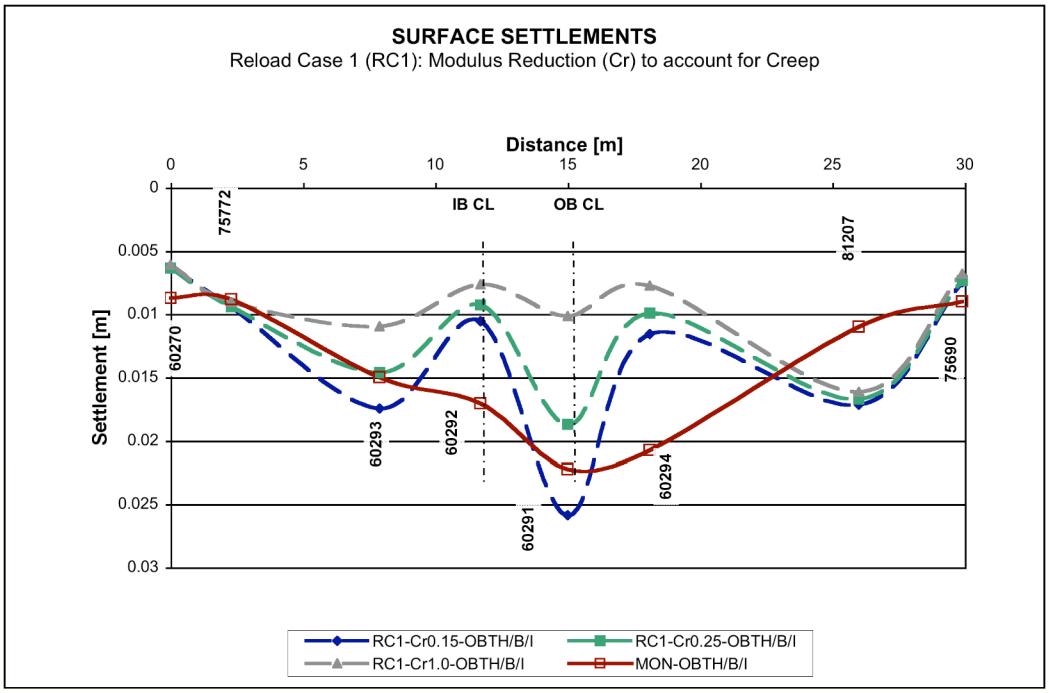

Figure 6.15.b: Comparison of Monitored (MON) vs. Calculated Surface Vertical Deformations for Reload Case 1 (RC1) – OB TH/B/I

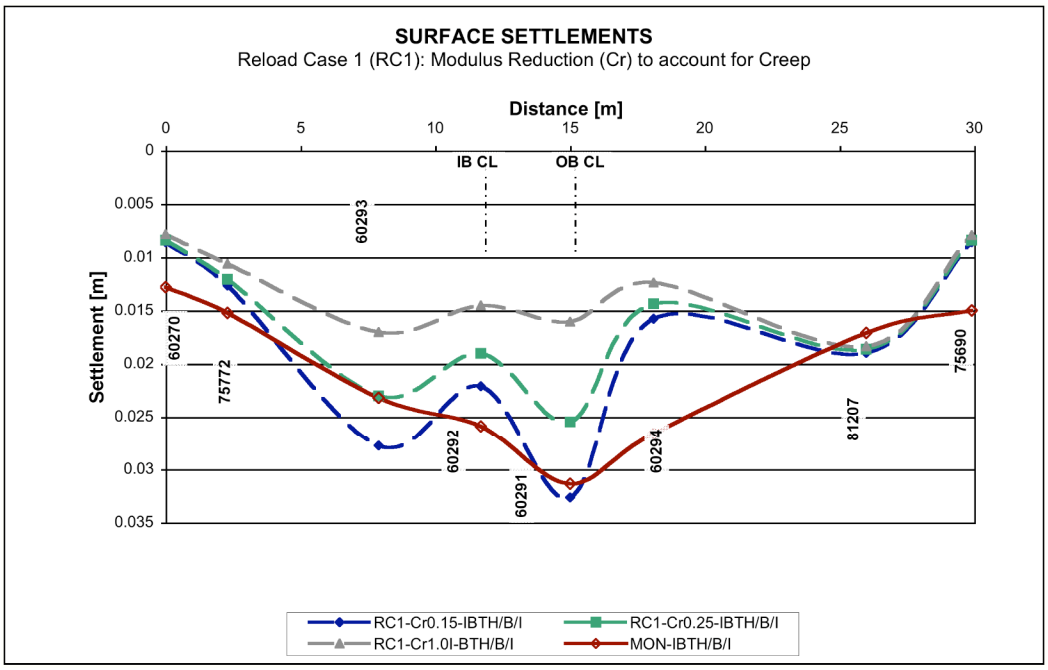

Figure 6.15.c: Comparison of Monitored (MON) vs. Calculated Surface Vertical Deformations for Reload Case 1 (RC1) – IB TH/B/I

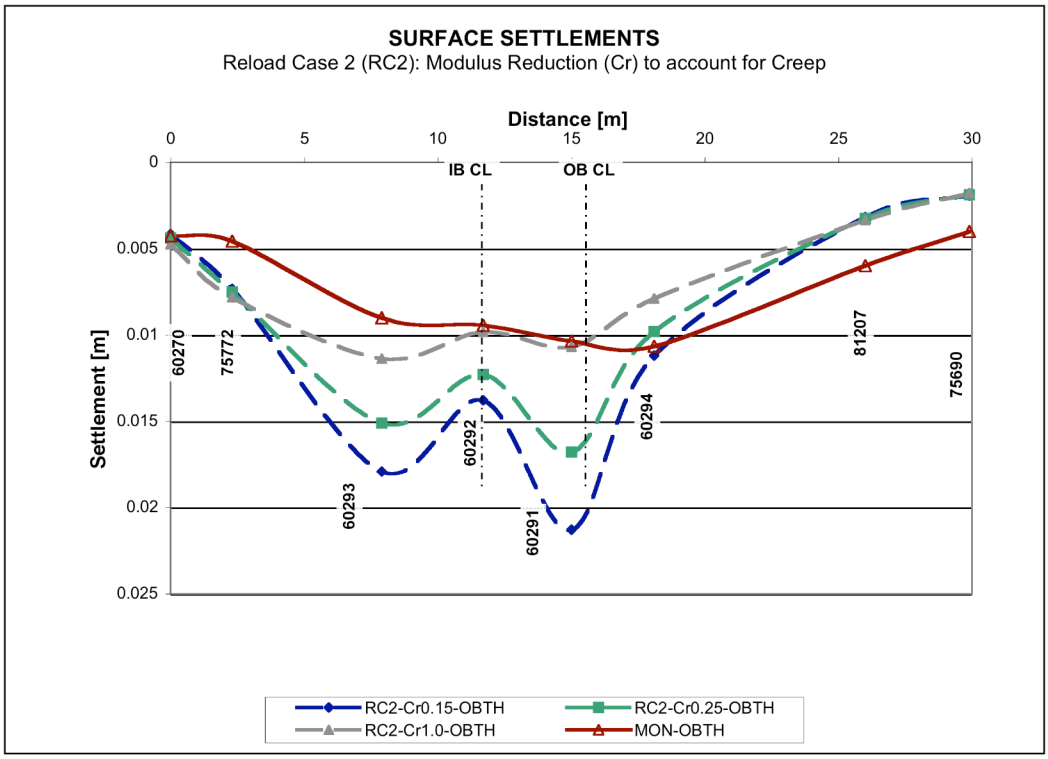

Figure 6.16.a: Comparison of Monitored (MON) vs. Calculated Surface Vertical Deformations for Reload Case 2 (RC2) – OB TH

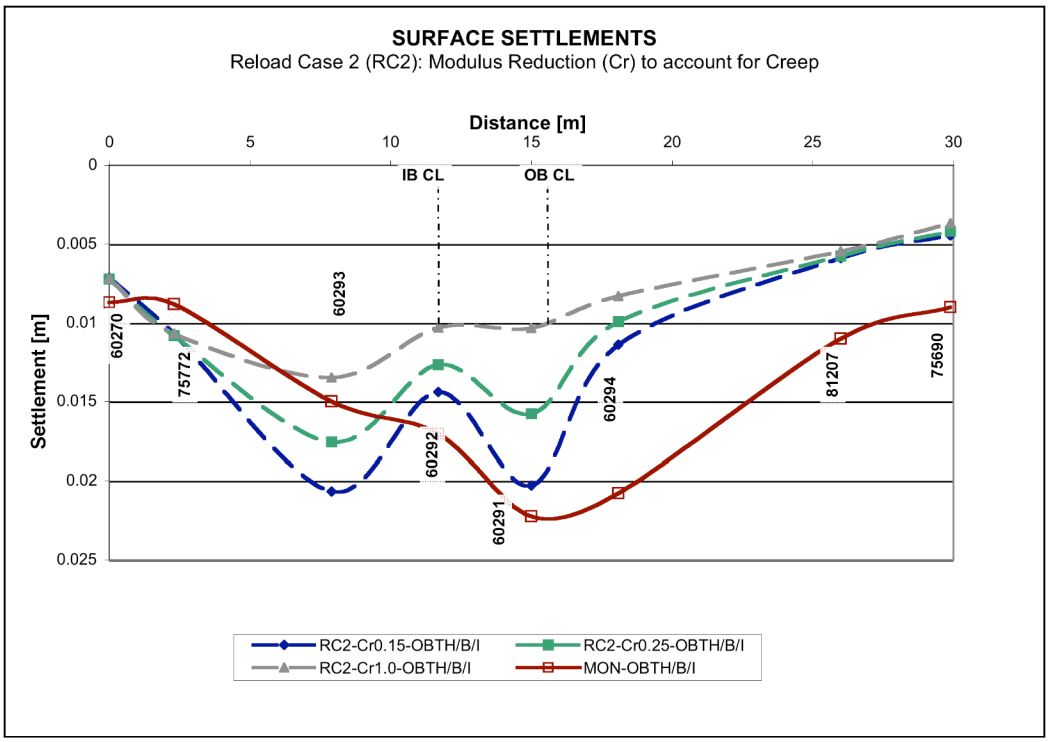

Figure 6.16.b: Comparison of Monitored (MON) vs. Calculated Surface Vertical Deformations for Reload Case 2 (RC2) – OB TH/B/I

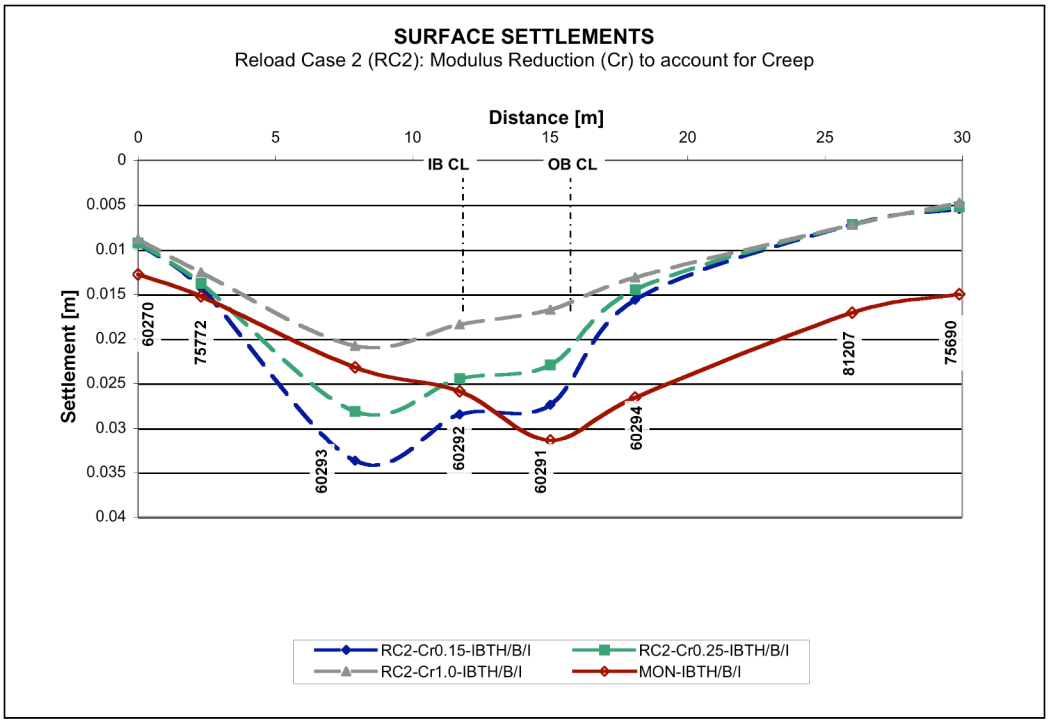

Figure 6.16.c: Comparison of Monitored (MON) vs. Calculated Surface Vertical Deformations for Reload Case 2 (RC2) – IB TH/B/I

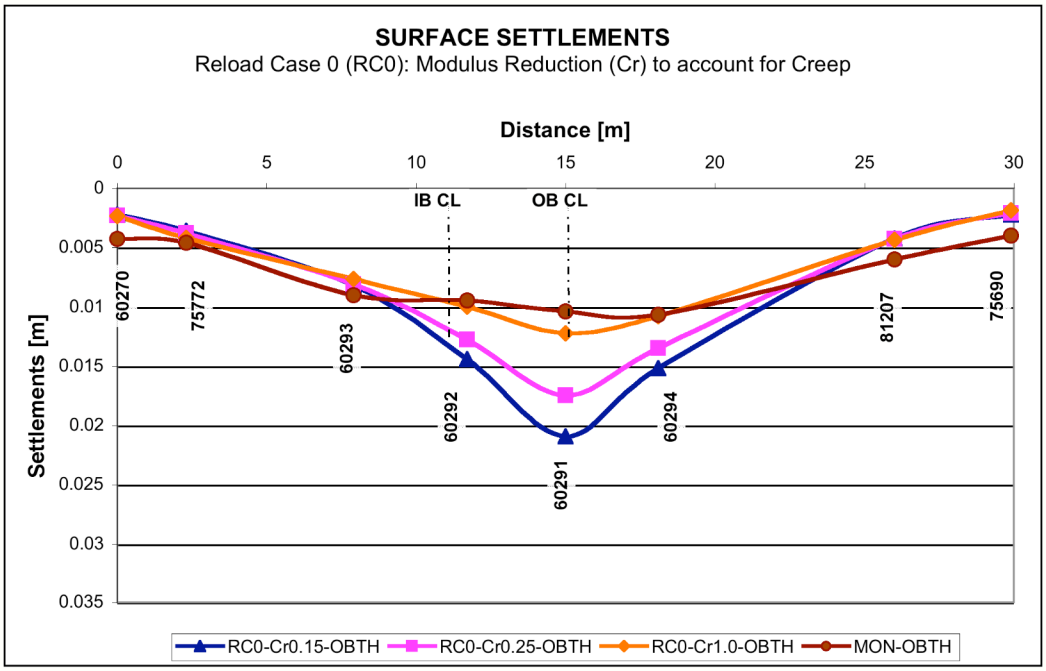

Figure 6.17.a: Comparison of Monitored (MON) vs. Calculated Surface Vertical Deformations for Loads on Pile Caps (RC0) – OB TH

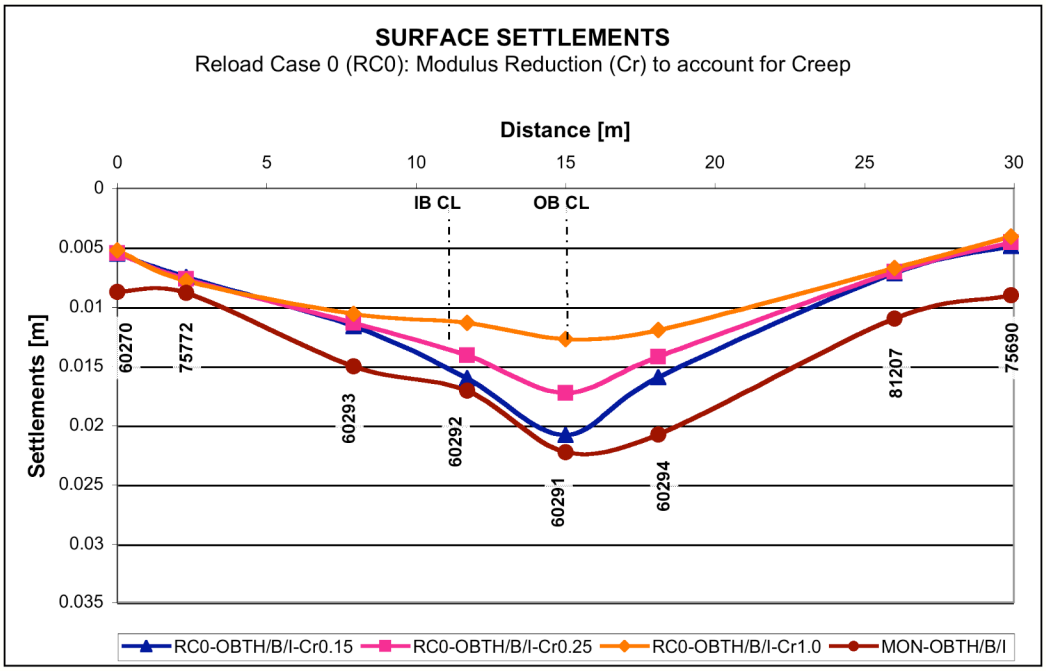

Figure 6.17.b: Comparison of Monitored (MON) vs. Calculated Surface Vertical Deformations for Loads on Pile Caps (RC0) – OB TH/B/I

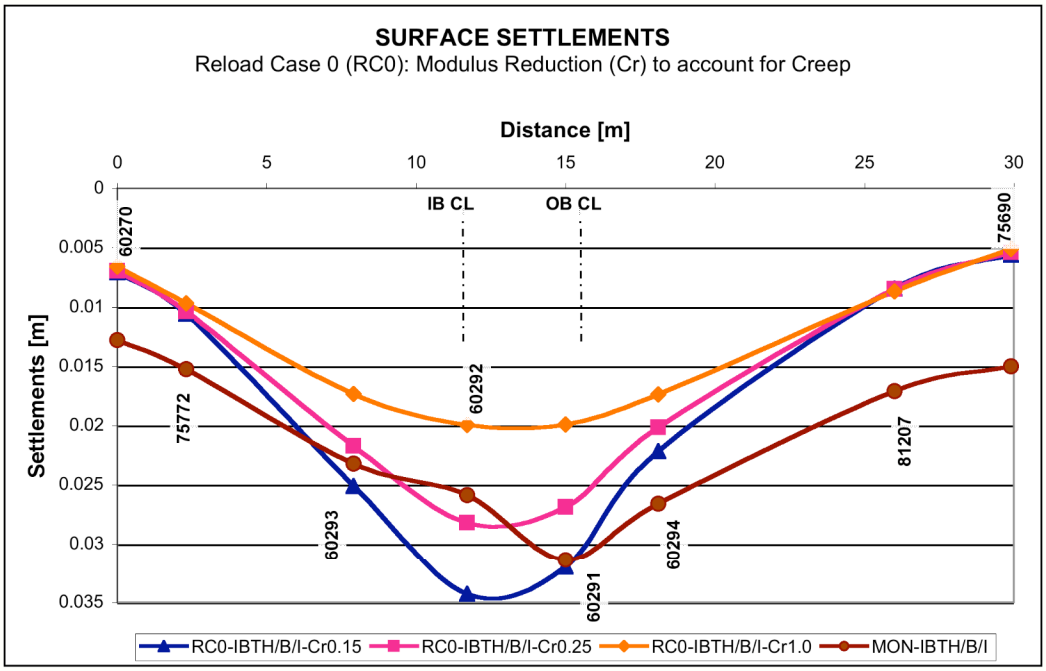

Figure 6.17.c: Comparison of Monitored (MON) vs. Calculated Surface Vertical Deformations for Loads on Pile Caps (RC0) – IB TH/B/I

The influence of lining thickness (Chapter 6.3.3) on surface settlement prediction was investigated with a reduction factor of Cr=0.15 for the elastic frozen soil moduli using surface monitoring point 60291 for the reload cases RC1 and RC2. The results are summarized in Figure 6.18. The lining thickness in the FE model has little influence on surface settlements and therefore the design lining thickness of 0.30 m was retained in subsequent modeling.

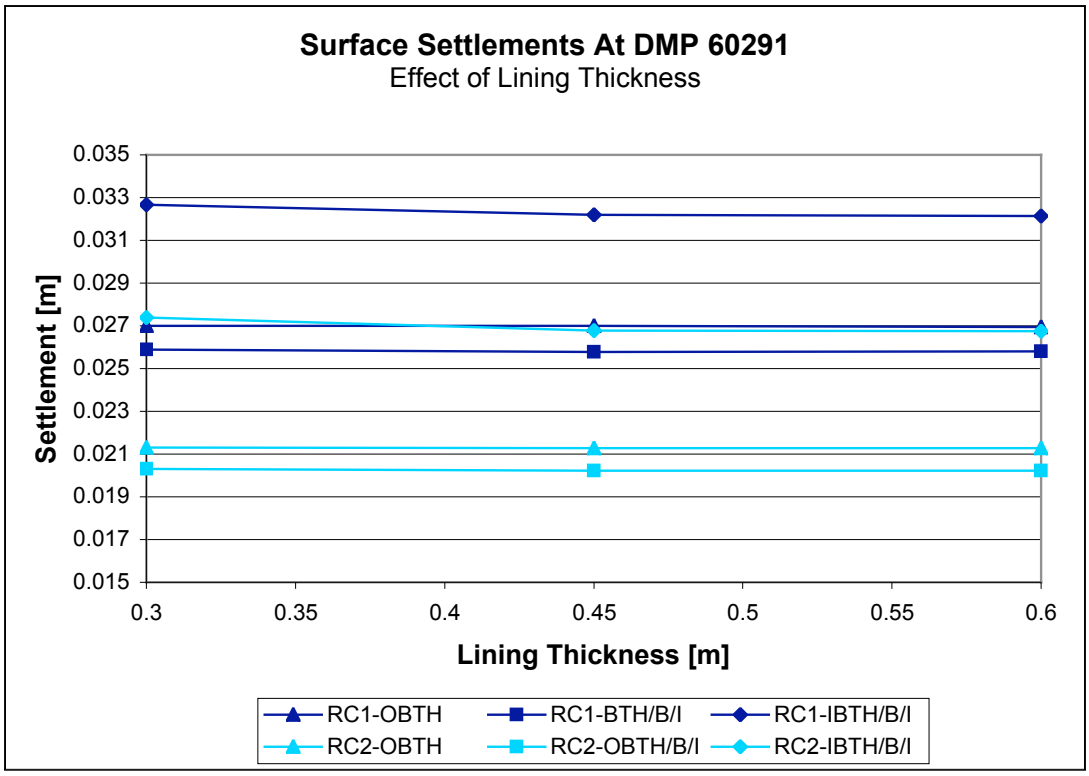

Figure 6.18: Effect of Lining Thickness on Surface Settlements

Any creep that may be associated at the pile - frozen soil interface is assessed using equation 6.3 after Bowles (1982):

$$\frac{\dot{u}_a}{D} = \frac{3^{(n+1)/2} B (f_{ad})^n}{n-1} \qquad (6.3)$$

where:

$\dot{u}_a$ = creep rate per year [-],
D = pile diameter [m],
B = creep parameter, at –10 ºC of 0.56 x 10^{-8} [kPa^{-n}/year],
n = creep parameter; 3,
f_{ad} = design (actual) adfreeze stress [kPa].

Evaluating equation 6.3 for a total project duration of 14 months (approximately 1.2 years between start and end of tunneling), and the lowest adfreeze value of 0.250 MPa in the Organic Deposits (according to Table 3.4) and a pile diameter of 0.2 m:

$$\frac{\dot{u}_a}{0.2} = \frac{3^{(3+1)/2} 0.56 \times 10^{-8} (0.250)^3}{3-1} \text{ or}$$

$\dot{u}_a = 7.875 \times 10^{-11}$ per year. Therefore, any creep associated with the frozen soil – pile interface is negligible.

6.3.7 Heave

Using observed surface heave, freeze test data, and the temperature regime in the frozen soil, an analysis is performed for the value of a site representative segregation potential. This value is then compared with literature data provided by Deix (1992), thus providing a cross reference between heave observed at the Graphic Arts building and other, relevant ground freezing projects.

Equation 3.7 provided in Chapter 3 is evaluated as follows:

$$h(t) = d(t) \cdot n \cdot F + SP \int_0^{t_1} gradT(t_1) d\, t_1 + SP \cdot gradT(t - t_1)$$

where:

h(t) = Frost heave prior to tunneling at selected points (DMP locations see Figure 6.11):

60291: 36.27 mm,
60292: 21.95 mm, and
60294: 31.70 mm.

d(t) = Frozen soil thickness contributing to heave, which considers the thickness of the cohesive soils (Marine Clay and Organic Deposits, 3.1 m thick at Station 95.20) only.

n = Void ratio, or initial moisture (water) content, see Table 6.2.

F = F ranges between 0 and 0.09. The maximum value of 0.09 would represent all pore water undergoing the maximum theoretical expansion due to ice formation. The value is evaluated based on freeze tests by Mueser Rutledge Consulting Engineers, 1998 in Table 6.2.

Table 6.2: Summary of Frozen Test Data for Heave Assessment Due to Ice Formation

Sample	Soil	Initial moisture content	Applied stress on sample	Percent of theoretical maximum heave, p	F = 0.09 x p
RW-5 UF5	Organic Deposits	61.3%	0.06 MPa	4.9%	0.0044
RW-5 UF8	Marine Clay	28.9%	0.09 MPa	18.5%	0.0167

grad T (t_1) = Temperature gradient at the frozen soil boundary during the initial freezing period (establishing the frost body): As mentioned in Chapter 6.3.4, a representative temperature gradient in the horizontal direction of the freezing of -10 ºC / 6 m = 0.0017 ºC / mm can be assumed during the initial freezing period. In comparison, Deix (1992) reports from the Metro Vienna, Contract Section U6/3 (Appendix, Project 15) a value ranging between 0.01 ºC / mm and 0.02 ºC / mm for clays and clayey silts.

grad T = Temperature gradient at the frozen soil boundary during maintenance freezing period. This portion is not further investigated for the purpose of initial heave calculations presented here.

t_l = Time duration of initial freezing period in seconds (s): Mass freezing began on 16 April 2002 and frozen soil temperatures decreased until about the beginning of November 2002. The surface deformation graphs in Figure 6.13 indicate a constant increase of heave until about 15 November 2002. t_l is therefore assumed to be 7 months or 210 days.

t = Time duration for total freezing period; is not further evaluated for the initial heave calculations presented here.

Therefore:

h (t), Marine Clay = 1,700 [mm] x 0.289 x 0.0167 + SP x 0.0017 [°C / mm] x (210 x 24 x 3600) [s]
= 8.20 mm + SP x 30,240 [°C s / mm]

h (t), Org. Deposits = 1,400 [mm] x 0.613 x 0.0044 + SP x 0.015 [°C / mm] x (210 x 24 x 3600) [s]
= 3.78 mm + SP x 30,240 [°C s / mm]

h(t), Marine Clay + h(t), Org. Deposits = 8.20 [mm] + 3.78 [mm] + 2 x SP x 30,240 [°C s / mm]

For the purpose of these back-calculations to verify an order of magnitude SP is evaluated at DMP 60291 assuming a "smeared" SP for both soil layers:

36.27 [mm] = 11.98 [mm] + 2 x SP x 30,240 [°C s / mm]

SP = 40.5×10^{-5} [mm^2 / °C s]

Similarly, computing SP for DMP 60294 and for DMP 60292 gives values of SP = 32.67 x 10^{-5} [mm^2 / °C s] and 16.47 x 10^{-5} [mm^2 / °C s] respectively.

Deix (1992) reports a range of SP values for clayey soils as a function of applied overburden pressure. These relationships are of linear type. For overburden pressures ranging between 0.090 MPa and 2.0 MPa the SP values given range between about 8 x 10^{-5} [mm^2 / ºC s] and 25 x 10^{-5} [mm^2 / ºC s] depending on the composition of the clayey soil. Acknowledging the various uncertainties and assumptions in the above calculations, including among others:

- The very limited sample space considered in derivation of heave values as only two samples were investigated (Table 6.2), and
- The assumption of the average or "smeared" temperature gradient,

the SP values computed compare well with those reported for similar applications in similar soils and surface loading conditions. In other words, the heave measured at the Graphic Arts building compares well with case history data and SP values from the literature. These values can be readily utilized to estimate heave associated with soil freezing and consider applied stresses.

6.3.8 Tunnel Deformations

Five individual deformation points in the tunnels were selected for the evaluation of tunnel deformations. These are the roof leveling points (RLs) located in the crown that measure the vertical deformation and convergence bolts (CBs) measuring the horizontal deformation as displayed in Figure 6.11. The measured tunnel deformations were

compared with the computed deformations utilizing the reduced elastic frozen soil moduli (Cr = 0.15). In the computations, the deformations caused by the softening of the individual excavation steps were subtracted. For example, the deformations in stage 6 (OB TH) do not include the deformations in stage 5 where excavation was simulated by softening the materials in the top heading. This is appropriate since the ground pre-deformations caused by the approaching tunnel face and those caused by the excavation at the monitoring cross section are not included in the measured tunnel deformation values.

Three surface load cases were investigated for this purpose. The comparison of measured (MON) and computed deformations is graphed in Figure 6.19 for the RL values and Figure 6.20 for the CB values. Both graphs include reload case 1 (RC1), reload case 2 (RC2) and the case where the pile cal loads remain on the granite pile caps (RC0).

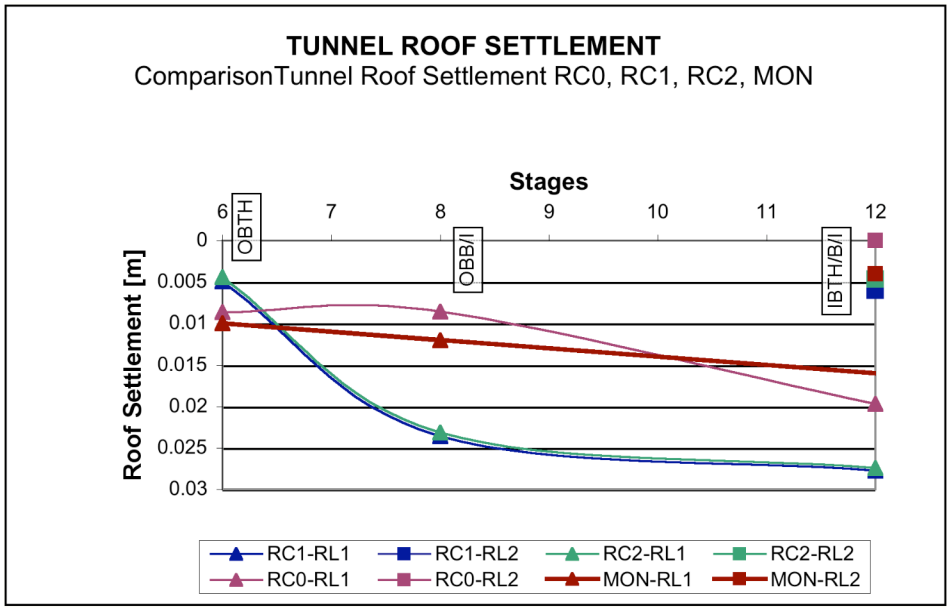

Figure 6.19: Comparison of Monitored (MON) vs. Calculated Tunnel Roof Settlements (RL1, RL2) for Reload Case 1 (RC1), Reload Case 2 and Column Loads on Pile Caps (RC0)

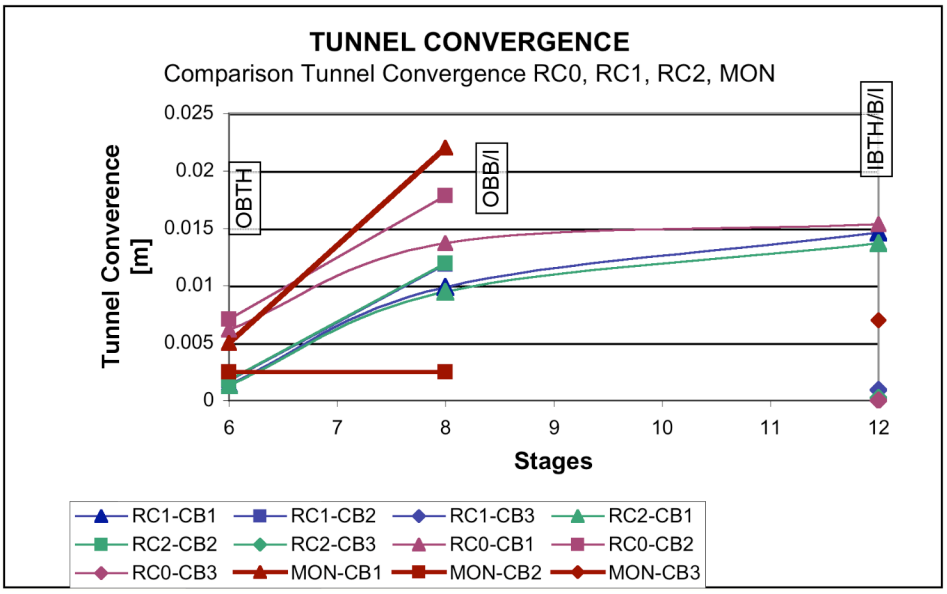

Figure 6.20: Comparison of Monitored (MON) vs. Calculated Tunnel Convergences (CB1, CB2, CB3) for Reload Case 1 (RC1), Reload Case 2 (RC2), and Column Loads on Pile Caps (RC0)

With regard to the roof leveling points (RL1, RL2, Figure 6.19) the case where the column loads remain on the pile caps (RC0) closely approximates the deformation of RL1 in the OB tunnel. A comparison between calculated and monitored deformations for RL2 in the IB tunnel is difficult because only a very small value of about 5 mm was monitored. Load cases RC1 and RC2 approximate the monitored results well while RC0 underestimates the deformation.

With regard to the convergence deformations (Figure 6.20) all load cases approximate the order of magnitude measured for the OB TH situation. For the OB TH/B/I situation the calculations overestimate monitoring point CB2 and underestimate CB1; however, the overall range of predicted deformations between 10 to 18 mm is well within the measured range of 3 to 15 mm in all cases. All load cases underestimate the convergence in the IB TH/B/I tunnel by indicating only up to 20% of the measured value

of about 7 mm. However, this is due in part because of construction activities that are not simulated by the model (Dr. G. Sauer Corporation, 2003) and also some measuring inaccuracies.

6.3.9 Lining, Ground, and Pile Stresses

The measured stresses in the shotcrete lining and ground pressures on the shotcrete lining were close to zero (Dr. G. Sauer Corporation, 2003) and are therefore deemed unreliable. It is believed that the stress measurement problems were due to either faulty installation or monitoring. Similarly, pile pressure cells at monitoring section 2A (Chapter 4) have shown negative values with decreasing trend. Construction problems including incidental cutting of cables were reported (Dr. G. Sauer Corporation, 2003). Therefore, a comparison of measured vs. calculated stresses was not possible for model verification.

6.3.10 Summary of Model Verification for As-Built Conditions

This chapter analyzed the tunnel construction and compared measured data with calculated results from the 2-D FE model. The main assumptions that influence results of the modeling including the frozen soil and its strength parameters, number of piles encountered during tunneling, lining thickness, and tunnel excavation sequencing using a softening factor of 0.55 were verified. The model predicts the general range of deformations. Depending on the tunnel excavation stage the model predicts surface settlements to between 60% and close to 100%. To achieve a closer prediction of surface

settlement ranges in the final tunneling stages the moduli of elasticity of the frozen soils were reduced. While this in part accurately represents deformations caused by frozen soil creep it also accounts for construction realities that were not in accordance with model and design assumptions. A reduction factor of 0.15 has been implemented for the reduction of frozen soil elastic moduli.

This verified and calibrated 2-D FE model has been adopted for the prediction of tunneling induced phenomena in Chapter 7 that is concerned with the development of a new support mechanism. Unlike in this chapter the wooden piles become an integrated element in the frozen soil-pile-tunnel building support system during tunneling.

Chapter 7: Frozen Soil Requirements For Integrated Pile Support System

7.1 General

Chapter 6 provided the verification and calibration of the model for observed field conditions. Generally a good agreement was found between model predictions and observations. In this chapter, the model is used to investigate further the interactions between the piles, frozen soil and tunnel liner. The purpose of this investigation is to determine the minimum required extent of frozen ground around the tunnel and the required adfreeze strength. By reducing the frozen soil in its extent a new support mechanism is proposed. Column loads are no longer supported by the frozen soil but remain supported by the timber piles. Unlike the as-constructed scenario in Chapter 6, the piles now become a support member of an overall system that includes the piles, frozen soil and tunnel lining. This composite support system with its reduced frozen soil zone offers several benefits. Specifically energy needs for the build-up and maintenance of the frozen soil body are reduced, as are the problems associated with frost heave and thaw settlements. However, reduction of the frozen soil mass in thickness and width and reliance on the wooden piles as a structural member, requires a more detailed investigation of a more complex support system. Furthermore, the question arises as to the limits of the reduction, i.e. the minimum size of the frozen soil. A set of acceptance criteria has therefore been developed for the evaluation of the supporting capability of this support system.

7.2 Variations

7.2.1 Variations of the Frozen Soil Mass

Variations of the frozen soil extent have been defined as shown in Figure 7.1. The frozen soil mass is sequentially reduced in horizontal extent between distances d1 through d4 and the vertical height of the frozen soil is reduced from h1 through h5. The vertical height of the frozen soil was not reduced below a thickness of 1.2 m, which is viewed as a minimum thickness based on practical considerations to develop a consistent and structurally competent frozen soil mass. The frozen soil geometry has been kept rectangular in shape. This is viewed as a practical limitation for a vertical freeze pipe arrangement.

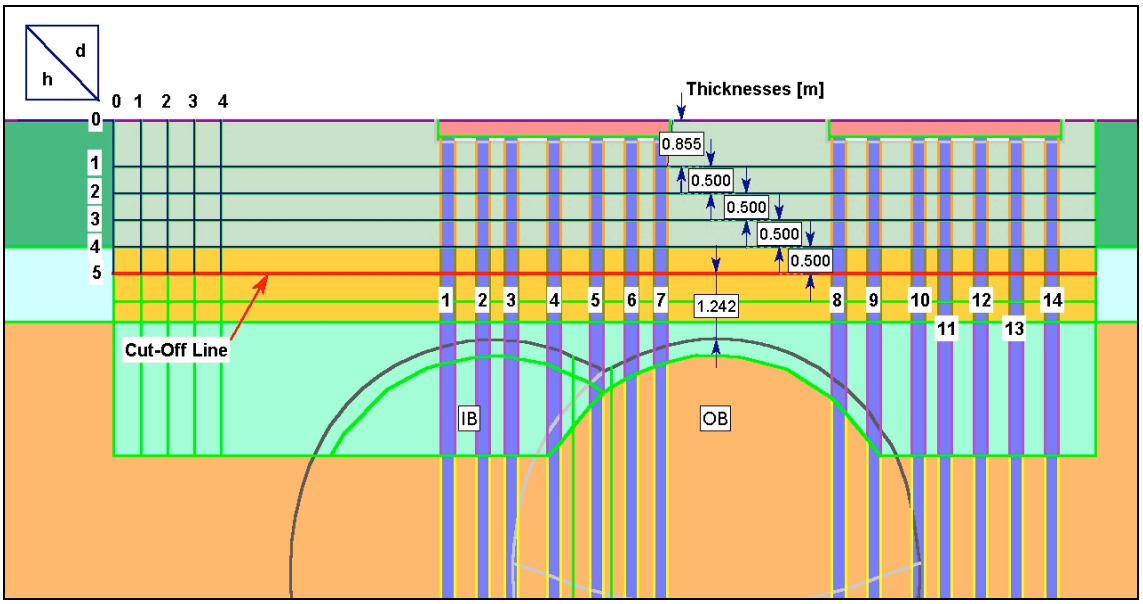

Figure 7.1: Geometric Variations of the Frozen Soil Mass in Extent (d), Height (h) and Pile Number Definitions

7.2.2 Variations of Adfreeze Strength

A range of adfreeze strength values reported in the literature was presented in Chapter 3. The upper and lower boundary values have been implemented in the variations. In addition, a set of lower adfreeze strength values was implemented as 50% of the lower range to increases the overall range in a conservative way. Table 7.1 lists the adfreeze strengths used in the calculations, grouped into sets S1, S2, and S3.

Table 7.1: Adfeeze Strength Sets

Frozen Soil	Adfeeze Strength Sets in MPa		
	S1	S2	S3
Fill	0.935	0.350	0.175
Organic Deposits	0.496	0.250	0.125
Marine Clay	0.600	0.300	0.150

For piles located outside of the frozen soil mass, pile skin strength was assumed equal to the undrained shear strength of the surrounding soil according to Chapter 6.

7.2.3 FE Model Tunneling Stages

Variations of the frozen soil extent were investigated for staged tunnel excavation and support in accordance with Chapter 5 as follows:

- *Stage 1 through 4:* Geostatic stress conditions, freezing of the ground, insertion of pile caps and loading of the model with pile loads.
- *Stage 5:* Excavation of top heading (TH) of the outbound (OB) tunnel by reducing the elastic modulus of the soil within the TH using the softening factor S=0.55 derived in Chapter 5.

- *Stage 6:* Application of beam elements representing shotcrete in the TH and the temporary invert of the OB tunnel and removal of the TH soil elements and the cut-off piles. This stage is also labeled OBTH in the Figures.
- *Stage 7:* Excavation of bench and invert (B/I) of the OB tunnel by reducing the elastic modulus of the soil within the B/I using S=0.55.
- *Stage 8:* Application of beam elements representing shotcrete in the B/I of the OB tunnel and removal of soil elements. This stage is also labeled OBTH/B/I in the Figures.
- *Stage 9 and 10:* During this stage the shotcrete in the OB tunnel is "hardened", i.e. its elastic modulus is set to its 28-day strength and the final lining and the middle-supporting column is inserted into the model.
- *Stage 11:* Similar to Stage 5 the inbound (IB) tunnel is excavated.
- *Stage 12:* Similar to Stage 6 the IB tunnel is supported.
- *Stage 13 and 14:* Similar to Stage 9 and 10 the IB tunnel shotcrete is hardened and the final shotcrete lining is inserted. This stage is also labeled IBTH/B/I in the Figures.

Stages 5 through 14 are utilized selectively to report on the behavior of the hybrid support system.

7.3 Acceptance Criteria

Acceptance criteria were developed for admissible, structural support performance of the individual support elements. An assumption is further made that the frozen soil mass may not decrease below a practical minimum size to serve reliably for tunneling pre-support, groundwater cut-off and embedment of the wooden piles within

the frozen soil. A minimum thickness of the frozen soil of 1.2 m was assumed for this purpose. Deformations of the surface and tunnel are evaluated but do not form part of the acceptance criteria. It is assumed that implementation of the proposed concept would rely on a heave/settlement compensation system, similar to the one carried out for the project and therefore, by activating this system the building would be kept within permissible limits. However, information on surface as well as tunnel deformations is provided to indicate tendencies. Using maximum allowable settlements and building distortion levels of 6 mm and 1/700 respectively for this project (Lacy *et al*., 2004) jacking efforts may be estimated.

Specific acceptance criteria for each structural component are described in the following subsections. Based on these acceptance criteria the overall support system is evaluated.

7.3.1 Strength of the Wooden Pile – Frozen Soil Interface

It has been assumed that pile-supporting capacity is derived from the embedment lengths within the frozen soil only. The capacity is computed by a summation of adfreeze strengths within the respective frozen soils multiplied by the given embedment lengths. It is then compared with the calculated load of the pile that is obtained from a summation of shear stresses within the pile joints multiplied by the respective lengths. The criterion is established as the ratio between the load capacity and calculated load in the pile-frozen soil interface (joint) for each individual pile. Two interfaces for each pile are considered in this computation. The ratio is termed load capacity ratio (LCR) and has to be ≥ 2. With respect to the proposed and complex system this is viewed to be an

acceptable factor of safety. The percentage of yielded joint lengths is also reviewed and reported. Yielded joints are considered failed and therefore not included in the evaluation of the pile load capacity. Joints located up to approximately 0.45 m above the tunnel crown are also not considered in this evaluation. This portion of the pile is typically excavated for the installation of pile shoes (Chapter 4 and 6) and does not provide any supporting strength. Equation 7.1 defines the load capacity ratio as follows:

$$LCR_j = \frac{\sum_{i=1}^{i=E} l_i S_i}{\sum_{i=1}^{i=E} l_i \, |\tau_i|} \tag{7.1}$$

LCR_j = Load Capacity Ratio of joints of a pile j
$\boldsymbol{i}$ = 1 … E (maximum number of joint elements representing the pile-frozen soil interface, excluding yielded elements, varies),
j = 1 … 14 (number of piles),
Si ∈ (S1, S2, S3) adfreeze strength on joint element,
l_i = Length of joint element, and
$|\tau_i|$ = Absolute value of shear stress in joint element.

In equation 7.1 the absolute value of the shear stress is considered, thereby neglecting its direction. The derivation of LCR thus considers the resistance of the pile against a deformation or "pull-out" regardless of the pile deformation direction. During the tunnel excavation process the piles undergo deformations dependent on their location relative to the excavation. Generally piles move toward the excavated space. The LCR therefore describes not only pile supporting capacity but also a resistance against deformation and their function in this respect may be compared to the concept of steel reinforcement in concrete.

7.3.2 Stresses in the Wooden Piles

The wooden piles may not be stressed beyond their uniaxial compressive strength. Utilizing a safety factor of 2 this results in a maximum value of approximately 7.5 MPa.

7.3.3 Section Forces in the Shotcrete Lining

Once the wooden piles are cut, they are embedded into the shotcrete initial lining. To some extent, loads will be transferred through the pile tips into the shotcrete lining. The capacity of the shotcrete lining is evaluated using interaction diagrams that plot the existing axial force / moment combinations vs. an envelope of permissible combinations. The evaluation adheres to the design requirements for reinforced concrete.

7.3.4 Strength of the Frozen Soil

The strength of the frozen soil is inspected at two characteristic horizons above the tunnel crown using strength factors. The strength factor is calculated by dividing the material strength based on the Mohr-Coulomb failure criterion by the induced stress at the selected locations.

7.4 Results

7.4.1 Load Capacity Ratio (LCR)

Variations of the width of the frozen soil mass indicated no significant difference of supporting strength of the frozen soil mass. Therefore only the width labeled “d4” (see Figure 7.1) has been considered in the presentation of results. Similarly to a minimum vertical extent this is viewed appropriate from a practical view and to provide a reliable

ground water cut-off. The load capacity ratios were investigated for all combinations between h and S for all piles. Only selected results are reported herein, although the general trends are also described. Graphs indicating LCR for all piles as a function of FE Model tunneling stages are presented for the combination h1S1 in Figure 7.2, for h3S2 in Figure 7.3, and for h5S3 in Figure 7.4, thus reporting for conditions of highest capacity to lowest capacity of frozen soil and adfreeze strength. A general tendency of decreasing LCR can be observed with decreasing height of the frozen soil mass and decreasing adfreeze strength through the excavation of the OB tunnel. Excavation of the IB tunnel however, indicates a general increase of LCR for piles located above the IB tunnel while the LCR of the piles located outside and to the side of the OB tunnel further decreases.

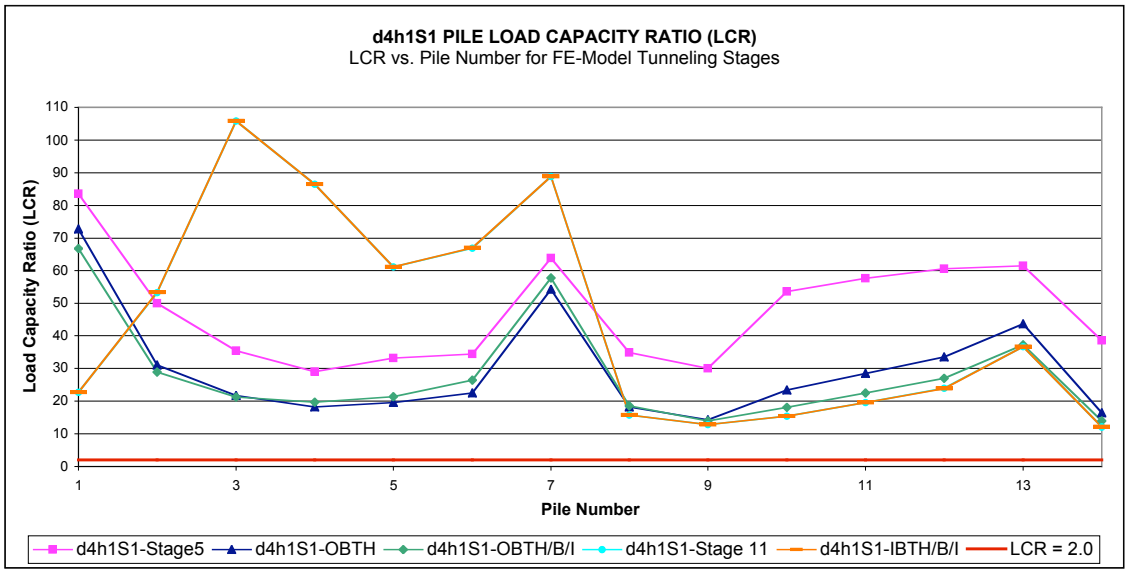

Figure 7.2: Load Capacity Ratio (LCR) for All Piles as a Function of FE Model Tunneling Stages: Frozen Soil Thickness h1, Adfreeze Strength S1

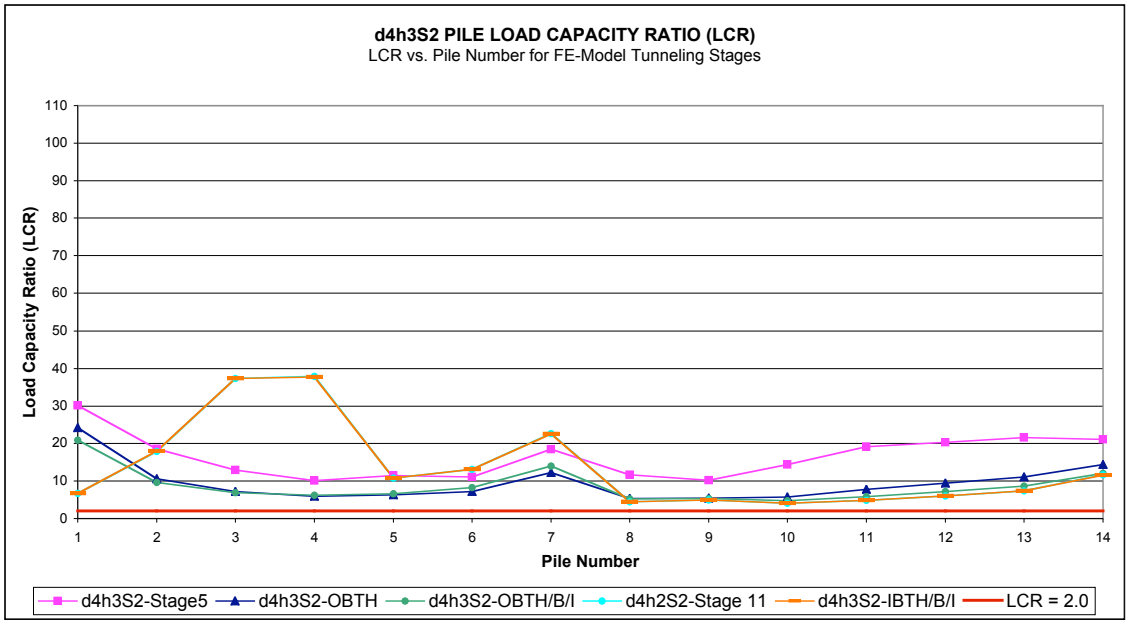

Figure 7.3: Load Capacity Ratio (LCR) for All Piles as a Function of FE Model Tunneling Stages: Frozen Soil Thickness h3, Adfreeze Strength S2

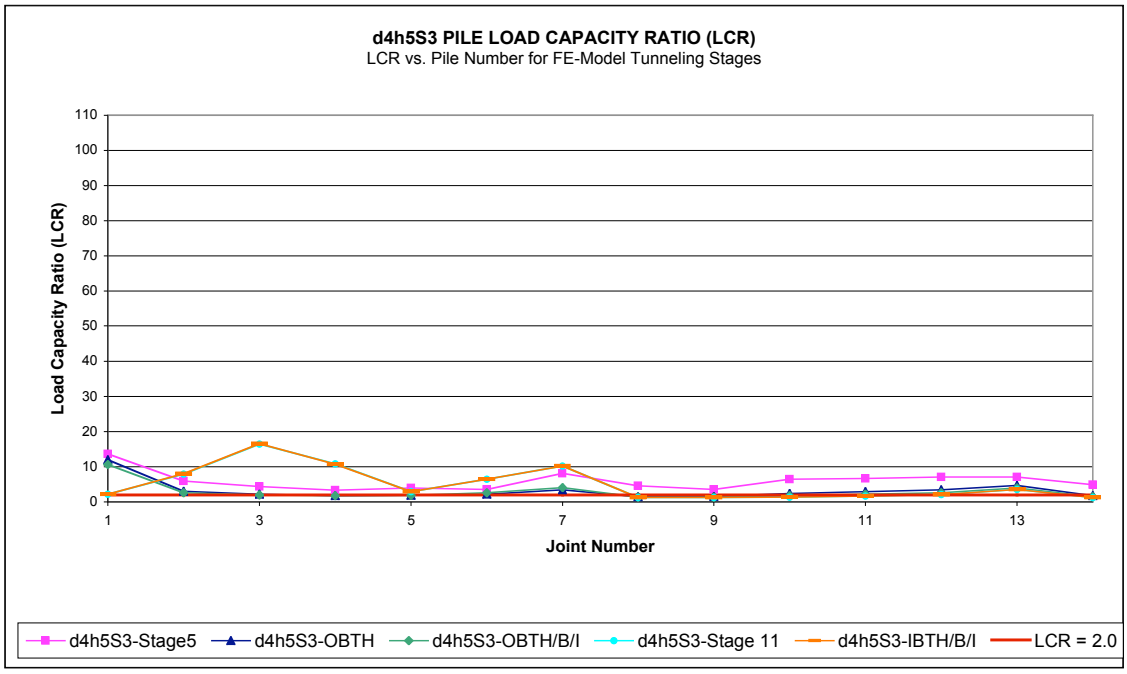

Figure 7.4: Load Capacity Ratio (LCR) for All Piles as a Function of FE Model Tunneling Stages: Frozen Soil Thickness h5, Adfreeze Strength S3

To further evaluate the different loading tendencies of piles located above the IB tunnel vs. those located to the side of the OB tunnel, piles 3 and 11 (see Figure 7.1 for pile locations) were selected for closer examination. The respective LCR values vs. the FE model tunneling stages for frozen soil height and adfreeze strength combinations h1S1, h3S1, h5S1, h1S2, h3S2, h5S2, h1S3, h3S3, and h5S3, were graphed in Figure 7.5.a for pile 3 and Figure 7.5.b. Figure 7.5.a shows the decrease of LCR through completion of the OB tunnel and an increase through IB tunnel completion. While the LCR values decrease to about 20 for h1S1 and then increase to over 100, the LCR values for h5S3 decrease to about 2, and then increase to about between 15 and 20. A clear dependency on the adfreeze strength and height of the frozen soil mass and adfreeze strength is demonstrated. Figure 7.5.c is a zoom into stages 6 through 8 for investigation of the LCR values close to 2. LCR is smaller than 2 for the combinations h3S3 and h5S3 for pile 11 and h5S3 for pile 3. With the established criterion of LCR $\geq$ 2, use of frozen soil thicknesses h3 and h5 for frozen soil having adfreeze as low as those in set S3 is unfeasible.

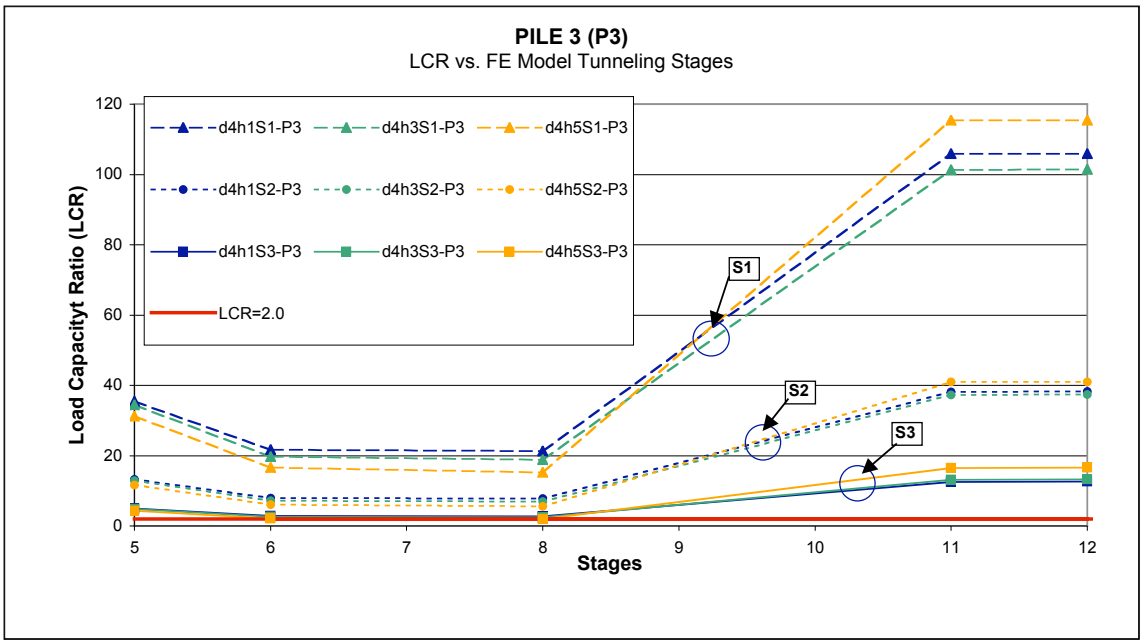

Figure 7.5.a: Load Capacity Ratio (LCR) vs. FE Model Tunneling Stages for Pile 3

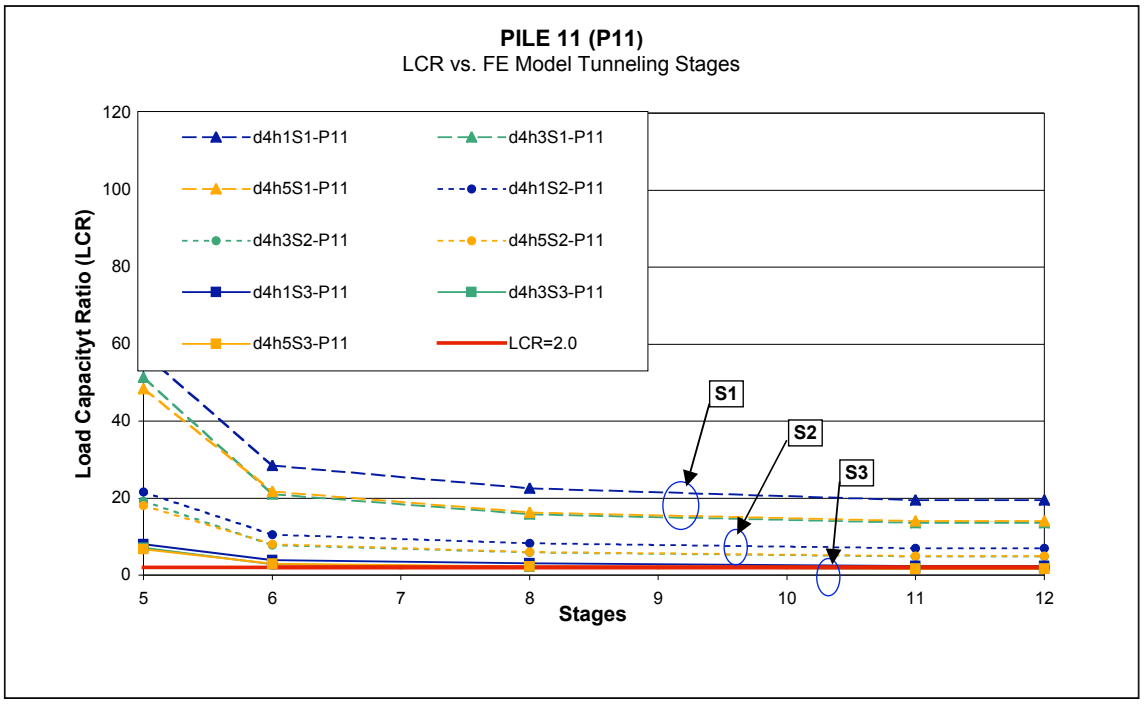

Figure 7.5.b: Load Capacity Ratio (LCR) vs. FE Model Tunneling Stages for Pile 11

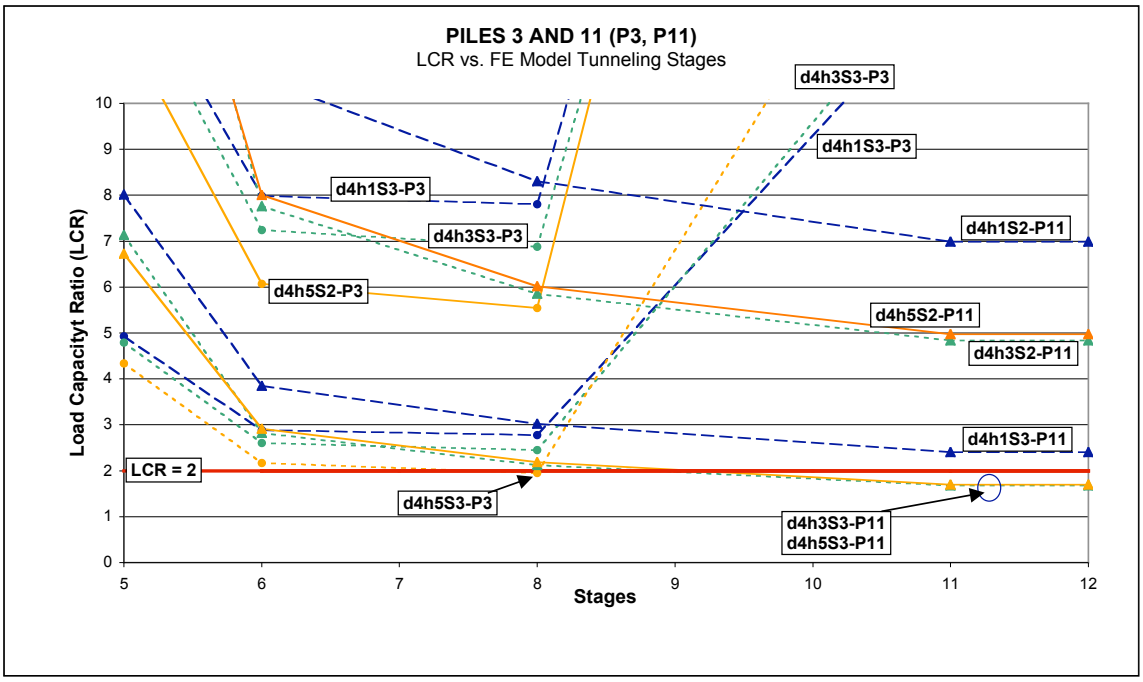

Figure 7.5.c: Load Capacity Ratio (LCR) vs. FE Model Tunneling Stages for Pile 3, 11 (Zoom for LCR < 2)

The study of the load capacity ratio for the piles as a function of the FE model tunneling stages enables a qualitative interpretation of the pile load redistribution as presented in Figure 7.6. Excavation of the OB tunnel top heading and subsequently bench and invert leads to an increased loading of the piles to both sides of the tunnel. Upon excavation of the IB tunnel the piles to the side of the OB tunnel become more loaded and the ones above the IB tunnel are unloaded. Direction and change in the LCR are taken from piles 3 and 11. The unloading of the piles above the tunnel is plausible because the tunnel lining acts as a support member in the overall support system of frozen soil-piles-tunnel lining. Due to the excavation of the tunnel the frozen ground and piles become more loaded to the side of the OB tunnel, although the additional load increment due to IB tunnel excavation is small.

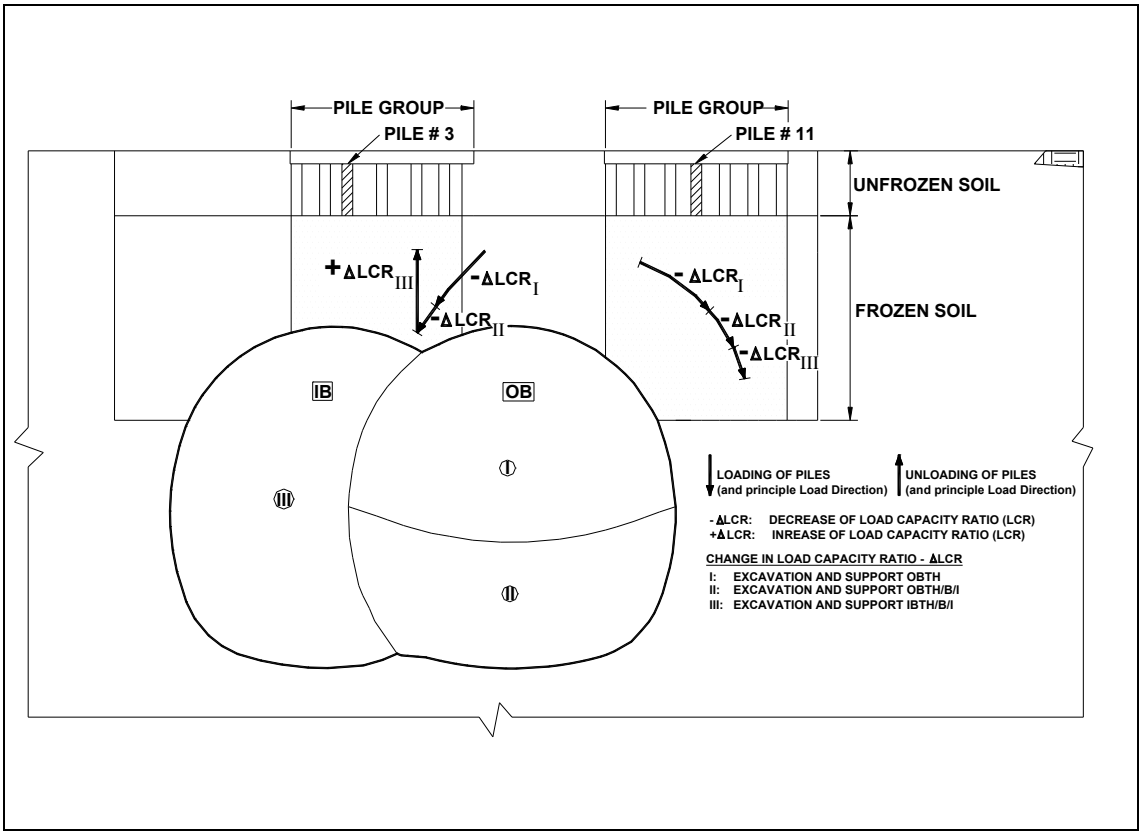

Figure 7.6: Qualitative Interpretation of Pile Load Redistribution Process

7.4.2 Stresses in the Wooden Piles

Axial stresses in the wooden piles have been examined for pile elevations about 0.6 m above the tunnel crown and 0.6 m above the bottom elevation of the frozen soil where piles are located to the outside of the OB tunnel. Axial stresses have been graphed for the FE model tunneling stages in Figures 7.7, 7.8, and 7.9 for the frozen soil-adfreeze set combinations h1S1, h3S2, and h5S3 respectively. The development of pile stresses throughout the tunnel modeling stages is similar for all graphs. During the excavation of the OB tunnel piles located directly above it become less stressed and those outside of it are stressed more because of the load re-distribution that takes place to these regions.

When the IB tunnel excavation takes place the piles above the IB tunnel are unloaded indicated by a decrease in pile stresses. Unlike for the pile load capacity or pile skin friction the piles to the outside of the OB tunnel tend to unload to a minor extent during the final tunneling stage. The development of the pile stresses in principle indicates that the frozen soil mass rests on the tunnel lining and this becomes a load-carrying element of the overall system.

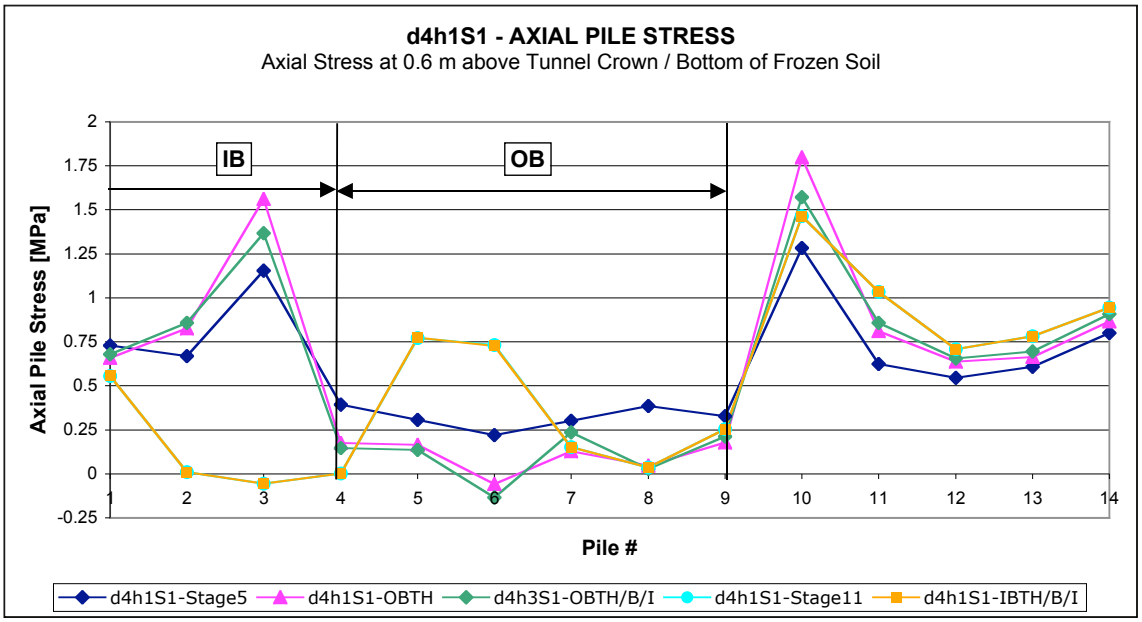

Figure 7.7: Pile Stresses at Elevation of 0.6 m Above the Tunnel Crown / Bottom of Frozen Soil: Frozen Soil Thickness h1, Adfreeze Strength Set S1

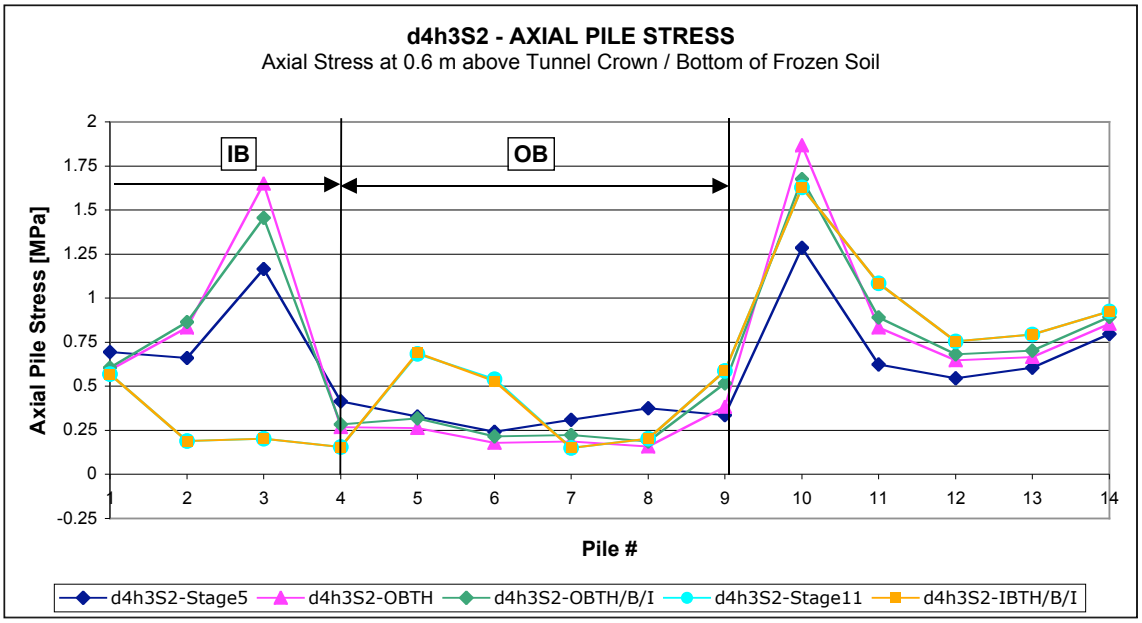

Figure 7.8: Pile Stresses at Elevation of 0.6 m Above the Tunnel Crown / Bottom of Frozen Soil: Frozen Soil Thickness h3, Adfreeze Strength Set S2

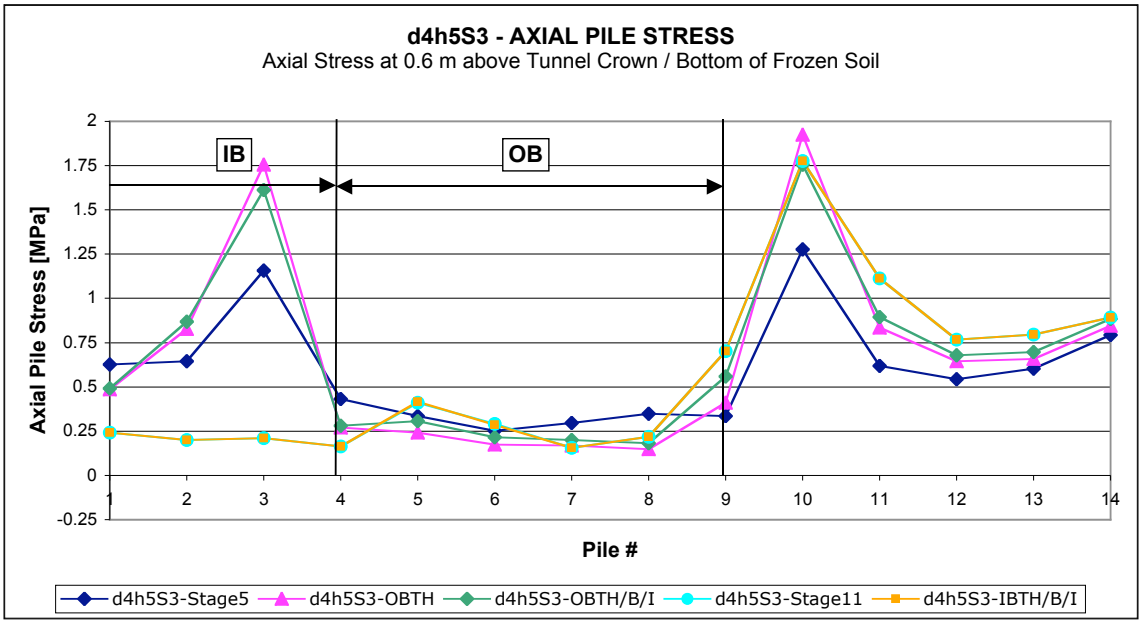

Figure 7.9: Pile Stresses at Elevation of 0.6 m Above the Tunnel Crown / Bottom of Frozen Soil: Frozen Soil Thickness h5, Adfreeze Strength Set S3

7.4.3 Section Forces in the Shotcrete Lining

Section Forces in the initial and final linings have been examined by plotting moment / axial force combinations in interaction diagrams (Sauer *et al.*, 1994) that provide an envelope of permissible combinations for a concrete reinforced section with the project lining design thickness of 0.3 m and the reinforcement with lattice girders every about 0.8 m and two layers of welded wire fabric (W8 x W8, 6 inch x 6 inch). These envelopes take into account material reduction and load factors according to ACI 318. Frozen soil height and adfreeze set combinations of h1S1, h3S2, and h5S2 have been plotted for all FE Model tunneling stages in the graph of Figure 7.10. As can be seen the existing section axial force / moment combinations lie well within the envelope, thus indicating reserves in the structural lining.

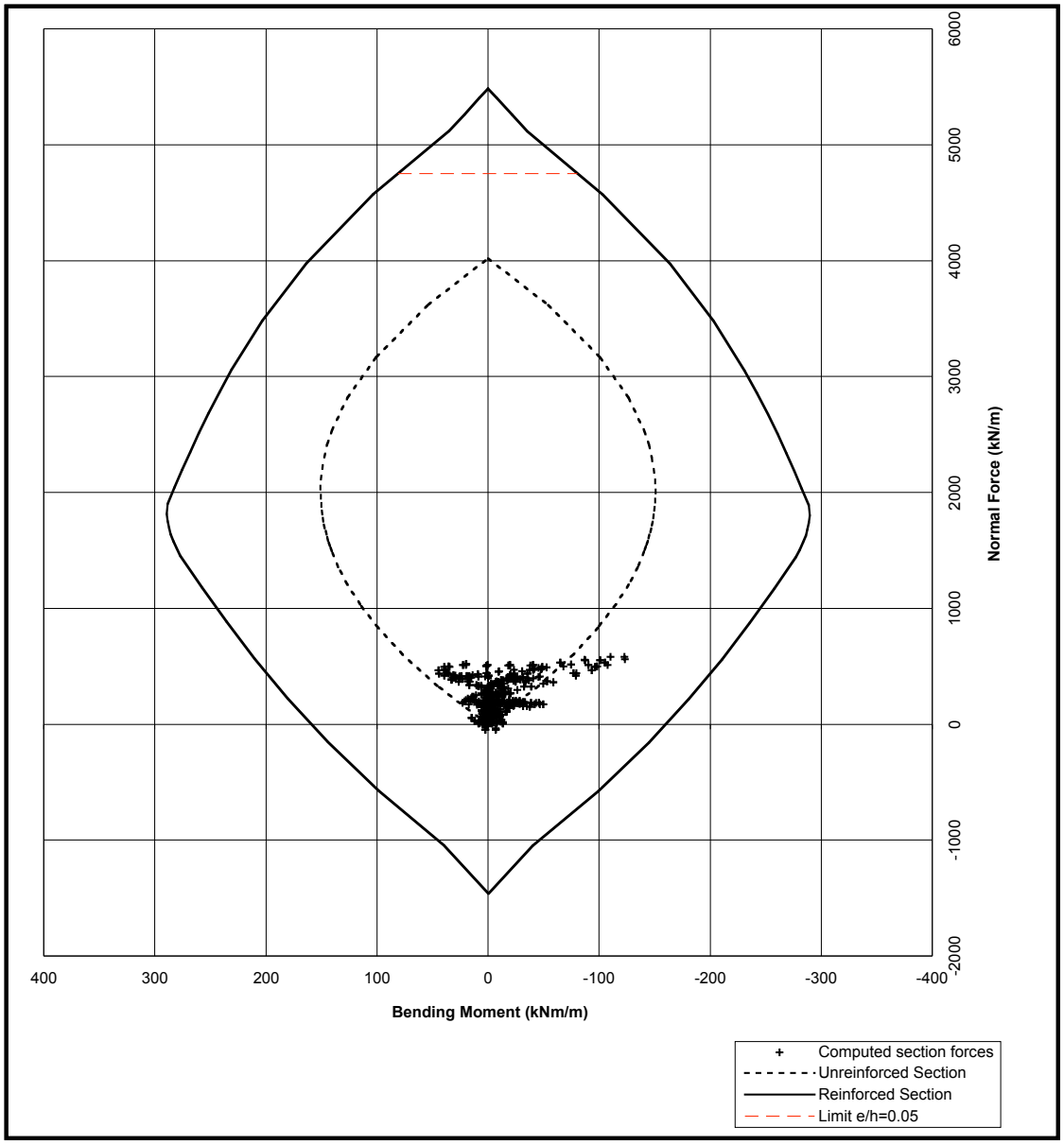

Figure 7.10: Interaction Diagram for Lining Capacity Verification

7.4.4 Strength of the Frozen Soil

Figure 7.11 indicates two horizons in the frozen soil mass that have been selected for a representative investigation of frozen soil strength. At the locations shown the strength factors have been graphed along the width of these horizons and presented in

Figures 7.12, 7.13 and 7.14 for adfreeze strength sets S1, S2, and S3 respectively. Each of these figures displays strength factors for each tunneling stage and frozen soil height h1, h3, and h5.

The strength factors are similar for the different adfreeze strength sets, although a tendency to lower strength factors, thus increased stressing of the frozen soil is observed with decreasing adfreeze strength. With decreasing adfreeze strength the frozen soil itself contributes increasingly in the frozen soil-pile-tunnel lining system.

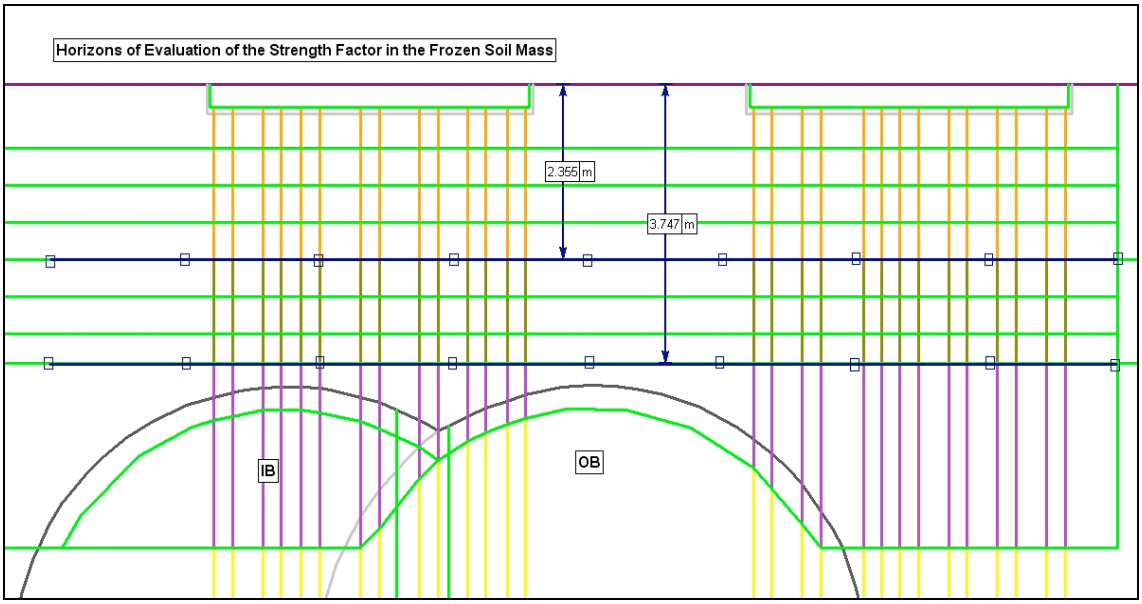

Figure 7.11. Horizons in Frozen Soil for the Evaluation of Strength Factor of Frozen Soil

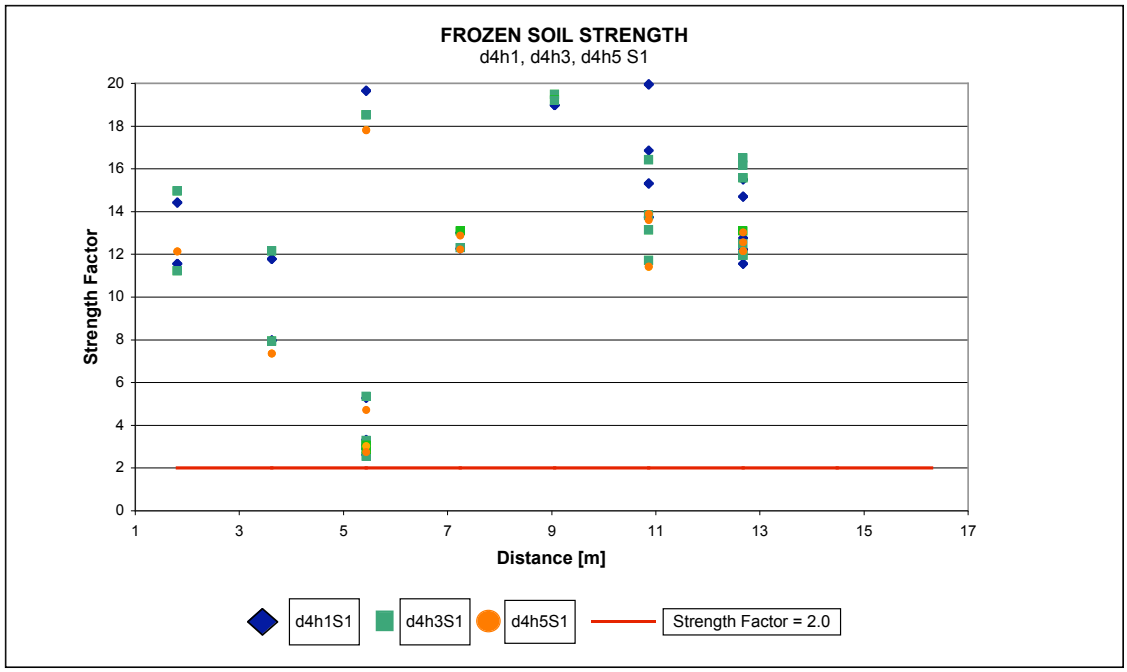

Figure 7.12: Strength Factor of Frozen Soil for FE Model Tunneling Stages for Adfreeze Set S1

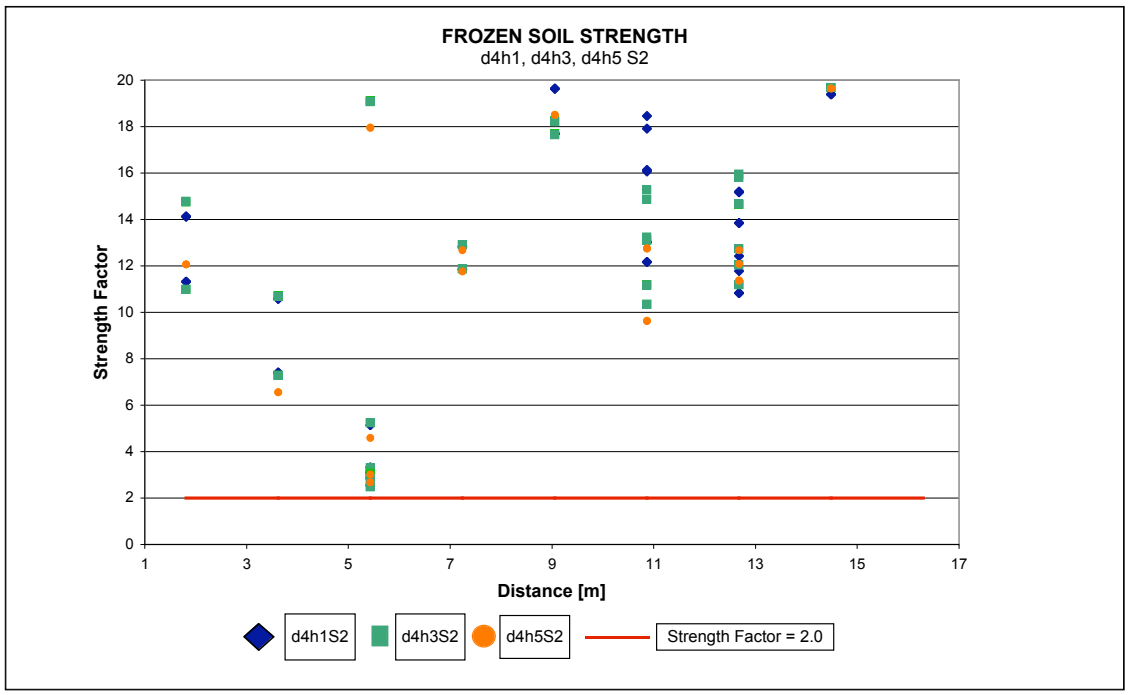

Figure 7.13: Strength Factor of Frozen Soil for FE Model Tunneling Stages for Adfreeze Set S2

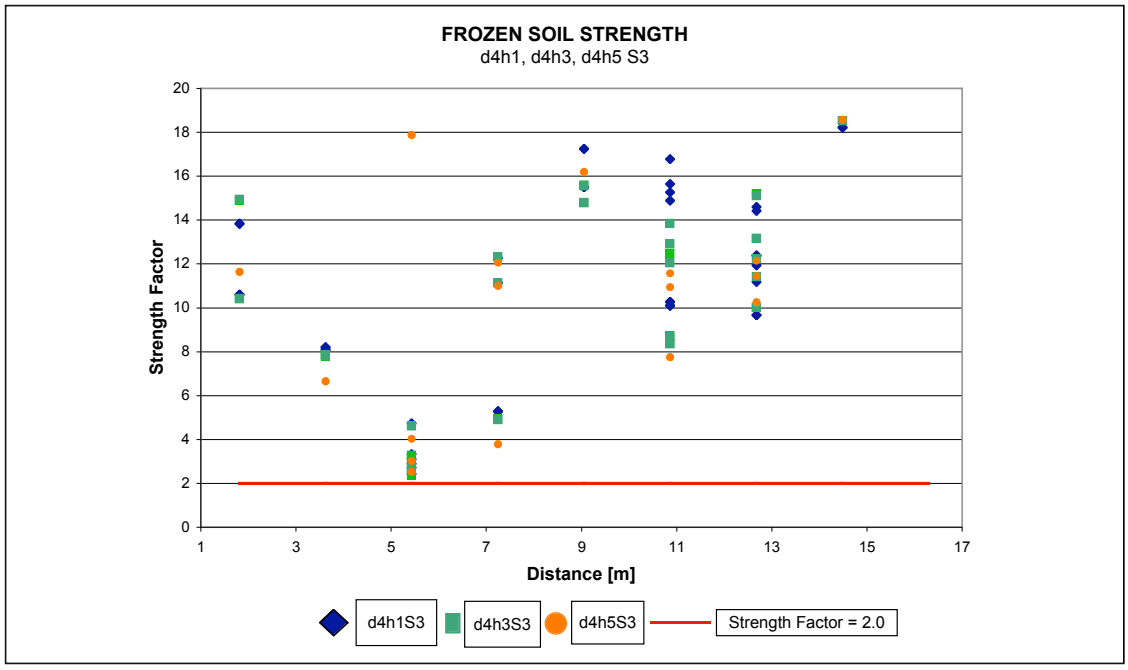

Figure 7.14: Strength Factor of Frozen Soil for FE Model Tunneling Stages for Adfreeze Set S3

7.4.5 Summary of Results

A summary of results is presented in form of an evaluation matrix in Table 7.2. The criteria established have been evaluated for the combination of frozen soil thickness and adfreeze values as presented in the first column. Subsequent columns include evaluation criteria for these combinations including the load capacity ratio LCR, pile stresses, shotcrete lining capacity, and frozen soil strength factor. Maximum vertical surface displacements, maximum distortion or relative displacement between the two columns resting on the two pile caps, and tunnel deformations at selected locations are also provided for information purposes, although these are not used in assessing the adequacy of the overall structural system.

The table shows that the adfreeze strength and thickness of the frozen soil are the critical acceptance criteria. Already with the completion of the OB tunnel top heading LCR become less than 2 for the lower capacity frozen zones. While the load capacity is exceeded for just one pile for frozen soil height of h1, 7 piles show excess loads for height h5. These include piles 3, 4, 5, 8, and 9, indicating that pile load capacity has been exceeded for piles to the outside of the tunnel and above it. The minimum LCR value is 1.2 for h5S3. Maximum surface vertical deformation associated with this case is 55 mm. However, this total surface displacement is only about 52% more than the surface displacement monitored at the project. The surface deformations cause an angular distortion between the two columns of 1/230. Based on the evaluation of strength the adfreeze set S3 provides insufficient shear capacity in the frozen soil-pile interface. Adfreeze set S3 would therefore not be accepted for the proposed support mechanism.

For the adfreeze value set S2 the frozen soil thickness may be reduced to height h5, or a total minimum thickness of 1.2 m measured above the tunnel crown. This thickness provides for a minimum LCR value of 3.5. The associated maximum vertical surface displacement predicted is 44 mm at the pile cap, thus for the column. An angular distortion of 1/340 is associated with this configuration.

Vertical deformations occur at all pile caps, thus it is expected that a settlement compensation system would be required for all cases investigated. However, the settlement values computed do not consider any heave amounts associated with freezing. These will compensate for some amount of the settlements predicted.

Tunnel deformations reach a maximum of 56 mm at the roof leveling points. These are viewed as acceptable. In practical tunneling applications anticipated

deformations are considered by over-excavation as not to violate the clearance requirements of the finished opening of the tunnel.

Contour plots of vertical displacements for the FE model tunneling stages OBTH, OBTH/BI, and IBTH/B/I are provided in Figures 7.15, 7.16, and 7.17 respectively. Stress regimes associated with these displacements are represented in respective Figures 7.18 through 7.20 using major principal stresses.

In summary, the evaluation framework developed in Table 7.2 may be used in the systematic planning of ground freezing projects with similar challenges as those found on this project. Beginning with a confidence level expressed by the load capacity ratio LCR, a frozen soil extent – adfreeze strength combination may be selected. This selection may be based on refrigeration plant economy in terms of frozen temperature and frozen soil volume. The ground freezing planner may select a colder temperature which yields higher adfreeze strengths at a lower frozen soil mass height or accept a thicker frozen soil mass with lower adfreeze strengths. An optimum balance of frozen soil mass at a given temperature may thus be determined. Heave considerations will also enter such a selection process.

Table 7.2: Summary Evaluation Matrix

Combination of Frozen Soil Height and Adfreeze Strength (all d4)	Evaluation of Pile Capacity (No. of Piles LCR < 2) and Minimum LCR						Pile Vertical Stress (> 7.5 MPa)					Lining Capacity (Satisfies ACI Requirements: Yes=Y, No=N)					Minimum Frozen Soil Strength Factor at Representative Locations (< 2)					Maximum Surface Deformation		Maximum Tunnel Deformation (for Locations see Figure 6.11, Chapter 6)			
	Stage 5	OBTH	OBTH/B/I	Stage 11	IBTH/B/I	Min. LCR All Piles	Stage 5	OBTH	OBTH/B/I	Stage 11	IBTH/B/I	Stage 5	OBTH	OBTH/B/I	Stage 11	IBTH/B/I	Stage 5	OBTH	OBTH/B/I	Stage 11	IBTH/B/I	Vertical Settlement (mm)	Distortion (between Columns)	RL1 (mm)	RL2 (mm)	CB1 (mm)	CB3 (mm)
h1S1	0	0	0	0	0	12.4	0	0	0	0	0	Y	Y	Y	Y	Y	0	0	0	0	0	37	1/500	37	37	12	14
h3S1	0	0	0	0	0	11.3	0	0	0	0	0	Y	Y	Y	Y	Y	0	0	0	0	0	38	1/460	39	39	12	14
h5S1	0	0	0	0	0	9.7	0	0	0	0	0	Y	Y	Y	Y	Y	0	0	0	0	0	40	1/400	40	41	12	13
h1S2	0	0	0	0	0	4.3	0	0	0	0	0	Y	Y	Y	Y	Y	0	0	0	0	0	40	1/430	40	40	12	14
h3S2	0	0	0	0	0	4	0	0	0	0	0	Y	Y	Y	Y	Y	0	0	0	0	0	41	1/400	42	42	12	13
h5S2	0	0	0	0	0	3.5	0	0	0	0	0	Y	Y	Y	Y	Y	0	0	0	0	0	44	1/340	44	45	11	13
h1S3	0	1	2	4	4	1.5	0	0	0	0	0	Y	Y	Y	Y	Y	0	0	0	0	0	45	1/360	46	46	11	13
h3S3	0	2	3	4	4	1.4	0	0	0	0	0	Y	Y	Y	Y	Y	0	0	0	0	0	48	1/320	49	48	11	13
h5S3	0	5	7	5	5	1.2	0	0	0	0	0	Y	Y	Y	Y	Y	0	0	0	0	0	55	1/230	56	56	11	13

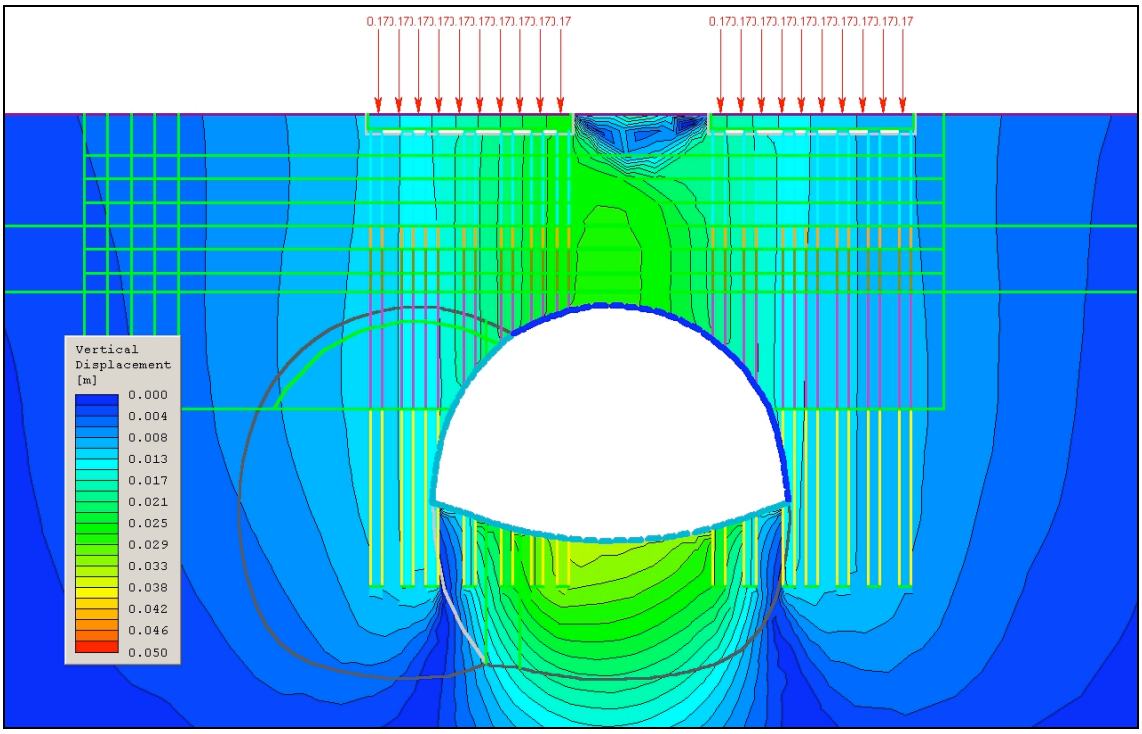

Figure 7.15: Vertical Displacements for h5S2 and FE Model Tunneling Stage OBTH

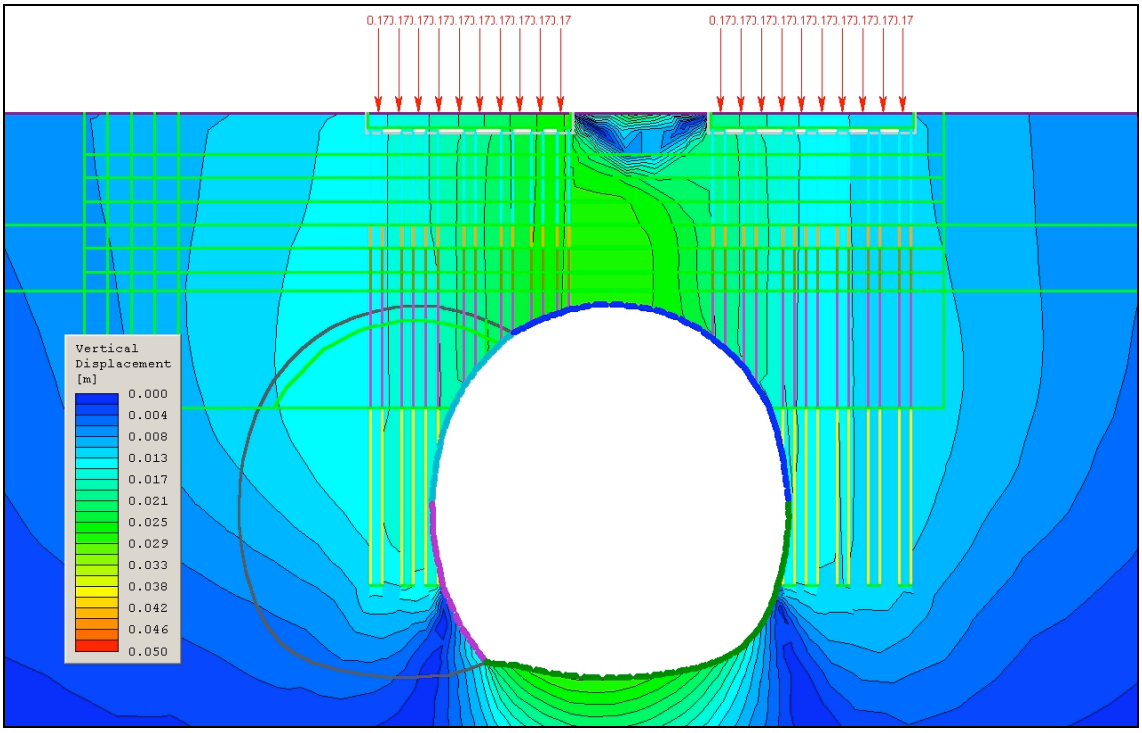

Figure 7.16: Vertical Displacements for h5S2 and FE Model Tunneling Stage OBTH/B/I

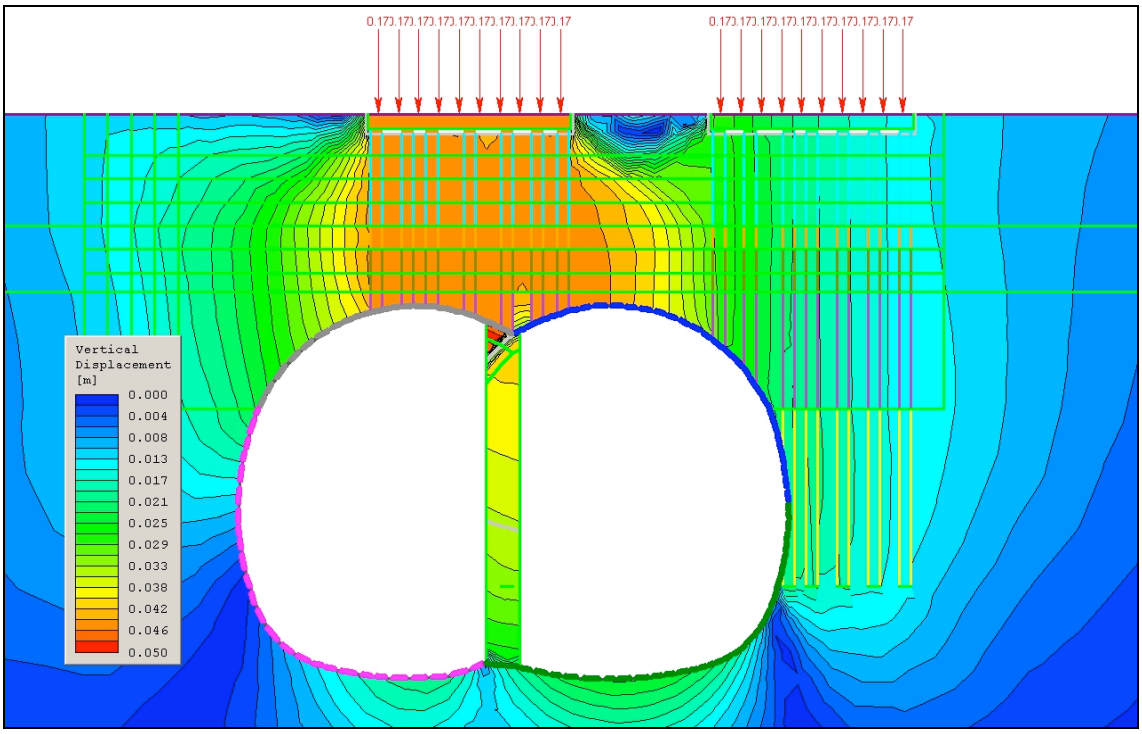

Figure 7.17: Vertical Displacements for h5S2 and FE Model Tunneling Stage IBTH/B/I

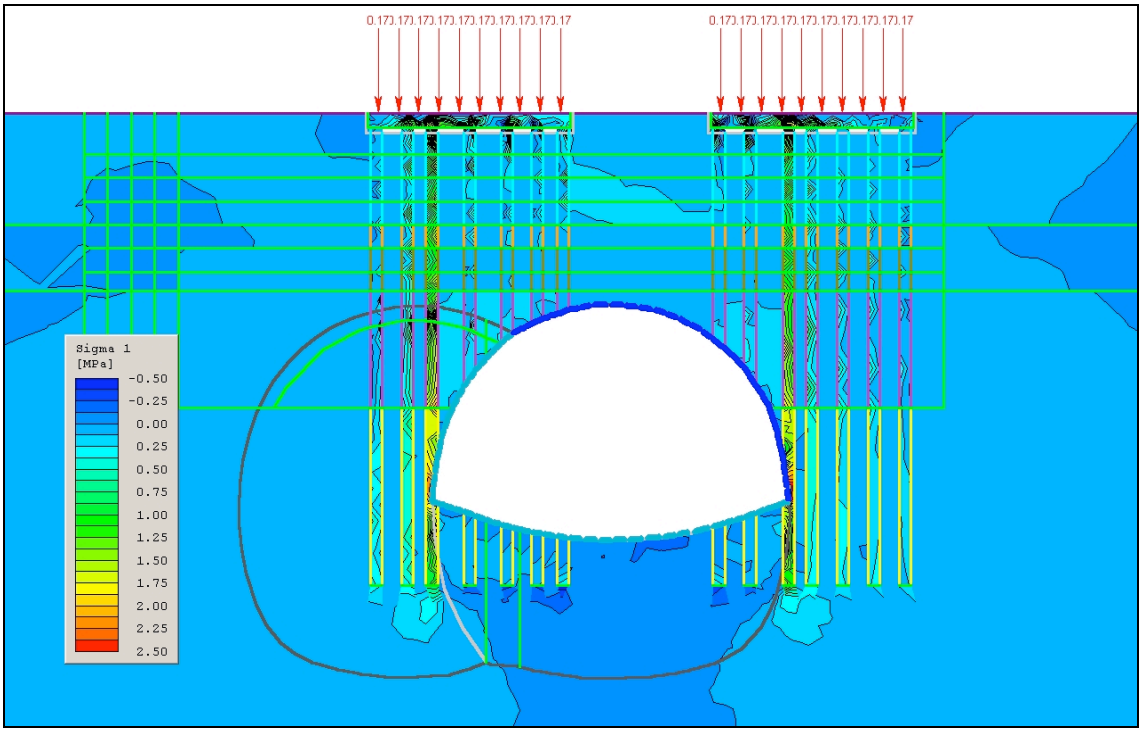

Figure 7.18: Major Principal Stresses for h5S2 and FE Model Tunneling Stage OBTH

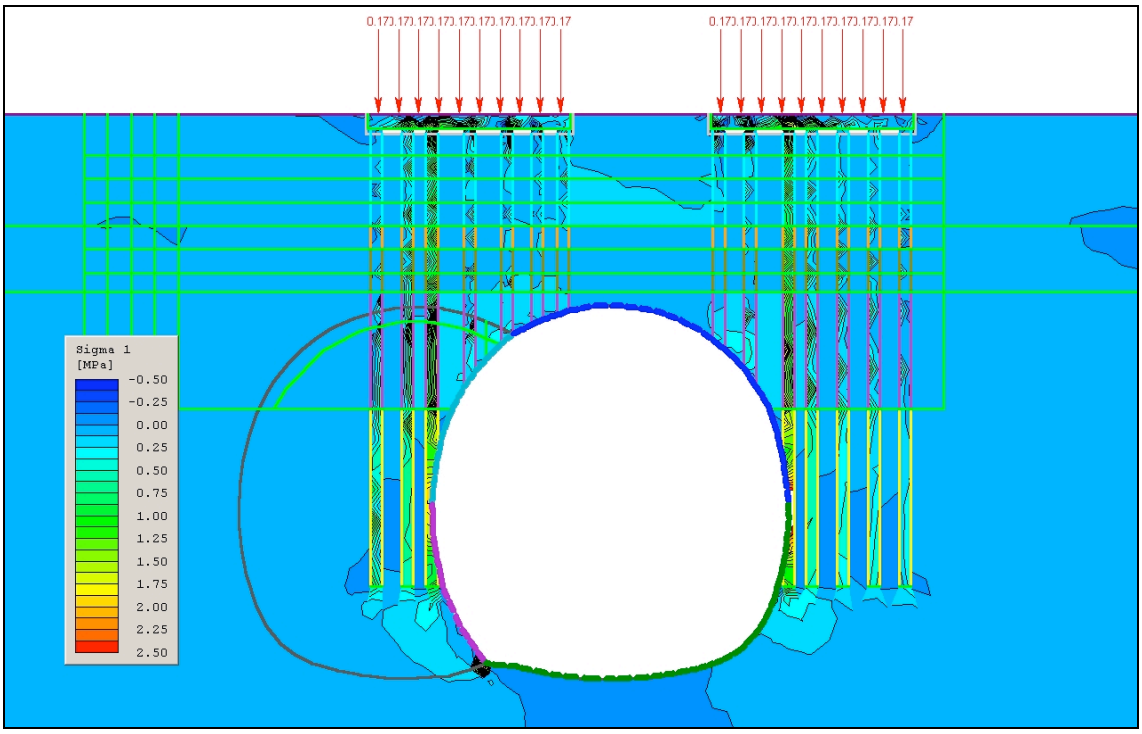

Figure 7.19: Major Principal Stresses for h5S2 and FE Model Tunneling Stage OBTH/B/I

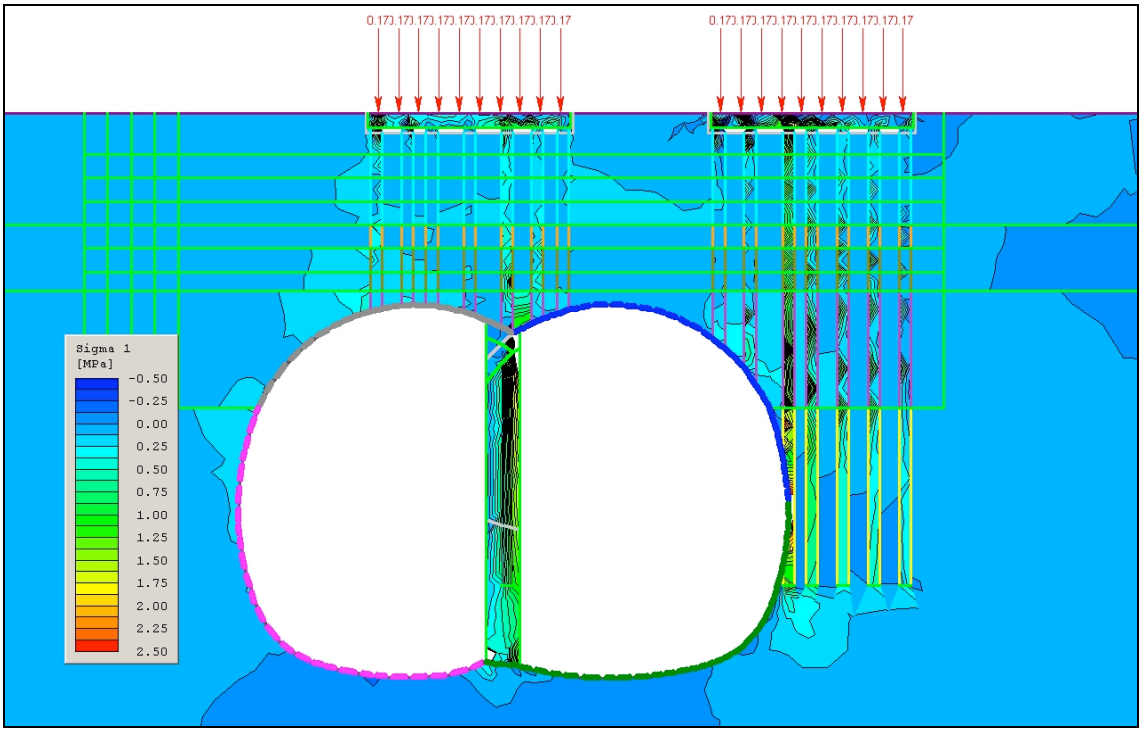

Figure 7.20: Major Principal Stresses for h5S2 and FE Model Tunneling Stage IBTH/B/I

7.4.6 Cost Savings

To demonstrate potential cost savings by the proposed approach a generic cost estimate was developed for the reduced frozen soil extent based on prices commonly used in the underground construction industry for ground freezing. This generic cost estimate is free of any site specifics at Russia Wharf. For example, increased difficulties of vertical freeze pipe installation under low headroom and thus higher installation costs have not been considered. Similarly, any cost savings associated with the proposed approach resulting from a lesser effort in heave compensation have not been included. This generic cost estimate is thus intended for use in estimating cost when adopting the proposed concept in similar, future applications.

According to 2004 cost data, the installation of freeze pipes, establishment of the frozen soil body and dismantling of the freezing system ranges between \$400-\$600 / m^3 or an average of \$500 / m^3. The freezing operation costs between \$1.40 and \$2.20 / m^3 per week or an average of \$1.80 / m^3 per week. Energy costs based on an energy rate of \$0.15 / kWh are between \$1.10 and \$1.60 / m^3 per week or an average of \$1.35 / m^3 per week.

Based on the assumption that a sufficient frozen soil height above the tunnel crown would be 1.2 m and the horizontal frozen soil extent would be reduced by approximately 2 m as proposed, then approximately 1,800 m^3 less volume of frozen soil would be required at the Graphic Arts building. Utilizing the cost data above, the establishment of the frozen soil body would save approximately \$900,000.00. The cost savings for maintaining the frozen soil body for a duration of about 14 months of

tunneling would be about $190,000.00, and savings in energy cost would be about $150,000.00. In total, cost savings of about $1.24 million could be realized with the proposed frozen soil concept.

Chapter 8: Summary of Results and Conclusion

8.1 Summary of Results

Tunneling beneath buildings supported by an array of timber piles was successfully accomplished at the Russia Wharf Site in Boston, MA. A complex, state-of-the-art design combining NATM tunneling procedures, pile cutting, and pile integration into the shotcrete lining was required to meet the complex challenges of the project. Ground freezing was successfully used for tunnel pre-support and building underpinning in this design. Performance of the tunneling and its impact on surface and building settlements compare well with experiences at other, similar urban tunneling projects employing ground freezing.

Three-dimensional (3-D) finite element numerical computations were performed to assess the three-dimensional stress re-distribution effect around the active tunnel face. These results were then used to derive a modulus reduction or "softening" factor to be used to approximate the stress relaxation at the tunnel face in two-dimensional (2-D) calculations. A softening factor of S=0.55 provided a good agreement between the 2-D and 3-D results. The 2-D model then enabled enhanced modeling of the wooden piles utilizing elements with a Mohr-Coulomb failure criterion along the pile-soil interface. The 2-D modeling has shown to be suitable for the representation of these complex support and excavation systems.

Monitoring data obtained from geotechnical, tunnel and ground freezing related instruments were collected over a period of about 24 months along with reports documenting tunnel excavation and support. Evaluation of the data allowed verification

of the 2-D model. Given that the design intent and assumptions were generally realized in the field, parameters describing the constitutive behavior of soils and frozen soils as derived from laboratory tests were found valid for the representation of in-situ conditions. In the absence of a material model within the calculations to describe creep phenomena, a quasi-static reduction of the elastic moduli of the frozen soils was used instead.

Monitored surface and column heave data at characteristic locations were utilized for the back-analysis of the site-specific segregation potential. Utilizing monitored frozen soil temperature gradients and vertical stresses acting on the frozen soil strata from the 2-D FE model a range for the segregation potential of between 16 x 10^{-5} [mm^2 / °C s] and 41 x 10^{-5} [mm^2 / °C s] was determined. This range compares well with the range of reported values in the case histories for similar site conditions and problem statements.

The verified 2-D FE model, laid out suitably to assess the supporting capacity of piles when embedded in surrounding ground, was utilized to investigate an alternative hybrid support system during tunneling consisting of frozen ground, timber piles and the tunnel lining. In contrast to the support mechanism as constructed, which practically neglects the existence of piles during tunneling and merely relies on a full thickness of frozen soil between pile caps and tunnel crown for building support, the proposed hybrid support relies on pile support during tunneling. Strength between piles and frozen soil is derived from the adfreeze strength that develops along the interface between the piles and the surrounding frozen soil mass.

Adfreeze strength values taken from the cold regions engineering literature were used to estimate adfreeze strength values for parametric variations designed to evaluate

the influence of this parameter on the supporting capacity of the hybrid system. Along with the variations of the adfreeze strength, the frozen zone extent, and in particular the frozen soil height, was varied. Minimum required frozen soil extent along with a minimum required adfreeze strength was evaluated in terms of the stress within the frozen soil, the load carrying capacity of the piles embedded in the frozen soil, pile stresses, and tunnel lining capacity. The results indicate that for the frozen temperature regime utilized in the Russia Wharf project a frozen soil thickness of 1.2 meter is sufficient in combination with adfreeze strength values commonly reported for similar frozen soils. The maximum surface vertical settlement for this alternate scenario would be about 22% higher than monitored during the project construction. Thus, a jacking system to compensate column settlement / heave would still be needed.

8.2 Conclusions

The investigations performed here indicate that ground freezing may be very effective for supporting vertical, slender underground support members such as piles to enable their partial removal or cut-off by tunneling operations. To minimize the stressing and deformation of the frozen soil-vertical support interface the NATM has proven to be the method of choice for tunneling.

The interface strength between pile and frozen soil is derived from adfreeze strength. This interface shear strength depends on soil composition and temperature. Therefore, an optimum combination of pile embedment length in frozen soil and frozen soil temperature must be determined.

It is suggested that the hybrid support concept of frozen soil-pile-NATM tunnel be considered as a methodical tool for tunneling applications in soft ground where existing pile supports interfere with proposed tunnel alignments and have to be cut during the tunneling process while maintaining their supporting function for the structure above. The extent of the frozen soil zone and the required temperature regime must be adjusted to meet local soil and spatial restrictions.

Any such implementation must be supported by calculations and evaluation criteria. Those presented herein provide a methodological approach for such an assessment. The application will produce a rational design process that will lead to an efficient and economical ground freezing and tunneling design. Because of the significance of adfreeze strength, specific tests must be required to assess its magnitude. Measurement may involve scaled laboratory test and / or field tests on representative pile cross sections and soil materials.

8.3 Recommendation for Further Research

In support of the proposed support system research is recommended in three areas. Because of the importance of adfreeze strength its development and magnitude as a function of soil type, temperature and pile material should be investigated.

Further, and to be able to rely on the strength between pile and surrounding soil monitoring devices shall be developed to verify the magnitude of the established interface strength.

The incorporation of building supporting piles into a tunnel lining creates a structural connection that transmits tunnel-induced vibrations into the building. This is in

particular the case for transportation tunnels that accommodate rail based vehicles. For critical applications research into vibration attenuating systems and type of materials to be used will benefit the proposed application.

Appendix

Case Histories Using Frozen Soil as Pre-Support

Project 1	**Syracuse Tunnel**
Location:	Syracuse, NY, USA
Nature of Work:	- Freezing to allow construction of tunnel under active, high speed railroad tracks
Construction Period:	- Start drilling: 15 May 1980 Start freezing: 25 Aug 1980 Start tunnel excavation: 16 Sep 1980 Completion date: April 1983
Project Details: Tunnel Cross Section: Tunnel Length: Geotechnical Conditions: Tunneling Under: Depth of Cover: Freezing: Miscellaneous: Ground Surface Deformation: (at tunnel centerline) Additional Information:	 - Diameter approximately 3.0 m - 36.6 m - Fine sand beneath gravel and silt of varying thickness, Groundwater table 1.5 - 2.1 m above tunnel - Highspeed railroad tracks - 2.0 m min. Horizontal freezing, brine - N/A - General settlement of approx. 23 mm/year Maximum heave during artificial freezing 60 mm, no discernable settlement occurred during tunneling after the freeze unit was turned off approximately 30 to 40 mm settlement - See Figure below
Owner:	- County of Onondaga, New York
Source of Project Information:	- Lacy *et al*., 1982

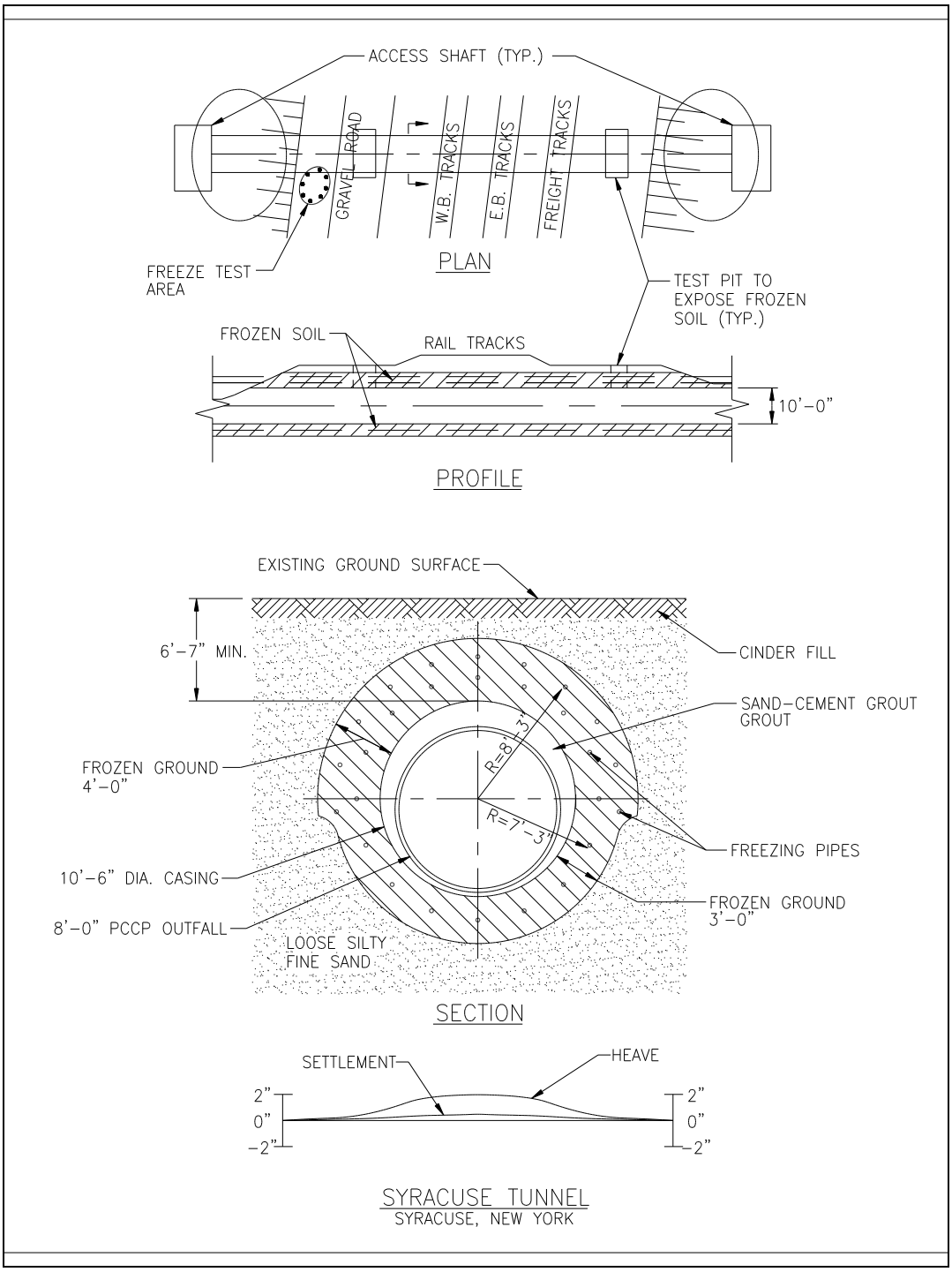

Syracuse Tunnel, Syracuse, NY

Project 2	**Heights-Hilltop Interceptor Sewer Tunnel**
Location:	Cleveland, Ohio, USA
Nature of Work:	- Freezing to allow construction of tunnel beneath active main railroad tracks without interruption
Construction Period:	- Freeze pipe installation: April 1987 - Beginning of ground freezing: 25 Aug 1987 - Start of tunnel excavation: 24 Sep 1987 - Hole-through: 19 Oct 1987
Project Details: Tunnel Cross Section: Tunnel Length: Geotechnical Conditions: Tunneling Under: Depth of Cover: Freezing: Miscellaneous: Ground Surface Deformation: (at tunnel centerline) Additional Information:	 - Diameter 4.6 m, steel liner plate tunnel - 42.7 m - Medium silty clay, lenses and pockets of clean sand and gravel - Railroad tracks - 2.7 m below railroad ties - Horizontal freezing pipes, brine refrigeration plant of minimum 350 kW capacity - Road header excavation, strength of frozen clay 5,000 to 10,000 kPa - N/A - see Figure below
Owner:	- Northeast Ohio Regional Sewer District
Source of Project Information:	- Lacy *et al*., 1989 and Hayward Baker, Case Histories Ground Freezing

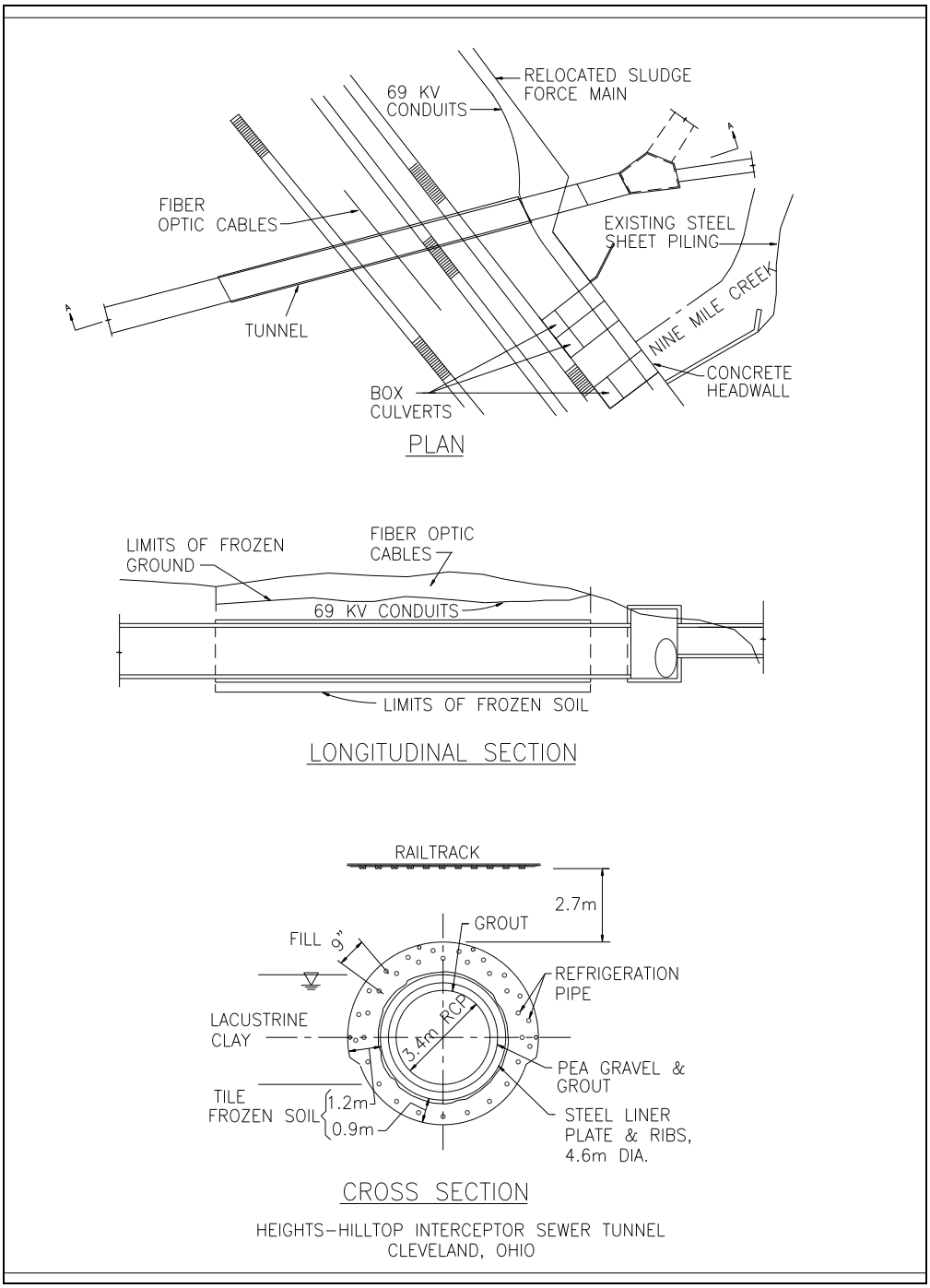

Heights-Hilltop Interceptor Sewer Tunnel, Cleveland, Ohio

Project 3	**Large Acoustic Tank for Naval Research Laboratory**
Location:	Washington, DC, USA
Nature of Work:	- Freezing of a 16.8 m deep shaft to allow construction of a 19.5 m diameter tank inside an existing building, underpinned and supported by the freezing
Construction Period:	- 1989, six weeks of freezing prior to excavation
Project Details: Shaft Diameter: Shaft Depth: Geotechnical Conditions: Tunneling Under: Depth of Cover: Freezing: Miscellaneous: Ground Surface Deformation: Additional Information:	 - 19.5 m - 16.8 m - Sands and gravels with lenses of silty clay - Laboratory building - N/A - N/A - Vertical freezing pipes with a refrigeration plant capable of cooling the calcium chloride coolant to approximately –30 ^{0}C - Refrigeration pipes installed to a depth of approximately 21.3 m - After six weeks of refrigeration, the excavation operations began - N/A - N/A - see Figure below
Owner:	- United States Navy
Source of Project Information:	- Hayward Baker, Case Histories - Ground Freezing

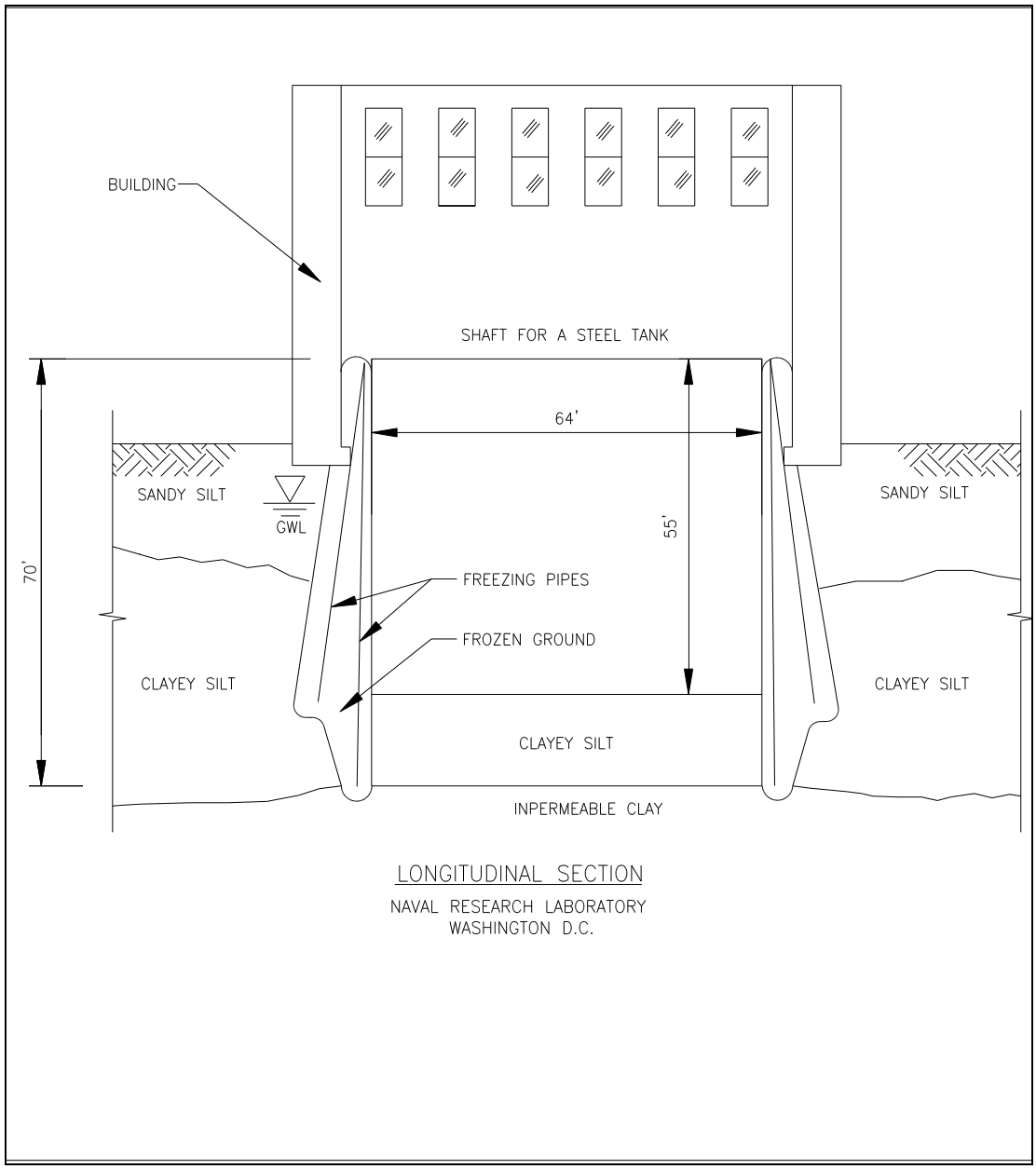

Naval Research Laboratory, Large Acoustic Tank, Washington, DC

Project 4	**Urban Rapid Transit Rail Stuttgart - Contract Section 12**
Location:	Stuttgart, Germany
Nature of Work:	- Construction of a single track rail tunnel with manifold
Construction Period:	- 1974 - 1978
Project Details: Tunnel Cross Section: Tunnel Length: Geotechnical Conditions: Tunneling Under: Depth of Cover: Freezing: Miscellaneous: Ground Surface Deformation: (at tunnel centerline) Additional Information:	 - 50 m^2 (Diameter: 8.1 m) to 162 m^2 (Diameter: 13.15 m) - 1,600 m of which 505 m were with ground freezing - Leached and non leached gypseous keuper, marl, clayey silt, draw down of water table - Road with services and residential buildings - 18 m - Horizontal freezing pipes, brine, 9,700 m^3 of frozen ground - 3 freeze sections: 30 m, 41 m, and 40 m with total length of boreholes of 6,190 m Tunneling using shotcrete support method (NATM) - N/A - see Figure below
Owner:	- German Federal Railroad (DB), Stuttgart
Source of Project Information:	- Holzmann P., 1975, Project Brochure / Holzmann, P., 1979, Technical Report / Deutsche Bundesbahnen, 1985

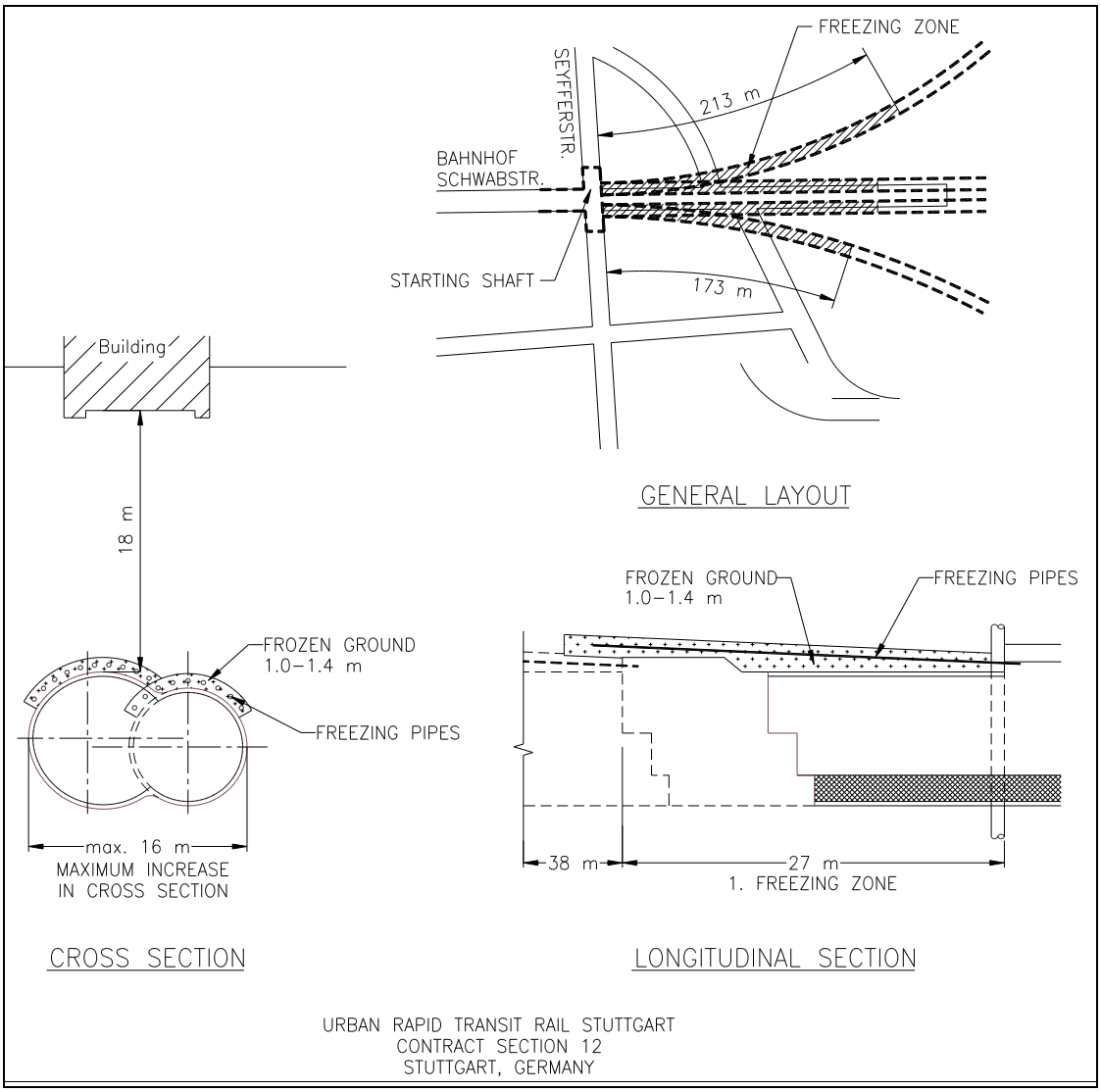

Urban Rapid Transit Rail, Stuttgart, Germany

Project 5	**Sewage Collector - Center, Düsseldorf**
Location:	Düsseldorf , Germany
Nature of Work:	- Trial section for the application of ground freezing for large caverns
Construction Period:	- 1978
Project Details: Tunnel Cross Section: Tunnel Length: Geotechnical Conditions: Tunneling Under: Depth of Cover: Freezing: Miscellaneous: Ground Surface Deformation: (at tunnel centerline) Additional Information:	 - 25 m^2 cross section area (6.30 m x 5.20 m) - 115 m (single freezing section) - Sand, silty gravel, groundwater at invert level - Highway with 7 lanes - 3.20 m - Horizontal freezing pipes, brine, freezing plant 2 x 220,000 kcal/h - 350 kW power supply - Shotcrete support method (NATM), full face excavation - Heave maximum 3 mm, settlement max 15 mm - N/A - N/A
Owner:	- Kanal und Wasserbauamt der Landeshauptstadt Düsseldorf
Source of Project Information:	- Holzmann, P., 1979, Technical Report

Project 6	**Metro Frankfurt - River Main Crossing Contract Section 81**
Location:	Frankfurt am Main, Germany
Nature of Work:	- Twin metro tunnel under the river Main
Construction Period:	- 1976 to 1981 Start of the freezing operation began on 12 Apr 1977 and the first tunnel hole through occurred on 10 May 1978
Project Details: Tunnel Cross Section: Tunnel Length: Geotechnical Conditions: Tunneling Under: Depth of Cover: Freezing: Miscellaneous: Ground Surface Deformation: (at tunnel centerline) Additional Information:	 - 2 x 38.5 m^2 (Diameter: 7 m) - 2 x 193 m, entire length of frozen ground of 154 m under the river - Frankfurt clay with limestone banks with sand and silt lenses - River bed (river Main) - 6.0 - 9.5m - Brine with a freezing plant with two stages with 200,000 to 400,000 kcal/h Maximum brine output 25,000 l $CaCl_2$/hour - Lengths of freezing stages 32 to 43 m with 14 to 18 freezing pipes installed using a horizontal drilling system Tunneling by shotcrete support method (NATM) - N/A - see Figure below
Owner:	- City of Frankfurt am Main, Construction and Municipal Works Department
Source of Project Information:	- Holzmann, P., 1977, Project Brochure / Holzmann, P., 1979, Technical Report / Haack, 1995

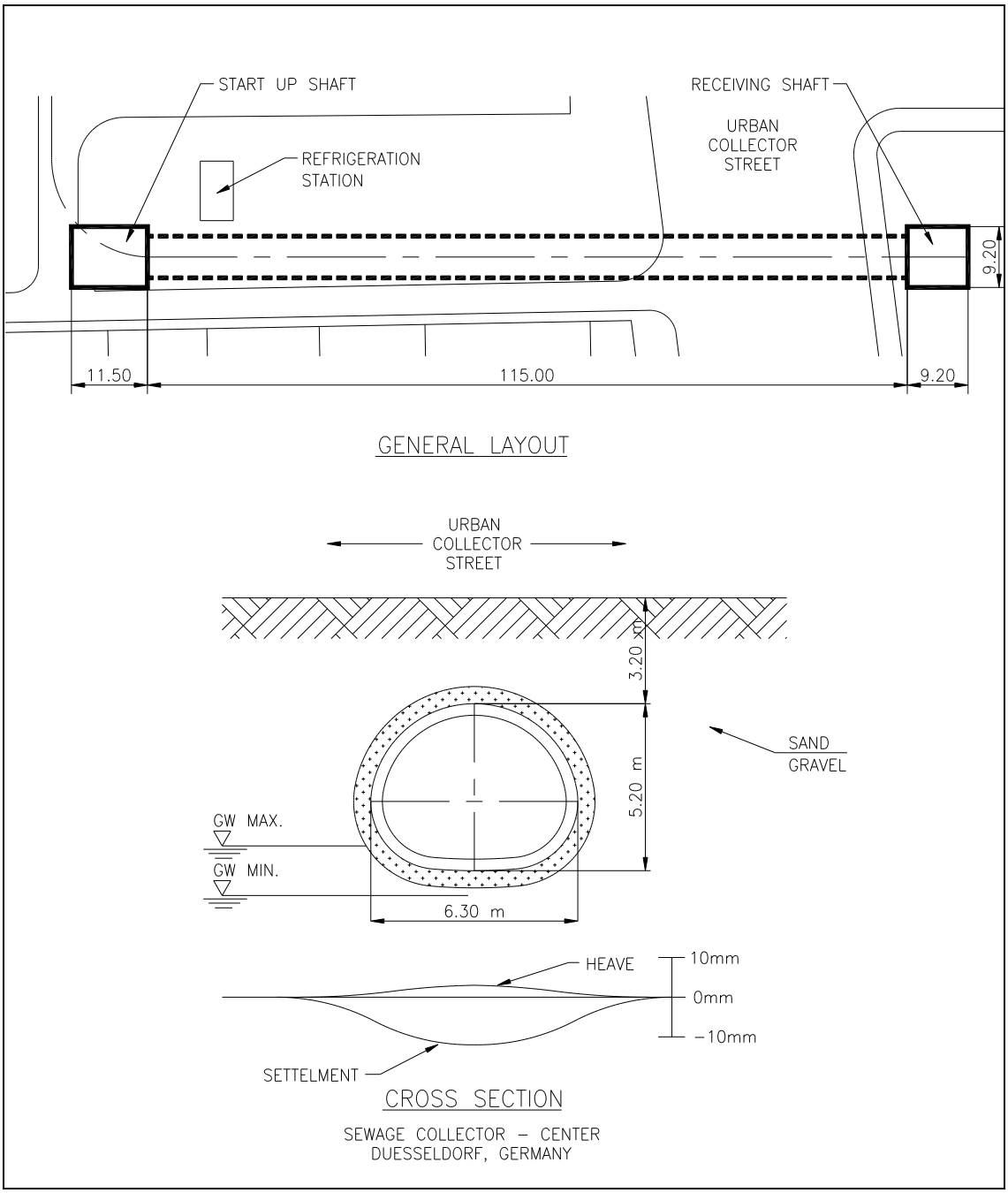

Metro Frankfurt am Main, Tunneling Under the River Main, Contract Section 81, Frankfurt, Germany

Project 7	**Metro Nuremberg, Contract Section 258/1.3**
Location:	Nuremberg, Germany
Nature of Work:	- Mining a tunnel underneath the Main-Danube Ship Canal
Construction Period:	- 1984
Project Details: Tunnel Cross Section: Tunnel Length: Geotechnical Conditions: Tunneling Under: Depth of Cover: Freezing: Miscellaneous: Ground Surface Deformation: (at tunnel centerline) Additional Information:	 - Diameter: approximately 5.6 m - 2 x 1,050 m of which 11 m were frozen - Clay cemented sandstone and claystone, with the freezing section located in a in fault zone and the groundwater level above the tunnel roof level - Ship canal - (Main-Danube) - Approximately 5.0 m - Liquid Nitrogen (LIN), 650,000 l were used, creating a volume of frozen ground of approximately 500 m^3 - Insulation blanket was placed on the river bed Horizontal drilling system was used and freezing began one week before tunneling - Tunneling by shotcrete support method (NATM) with backhoe and hoe ram - N/A - see Figure below
Owner:	- City of Nuremberg, Department for underground constructions
Source of Project Information:	- Adams, 1985 / Rebhan, 1990

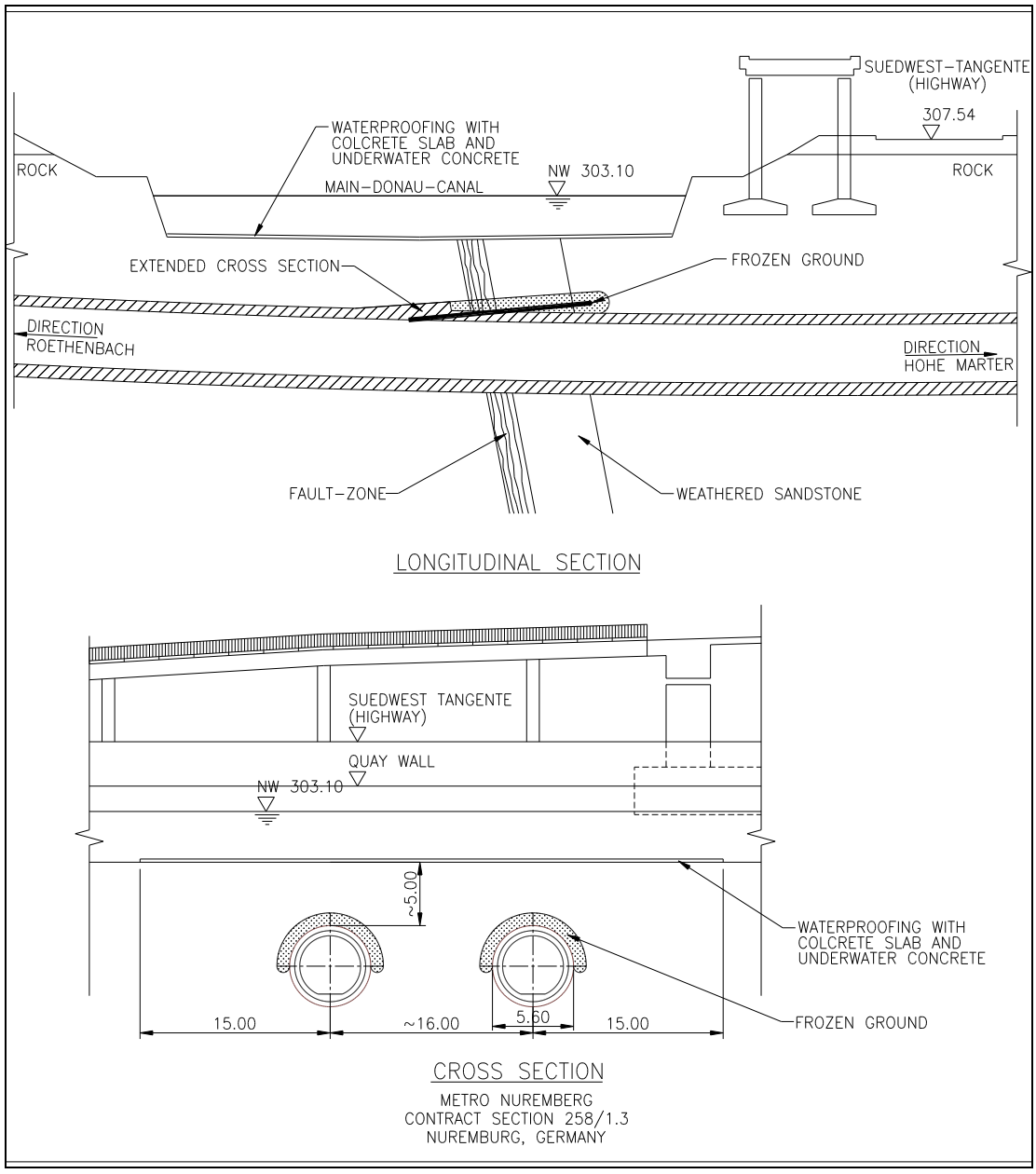

Metro Nuremberg, Contract Section 258/1.3, Nuremberg, Germany

Project 8	**Urban Rail System Hannover, Contract Section C 23**
Location:	Hannover, Germany
Nature of Work:	- Construction of twin railroad tunnel in an urban area
Construction Period:	- 1988 to 1991
Project Details: Tunnel Cross Section: Tunnel Length: Geotechnical Conditions: Tunneling Under: Depth of Cover: Freezing: Miscellaneous: Ground Surface Deformation: (at tunnel centerline) Additional Information:	 - 37.4 m^2 to 55.4 m^2 - 475 m and 251 m in frozen ground - Fill, sand, gravel, silt, and clay with ground water approximately 4 m beneath the surface - Residential and commercial buildings - 8 to 12 m - Horizontal freezing pipes (10 or 11) with a brine freezing plant of 650 kW power supply and volume of frozen ground of approximately 3,600 m^3 - Tunneling by shotcrete support method (NATM) under compressed air (1.3 bar) - N/A - see Figure below
Owner:	- Hannover Municipality
Source of Project Information:	- Holzmann Project Brochure, 1990 / Haack, 1995

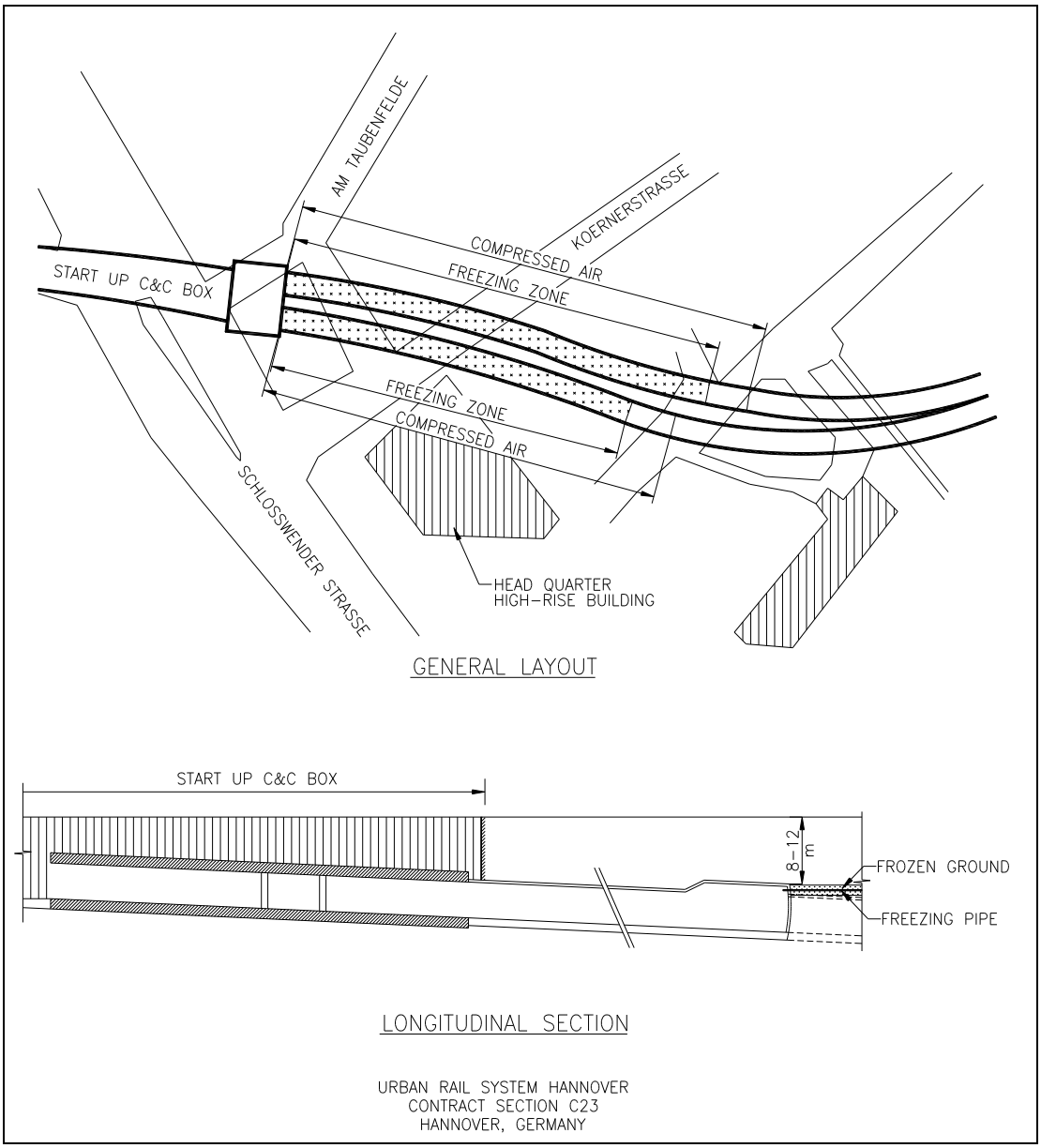

Urban Rail System Hannover, Contract Section C 23, Hannover, Germany

Project 9	**Fahrlach Highway Tunnel, Mannheim**
Location:	Mannheim, Germany
Nature of Work:	- Construction of a twin-tube road tunnel
Construction Period:	- 1989 to1992
Project Details: Tunnel Cross Section: Tunnel Length: Geotechnical Conditions: Tunneling Under: Depth of Cover: Freezing: Miscellaneous: Ground Surface Deformation: (at tunnel centerline) Additional Information:	 - 2 x 100 m^2 (6.6 to 10.2 m) - Total length of 2 x 489 m, with approximately 2 x 184 m in frozen ground - Man-made railroad embankment consisting of quaternary silt layers, sand and gravel, groundwater level between 3.5 and 7.0 m below the ground surface, and the tunnel crown above the ground water table - 70 m wide railroad embankment with 11 highly frequented tracks at about 1,000 trains per day, a high pressure gas pipeline, and a main sewage collector - At a distance of approximately 2.6 m to the tracks - Combination of horizontal and vertical freezing pipes, with 30 % $CaCl_2$ brine with a freezing plant of 9.0 M KJ/h, approximately 1,680 kW 27,000 m^3 of frozen ground, four freezing sections (two each tube) - Pilot tunnel (3.3 m) above the two road tunnels Artificial water irrigation as the tunnel crown was above the groundwater Grout curtain to decrease the permeability of the soils 42 freeze holes, 92 m in length, excavated with a micro tunneling machine (470 mm in Diameter) Tunneling by shotcrete support method (NATM) - heave of 0 to 6 mm, settlement of 10 to 30 mm - see Figure below
Owner:	- City of Mannheim, Mannheimer Wohnungs- und Städtebaugesellschaft
Source of Project Information:	- Jordan, 1992 / Jessberger & Partner Project Brochure / Haack, 1995

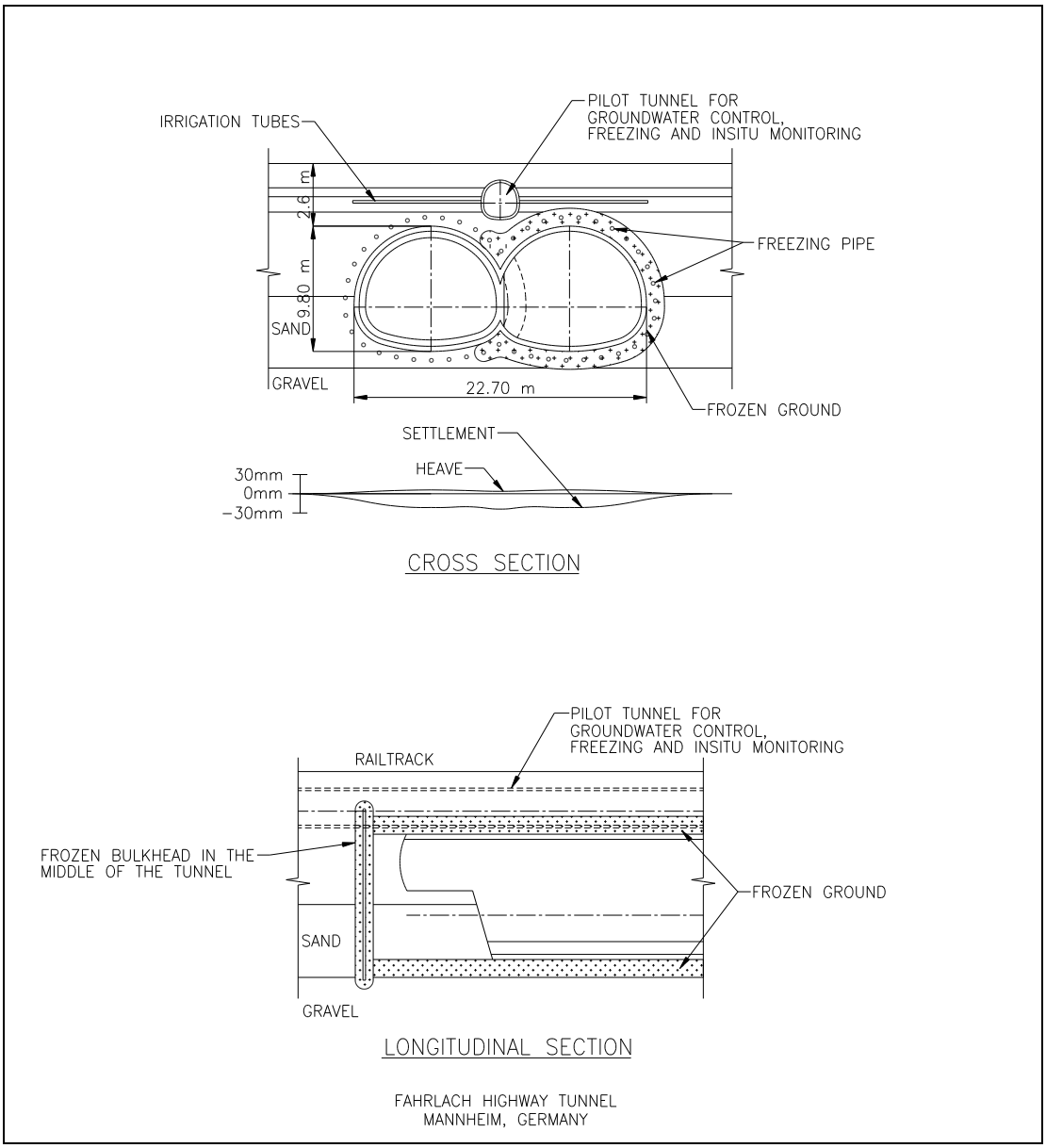

Fahrlach Highway Tunnel, Mannheim, Germany

Project 10	**Urban Railroad Mühlheim an der Ruhr Contract Section 8**
Location:	Mühlheim an der Ruhr, Germany
Nature of Work:	- Enlargement of an existing segmental lined tunnel to a station tunnel
Construction Period:	- October 1991 to February 1992
Project Details: Tunnel Cross Section: Tunnel Length: Geotechnical Conditions: Tunneling Under: Depth of Cover: Freezing: Miscellaneous: Ground Surface Deformation: (at tunnel centerline) Additional Information:	 - Enlargement from 38 m^2 (Diameter: 6.9 m) to 65 m^2 (Diameter: 9.1 m) - 90 m of which 30 m were frozen - Alluvial gravel, silt, buried valley, rock (freeze-section in gravel) - Street with services, commercial building - Approximately 9 m - Horizontal freezing pipes, Nitrogen freezing / storage tank with 40,000 l capacity Freezing plant with 500,000 kcal/h (20,900 MJ/h) and 600 kW power supply Working pressure of the liquid gas of 5 bar at –196 ^0C - Mining by shotcrete support method (NATM) - Heave of 1 to 4 mm and settlement of maximum 10 mm - see Figure below
Owner:	- Urban Railroad Rhein - Ruhr
Source of Project Information:	- Elmer *et al*., 1994

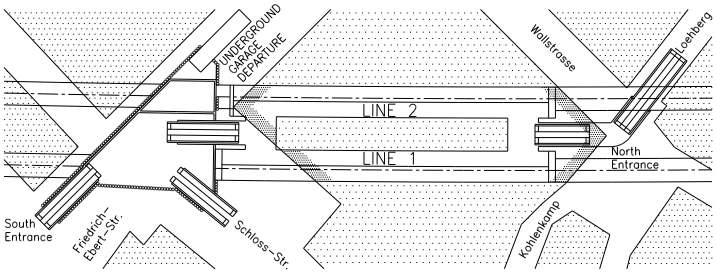

GENERAL LAYOUT

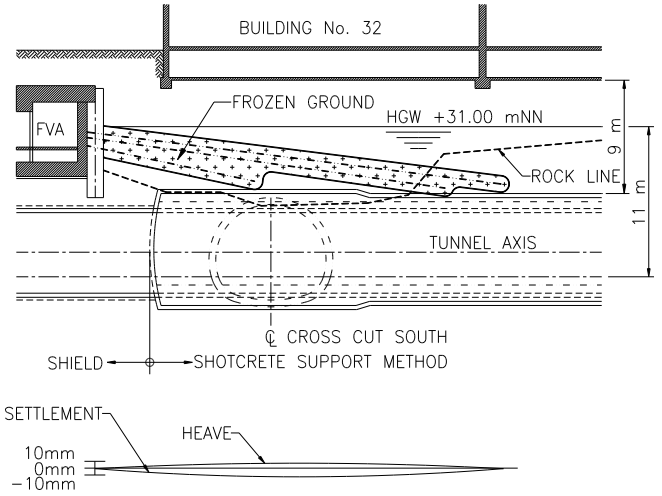

LONGITUDINAL SECTION

URBAN RAIL MUEHLHEIM AN DER RUHR
CONTRACT SECTION 8
MUEHLHEIM AN DER RUHR, GERMANY

Urban Railroad Muehlheim an der Ruhr, Muehlheim, Germany

Project 11	**Metro Düsseldorf, Contract Section 3.4 H**
Location:	Düsseldorf, Germany
Nature of Work:	- Construction of three metro tunnels under buildings and railroad tracks
Construction Period:	- 1991 to 1993 Freezing from June to August 1991
Project Details: Tunnel Cross Section: Tunnel Length: Geotechnical Conditions: Tunneling Under: Depth of Cover: Freezing: Miscellaneous: Ground Surface Deformation: (at tunnel centerline) Additional Information:	 - Largest cross section area at 96 m^2 - Each tunnel approximately 40 m long - Fill, sandy gravel, tertiary fine sands, water saturated (lower part) - Residential buildings, railway tracks - 1 to 9 m under the building foundation - Installation of horizontal freezing pipes for a volume of frozen soil of 2,600 m^3, 1,500 m^3, and 2,900 m^3 Freezing plant for brine cooling with maximum 540,000 kcal/h, and 600 kW power supply, Utilization of intermittent freezing 98 freezing pipes, length 36 to 48 m - Installation of a grout curtain to reduce the permeability to water Artificial infiltration of water in upper parts of frozen ground Dewatering of the ground within the excavation section by vacuum lances prior to tunneling Tunneling using the shotcrete support method (NATM) - Settlement of maximum 13 mm - see Figure below
Owner:	- City of Düsseldorf
Source of Project Information:	- Boening *et al*., 1992 / Jordan, 1992 / Jessberger and Partner - Project Brochure

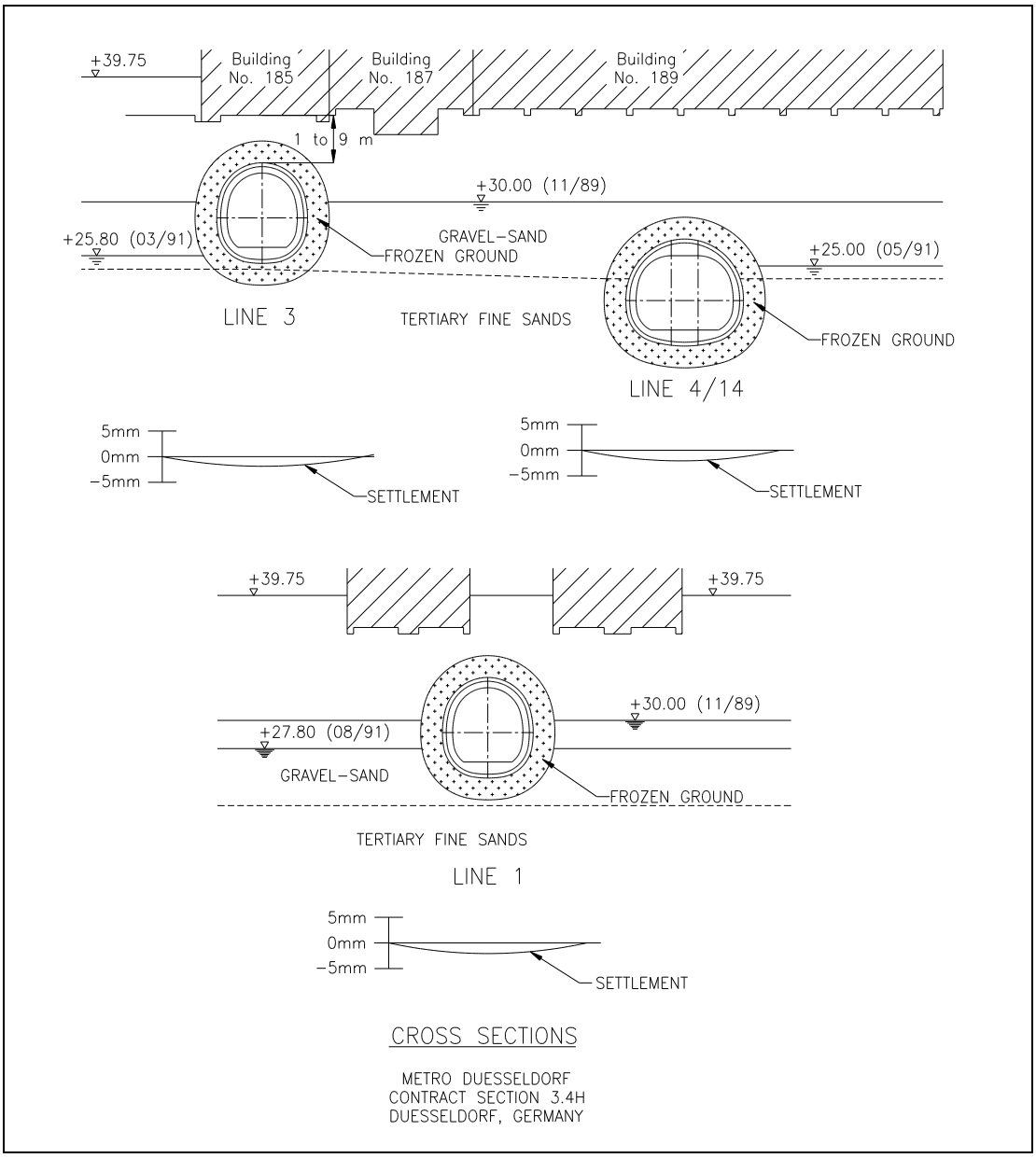

Excavation at Metro Düsseldorf, Contract Section 3.4H, Duesseldorf, Germany

Project 12	**Metro Düsseldorf, Contract Section - Oberbilker Markt**
Location:	Düsseldorf, Germany
Nature of Work:	- Construction of a tunnel under a building under shallow cover
Construction Period:	- 1995 to 1998
Project Details: Tunnel Cross Section: Tunnel Length: Geotechnical Conditions: Tunneling Under: Depth of Cover: Freezing: Miscellaneous: Ground Surface Deformation: (at tunnel centerline) Additional Information:	 - Approximately 60 m^2 cross section area - Approximately 38 m - Gravel, sand, fine sand, and groundwater approximately 1 m below tunnel roof level - 2 m to foundations of multiple story residential buildings - Horizontal freezing pipes, 30% $CaCl_2$ brine and freezing plant of 250,000 kcal/h - Artificial water infiltration to saturate soil strata above groundwater table - Installation of a grouting curtain and a slurry wall for ground water control - Tunneling using the shotcrete support method (NATM) - N/A - N/A
Owner:	- City of Düsseldorf
Source of Project Information:	- Jessberger and Partner - Project Brochure

Project 13	**Milchbuck Road Tunnel, Zürich**
Location:	Zürich, Switzerland
Nature of Work:	- Two lane road tunnel to extend the Swiss Interstate System
Construction Period:	- Excavation of the first section started in May 1978 and the final section was completed in June 1980
Project Details: Tunnel Cross Section: Tunnel Length: Geotechnical Conditions: Tunneling Under: Depth of Cover: Freezing: Miscellaneous: Ground Surface Deformation: (at tunnel centerline) Additional Information:	 - Horseshoe-shaped tunnel of 12,10 m height and 14,40 m width and a cross section of 145 m^2 At drill chambers the cross sections were 195 m^2 - 1,310 m with 350 m ground freezing length - Dense to very dense gravel (till), marlstone, siltstone, artesian groundwater (maximum 3 bar) - Street, multiple story private and commercial buildings with 5.50 m minimum cover - Horizontal freezing pipes, freezing plant with brine at 500,000 kcal/h (20,900 MJ/h) and 600 kW power supply - The section within the till was subdivided into 32, 33 m long freezing subsections The groundwater was lowered to reduce frost heave The tunnel was excavated in a full face excavation according to the NATM - After initial high heave the intermittent freezing method was utilized for heave control: 1st freezing section: maximum 105 mm heave, maximum 50 mm settlement 3rd freezing section: maximum 10 mm heave, maximum 10 mm settlement Other freezing sections: 4 to 6 mm heave and maximum 5 mm settlement - see Figure below
Owner:	- Canton of Zürich, Kantonale Baudirektion - Tiefbauamt
Source of Project Information:	- Aerni and Mettier, 1980 / Schmid, 1981 / Bebi and Mettier, 1979 / Braun and Schuster, 1979

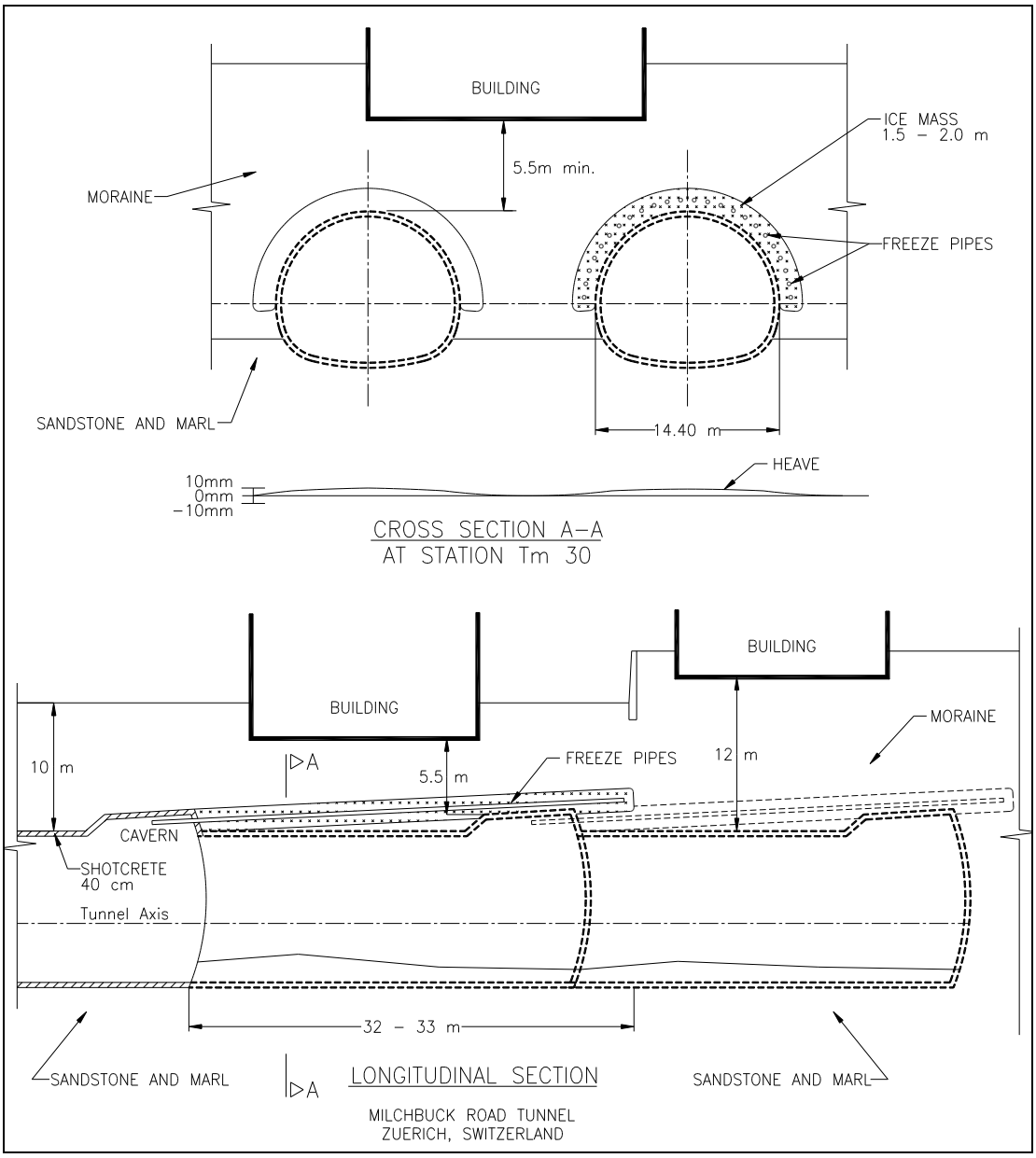

Milchbuck Road Tunnel, Zürich, Switzerland

Project 14	**Station Quay / Limmat (a) Contract section 2.04 Neumühle Quay / Publicitas (b) Contract section 4.03**
Location:	Zürich , Switzerland
Nature of Work:	- a) Double track railroad tunnel under the river Limmat b) Twin single track railroad tunnel under a river quay wall and a street
Construction Period:	- 1987
Project Details: Tunnel Cross Section: Tunnel Length: Geotechnical Conditions: Tunneling Under: Depth of Cover: Freezing: Miscellaneous: Ground Surface Deformation: (at tunnel centerline) Additional Information:	 - a) 13.50 x 10.50 m b) Two 7.65 x 9.30 m - a) Approximately 80 m b) Approximately 40 m - River deposit gravels, lake deposits, glacial till - a) River Limmat b) River quay wall, street - 2.5 to 3.5 m - Horizontal freezing pipes, brine freezing plant with 200,000 to 430,000 kcal/h - Insulation at the river bed Shotcrete support method (NATM) by road header - N/A - see Figures (2) below
Owner:	- Swiss Federal Railroad (SSB)
Source of Project Information:	- Holzmann, 1988 / Jordan, 1992 / Gruendler, *et al*. / Haack, 1995

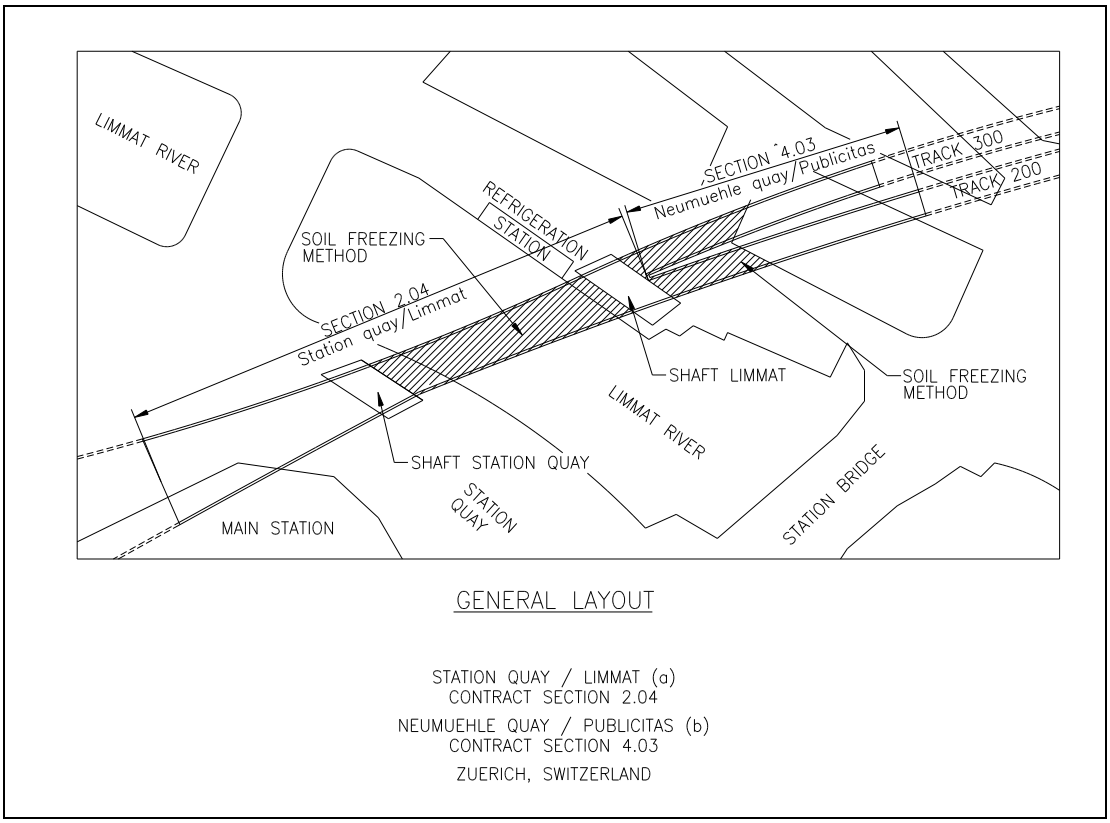

Station Quay / Limmat (a) Contract Section 2.04, Neumühle Quay / Publicitas (b) Contract Section 4.03, Zürich, Switzerland

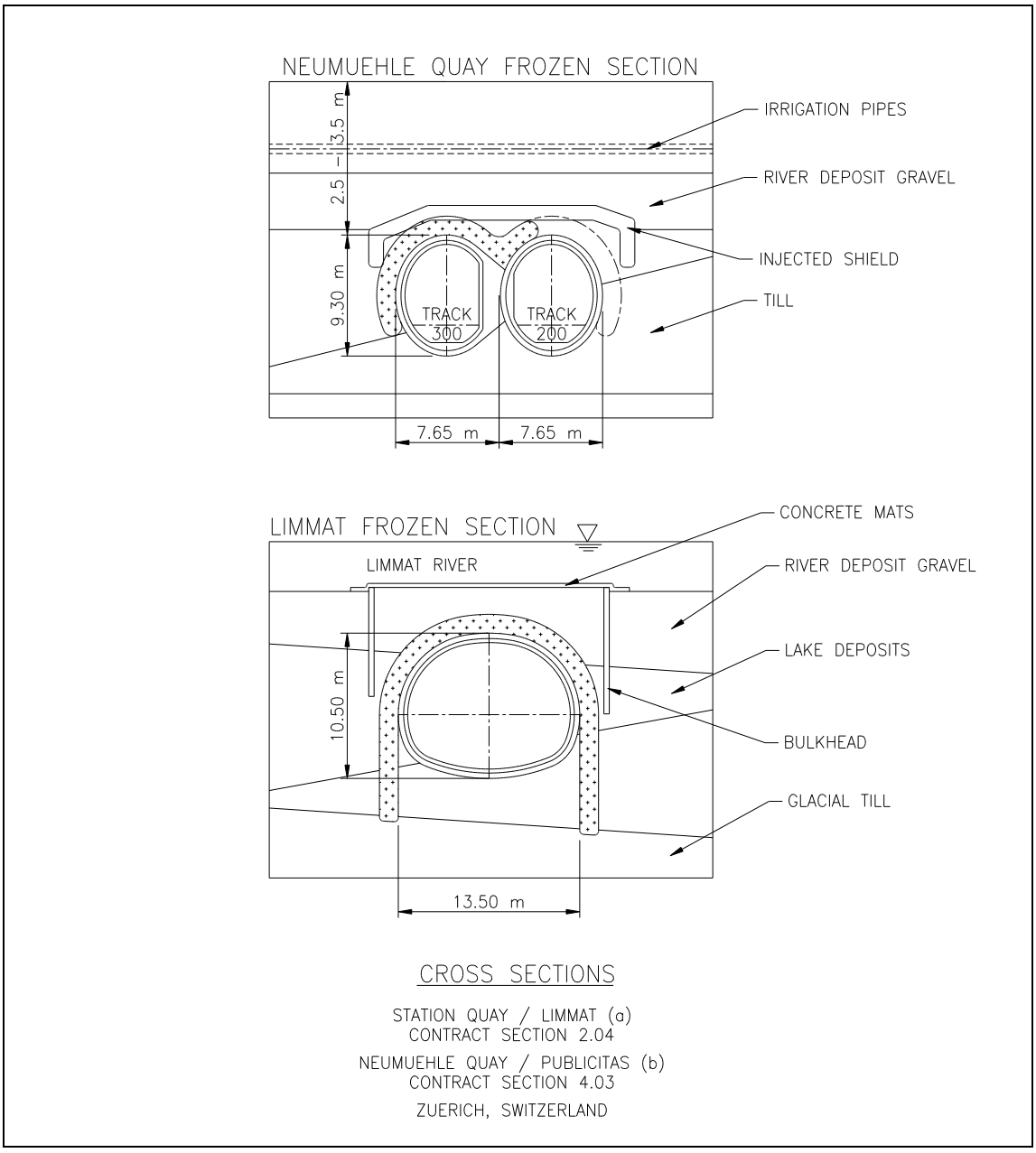

Station Quay / Limmat (a) Contract Section 2.04, Neumühle Quay / Publicitas (b) Contract Section 4.03, Zürich, Switzerland (Continued)

Project 15	**Metro Vienna, Contract Section U6/3 - Vivenotgasse**
Location:	Vienna, Austria
Nature of Work:	- Tunneling under a multiple story post office - telecommunication building with a very sensitive automatic relay telephone system
Construction Period:	- 5 Aug 1985: start of excavation work 12 Jan 1987: start of the freezing operation 28 Feb 1987: end of freezing and excavation
Project Details: Tunnel Cross Section: Tunnel Length: Geotechnical Conditions: Tunneling Under: Depth of Cover: Freezing: Miscellaneous: Ground Surface Deformation: (at tunnel centerline) Additional Information:	 - 2 x 34 m^2 cross section area - 1,100 m double and 240 m single track, with about 60 m and 64 m frozen ground - Alluvial deposits, sands, gravel, clays with sand layers, and silts Groundwater above the tunnel crown - Multiple story post office - telecommunication building - 1.6 m to building foundation - LIN, 2 x 750,000 kJ/h, 2,400 LIN/day, 100 kW, 1,800 m^3 frozen ground, 33 m long freeze pipes in a horizontal installation for a rectangular frozen section above tunnel roof (1 x 65 x 22m) - Shotcrete support method (NATM) under compressed air (0.7 to 0.9 bar) - Very strict restrictions were imposed for allowed ground settlements (maximum 5 mm) and distortion within 1:500 to 1:1000 limits Heave during freezing: 10 to 13 mm Settlement due to tunneling: 4 to 6 mm Settlement after tunneling and thawing: 16 to 18 mm Final and total subsidence: 10 to 14 mm - see Figure below
Owner:	- Municipal of Vienna, Magistrat der Stadt Wien, Magistratsabteilung 38 - U-Bahn-Bau
Source of Project Information:	- Fischer, 1987 / Magistrat der Stadt Wien - Publication / Jordan, 1992 / Deix, 1988 / Harris, 1995

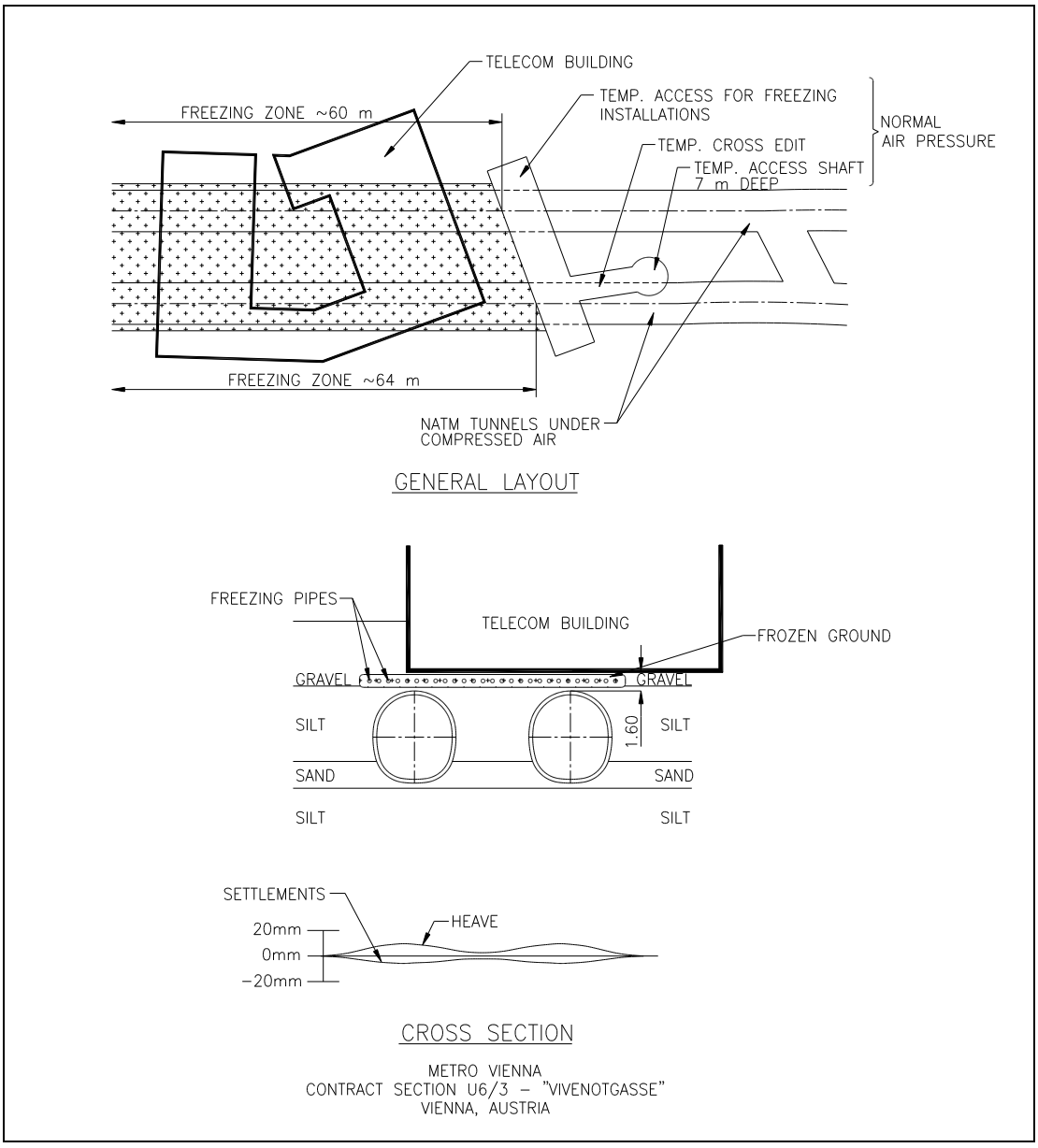

Metro Vienna, Contract Section U6/3 - Vivenotgasse, Vienna, Austria

Project 16	**Metro Vienna, Contract Section U3/10**
Location:	Vienna, Austria
Nature of Work:	- Tunneling under a five story commercial building (department store Herzmansky)
Construction Period:	- 1987
Project details: Tunnel Cross Section: Tunnel Length: Geotechnical Conditions: Tunneling Under: Depth of Cover: Freezing: Miscellaneous: Ground Surface Deformation: (at tunnel centerline) Additional Information:	 - Diameter: 6.60 to 8.60 m - Approximately 70 m, with two freezing sections of approximately 35 m in length - Clayey silts, sandy gravels, groundwater table below tunnel - Multiple story commercial building - Approximately 2 m - Horizontal freeze pipe installation, use of LIN for freezing Tunneling using shotcrete support method (NATM) - Frost heave from 1 to 2 mm Settlement during tunneling from 8 to 11 mm Resultant settlement between 7 to 9 mm - see Figure below
Owner:	- Municipal of Vienna, Magistrat der Stadt Wien, Magistratsabteilung 38 - U-Bahn-Bau
Source of Project Information:	Magistrat der Stadt Wien - Project Brochure / Jordan, 1992 / Rebhan, 1990 / Szadecky, 1988 / Soletanche Project Brochure, 1987

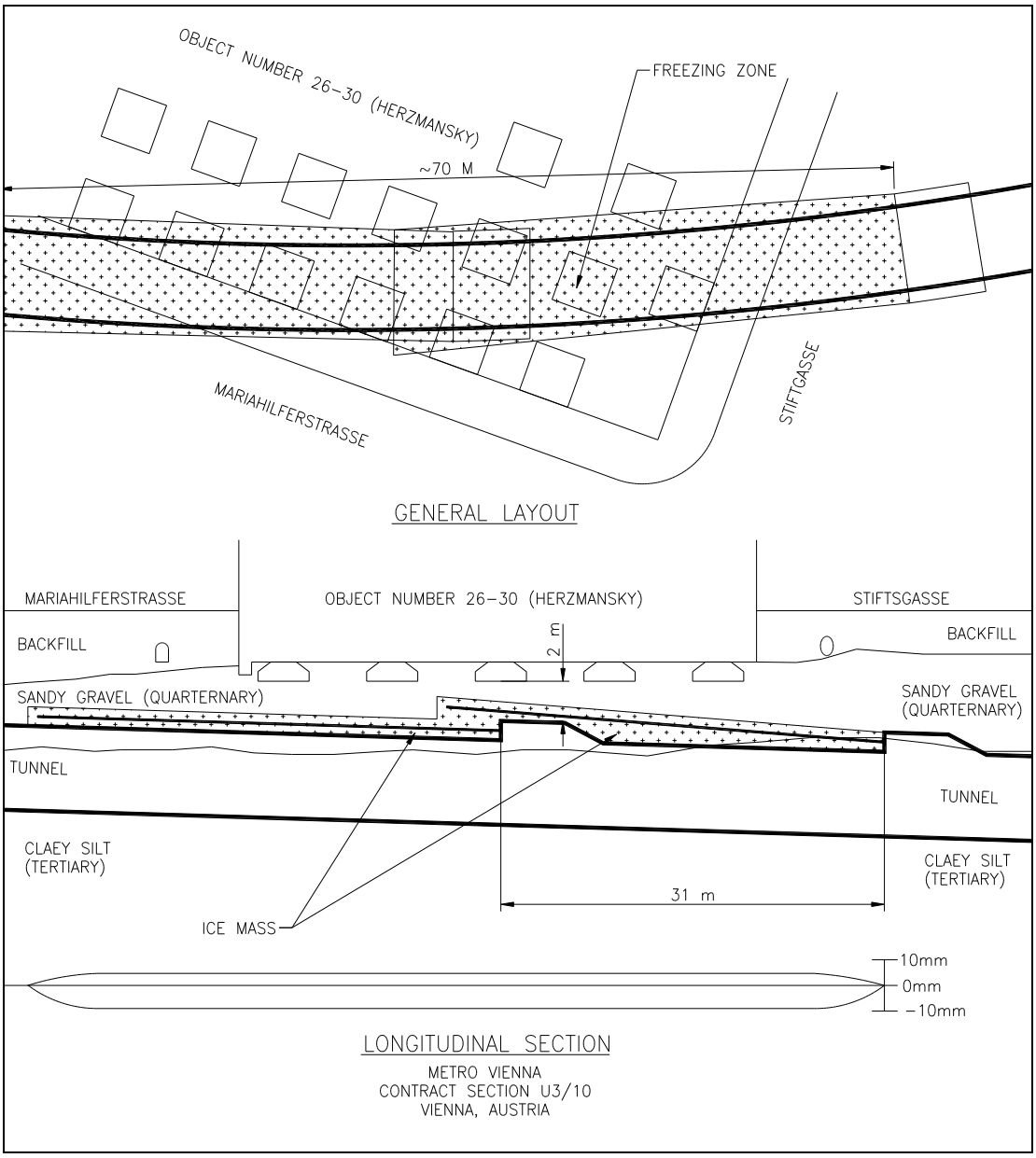

Metro Vienna, Contract Section U3/10, Vienna, Austria

Project 17	**Santa Lucia Tunnel**
Location:	Salerno, Italy
Nature of Work:	- Double track railroad tunnel section
Construction Period:	- 1973, time of operation of freezing unit one, about 15.5 weeks and unit two about 14 weeks
Project Details: Tunnel Cross Section: Tunnel Length: Geotechnical Conditions: Tunneling Under: Depth of Cover: Freezing: Miscellaneous: Ground Surface Deformation: (at tunnel centerline) Additional Information:	 - 85 m^2 (11.0 m wide and 5.5 m high) - 10,263 m total length / 71 m ground freezing length - Soil of volcanic origin, alluvial sands, friable dolomite, weathered granite, groundwater table above tunnel roof level - Residential and commercial buildings - Approximately 7.5 m - Vertical and subvertical freeze pipes, brine, freezing plant of 500,000 kcal/h, 500 KVA, frozen ground volume of about 6000 m^3 - Prior to tunneling all buildings located in the vicinity were underpinned by mini piles - N/A - see Figure below (2)
Owner:	- Azienda Autonoma Ferrovie dello Stato - Servicio Lovari e Costruzioni, Rome
Source of Project Information:	- Braun, *et al*., 1974

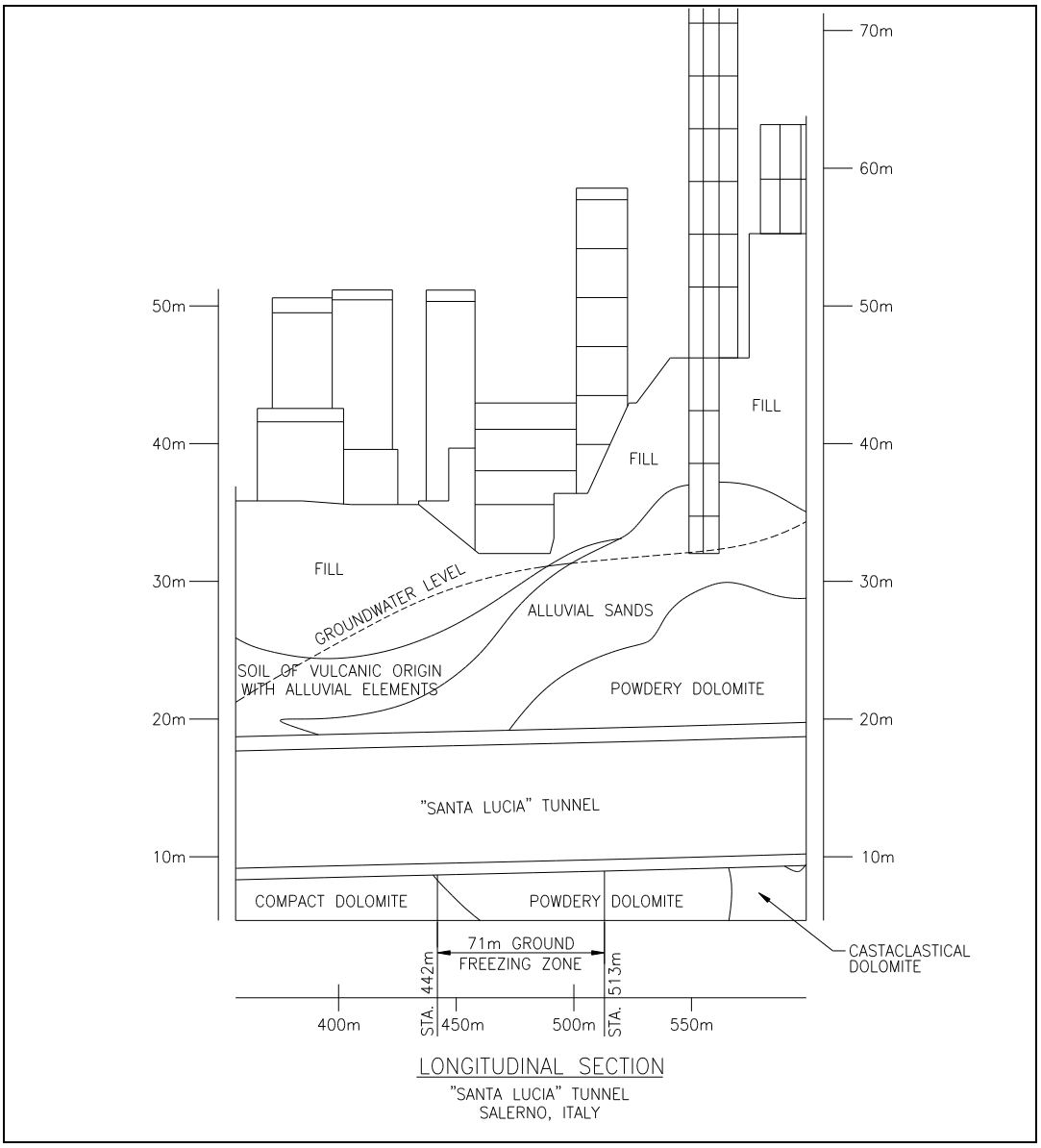

Santa Lucia Tunnel, Salerno, Italy

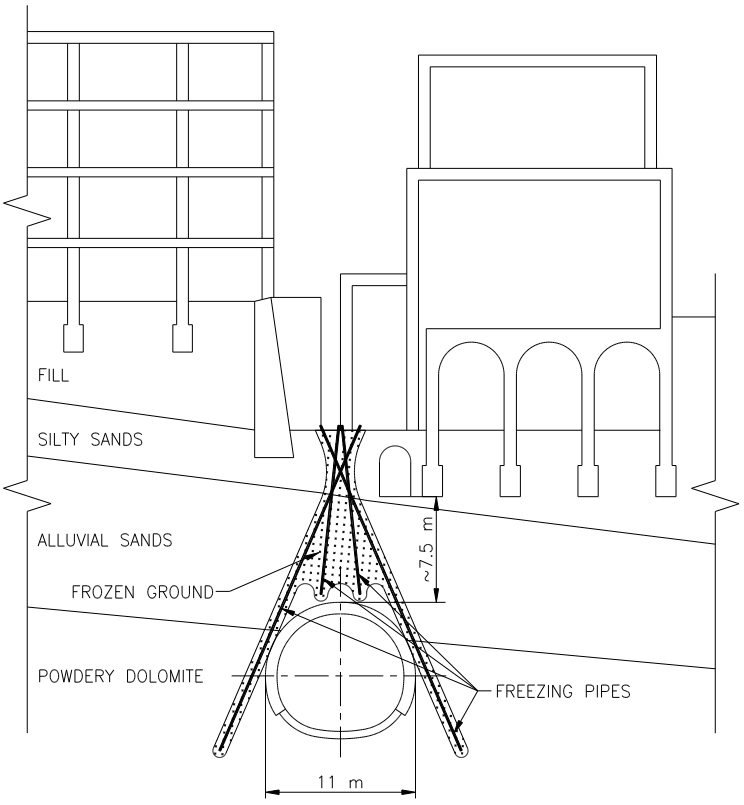

CROSS SECTION

"SANTA LUCIA" TUNNEL
SALERNO, ITALY

Santa Lucia Tunnel, Salerno, Italy (Continued)

References

ABAQUS, Inc., 2002, Abaqus/Standard, Ver. 5.8 User's Manual.

Aerni, K. and Mettier, K., 1980, "Groundfreezing for the Construction of the Three-Lane Milchbuck Road Tunnel in Zurich, Switzerland," *2nd International Symposium on Groundfreezing*, Trondheim, Norway, pp. 889-895.

Aerni, K., "Das Gefrierverfahren aus der Sicht des Projektierenden Ingenieurs."

Andersland, O.B. and Ladanyi, B., 1994, An Introduction to Frozen Ground Engineering, Chapman & Hall.

Bebi, P.C. and Mettier, K.R., 1979, "Groundfreezing for the Construction of the Milchbuck Road Tunnel, Zurich, Switzerland," *Proceedings, Tunneling '79, IMM*, London, UK, pp. 245-255.

Bilfinger und Berger, 1992, "Durchschlag am Fahrlach Tunnel in Mannheim," Bilfinger und Berger Aktuell, No. 1, July pp. 41-42.

Boening, M., Jordan, P., Seidel, H.W., and Uhlendorf, W., 1992, "Baugrundvereisung beim Teilbaulos 3.4 H der U-bahn Duesseldorf," *Bautechnik 69*, pp. 693-705.

Bowles, J.E., 1982, Foundation Analysis and Design, McGraw Hill, Inc., Third Edition.

Braun, B. and Shuster, J.A., 1979, "Ground Freezing: Technology Opens New Applications," *World Construction*, November.

Braun, B., Macchi, A., and Recchi, E., 1974, "Groundfreezing Techniques at Salerno, *Tunnels and Tunnelling*," March Issue, pp. 81-89.

Chen, L.T., Poulos, H.G., and Loganathan, N., 1999, "Pile Responses Caused by Tunneling," *Journal of Geotechnical and Geoenvironmental Engineering*, March Issue, pp. 207-215.

Coulter, S. and Martin, D.C., 2004, "Ground Deformations Above Large Shallow Tunnel Excavated Using Jet Grouting," In Print: *EUROCK 2004 & 53rd Geomechanics Colloquium*, Schubert (Ed.), VGE.

Deix, F., 1992, "Kombination Setzungsmindernder und Umweltschonender Massnahmen (Solevereisung, Druckluft, Ausbruchsicherung) beim Innerstaedtischen Tunnelbau in Kritischen Bereichen," Dissertation, Technical University of Vienna, Austria.

Deix, F., and Braun, B., 1988, "Vienna Subway Construction - Use of Brine Freezing in Combination with Shotcrete Support Method Under Compressed Air," *Proceedings, 5th International Symposium on Ground Freezing*, Jones and Holder (Eds.), Balkema, pp. 321-330.

Deutsche Bundesbahnen, Bundesbahndirektion Stuttgart, 1985, "Die Wendeschleife - Verbindungsbahn der S-Bahn Stuttgart, Dokumentation Ihrer Entstehung, Stuttgart," Der Tunnel, pp. 106-113.

Dr. G. Sauer Corporation, 1996, "Shotcrete Support Method with Groundfreezing at MBTA South Boston Piers Transitway Section CC03A," Feasibility Study, Prepared for MBTA on behalf of Frederic R. Harris, Inc.

Dr. G. Sauer Corporation, 1999, "Structural Analysis and Design Report," Prepared for MBTA on behalf of Frederic R. Harris, Inc.

Dr. G. Sauer Corporation, 2002, "December Monthly Inspection Report," MBTA South Boston Piers Transitway Section CC03A.

Dr. G. Sauer Corporation, 2003, "November Monthly Inspection Report," MBTA South Boston Piers Transitway Section CC03A.

Drucker, D.C. and Prager, W., 1952, "Soil Mechanics and Plastic Analysis or Limit Design," *Quart. Appl. Math.*, Vol. X, No. 2, pp. 157-165.

Elmer, H., Kramer, J., Lehmann, F., Seidel, H.W., and Tuente, B., 1994, "Bahnhofsaufweitung in Gestoertem Gebirge im Schutze einer Bodengefrierung - Stadtbahn Muelheim a.d. Ruhr," Taschenbuch Tunnelbau, Verlag Glueckauf, Essen, Germany, pp.123-154.

Fischer, P.,1987, "Eisbaeren in Wien, Gefrierprojekt U-Bahnlos 6/3 - Vivenotgasse," Unser Betrieb, No. 45, August, pp. 21-25.

Floess, CH., Lacy H.S., and Gerken, D.E., 1989, "Artificially Frozen Ground Tunnel – A Case History," *Proceedings 12th Int. Conf. SM & FE*, Brazil, Vol. II, pp. 1445-1448.

Gall, V., Urschitz, G., and Zeidler, K., "Frozen Ground for Building Support - Implementation of Innovative Engineering Concepts for Tunneling at Russia Wharf," *Proceedings, North American Tunneling 2000*, Boston, Massachusetts, pp. 447-456.

GEI Consultants, Inc., 1998, CC03A/CC05 "Draft Geotechnical Engineering Report," South Boston Piers Transitway, MBTA Contract S0PS08 Boston, MA submitted to F.R. Harris, Inc.

GEI Consultants, Inc. (GEI), 1998, "Final Geotechnical Data Report," MBTA South Boston Piers Transitway, Sections CC03A and CC05, MBTA Contract S0PS08, Boston, MA,' Report Prepared for Massachusetts Bay Transportation Authority.

Gruendler, H., Letta, G., Hagmann, A.J., and Bischoff, N., "Bahnhof Museumstrasse, Unterquerung Limat," Zuericher S-Bahn, Die Neubaustrecke der Zuericher S-Bahn, pp. 6-10.

Haack, A., 1995, "Unterirdisches Bauen in Deutschland," *Proceedings STUVA / ITA-Tagung '95*, Stuttgart, Germany, pp. 58-59, pp. 62-63, pp. 134-135, pp. 194-195.

Harris, J.S., 1995, Groundfreezing in Practice, Thomas Telford Services, Ltd., London, UK.

Hayward Baker - A Keller Company, "Case Histories - Ground Freezing."

Holzmann, P., 1975, "S-Bahn Stuttgart, Baulos 11 und 12 Urban Rail Stuttgart, Contract 11 and 12," Project Brochure.

Holzmann, P., 1977, "Stadtbahn Los 81, Frankfurt am Main, Mainquerung," Project Brochure.

Holzmann, P., 1979, "Soil Freezing in Tunnel Construction, Experience Gained on Major Road and Rail Tunnel Projects," Technical Report.

Holzmann, P., 1979, "Baugrundvereisung zur Herstellung von Tunnelbauwerken, Versuchslos Hauptsammler Mitte, Düsseldorf," Technical Report.

Holzmann, P., 1988, "Freezing Method for Construction of Metro Tunnel Under the Limmat River in Zurich," Project Brochure.

Holzmann, P., 1990, "Spritzbetonvortrieb unter Druckluft und Vereisung, Stadtbahn Hannover, Baulos C23," Project Brochure.

Jessberger, H.L., 1981, "A State-of-the-Art Report, Groundfreezing: Mechanical Properties, Processes and Design," Department of Civil Engineering, Ruhr University, Bochum, Germany.

Jessberger and Partner, "Oberbilker Markt," Project Brief in Company Presentation.

Jessberger and Partner, "Artificial Groundfreezing," Selected Projects Brochure.

Jessberger and Partner, "Erlaueterungsbericht - Sondervorschlag 2 - Hausunterfahrung im Schutze einer Vereisung, Stadtbahn Duesseldorf, U-Bahn Baulos Bhf Oberbilker Markt," Report.

Johnston, G.H. (Editor), 1981, Permafrost: Engineering Design and Construction, John Wiley&Sons, Canada Ltd., Toronto 540 p.

Joint Departments of the Army and Air Force USA, 1985, "Chapter 4, Arctic and Subarctic Construction: Building Foundations," Technical Manual, TM-852-2/AFM 88-19.

Jones, J.S. and Van Aller, H. W., 1982, "Artificial Groundfreezing, Final Report, Federal Highway Administration Office of Research Structural and Applied Mechanics Division," DOT-FH-1-9569, Washington, D.C. August.

Jordan, P., 1992, "Gefrierverfahren im Tunnelbau," Festschrift Anläßlich des 60. Geburtstages von Prof. Dr.-Ing. H.L. Jessberger, Ruhr-Universität Bochum, Schriftenreihe des Instituts für Grundbau - Heft 20; pp. 203-226, Bochum, Germany.

Kielbassa, S. and Duddeck, H., 1991, "Stress-Strain Fields at the Tunneling Face – Three-dimensional Analysis for Two-dimensional Technical Approach," *Rock Mechanics and Rock Engineering 24*, Springer Verlag, pp. 115-132.

Klein, J. and Gerthold, A., 1979, "Die Fliessbedingung von Drucker/Prager im Vergleich zu anderen Bruchkriterien bei der Bemessung von Gefrierschaechten," *Die Bautechnik, 11/1979*.

Klein, J. and Jessberger, H.J., 1979, "Creep Stress Analysis of Frozen Soil under Multiaxial State of Stress," *Engineering Geology*, 13, Elsevier Scientific Publishing Company, Amsterdam, pp. 353-365.

Lacy, H.S., Boscardin, B.D., and Becker, L.A., 2004, "Performance of Russia Wharf Buildings During Tunneling," *Proceedings, North American Tunneling 2004*, Atlanta, Georgia, pp. 121-127.

Lacy, H.S. and Floess, C.H., 1988, "Minimum Requirements for Temporary Support with Artificially Frozen Ground," *Artificial Ground Freezing and Soil Stabilization, Transportation Research Record 1190*, Transportation Research Board, Washington, D.C.

Lacy, H.S., Jones, J.S. and Gidlow, B., 1982, "A Case History of a Tunnel Constructed by Ground Freezing," *Proceedings, of the 3rd International Symposium on Ground Freezing*, Hanover, New Hampshire, pp. 389-396.

Magistrat der Stadt Wien, Magistratsabteilung 38 - U-Bahnbau, "Unterfahrung Post- und Fernsprechamt, U-Bahnbausabschnitt U6/3 in Wien," 1. Ergaenzungsblatt.

Magistrat der Stadt Wien, Magistratsabteilung 38 - U-Bahnbau, "Stickstoffvereisung unter dem Kaufhaus Herzmansky, U-Bahn Bausabschnitt U3/10 in Wien," 1. Ergaenzungsblatt.

Merritt, F. S., 1983, Standard Handbook for Civil Engineers, Third Edition, McGraw-Hill Book Company, New York.

Mohr, B and Pierau, B. 2004, "Unterfahrung der DB-Gaeubahnstrecke mit dem Strassentunnel B 14 in Stuttgart," Taschenbuch Tunnelbau 2004, DGGT, Deutsche Gesellschaft fuer Geotechnik, e.V., pp. 217-234.

Mueser Rutledge Consulting Engineers, 1998, "Supplemental Test Pit Investigation at Russia Wharf, South Boston Piers Transitway, Section CC03A - Russia Wharf," Report Prepared for Frederic R. Harris, Inc.

Mueser Rutledge Consulting Engineers, 1998, "Summary of Frozen and Unfrozen Laboratory Tests on Timber Pile Samples, South Boston Piers Transitway, Section CC03A - Russia Wharf," Report Prepared for Frederic R. Harris, Inc.

Mueser Rutledge Consulting Engineers, 1998, "Frozen Soil Laboratory Test Data and Interpretation, South Boston Piers Transitway Section CC03A – Russia Wharf," Report Prepared for Frederic R. Harris, Inc.

Mueser Rutledge Consulting Engineers, 1998, "Geotechnical Analysis of Tunnel Stability Using Artificially Frozen Soil, South Boston Piers Transitway, Section CC03A - Russia Wharf," Report Prepared for Frederic R. Harris, Inc.

Odkvist, F.K.G. and Hult, J., 1962, Kriechfestigkeit Metallischer Werkstoffe, Berlin: Springer Verlag.

Rebhan, D., 1990, "Baugrundverbesserung durch Stickstoffvereisung," *Proceedings, 5th Christian Veder Kolloquium*, Graz, Austria.

RocScience, Geomechanics Software Solutions, 2001, Users Guide, Phase^2, Finite Element Analysis and Support Design for Excavations, 2D Finite Element Program for Calculating Stresses and Estimating Support Around Underground Excavations.

Sauer, G., Gall, V., Bauer, E., and Dietmaier, P., 1994, "Design of Tunnel Concrete Linings Using Capacity Limit Curves," *Proceedings, Computer Methods and Advances in Geomechanics*, Siriwardance and Zaman, (Eds.), Balkema, Rotterdam, pp. 2621-2626.

Sauer, G., 1988, "When an Invention is Something New: from Practice to Theory in Tunnelling," 23rd Sir Julius Wernher Memorial Lecture of the Institution of Mining and Metallurgy, *Tunneling '88 Symposium*, London, UK.

Schmid, L., 1981, "Milchbuck Tunnel: Application of the Groundfreezing Method to Drive a Three Lane Highway Tunnel Close to the Surface," *Proceedings, Rapid Excavation and Tunneling Conference*, San Francisco, Vol. I, pp. 427-445.

Soletanche, 1987, "Vienna Metro Line U3 - Section U3/10 Groundfreezing."

Szadecky, B., 1988, "Anwendung der Stickstoffvereisung beim Wiener U-Bahnbau," Mayreder-Zeitschrift, 33. Jahrgang, January Issue.

Terzaghi, K., Peck, R. P., and Mesri, G.,1996, Soil Mechanics in Engineering Practice, Third Edition, John Wiley & Sons, Inc.

Ting, J.M., Martin, T.R., and Ladd, Ch. C., 1983, "Mechanisms of Strength for Frozen Sand," *ASCE Journal of Geotechnical Engineering*, Vol. 109, No. 10., pp. 1286-1300.

Wind, H., 1991, "Soil and Rock Improvement in Underground Works - Site Organization of Groundfreezing, Criteria and Recommendations," *ATTI Proceedings*, Vol. II, Milano, Italy.

Wittke, W., 1999, "Tunnelstatik, Grundlagen," *Geotechnik in Forschung und Praxis*, WBI-PRINT 4, Essen: Verlag Glueckauf.